Evaluation of One-Dimensional Seismic
Site Response Analyses at Small to Large Strain Levels

By

DANIEL HUTABARAT

A Thesis

submitted in partial fulfillment of the

requirements for the degree of

Master of Science in Civil Engineering

UNIVERSITY OF WASHINGTON

August 2016

Committee:

Professor Steven L. Kramer, Chair

Professor Pedro Arduino

Program Authorized to Offer Degree:

Department of Civil and Environmental Engineering

University of Washington

Abstract

Evaluation of One-Dimensional Seismic
Site Response Analyses at Small to Large Strain Levels

DANIEL HUTABARAT

Chair of the Supervisory Committee:
Professor Steven L. Kramer, Ph.D.

One dimensional (1D) site response analysis using total stress approach is a popular framework

for evaluating seismic hazard at a site where no significant excess pore water pressure generation

is expected. Several site response analysis codes are available, but their variabilities to predict

site response at shear stress levels approaching the shear strength of the soil have not been

demonstrated. This study evaluates the performance of different soil models employed in each

code to predict the nonlinearity behavior of soil over a wide range of strain levels. This research

performed a set of 1D site response analyses utilizing input motions, scaled to various intensity

levels, against sites that were underlain by cohesive deposits with determined shear wave

velocity profiles. The analyses utilized several available nonlinear soil models while the model-

to-model variability was characterized. These codes were then validated against free-field

downhole data from a vertical array at a relatively well characterized site. The evaluations of the

variabilities of ground motion amplitude, duration, response spectra and cyclic hysteresis loop at various strain levels were performed by comparing all predictions to data from a vertical array. The results showed that all codes give consistent predictions with reasonable accuracy at small to moderate shear strain levels. At larger shear strain levels, only some of current nonlinear soil models were capable of predicting reasonable cyclic behavior in terms of being able to approach the peak shear strength with reasonable damping behavior. The analyses show that the variability of predicted peak shear strain parameters are higher than peak acceleration and shear stress parameters. It also shows that the coefficient of variation of the ground motion parameters predicted by all codes tended to increase at greater shear strain levels.

ACKNOWLEDGEMENTS

First of all, I would like to thank the Lord Jesus Christ for His endless grace in my life until today. This achievement would never be complete without His consent and will.

Secondly, I would like to express my sincere gratitude to my supervising professor, Professor Steven L. Kramer for inspiring me in his *Geotechnical Earthquake Engineering* class and providing me an opportunity to gain valuable knowledges in the area of soil dynamics and earthquake engineering. His generous supports and guidances play an important role during my research and finishing this thesis. I would also like to acknowledge Professor Pedro Arduino as my committee for the reviewing this thesis and providing me with significant feedbacks. I found that their classes during my study in University of Washington to be one of the most crucial part in my academic career.

During my study in Seattle, I met so many people that gave impactful contributions to me and provided memories that I will always remember. I would like to thank all of the current and former graduate students in Geotechnical Engineering program: Mike Greenfield, Cyndi Lopez, Long Chen, Alborz Ghofrani, Alex Ciccone and other geotech folks. All the supports, discussions, comments and tough academic moments are greatly appreciated.

Full financial support during my study was provided by Indonesia Endowment Fund for Education (LPDP), for that, I would like to truly thank the Government of Republic Indonesia for making all the dreams come true. I am looking forward to be back and give significant contribution to the people of Indonesia in the future.

Finally, I would like to thank my dearest wife: Melo, my parents, my brother and sister, all families, and my truly mentor: Professor Masyhur Irsyam, who support me with very strong encouragement. I would not be where I am today without your supports and I believe that this thesis is just the beginning.

DANIEL HUTABARAT

Seattle, Washington

17 August 2016

DEDICATION

To my beloved wife, Melo

my mother, Ompu Davina (Rani); father, Ompu Davina (Robert)

my siblings, David, Ruth and Kristina.

This would not have been possible without your love.

TABLE OF CONTENTS

LIST OF FIGURES

LIST OF TABLES

Chapter 1. INTRODUCTION

1.1 BACKGROUND AND MOTIVATION

The evaluation of ground shaking under earthquake event is mandatory during the preliminary design stage to fulfill the seismic safety criteria of many high risk infrastructures. Many studies reveal that local soil condition play a significant role in the prediction of ground shaking during seismic loading (e.g., Seed et al., 1976, Seed et al., 1988, Vucetic & Dobry, 1991, Baise et al., 2003, Hashash, 2010). For many years, geotechnical earthquake engineers have evaluated this aspect by performing site response analysis in order to compute three important characteristics of seismic ground motion; 1) amplitude, 2) frequency content and 3) duration of the motion (Kramer, 1996) at any depth of interest. Principally, one-dimensional (1D) site response analyses model a specific site as a stack of 1D elements comprising a soil column shaken horizontally by an input motion applied at the base of the column (Figure 1.1). The analyses involve the simulation of seismic shear waves that travel vertically toward the ground surface while computing the response of soil deposit at any depth of interest. Ultimately, these analyses yield predictions of surface time histories and response spectra that are necessary for structural or geotechnical design.
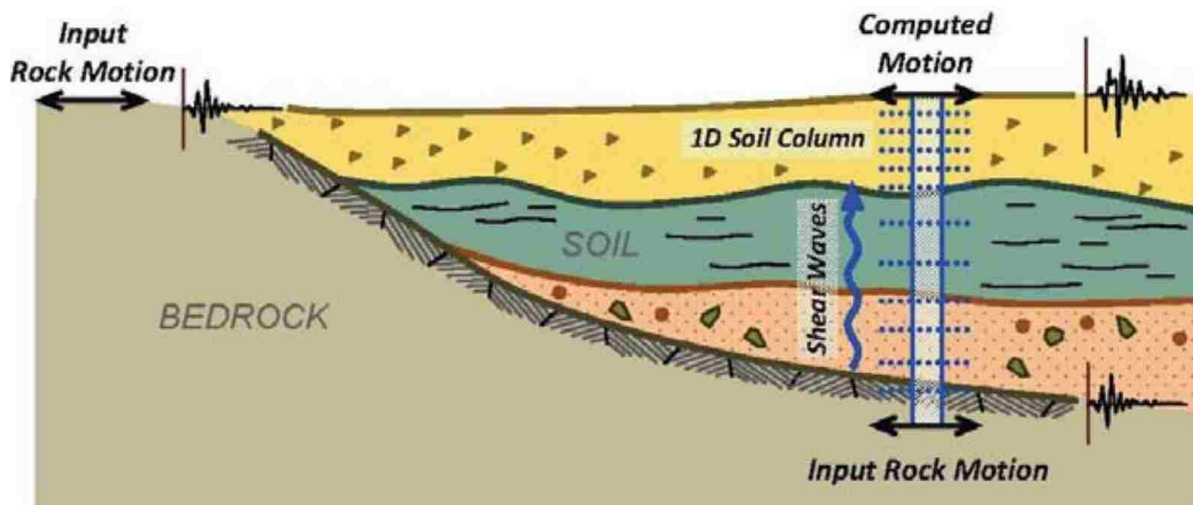
Figure 1.1. Illustration of 1-D seismic site response analysis that is simplified into a 1D soil column (Nikolaou & Go, 2009)

One of the most popular techniques in site response analysis is the equivalent-linear (EQL) approach (Kramer and Paulsen 2004), because it only requires relatively straightforward soil properties. Meanwhile, non-linear (NL) analyses have recently gained more popularity since they are able to predict the non-linear soil behavior during cyclic loading with more accuracy. They capture more reasonable NL soil behavior by keep updating the stiffness of the soil during the earthquake excitation. In addition to the prediction of motion characteristics, site response analyses have the capability of evaluating the cyclic stresses, cyclic strains and excess pore water pressure (only for effective stress analysis approach) in the soil skeleton that is beneficial to understand its behavior during cyclic loading.

During an earthquake, the seismic waves are assumed to excite the 1-D soil column in the horizontal direction, thus, they are usually modeled in a simple shear framework. Under this assumption, the shearing stiffness of the soil is described by the shear modulus (G) at various strain levels and the capability of soil to absorb energy termed as damping ratio (D), are two important dynamic soil properties. These basic parameters control the shape of cyclic stress versus cyclic strain curve (nonlinearity level). Nonlinearity of soil is the most important aspect in non-linear (NL) site response analysis, which are necessary for strong motion and soft soil where high strain level can develop in the soil column.

In practice, both EQL and NL analyses take the advantage of computer programming to perform the computation process. Available codes that are based on the EQL approach typically used the same method and soil model. They only provide different additional user interface features to make the analysis process easier. On the other hand, several NL codes are available but the codes are different in terms of computation methods and non-linear soil models. Currently, the variability in their predictions has not been characterized and the ability of each NL code to predict site response at shear stress levels approaching the shear strength of the soil has not been demonstrated. This research is conducted based on that motivation.

This thesis presents comparisons of available NL codes in predicting site response over a wide range of soil nonlinearity levels. The comparison includes analyzing various site profiles excited by low to high intensity motions and validation against vertical array data. Furthermore, the research in this thesis focuses upon the characterization of variability among all NL codes of interest. In conjunction with NL results, the EQL results are also compared and this research attempts to characterize the condition at which the EQL deviate significantly from NL analysis.

1.2   THESIS OVERVIEW

1.2.1   *Objectives of Research*

The objectives of this thesis are to evaluate the current available site response analysis codes in predicting the surface motion characteristics. It also provide a documentation of the variability of the results predicted by each code. In more detail, this work involves task such as:

1. Using available equivalent linear and non-linear codes to predict the surface motion characteristic for a wide range of intensity motion and strain level. Evaluation of the ability of each soil model in predicting the site response at shear stress levels approaching the shear strength of the soil is required, therefore, that will be one of the main objective of this thesis.

2. Characterize the model to model variability of the site response results (i.e. time histories, response spectra, arias intensity, cumulative absolute velocity, etc.) predicted by each codes. The sources of variability in terms of computation method, soil model and other aspects will be documented.

1.2.2   *Scope of Research*

The main objective of this thesis is to evaluate the variability of the 1D site response analysis computed by different available codes. It focuses on the EQL analysis and the available nonlinear analysis with total stress approach. The codes considered in this research include DEEPSOIL and STRATA for EQL approach and DEEPSOIL, FLAC, OPENSEES, NERA, DMOD2000, FLIP for NL approach. The details of the nonlinear soil models used for each code are briefly summarized in the next chapter. Although the total stress approach does not have capability to capture all the important aspects, such as prediction of the generation of pore water pressure for liquefiable soil during seismic loading, it is still reasonable for many types of soils and loading conditions. Multidimensional site response analysis is required for sites at which basin effects or topographical effects might affect the result (Kramer, 1996), but 1D assumption as employed in this thesis is adequate for many seismic design projects.

This thesis mainly focuses on the deposit where the development of pore water pressure is trivial. For this type of material, plasticity index (PI) become one of the most sensitive parameter in the prediction of the results. In order to accommodate the PI differences in the analysis, the

Darendeli (2001) curve will be used for all of the analysis except for the site that have individual G/G_{max} and damping curve. Another parameter that is important is undrained shear strength parameters, this research will use the correlation proposed by Dickenson (1994) that is established for cohesive soils and correspond to shear wave velocity in the San Francisco Bay Area. The undrained shear strength is important to adjust the original G/G_{max} degradation curve so that it will not exceed the real shear strength of the soil.

For the specification input motion assumption, this research follows the recommendations suggested by Kwok et al, 2007 as the guideline to choose the input motion (outcropping or within profile motion) and the model of underlying halfspace. Lastly, this thesis provides documentation of variability characterization in site response analysis using available nonlinear codes. It attempts to increase understanding of 1D site response analysis particularly in terms of nonlinear models or constitutive modeling of soil aspect in practice.

1.2.3 *Organization*

This thesis consists of six chapters. Chapter Two reviews the literatures and the important aspects that should be taken into account in 1D site response analysis. Chapter Three discusses a general overview of the 1D site response analysis method for each code including the analysis model and computational method. This chapter will discuss brief theories and 1D site response analysis model used in this thesis. Furthermore, the nonlinear and constitutive soil model will be briefly discussed in this chapter.

In Chapter Four, the analysis model of interest established in Chapter Three will be employed to analyze the seismic site response of site underlain by simple soil profiles that contain cohesive soils. Three models of simple site profile consisting of constant, layered and parabolic shear wave velocity profile will be generated. These sites represent the three NEHRP site classes (S_E, S_D and S_C). Moreover, a motion taken from 1989 Loma Prieta earthquake will be scaled from low to high intensity motion and each motion will be applied as the input motion at bedrock layer. These analyses will provide 36 results ranging from low to high strain level event and the variability of each case will be characterized.

Another evaluation of site response analysis codes against vertical array data from an actual earthquake is presented in Chapter Five. Chapter Six will use the Turkey Flat data that is shaken by relatively low intensity motion. A comparison will be performed between the real measurement

in the surface and the motion predicted by each codes. In order to take advantage of the soil properties data in Turkey Flat, the analysis case will be expanded by scaling the original input motion to higher motion and the variability of the results will be characterized. In addition, the summary and conclusion of the research findings and conclusions found in this thesis are presented in Chapter Six.

<div align="right">Chapter 2. LITERATURE REVIEW</div>

2.1   SOIL BEHAVIOR DURING CYCLIC LOADING

This section will briefly summarize basic aspects of soil behavior during cyclic loading as typically adopted in 1-D site response analysis. The 1-D framework only considers the horizontal component of seismic ground motion that is applied at the bottom of the soil column, therefore, the direct simple shear (DSS) concept is useful for representing the cyclic behavior of soil (Figure 2.1a). In the 1-D EQL approach, the soil is assumed to behave as a Kelvin-Voigt solid material, in which the shearing resistance of the material is proportional to the sum of the elastic (spring) and viscous (dashpot) resistance (Kramer, 1996) as illustrated in Figure 2.1b. The shear stress and strain response of this material is plotted in Figure 2.2. At strain level, γ, the elastic stiffness of the element is represented by G_{sec} (proportional to strain) and the viscous resistance is represented by the material damping ratio, D (proportional to strain rate).
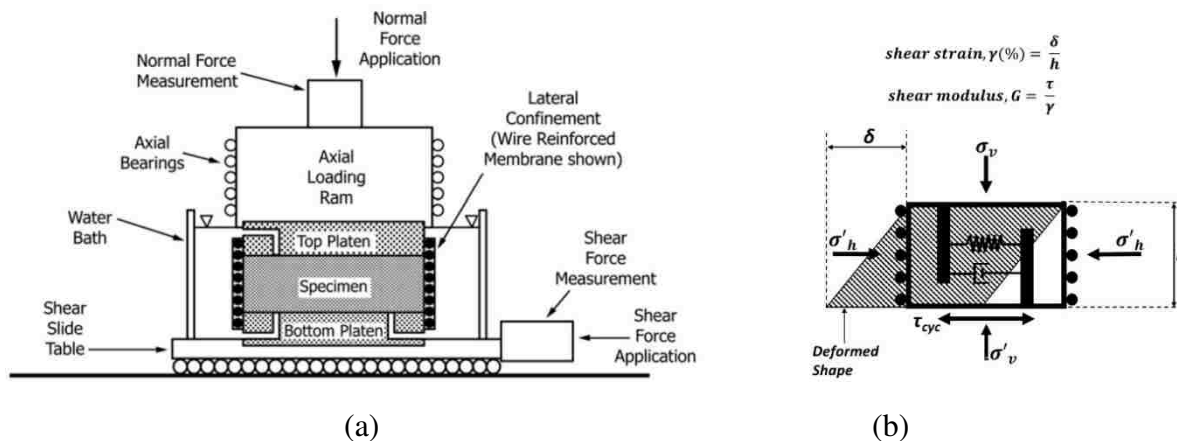
Figure 2.1. (a). Schematic diagram of DSS test in the laboratories (after ASTM, 2007), (b). Kelvin-Voigt model includes spring constant (G) and dashpot coefficient (μ) in the soil skeleton and deformed shape illustration during loading.

The viscous resistance theoretically represents the ability of a material to dissipate energy under cyclic loading. As shown in Figure 2.2, the peak stored energy during shearing is proportional to the area of the red triangle (A_{SE}) and the dissipated energy absorbed by the material

is proportional to the area of the hysteresis loop (A_{LOOP}). The ratio of dissipated energy to energy stored to the material is referred to material damping ratio, D.
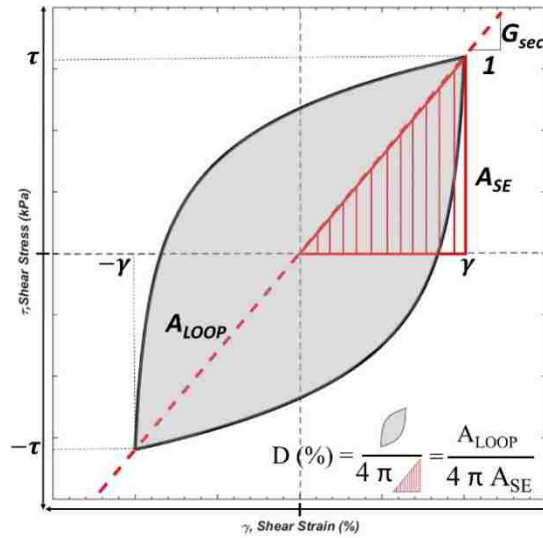
Figure 2.2. Illustration to estimate the secant shear modulus (G_{sec}) and material damping ratio (D) during cyclic loading.
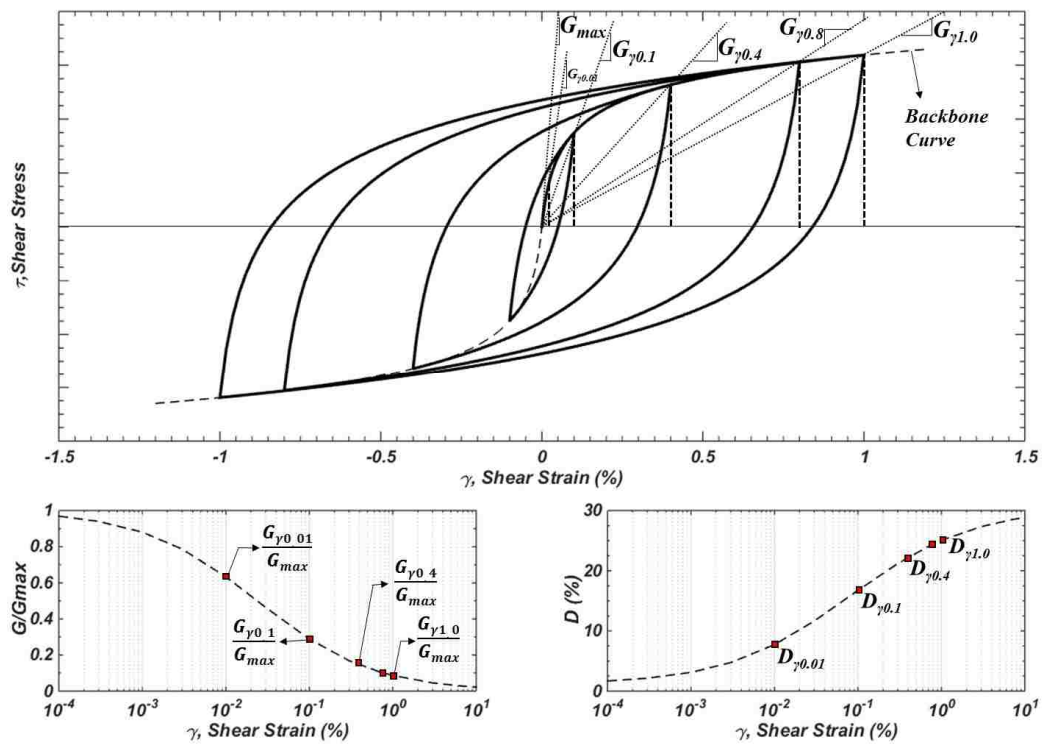
Figure 2.3. Cyclic stress-strain behavior and two important dynamic properties (G/G_{max} and Damping Ratio) of soil during cyclic loading.

The upper curve in Figure 2.3 shows the stress-strain response of soil under strain-controlled cyclic loading test. Initially, the shearing stiffness of the soil is usually referred to as small strain shear modulus or maximum shear modulus ($G_{max} = \rho \times V_s^2$) that is related to the mass density and shear wave velocity of the soil. As the strain increase, the shear modulus will decrease following the backbone curve of the soil as shown in the lower left curve. In contrast to the shear modulus, the material damping ratio will increase with strain amplitude, because the area of hysteresis loop is larger at higher strain levels. These two curves describe the most important dynamic soil properties during cyclic loading and they are critical parameters in site response analysis.

Darendeli (2001) reported that plasticity index (PI), mean effective confining pressure (σ_m), overconsolidation ratio (OCR) and number of loading cycles all influence nonlinear soil behavior at various strain levels. These parameters affect the threshold strain level at which the soil will start its nonlinear phase. At similar σ'_m, the threshold strain level for the material with lower PI is smaller than material with greater PI. In other words, lower PI will cause greater shear modulus reduction curve values for a given shear strain and confining pressure (Figure 2.4a).

(a) Similar σ'_m (b) Similar PI
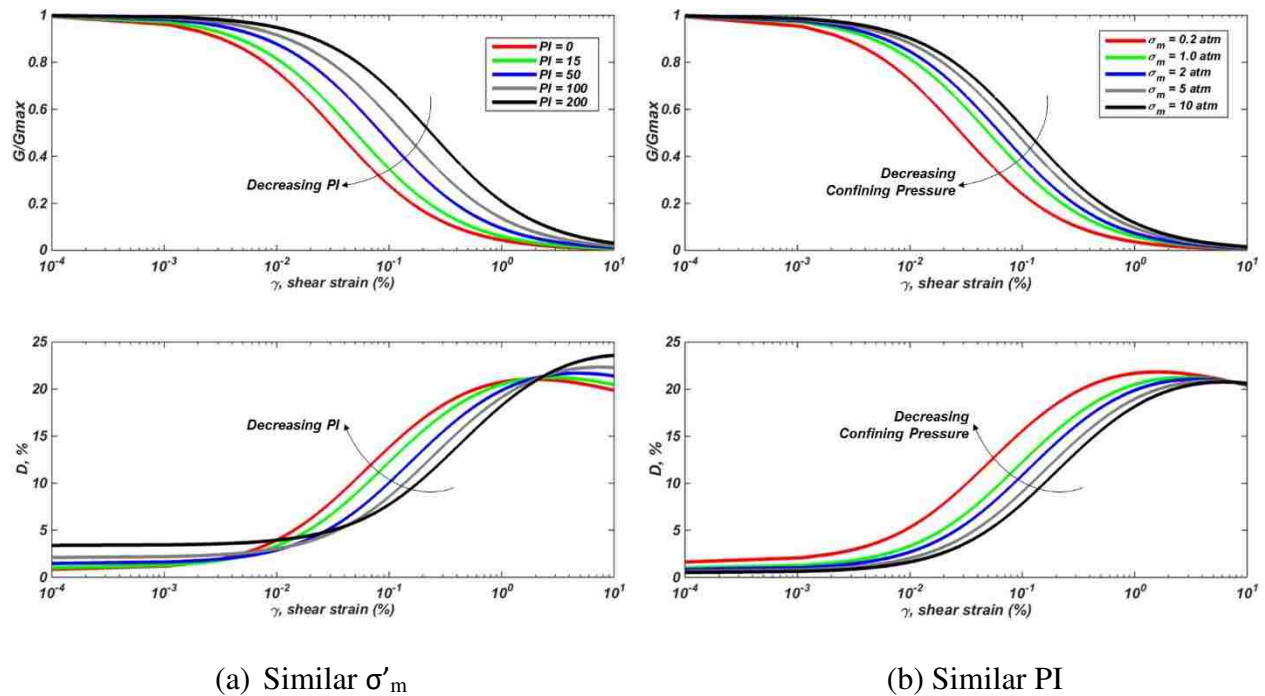
Figure 2.4. Effect of strain amplitude, plasticity index and mean effective confining pressure on the dynamic properties of soil during cyclic loading based on Darendeli (2001).

In terms of damping, at small strain, soil with higher PI will have greater small strain damping ratio but it will not be the same at moderate to higher strain level. Figure 2.4b shows the effect of mean confining pressure on the G/G_{max} and damping curves for different PI values. In conclusion, the degradation of shear modulus (non-linearity level) and the damping ratio will be less for soil with higher threshold strain level. This is important in site response analysis because with lesser damping, the soil will absorb less energy, allowing more energy to propagate and consequently cause greater intensity motion at the surface.

2.2 ONE-DIMENSIONAL SITE RESPONSE ANALYSIS

One-dimensional (1D) site response analysis assumes that the horizontal seismic wave motion propagates vertically from the underlying bedrock to the ground surface. During the analysis, horizontal layer boundaries are extended infinitely and must be perpendicular to the direction of wave propagation. As described earlier, EQL and NL approaches are the most common techniques to conduct 1D site response analysis. The answer when the EQL and NL approach should be selected depends mainly on the induced cyclic shear strain during earthquake event. Kaklamanos (2013) conducted numerous site response analyses to improve understanding about that issue using the Kiban-Kyosin network (KiK-net) downhole array data in Japan (Figure 2.5a).
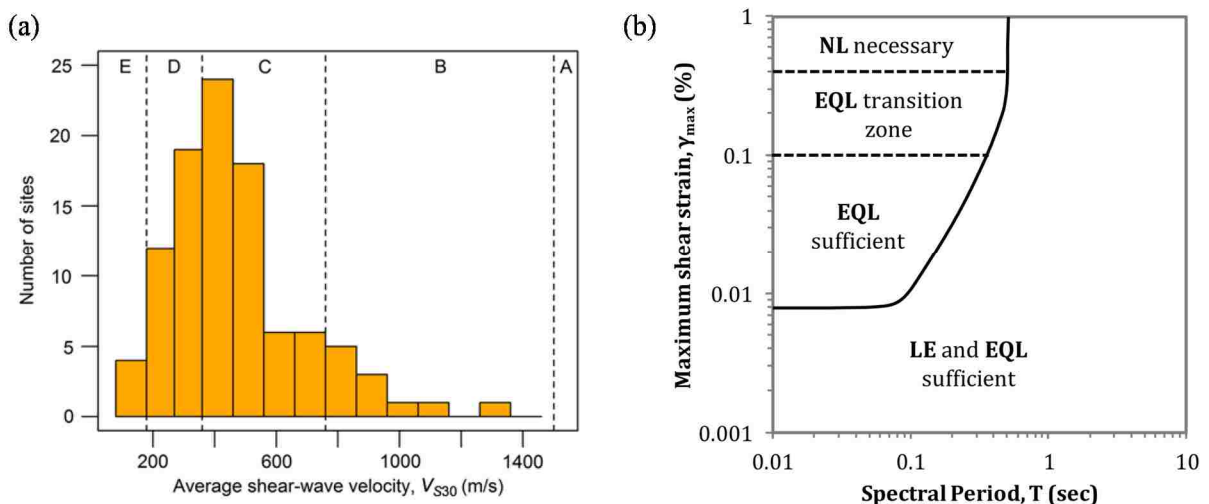
Figure 2.5. Study conducted by Kaklamanos et al. (2013). (a) range of data within KiK-net downhole array, (b) the threshold of shear strain and period that predicts at which strain level the accuracy of equivalent linear approach is no longer accurate.

This study concludes that if the shear strain is between 0.1% - 0.4% the EQL analysis might be not sufficient to predict accurate result. Furthermore, if the induced shear strain is greater than 0.4% the NL approach is necessary because EQL is no longer accurate (Figure 2.5b). Zalachoris and Rathje (2015) also show that within that threshold the residual value representing the different of measured and computed amplification factor is greater than 0.4.

2.2.1   *Equivalent Linear Analysis (EQL)*

The EQL approach is initiated by the work of Schnabel et al. (1972) as a modification of the linear approach to provide reasonable site response prediction. It is employed to solve the 1D shear wave propagation equation (Kramer, 1996). Principally, the linear approach uses a transfer function to determine the amplification factor and phase shift for each frequency during shaking. This function mainly depends on the soil column properties (i.e., impedance ratios -controlled by mass density and shear wave velocity- damping ratio and layer thicknesses) that determine the degree to which each frequency of input motion is amplified or deamplified by the soil column.

Once the transfer function is established, the input acceleration time histories in the time domain (bedrock input motion) will be transformed to the frequency domain using Fast Fourier Transform algorithm (FFT). The FFT will transform the input motion into Fourier Amplitude Spectrum (FAS) at various frequencies where the summation would be the original time history. This series is then multiplied by the transfer function, over a range of frequencies and its product will be the Fourier series of the output motion (surface motion). In order to obtain the time history of the output motion, the output Fourier series is then transformed back to the time domain using inverse FFT algorithm. A detailed explanation of the linear approach is explained in Kramer (1996).

As described previously, the linear approach assumes that the soil behaves as a Kelvin-Voight material with a constant small strain shear modulus, G_{max} and damping ratio, D_{min}. This assumption might be suitable for very small strain problems, but it must be modified for higher strain to yield reasonable predictions. This modification is referred to equivalent linear (EQL) procedure where the equivalent linear shear modulus (secant shear modulus) and damping ratio are selected from G/G_{max} and damping curves to estimate the nonlinear behavior at the strain level of interest. The selections of equivalent parameters follows an iterative procedure by repeating the computation process until the selected parameters give the strain level that is matched the effective shear strain,

γ_{eff} (usually 65% of maximum strain in a given layer) with tolerable computation error. The iterative procedure is illustrated in Figure 2.6 and explained in detail in Kramer (1996).
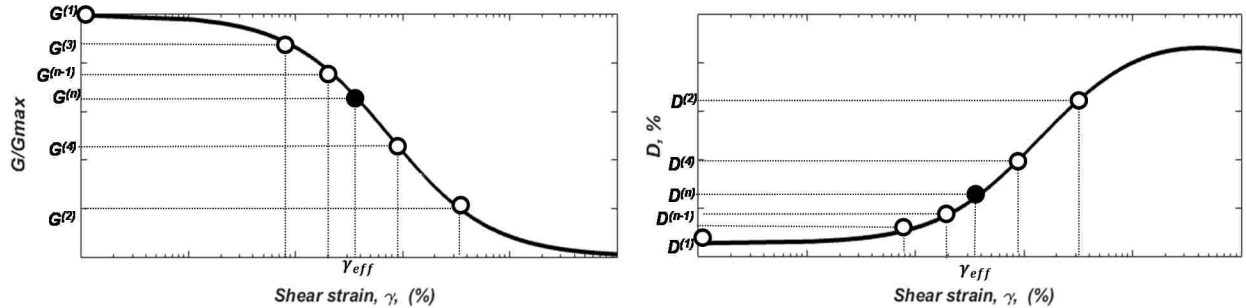
Figure 2.6. Iterative procedure of G and D in EQL analysis, the iteration is repeated for *n* times until computed effective strains are consistent with assumed effective strains. Initial estimation , using $G^{(1)}$ and $D^{(1)}$, predicts the γ^1_{eff} that is greater than the strain of assumed G/G$_{max}$ and Damping curve model. The computation process is repeated until the selection of G and D at the n-iterative yield the γ^n_{eff} matched the strain of the model with tolerable computation error (1-3%).

The EQL approach is commonly used in practice because it requires straightforward readily obtainable soil properties and low computational requirements since the computation process is performed in the frequency domain (Hashash et al, 2010). For seismic design problems at relatively low strain levels, the EQL is sufficient and provides reasonable results. Figure 2.7 present an example of cyclic stress and strain response of a soil deposit at low and high strain levels. Figure 2.7 illustrates that the EQL approach is no longer accurate due to the simplification of the dynamic soil properties (constant shear modulus). At high strain level, nonlinear approach should be employed because it is capable of representing the actual nonlinear cyclic behavior of soil much more accurately.

2.2.2   *Non-linear Analysis (NL)*

The NL approach is performed in the time domain to solve the dynamic wave equation problem. There are two type of equations that is commonly solved in NL approach, one is the lumped mass equation of motion (Eq. 2.1) and the other is the one-dimensional wave propagation equation (Eq. 2.2). To solve Equation 2.1, NL analysis is employed in a time-stepping procedure as usually performed in the analysis of structural response to input ground motion (Chopra, 2012).

$$[M]\{\ddot{u}\} + [C]\{\dot{u}\} + [K]\{u\} = -[M]\{I\}\ddot{u}_g \qquad (2.1)$$

$$\frac{\partial \tau}{\partial z} = \rho \frac{\partial^2 u}{\partial t^2} = \rho \frac{\partial \dot{u}}{\partial t} \qquad (2.2)$$

The soil mass matrix $[M]$ is constructed usually as a lumped mass (Figure 2.8a) system and the soil viscous damping matrix $[C]$ is constructed usually by using Rayleigh damping or frequency-independent approach (Phillips & Hashash, 2009). The key of NL approach is the construction of the soil stiffness matrix, $[K]$, that is continuously updated over the earthquake duration. The $[K]$ will adopt either a cyclic non-linear soil model (i.e., Matasovic & Vucetic 1993, Itasca 2009, Groholski et al 2016) or advanced constitutive soil model (i.e., Iwan 1967, Mroz 1967, Yang 2000, Iai et al 2011). Once the matrices are constructed, Equation 2.1 is solved numerically using a time integration method such as Newmark (1959) β-method for each time step and the response (i.e., displacement, velocity and acceleration) of each node of interest is resulted.
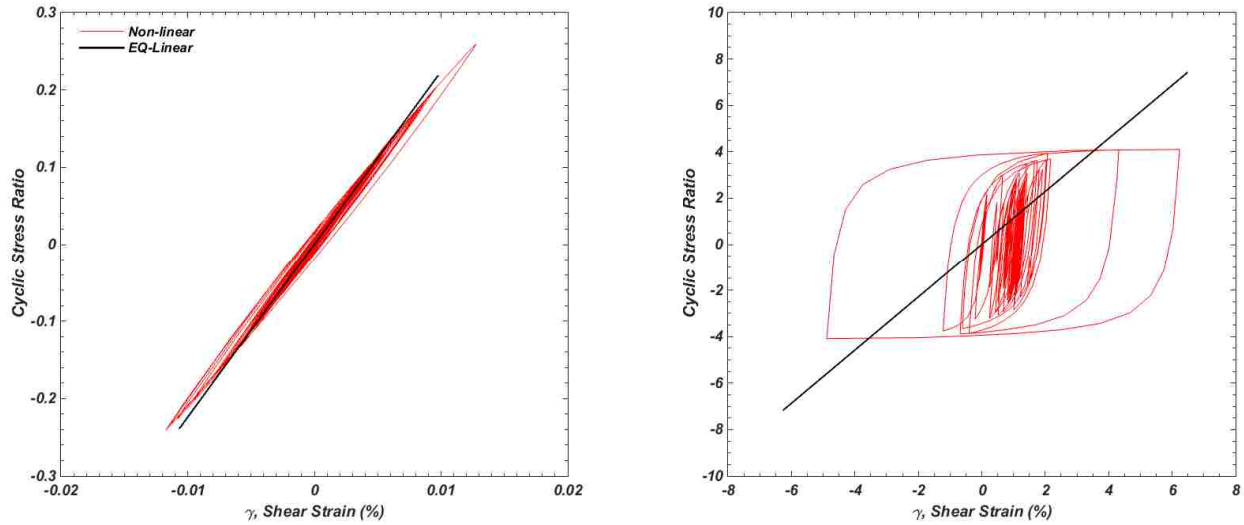
Figure 2.7. Example of two stress-strain curves at low and high strain level at 2.0 m depth at Turkey Flat vertical array site. (a) Response simulation ($\gamma_{max} = 0.01\%$) shaken by 2004 M_w 6.0 Parkfield Earthquake (PGA = 0.07g). (b) Response simulation ($\gamma_{max} = 6.6\%$) shaken by original motion scaled to PGA = 1.0g, predicted by Pressure Independent Multi-yield surface (Yang, 2000) soil model using OPENSEES. At low strain level, the response predicted by EQL and NL approach give similar prediction. At high strain level, EQL predicts stiffer stiffness without any softening behavior that is captured by NL approach with more accuracy. (Plot is not at the same scale)

Another option to perform NL site response analysis is to solve the equation of seismic wave propagation problem, given by Equation 2.2 by using forward finite-difference (FD) approximation (Kramer 1996, Bardet & Tobita 2001) or finite element anlaysis (FE). This approach divides the soil column into a number of sublayer with arbitrary thickness. By using FD approach, the partial differential equation is solved to obtain the response at each nodes (depth) and time steps.

Equation 2.1 requires the use of viscous damping to prevent oscillations and to accommodate the small strain damping to the system that is not captured by the NL models (Stewart et al 2008). It adopts Rayleigh damping that is not totally suitable for material like soil since it produces damping that is frequency dependent. On the other hand, Equation 2.2 does not require the construction of $[C]$ because it assumes that all the material damping is included in the stiffness component. Kaklamanos et al (2015) shows that the exclusion of Rayleigh damping may help to mitigate the issue of overdamping at high strain levels.
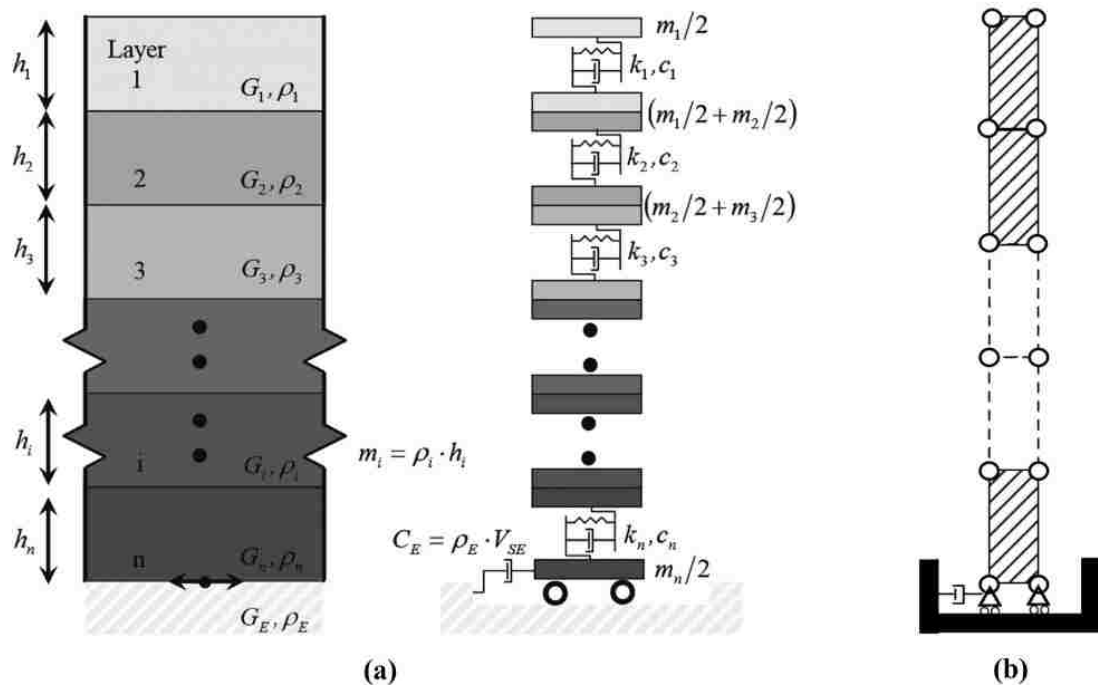
Figure 2.8. (a) Multi-degree of freedom system with lumped mass system corresponding to nonlinear spring and a dashpot for a viscous damping (Hashash, 2010). (b) Continuum discretized into finite elements with distributed mass (after Stewart, 2008). Both system utilize a dashpot at the base of the column to account for the finite rigidity of the halfspace.

Although these two approaches are performed to solve different equations in site response analysis, the process is similar. At the beginning of each time step, both their governing equations solve to yield the particle displacement, velocity and acceleration using initial soil dynamic properties (G_{max} and D_{min}). The result then is used to determine the shear strain within each layer. The amount of induced shear strain is then matched to the nonlinear soil model or advanced constitutive soil model to update the shear modulus of the soil that is used to compute the response in the next time step. This process is repeated over the duration of the input motion until the response at each node is computed (i.e., time histories of acceleration, velocity, displacement, shear stresses, shear strains and pore water pressure if the analysis is performed using the effective stress approach).

By updating the soil stiffness properties after each time step, the NL approach utilizes a stress-strain relationship to model the actual nonlinearity during cyclic loading. The accuracy of the prediction will be sensitively dependent on the nonlinear soil model used. An ideal NL soil model is expected to capture several important aspects of soil behavior: 1) stress vs strain behavior during monotonic loading (*backbone* curve); 2) stress vs strain behavior during unloading and reloading behavior (*hysteretic damping* rules); 3) the peak shear strength of the soil; 4) pore water pressure generation (for effective stress analysis model).

To accommodate the first two aspects, NL soil models (e.g., Matasovic & Vucetic 1993, Itasca 2009, Phillips & Hashash 2009) usually use target G/G_{max} and damping curves and try to fit their model by adjusting the basic equation of the model featured with curve fitting parameters. The fitting procedures are usually performed to fit one of three options: a) fit perfectly the modulus reduction by allowing less accuracy in damping curve; b) fit perfectly the damping curve by allowing less accuracy in the modulus reduction behavior and; c) fit less perfectly both of modulus reduction and damping by allowing greater accuracy in both of target curves.

Furthermore, for the third aspect, Yee et al (2013) proposed a procedure to adjust the target curve so that it could not exceed the peak shear strength of the soil (strength correction procedure). Groholski et al (2015) proposed a new equation to perform the curve-fitting procedure with much more accuracy by allowing peak shear strength of soil to be defined while providing flexibility to match the small strain soil behavior. The fourth aspect is required in the effective stress analysis approach and it will beyond the scope of this thesis.

2.3   OTHER IMPORTANT ASPECTS

Several important aspects beside the nonlinear model or constitutive modeling of soil must be considered to perform 1D seismic site response analysis. These aspects include the minimum thickness of the layer discretization, specification of input motion and underlying halfspace, calibration of Rayleigh damping and G/G$_{max}$ curve correction to match the target shear strength of the soil.

2.3.1   *Layer Thickness*

The minimum discretization of layer thickness depends on the natural frequency/period of the site given by Equation 2.3:

$$f_{max,i} = \frac{V_{s,i}}{4H_i} \; ; \quad T_{min} = \frac{1}{f_{max}} \tag{2.3}$$

where $f_{max,i}$ is the highest frequency that layer *i* can propagate, $V_{s,i}$ is the shear wave velocity of and H_i is the thickness of layer *i*. If a 30 m soil profile has V$_{s30}$ = 150 m/s, and it will only be discretized into a single layer, the maximum frequency of any motion that can be propagated by the layer is 1.25 Hz. It means that the component of the motion that have frequency more than 1.25 Hz would not be captured during the propagation because all of the high frequency waves are cut off.

The higher frequency of the soil layer can propagate, the more accuracy of the site response resulted. In terms of minimum frequency, T_{min} indicates that response spectra at periods below it tend to be flat and identical to the PGA value. The common recommendations for the maximum frequency are between 25 – 50 Hz (Hashash, 2015). To increase the maximum frequency of a layer, thinner layer discretization is required. The maximum frequency used in this research is 25 Hz.

2.3.2   *Specification of Input Motion and Half Space*

Specification of input motion is one of important aspects in 1-D site response analysis. Kwok et al (2008) summarized the recommendation procedure of treating bedrock as elastic or rigid

halfspace. At the base of the soil column (Figure 2.8), if the bedrock is modeled as elastic halfspace, the implementation of the dashpot (Lysmer & Kuhlemeyer, 1969) is necessary to account for finite rigidity of the underlying medium (Joyner & Chen, 1975). The dashpot coefficient is equal to the product of the mass density and the shear wave velocity of the bedrock. The input motion then is applied to the base of the column as force history proportional to the product of the dashpot coefficient and the velocity of the input motion.

The phenomenon of seismic wave propagation require special treatment when it approach the interface layer, for example, when it travel from stiffer material to softer material as encountered in 1D site response problem. Figure 2.9 (left figure) illustrate the common terminology used in ground response analysis. The implementation of rock outcropping motion or motion that is recorded within the depth (Bedrock motion) cause confusion in the practice of 1D site response analysis. To clarify this problem, the concept of impedance ratio in determining the reflected and transmitted wave of an incident wave at interface might be beneficial.

The product of the density and shear wave velocity of any material is the specific impedance. If an incident wave travel from material i to material j as shown in right figure in Figure 2.9, the impedance ratio, α_z is given by $\alpha_z = \dfrac{\rho_j \, v_{s_j}}{\rho_i \, v_{s_i}}$. The displacement and the stress amplitude of soil particle at the interface depends on the impedance ratio of the two layers and the formula to compute those parameters are given by Kramer, 1996. Table 2.1 listed the computed of displacement and stress amplitude for the transmitted and reflected wave corresponds to several impedance ratio value.
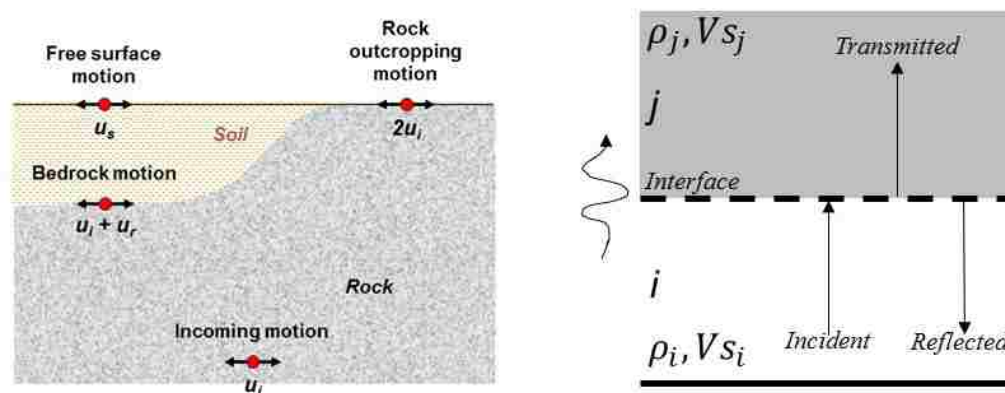
Figure 2.9. Nomenclature commonly used in site response analysis and the displacement amplitude at location of interest. (After Kramer, 1996). The right figure present the illustration of the wave propagation at the interface layer.

Table 2-1. Influence of Impedance Ratio to the reflected and transmitted wave at the interface

Impedance Ratio, α_z	Displacement Amplitudes			Stress Amplitudes		
	Incident	Reflected	Transmitted	Incident	Reflected	Transmitted
0 (free-end)	u_i	u_i	$2\,u_i$	σ_i	$-\sigma_i$	0
0.5	u_i	$u_i/3$	$4\,u_i/5$	σ_i	$-\sigma_i/3$	$2\sigma_i/3$
1	u_i	0	u_i	σ_i	0	σ_i
2	u_i	$-u_i/3$	$-2u_i/3$	σ_i	$\sigma_i/2$	$4\sigma_i/3$
4	u_i	$-3u_i/5$	$2\,u_i/5$	σ_i	$3\sigma_i/5$	$8\sigma_i/5$
∞ (fixed-end)	u_i	$-u_i$	0	σ_i	σ_i	$2\sigma_i$

Based on Table 2.1, an incident wave, u_i travel through identical material when impedance ratio is 1, and if it is less than 1 it can be thought of as approaching softer material. Such cases with $\alpha_z = 0$ and $\alpha_z = \infty$ are the main interest to explain the terminology of outcropping and within motion. The impedance ratio of zero implies that the incident wave approaching a "free-end" causing the material with no shear resistance (zero shear stress) as listed in Table 2.1. The "free-end" boundary condition causes the transmitted displacement amplitude, u_i to be twice the incident wave. The motion recorded at rock outcropping motion (illustrated in Figure 2.9) is one of the example of "free-end" condition.

An infinite impedance ratios implies that an incident wave is approaching a "fixed-end" boundary condition. It means all the incident wave will be completely reflected and the stress at the boundary is twice of the incident wave. A refracted seismic wave from ground surface that travel to very stiff (rigid) bedrock is an example of this condition. Since there is no transmitted displacement, all energy will be reflected back to the ground surface. This explains why the motion recorded at bedrock motion (within motion) will be the superposition of the incident and reflected wave ($u_I + u_R$) as shown in Figure 2.9. This is also valid for finite impedance ratio where not all the incident wave is reflected back to the ground surface. As a reminder, the application of Lysmer & Kuhlemeyer (1969) dashpot to input the stress history as the input motion procedure based on Joyner & Chen (1975) are used to represent this boundary problem.

From this explanation, the motion recorded at bedrock (within motion) and rock outcropping are not the same and should be treated differently to predict the free surface motion, u_s at the top

of the soil deposit. In order to address this issue, Stewart et al (2008) performs site response analyses using the combination of within motion + rigid base ($\alpha_z = \infty$), within motion + elastic base, outcropping motion + rigid base ($\alpha_z = \infty$), outcropping motion + elastic base and compared the result to an exact solution for an linear material properties as computed using SHAKE04. The result of this study is presented in Figure 2.10 and the recommendations are made as follows: 1) if the recorded rock outcrop motion is used, the motion should be used without any modifications but the base of the 1D soil column should be modeled as an elastic half-space, 2) if the recorded within motion is used like for the simulation of vertical array recording data, the within motion should be used without modifications in conjunction with a rigid base.
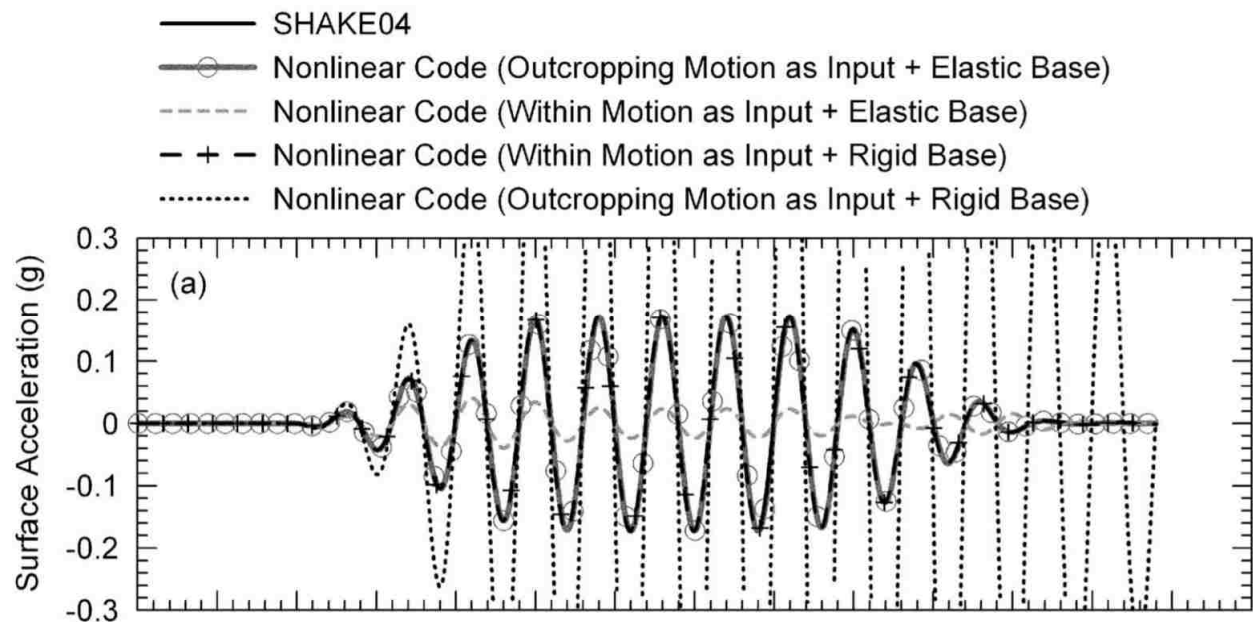
Figure 2.10. Summary of the comparison analysis to specify the input motion and halfspace material from the work of Stewart et al (2008)

2.3.3   *Damping*

The rules to construct unloading-reloading curve (hysteretic damping) in an NL soil model usually adopt the Masing (1926) rules. Some studies (Phillips & Hashash, 2009 and Arefi et al, 2013) reveal that Masing rules overestimate the damping ratio at moderate and large strain levels. It causes smaller estimation of shear strain in the soil layer that predicts lower intensity motion at

the ground surface. Damping represent the area of hysteresis loop, the larger the area the more energy is absorbed by the material (Figure 2.11).
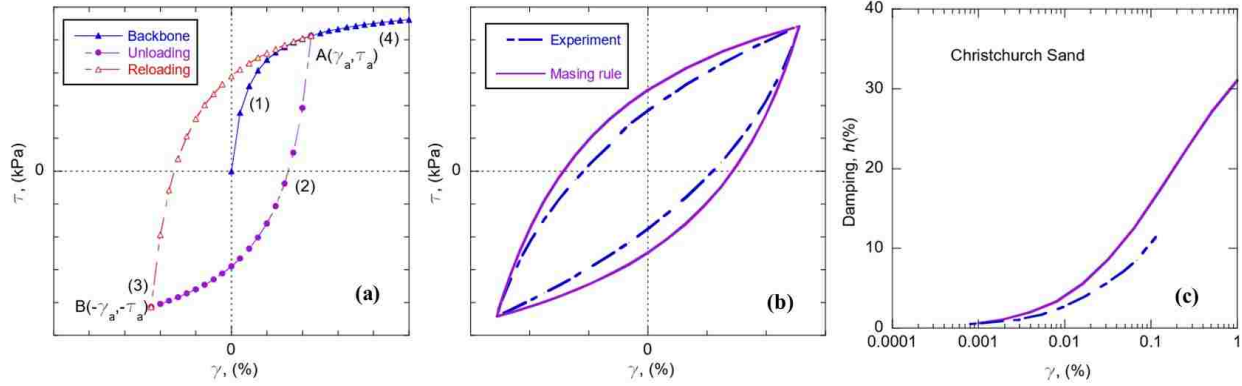
Figure 2.11. (a) Hysteretic cyclic response of soil constructed based on a NL soil model and using Masing criterion. (b) Comparison of experimental and Masing-based calculated loop. (c) Damping ratio curve predicted by Masing rules is greater than experiment at moderate to higher strain level of a sand material in Christchurch, NZ. Arefi et al (2013)

The implementation of Rayleigh damping is required in 1D site response analysis computation to construct the viscous damping matrix [C] at small strain levels. Viscous damping depends on the frequency (Figure 2.12) while the small strain damping in soil is not. Therefore, calibration is required to perform the 1D site response analysis to prevent overdamping condition due to the implementation of Rayleigh damping at frequencies other than the target frequency. Kwok, et al (2007) give recommendations to use full Rayleigh damping scheme (two target frequencies, f_m and f_n only) and the initial estimation to select the target frequencies. The formula to compute the target frequency is given by Kramer, 1996

$$f = \frac{V_s}{4H} \ (2n - 1) \tag{2.1}$$

where f is the 1D soil column's natural frequency of the corresponding mode and n is the mode number. Kwok et al (2007) proposed that the first target frequency, f_m shown in the Figure 2.24 should be the natural frequency at the 1st mode and the second target frequency, f_n is 5 f_m.
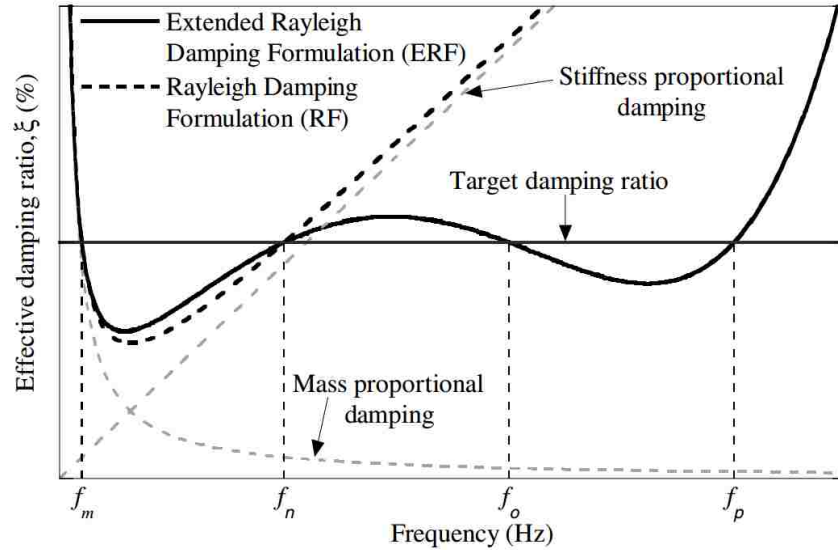
Figure 2.12. Illustration of the frequency dependency of Rayleigh damping and the extended Rayleigh damping formulation as proposed by Park and Hashash, 2004.

Once the two target frequencies are determined then the calibration is performed. Figure 2.13 show an example result of the calibration following the procedure used in this study as follow:

1. Perform the 1D EQL analysis against the soil column of interest using the design input motion.

2. If the result show that the induced shear strain is more than 0.05%, then the input motion need to be scaled to a lower intensity until the shear strain is low enough.

3. Perform 1D NL analysis using full Rayleigh damping scheme with the targeted material damping ratio equal to the published curve or target small strain damping ratio (0.5 – 2%) and target frequencies proposed by Kwok et al (2007).

4. Compare the 1D NL and 1D EQL result and adjust the second target frequency f_n until the 1D NL result give similar result to EQL.

2.3.4   *Shear Strength Correction*

As described earlier, most of 1D NL site response analysis codes utilize an hyperbolic equation to predict the cyclic behavior of soil although it is not always capable to perform well at high strain level. It is due to the overprediction of the shear strength of the soil at that strain level. This could overestimate the shear strength of the soil causing the soil has not failed yet which is completely incorrect. The adjustment of the peak shear strength is required but it might cause inaccuracy of

the stress strain behavior at small strain range. Yee et al (2013) proposed a procedure to address this issue by introducing a new equation to generate hybrid backbone curve.

Basically it allows the stress-strain curve to follow the published target curve until moderate strain level and then it will follow a new path drawn by proposed formula. A new recent procedure to solve this issue is proposed by Professor Youssef Hashash's research group that can be found in Groholski et al (2016). Theoretically, a new cyclic nonlinear soil model based on general quadratic and hyperbolic (GQ/H) equation is used. This research will follow the GQ/H equation for creating the adjusted shear modulus reduction and damping curves and it will be described in the Chapter 3.
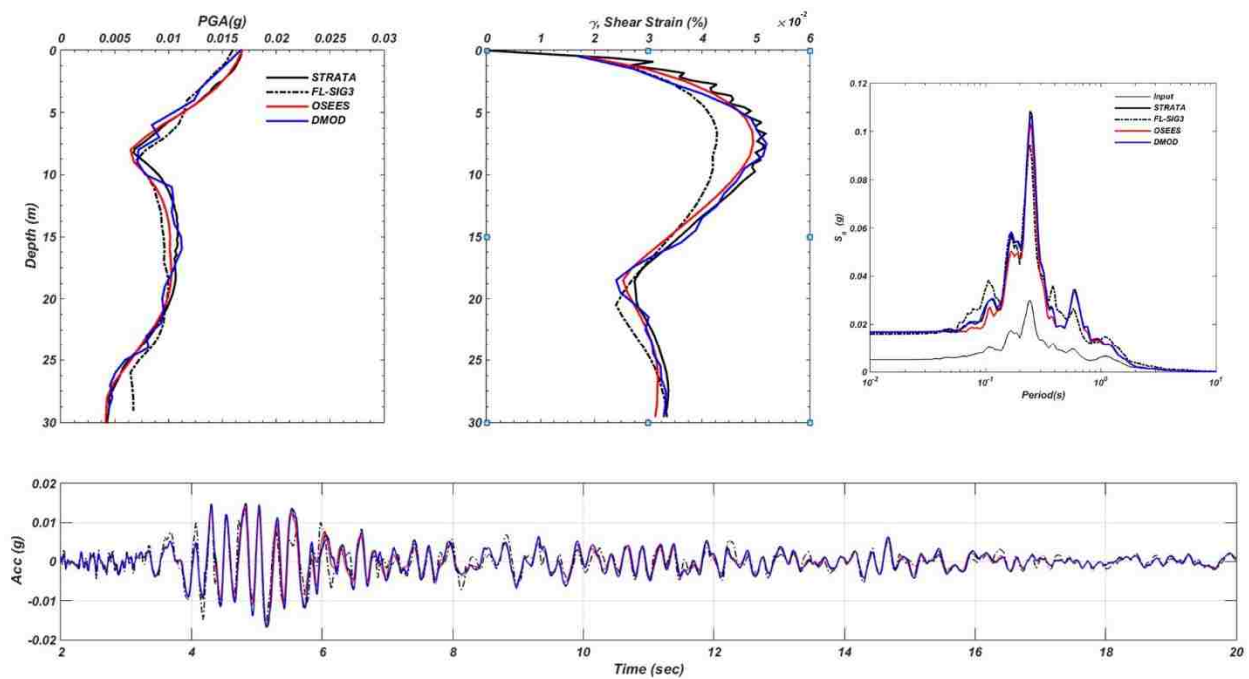
Figure 2.13. Result of 1D NL site response codes compared to EQL analysis after calibration of Rayleigh damping ($\xi_{tar} = 2\%$) and $f_n = 5\,f_m$

Chapter 3. 1-D GROUND RESPONSE ANALYSIS MODELS

This chapter provides a brief summary regarding computer codes used in this research, procedures employed in each code and the analysis used by each model (e.g., nonlinear soil model, hysteretic damping rules and boundary conditions, etc.). The first part of the chapter describes the codes representing the EQL approach and a comparison of the codes. The second part will describe NL 1D site response analysis codes utilized in this research including DEEPSOIL, NERA, FLAC, DMOD2000, OPENSEES and FLIP. Moreover, several important aspects related to the 1D site response analysis modeling are also discussed.

3.1   EQUIVALENT LINEAR (EQL) APPROACH

As described in Chapter One, most of all available EQL computer programs use similar approach and work in frequency domain as originally implemented in SHAKE (Schnabel et al, 1972). Figure 3.1 illustrates an example of the sequence of EQL computation procedure to predict the surface acceleration using STRATA and DEEPSOIL programs for the site profile presented in Figure 3.2. Every calculation uses a set of soil dynamic properties for each soil layer to compute a transfer function. Then, it is repeated using an iterative procedure until it matches the target G/G_{max} and damping curve with a range of error tolerance as illustrated in Figure 2.6. Despite the result at the surface, this procedure is able of computing the response of the soil within the depth of input motion and ground surface. Since all of these programs utilize the same basic computational procedure and concept, only one that will be used for further analysis. The EQL codes considered in this research included DEEPSOIL and STRATA. In their manuals (Hashash 2015, Kottke & Rathje 2008), the comparison between SHAKE and each codes exhibited consistent and similar results.

These two programs will be used to predict the site response underlain by a simple soil profile to understand the variability among all codes. Figure 3.1 presents a comparison of the results of STRATA and DEEPSOIL for a site that has two-layer soil profiles with V_{S30} = 150 m/s and subjected to input motions scaled to 0.05g, 0.20g and 1.00g. The results indicate that they are similar to each other in terms of the profile and time series (Figure 3.2 - 3.3). For this reason,

STRATA program will only be used to represent the EQL approach for further analysis in this research. STRATA has the capability to perform site variability analysis and perform the computation using random vibration theory approach. However, this research only consider the time series approach without considering the site variation. The error tolerance is set to 2.0% with 10 maximum numbers of iteration. The effective strain ratio will be dependent on earthquake magnitude as proposed by Idriss & Sun, 1992.
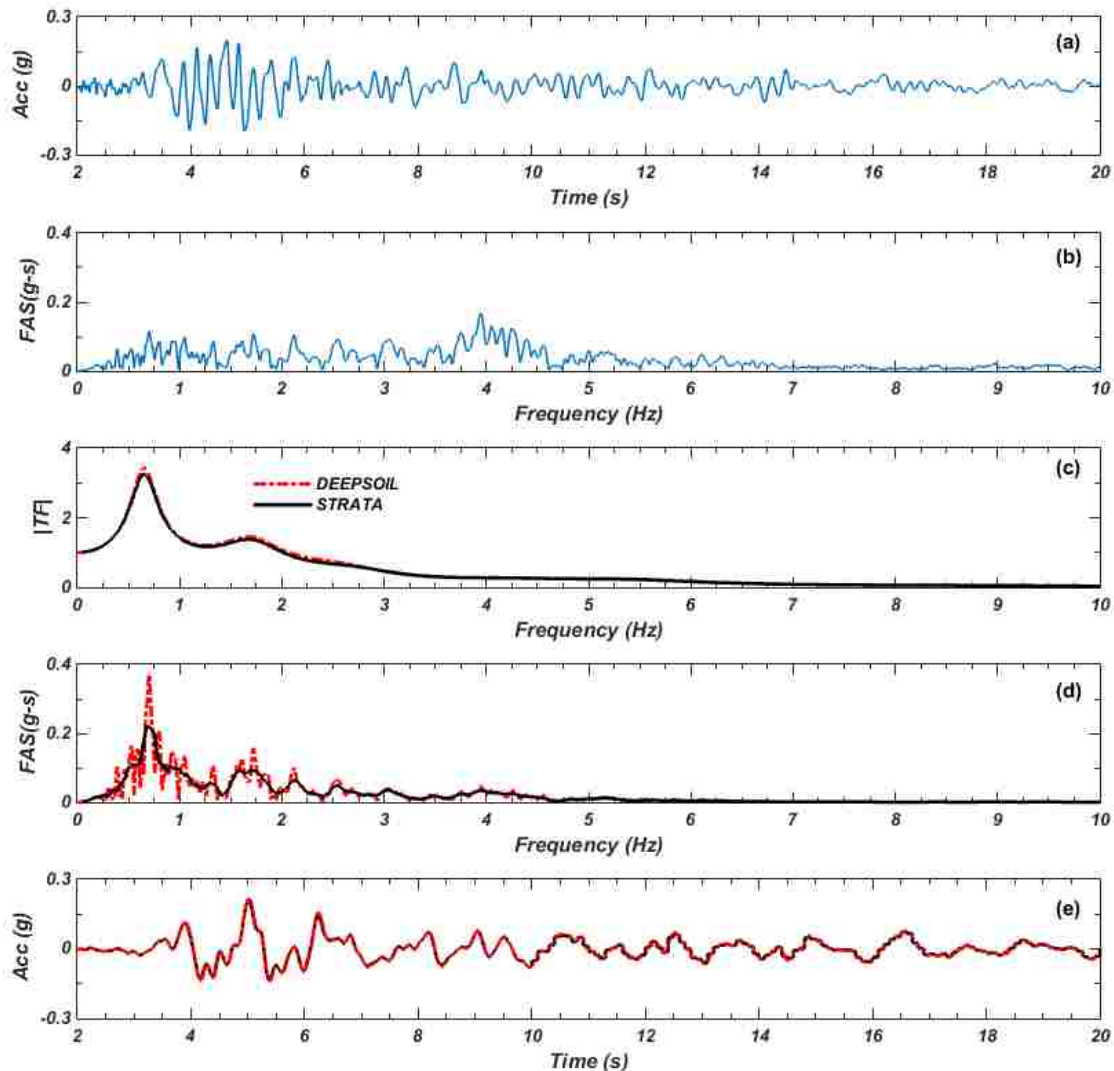
Figure 3.1. The sequence of EQL computational procedure: (a) input acceleration time history, (b) compute the Fourier amplitude spectrum (FAS) by transforming the input motion into frequency domain using FFT, (c) compute the transfer function depends on the properties of the soil profile, (d) compute the surface FAS by multiplying (b) to (c) over the frequency, (e) compute the surface acceleration time series by transforming back the (d) to time domain using inverse FFT. This procedure is repeated using iterative procedure (Figure 2.6). STRATA use smoothed FAS.
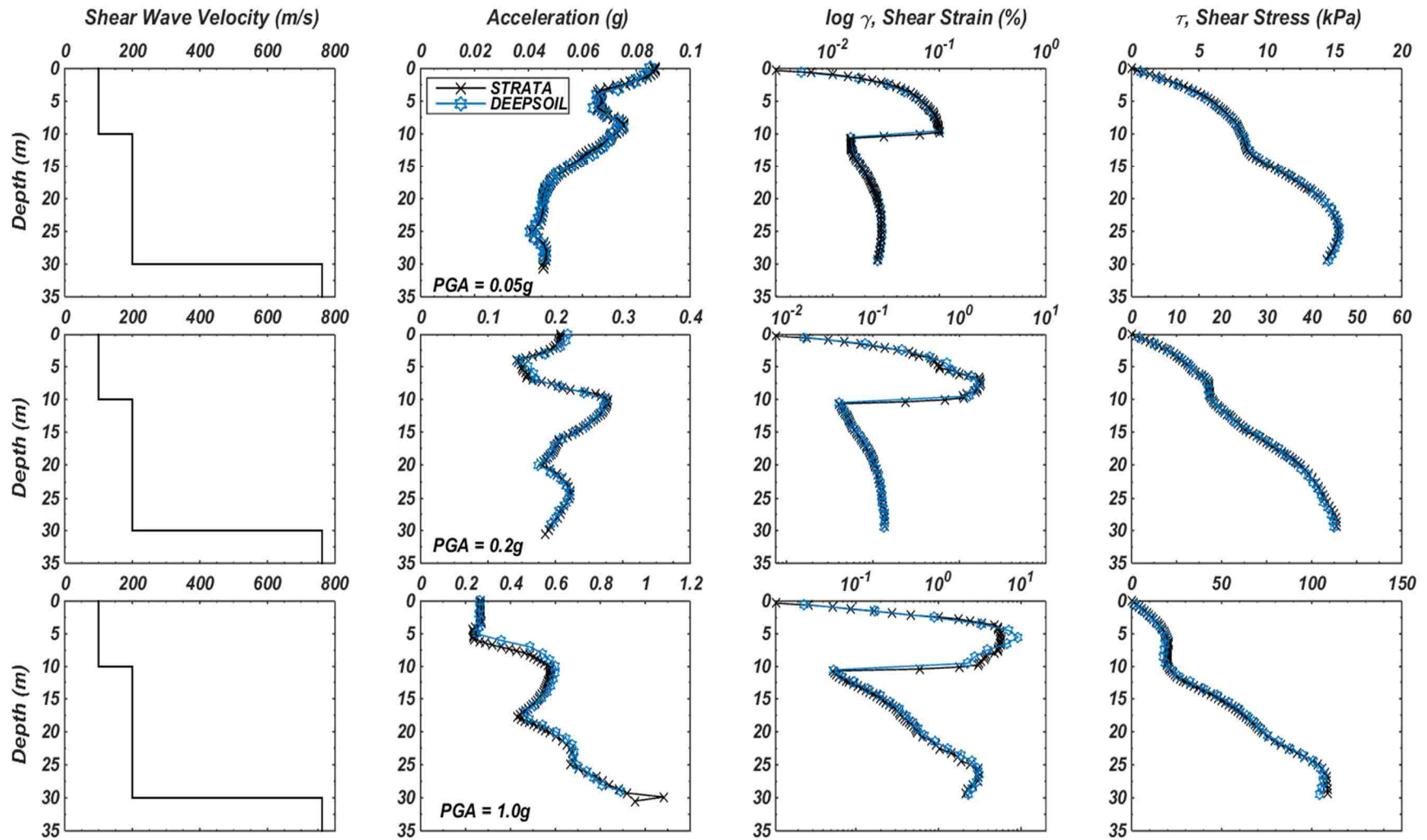
Figure 3.2. Result of EQL analysis predicted by STRATA (Kottke & Rathje, 2008) and DEEPSOIL (Hashash, 2015).
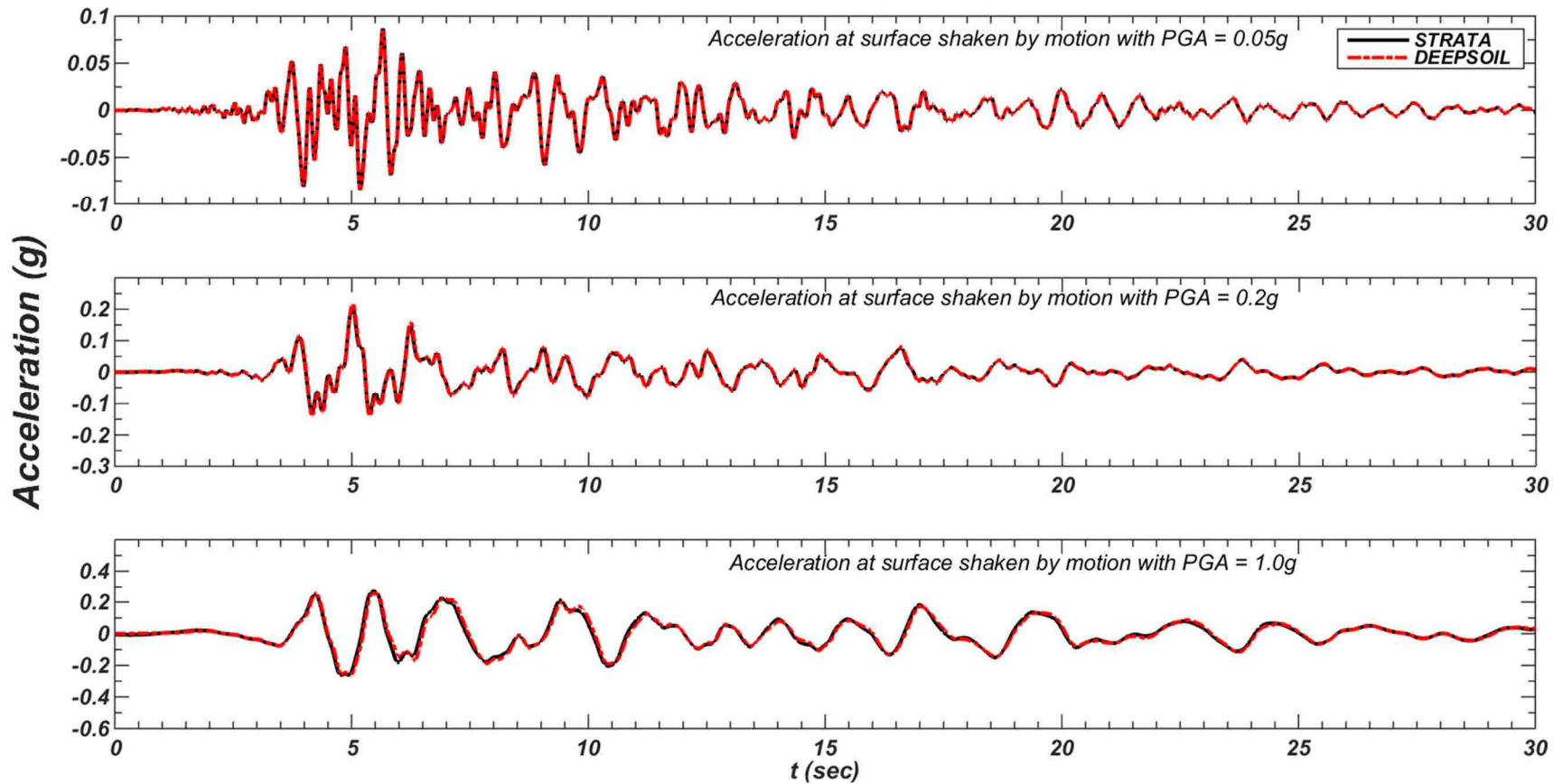
Figure 3.3. Time series at the surface predicted by each codes for site shown in Figure 3.1 shaken by a motion that is scaled to 0.05g, 0.2g and 1.0g. The result show identical prediction between each other.

3.2   NON LINEAR (NL) APPROACH

As illustrated in Figure 2.7, the prediction of responses by EQL and NL approaches will be similar at relatively small strain, or low nonlinearity, levels. The two predictions usually predict relatively similar soil stiffness and near zero damping ratio. However, the behavior of soil at higher shear stress levels is truly nonlinear and cannot be captured accurately using the EQL approach. For this reason, a better nonlinear soil model is necessary to incorporate soil non-linearity. This section will briefly summarize the nonlinear soil models used in this research with the computer programs listed in Table 3.1. It will review several important aspects that are necessary to be captured during the implementation of a nonlinear soil model as explained in Chapter One. The variability analysis of each codes in seismic site response prediction will be presented in the following chapters.

Table 3-1. Nonlinear site response analysis codes considered in this research

Codes	Soil Model	Mass Representation	Reference
D-MOD2000	Modified Kondner & Zelasko (MKZ)	Lumped Mass (1D)	Matasovic & Vucetic (1993)
DEEPSOIL	Extended MKZ; General Quadratic/Hyperbolic	Lumped Mass (1D)	Hashash and Park (2001); Groholski et al (2016); Hashash et al (2015).
NERA	Iwan (1967) & Mroz (1967)	Lumped Mass (1D)	Iwan (1967), Mroz (1967), Bardet & Tobita (2001)
FLAC	Elastic with Sigmoidal-3 hysteretic damping	Lumped Grid Point Mass (2D)	Itasca (2011)
OPENSEES	Pressure Independent Multi Yield Surface (PIMY)	Distributed Mass (2D)	Yang (2000)
FLIP	Multi-Spring Model	Distributed Mass (2D)	FLIP Consortium (2011)

3.2.1   *D-MOD2000*

One of the very first 1D NL site response analysis code is DESRA that was originaly written by Michael K.W. Lee and W.D. Finn at the University of British Columbia in 1975-1978. DESRA

uses the nonlinear soil model proposed by Kondner & Zelasko (1963) and was later modified by Matasovic & Vucetic (1993) to be implemented in D-MOD code. D-MOD2000 is an interactive Windows version of D-MOD which combined the dynamic response model as implemented in DESRA with the modified Kondner & Zelasko (MKZ) stress-strain model (Matasovic & Ordonez, 2011). D-MOD2000 performs an NL site response analysis by solving the full dynamic equation of motion (Equation 2.1) in the time domain using Newmark β time step integration scheme as usually adopted in structural dynamic problems (Chopra, 2012, Towhata, 2008). The soil column is idealized as a discrete lumped-mass system as illustrated in Figure 2.8a during the construction of the mass matrix [M]. The stiffness matrix [K] is represented by nonlinear springs to capture the soil stiffness and hysteretic behavior. The damping matrix [C] is constructed through the Rayleigh damping formulation to capture the small strain damping behavior. D-MOD2000 can also perform effective stress analyses but they are beyond the scope of this thesis. D-MOD2000 implemented the pore-water pressure model originally developed by Dobry et al. (1985) and modified by Vucetic and Dobry (1986).

Nonlinear Soil Model

The idea of the nonlinear soil model is to construct the stress-strain curve using a nonlinear function to fit the target G/G$_{max}$ (backbone) curve. One of the very first nonlinear soil models was the hyperbolic model by Kondner & Zelasko (1963), abbreviated as the KZ model, that requires two constant parameters (i.e., small strain shear modulus, G_{m0} and peak strength of the soil, τ_{m0}). Matasovic & Vucetic (1993) revealed that the KZ model was often incapable to describe the stress-strain behavior accurately, thus by adding only two curve-fitting constants (i.e., β and *s*) the accuracy of the prediction could be improved. The addition of these two parameters into the original KZ model then is termed as Modified KZ nonlinear soil model (MKZ) and the normalized form is given by:

$$\tau^* = f^*(\gamma) = \frac{G_{m0}^* \gamma}{1 + \beta \left(\frac{G_{m0}^*}{\tau_{m0}^*}\gamma\right)^s} \tag{3.2}$$

where $G_{m0}^* = G_{m0}/\sigma_{vc}'$, $\tau_{m0}^* = \tau_{m0}/\sigma_{vc}'$, σ_{vc}' = initial vertical effective stress.

The original KZ hyperbolic model corresponds to the $\beta = s = 1.0$ indicating that these two parameters adjust the position of the curve along the y-axis and control the curvature shape of the backbone curve of the MKZ model (Figure 3.4a). Matasovic & Vucetic (1993) validate the model by fitting the curve to the experimental Norwegian Geotechnical Institute (NGI) direct simple shear (DSS) apparatus data of Santa Monica Beach (SMB) sand as shown in Figure 3.4b.
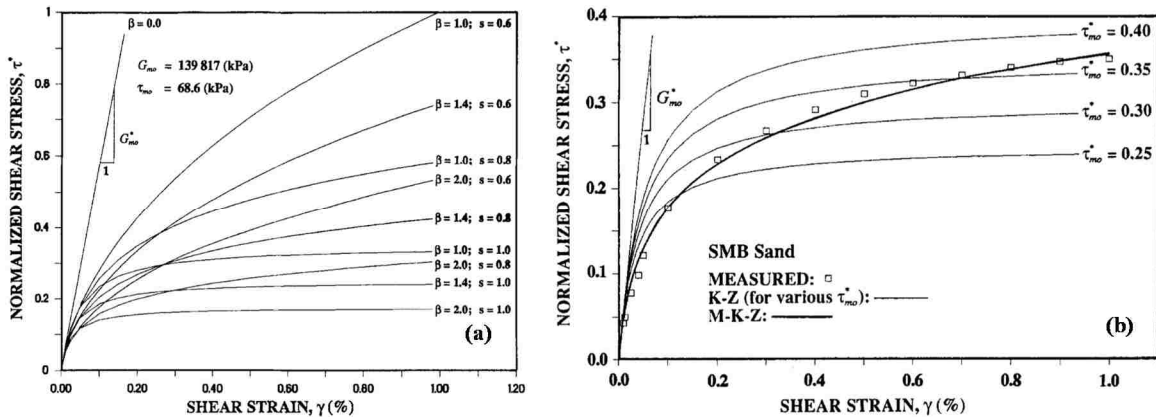
Figure 3.4. (a) Effect of values of β and s on shape of stress-strain curve predicted by MKZ model, (b) Comparison between KZ and MKZ model to predict the DSS test data of SMB sand (Matasovic & Vucetic, 1993)

One of the objectives of this thesis is to evaluate the nonlinear soil model to predict the behavior of soil at shear stress levels corresponding to the peak shear strength of the soil. From Figure 3.4, it could be concluded that when the value of $s = 1.0$ (KZ model), the shape of stress-strain curve will be asymptotic to a value (peak shear strength of the soil) but the accuracy of the stress-strain relationship at lower strain levels can decrease. On the other hand, if the MKZ model is used to fit the lower strain level the $s < 1.0$, the shape of the model can exceed the shear strength of the soil since it is the nature of the MKZ model's equation. This circumstance is shown in Figure 3.5 for a case taken from Turkey Flat vertical array data that will be explained later in Chapter Five.

In order to fit the target Turkey Flat backbone curve based on data from Real (1988), the β and s values have to be adjusted. When this model is evaluated for a high shear strain level ($> 5\%$), the nature of the equation will construct the stress-strain relationship that exceeds the peak shear strength of the soil. However, the strains induced in the seismic site response problem is less than 1-3% (Stewart, 2008), and experimentally, the MKZ model is capable to fit the measured data with

relatively good accuracy. For these reasons, it is still considered to be used in practice even though careful analysis is required for a site subjected to high intensity motion where the peak shear strength of the soil will be the controlling properties.
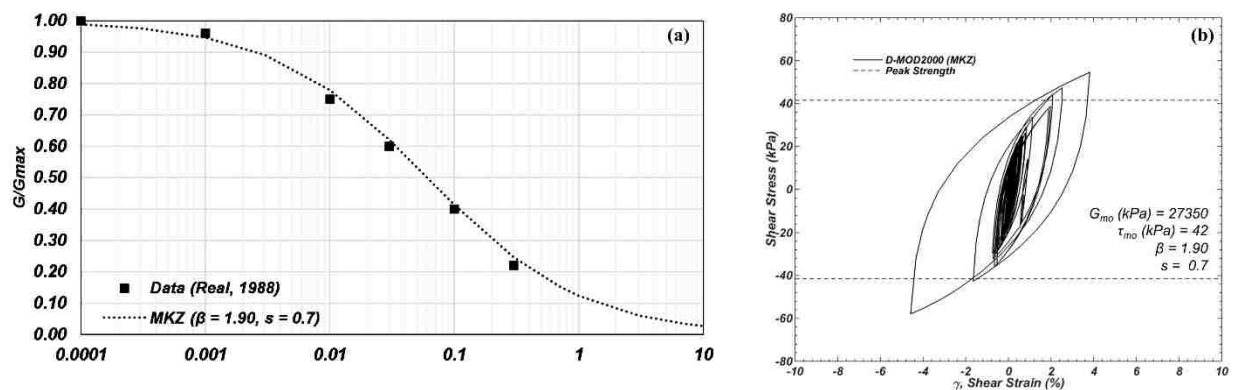
Figure 3.5. (a) The backbone curve predicted by MKZ model to fit the measured data from Turkey Flat vertical array data. (b) Example of cyclic stress-strain curve predicted by MKZ soil model and extended Masing rules (Vucetic, 1990). The form of MKZ's equation does not allow the predicted stress-strain curve to fit the peak shear strength of the soil at high strain level.

Damping Model

Two main types of damping are incorporated in NL site response analyses. The first one is the viscous damping matrix (small strain damping) that is implemented during the construction of [C] matrix. The second other damping is termed as hysteretic material damping that is constructed together with the stress-strain relationship and hysteretic behavior rules (e.g., Masing, 1926; Vucetic, 1990). Hysteretic damping is obtained automatically by updating the stiffness matrices [K] for each time step along earthquake duration.

D-MOD2000 constructs the viscous damping matrix [C] using the full Rayleigh damping formulation (Rayleigh & Lindsay, 1945) that is proportional to the mass and stiffness matrix. Viscous damping in a 1D soil column is required to prevent near zero damping for small strains. For hysteretic damping, Masing rules (Masing 1926) and extended Masing rules (Vucetic, 1990) are used to describe hysteretic behavior. The four rules of Masing (1-2) and extended Masing rules (1-4) is illustrated in Figure 3.6 and Figure 3.5b show an example of its application:

1. The original backbone curve is the initial path for the stress-strain relationship.
2. The unloading & reloading behavior follow the shape of original backbone curve but it is enlarged by a factor of two.

3. If the unloading or loading exceeds the maximum past strain and intersects the backbone curve, it will follow the backbone curve until the next reversal point.

4. If an unloading or loading curve crosses an unloading or loading curve from a previous cycle, the stress-strain curve follows the previous cycle.

Masing rules are known to overestimate the damping at large strains even though it is commonly used in NL site response analysis. Figure 3.7 shows that the application of Masing rules tend to overpredict the damping ratio that might cause more seismic energy to be absorbed. It indicates less energy to be propagated causing lower intensity motion predicted at the ground surface.
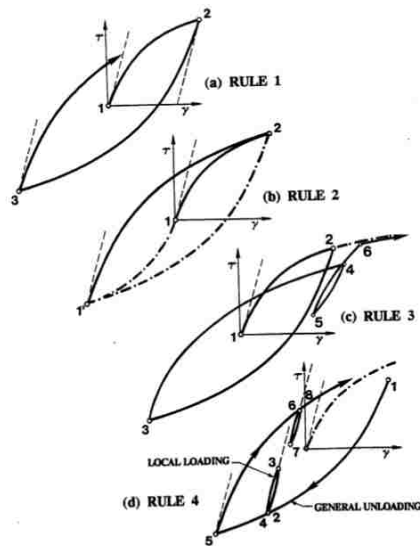
Figure 3.6. Masing, 1926 rules (1–2) and extended Masing rules proposed by Vucetic, 1990 (1-4)
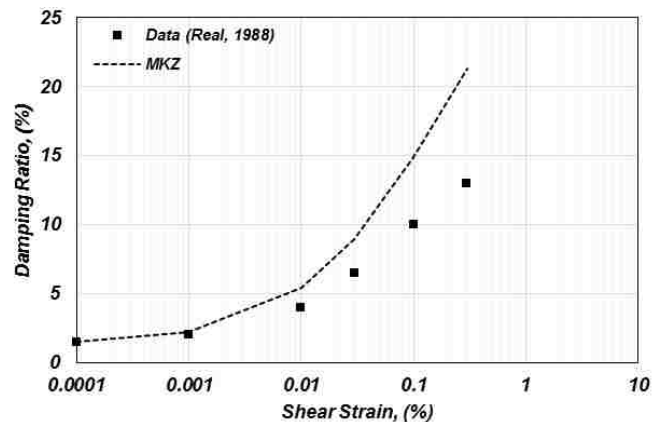
Figure 3.7. Comparison of damping ratio predicted by MKZ soil model in this study from and Turkey Flat data measured in the laboratory by Real, 1988.

3.2.2 *DEEPSOIL*

DEEPSOIL was originally developed at the University of Illinois at Urbana-Champaign to predict the 1D seismic site response of a deep soil deposit (more than 100 m) as encountered in Mississippi Embayment (Hashash & Park, 2001). It extends the basic MKZ model by adding the confining pressure effect on dynamic behavior of soil during cyclic loading. Recently, DEEPSOIL is developed to be a 1D site response program with friendly user interface that is capable to perform EQL and NL approach at the same time. It solves the full dynamic equation using similar procedure as implemented in DESRA-2 and D-MOD2000. The version considered in this research is V6.1 (Hashash et al, 2015) where two available models (i.e., Extended MKZ and General/Quadratic Hyperbolic model) are used in this research and explained in this section.

Nonlinear Soil Model

The MKZ soil model has been used extensively to estimate several well-documented case histories for soil profiles up to 88 m in depth (Hashash & Park, 2001). For soil deposit at deeper location, several studies recognize that the effect of confining pressure on dynamic properties of soil is significant (Laird and Stokoe, 1993; Stokoe et al, 1999; Darendeli, 2001). Hashash & Park (2001) extended the MKZ model to capture the effect of confining pressure by adding several curve fitting parameters to the original equation (Equation 3.2). The extended equation of MKZ model in DEEPSOIL is described by the following equation:

$$\tau^* = f^*(\gamma) = \frac{G_{m0}^* \gamma}{1 + \beta \left(\frac{G_{m0}^*}{\tau_{m0}^*} \gamma \right)^s} = \frac{G_{m0}^* \gamma}{1 + \beta \left(\frac{\gamma}{\gamma_{ref}} \right)^s} \tag{3.3}$$

The MKZ model used the reference strain, γ_{ref} based upon Hardin and Drnevich, 1972 whereas DEEPSOIL modifiy the γ_{ref} to be dependent on confining stress as given by:

$$\gamma_{ref} = a \left(\frac{\sigma'_v}{\sigma_{ref}} \right)^b \tag{3.4}$$

Laird and Stokoe (1993) data also show that the confining stress will influence the small strain soil damping ratio. Besides modifying the backbone curve, Hashash & Park, 2001 also introduce a new equation to estimate the small strain damping ratio as given by:

$$\xi = \frac{c}{(\sigma_v')^d} \tag{3.5}$$

The value of *a, b, c* and *d* are the curve fitting parameters that is adjusted to fit a target backbone curve and σ_{ref} is a reference confining pressure of 0.18 MPa. Figure 3.8 shows the accuracy of Eq. 3.3 and Eq. 3.4 fitted to the laboratory data from a wide range of confining stresses. At shallow depth, the shape of this model will be similar to MKZ model. This research will utilize the extended MKZ model and it will be termed as DS-MKZ.
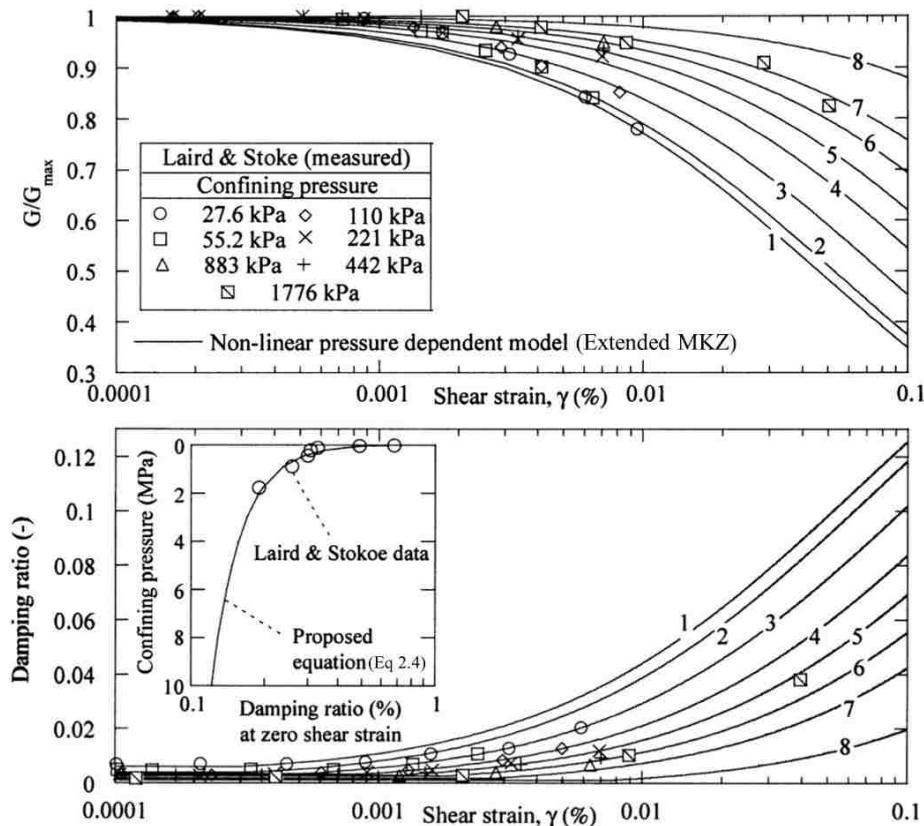
Figure 3.8 Influence of confining pressure on G/Gmax and Damping ratio curve from data of Laird and Stokoe (1993) compared to the prediction of Extended MKZ model to fit the laboratory data (after Hashash & Park, 2001).

The recently developed GQ/H model is the latest nonlinear soil model implemented in DEEPSOIL. This model allows the peak shear strength of the soil to be defined while providing flexibility to match the small strain behavior (Groholski et al, 2016). Theoretically, this model will give a better prediction of the cyclic behavior at high strain level when the shear stress level approaching the peak shear strength of the soil. In this research, this model will be termed as DS-GQ/H soil model and the equation to construct the backbone curve is given by:

$$\frac{\tau}{\tau_{max}} = \frac{2\left(\gamma/\gamma_{ref}\right)}{1+\left(\gamma/\gamma_{ref}\right)+\sqrt{\left\{1+\left(\gamma/\gamma_{ref}\right)\right\}^2-4\theta_\tau\left(\gamma/\gamma_{ref}\right)}} \tag{3.6}$$

where τ is shear stress, τ_{max} is the peak shear strength of the soil, γ is shear strain, γ_{ref} is the reference shear strain based on the Kondner & Zelasko (1963) and θ_τ is the curve fitting parameter. Similar to the Extended MKZ model, the DEEPSOIL program provides the user with the curve fitting tools to make the fitting process easier. The equation of curve fitting parameter for this model is given by:

$$\theta_\tau = \theta_1 + \frac{\theta_2 \cdot \left(\gamma/\gamma_{ref}\right)}{\theta_3 + \left(\gamma/\gamma_{ref}\right)} \leq 1 \tag{3.7}$$

The capability of this model to match the peak shear strength of the soil while providing the flexibility to match the small strain behavior is illustrated in Figure 3.9. It shows that if MKZ is forced to match the peak shear strength of the soil (by adjusting β and *s* value), the MKZ will predict the soil behavior with less nonlinearity level. The degradation of shear modulus will be greater that predict stiffer behavior at small to moderate shear strain level. From this standpoint, the DS-GQ/H is assumed to be more reliable model due to its flexibility to perform 1D site response analysis at low to high strain level. The more advanced curve fitting parameters (Equation 3.6) allows the peak strength to be defined but maintain the flexibility to match the backbone curve at small strain level.

Damping Model

The construction of the viscous damping matrix, [C] in DEEPSOIL is available either using Rayleigh damping (e.g., simplified, full and extended [Park & Hashash, 2004]) or frequency inde-
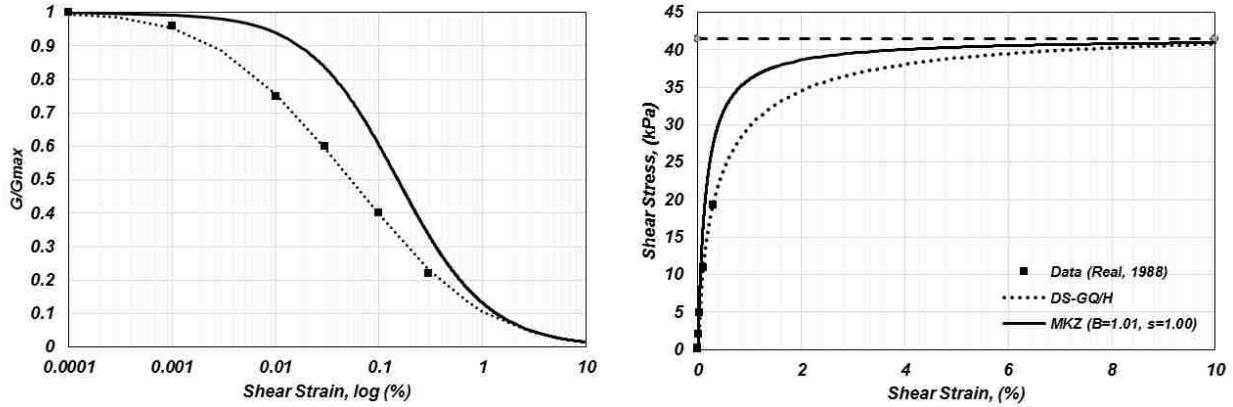
Figure 3.9 The shear modulus reduction curve (left curve) predicted by DS-GQ and MKZ nonlinear soil model to fit the measured data from Turkey Flat vertical array data. The right curve show the backbone curve constructed using DS-GQ/H and MKZ model. The MKZ model is adjusted to be asymptotic to peak shear strength of soil.

pendent formulation (Phillips & Hashash, 2009). The extended Rayleigh damping uses four target modes that might increase the accuracy even though it is still a frequency dependent formulation. The selection of four target frequencies might cause confusion in practice and it still over or under predicts the damping ratio at frequencies different from the target modes. Phillips & Hashash (2009) proposed a new frequency independent formulation to construct the [C] matrix and their study show that this new formulation predicts better results and it does not require the selection of target frequencies. For this reason, the frequency independent damping will be implemented for this research.

Figures 2.11, 3.7, and later in 3.10 illustrate the implementation of original or extended Masing rules in hyperbolic model will result greater computed damping ratio compared to what is measured in the laboratory, particularly for medium to high strain levels (e.g., Phillips & Hashash, 2009; Arefi et al, 2013). It leads to an underestimation of the propagated seismic energy towards ground surface. One of the main feature of DEEPSOIL is the option to use "non Masing" rules to construct the stress-strain curve for unloading and reloading stage (Hysteretic damping). Phillips & Hashash (2009) attempts to solve this issue by multiplying the damping ratio computed based on Masing rules to a damping reduction factor $F(\gamma_m)$ that is given by:

$$F(\gamma_m) = p_1 - p_2 \left(1 - \frac{G_{\gamma_m}}{G_0}\right)^{p_3}$$

(3.8)

where p_1, p_2 and p_3 are determined iteratively until the best possible fit with the target damping curve is obtained. The example of implementation of this non-Masing rules together with the DS-MKZ and DS-GQ/H nonlinear soil model are indicated in Figure 3.10. The areas of the hysteresis loops predicted by these model are smaller than the one predicted by D-MOD2000 shown in Figure 3.5.

Basically, this set of procedure calibrates the modulus reduction and damping ratio curve at the same time. This is the reason why it is termed as MRDF (Modulus Reduction & Damping with reduction Factor) procedure that is performed by following these steps:

1. Determine the target G/G_{max} curve from laboratory test or published curve.
2. Fit the target G/G_{max} curve by adjusting the curve fitting parameters (θ_τ for DS-GQ/H model and a,b,c,d for DS-MKZ model respectively)
3. Compute the corresponding damping ratio (ξ_{masing})following the Masing rules based on backbone curve in procedure No.2.
4. Fit the target damping curve from laboratory test or published curve, by multiplying the damping ratio from procedure No.3 with the reduction factor, $\xi_{MRDF} = F(\gamma_m) \cdot \xi_{masing}$.

Phillips & Hashash (2009) presents the accuracy of the fitting quality of MRDF procedure to 50 target damping ratio curves that give a relatively good result with $R^2 > 0.96$. For this reason the MRDF procedure will be used in this research to construct the hysteretic damping in DEEPSOOIL.
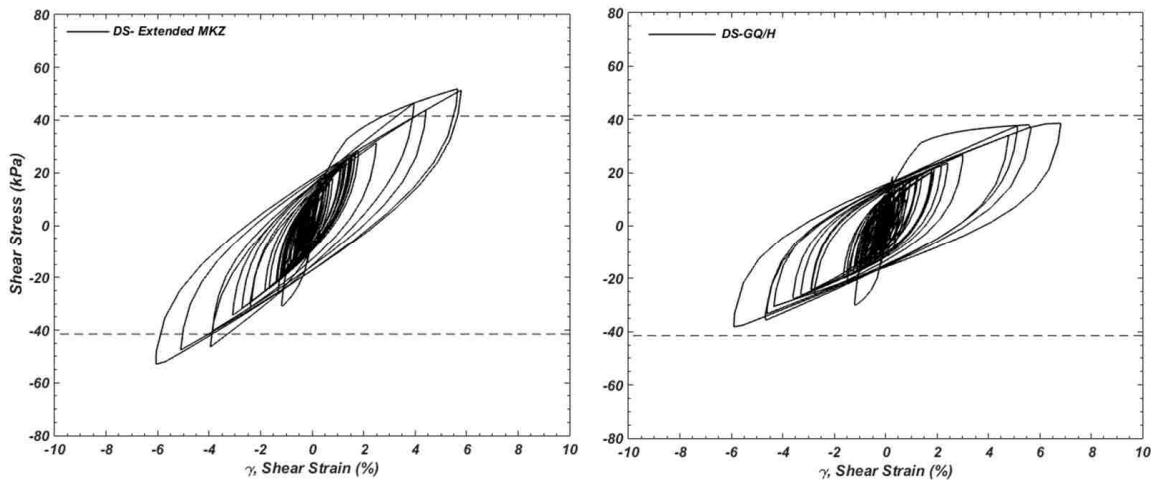
Figure 3.10. The stress-strain behavior based on DS-MKZ and DS-GQ/H nonlinear soil model using the "non Masing" MRDF procedure to construct the unloading and reloading stage at identical depth, site profile, input motion and other aspects. The DS-GQ/H allow peak strength to be defined whereas DS-MKZ exceeds the peak strength at high strain level.

3.2.3 *NERA*

NERA (Bardet & Tobita, 2001) is a one-dimensional NL site response analysis computer program that employs a soil constitutive relation to construct the stress-strain curve instead of using a curve fitting parameters equation to match the target backbone curve. It is developed based on the constitutive relation proposed by Iwan (1967) and Mroz (1967) and referred as IM model in NERA. The governing equation to be solved to compute the response of soil column in NERA is given by Equation 2.2 which is the one dimensional dynamic stress wave propagation problem (Kramer, 1996; Bardet & Tobita, 2001). It is solved by using forward finite difference approach based on the Newmark algorithm which is the central difference method. NERA employs the procedure similar to the Joyner & Chen (1975) in terms of the soil constitutive model and the boundary condition that allows the reflected energy to be radiated back into the underlying bedrock with finite rigidity.

Soil Constitutive Model

The application of Iwan (1967) soil model in nonlinear site response analysis was first proposed by Joyner & Chen (1975). This model is composed of linear springs having stiffnesses k_i and Coulomb friction elements having sliding resistances R_i, arranged as shown in Figure 3.11. At first, the friction element remain locked until the stress exceeds the sliding resistance R_1 with spring stiffness k_1. Once the stress yield the first resistance of friction element, R_1, the system will have stiffness influenced by k_1 and k_2 until the next sliding resistance R_2 is reached. This is continued until the last sliding resistance, R_n which is set to zero is reached. At this stress level, the shear stress working on the system has reached the peak strength of the soil and all springs is active.
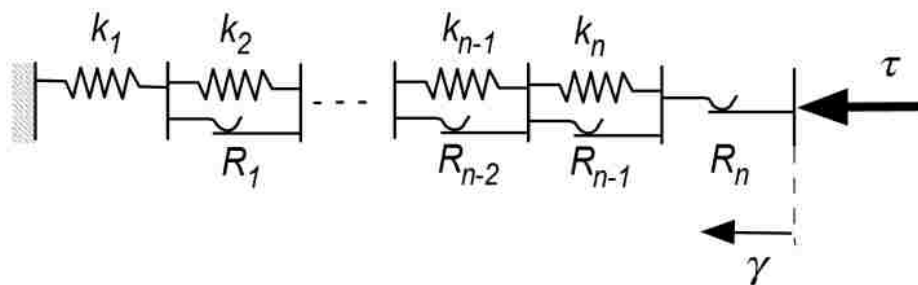
Figure 3.11. The rheological model of IM model implemented in NERA (Bardet & Tobita, 2001)

The stiffness of each stress level will correspond to the tangential modulus associated to the number of spring and friction element used in the analysis. Figure 3.12 illustrate a generated stress-strain curve by the IM model using two elements (i.e., n = 2) and the proportion of spring stiffness formulation for each stage of R_i. With greater numbers of spring and friction element, this model is capable of tracing nearly any shape of stress-strain curve and hysteretic loading.

Joyner & Chen, 1975 recommended that 50 elements should be sufficient for 1D NL site response analysis problems. They had used as many as 100 elements without significant computation time at that year. In this circumstance, the peak strength issue encountered in the MKZ soil model will not exist because the flexibility of constitutive model is capable to track the stress-strain curve until it reaches the peak shear strength of soil. An example of full stress-strain curve generated using this model with the Masing rules is presented in Figure 3.13.

$$H = \begin{cases} H_1 = k_1 & \text{if } 0 \leq \tau < R_1 \\ H_2 = \left(k_1^{-1} + k_2^{-1}\right)^{-1} & \text{if } R_1 \leq \tau < R_2 \\ \vdots & \\ H_{n-1} = \left(k_1^{-1} + k_2^{-1} + ... + k_{n-1}^{-1}\right)^{-1} & \text{if } R_{n-2} \leq \tau < R_{n-1} \\ H_n = \left(k_1^{-1} + k_2^{-1} + ... + k_{n-1}^{-1} + k_n^{-1}\right)^{-1} & \text{if } R_{n-1} \leq \tau < R_n \\ 0 & \text{if } \tau = R_n \end{cases}$$
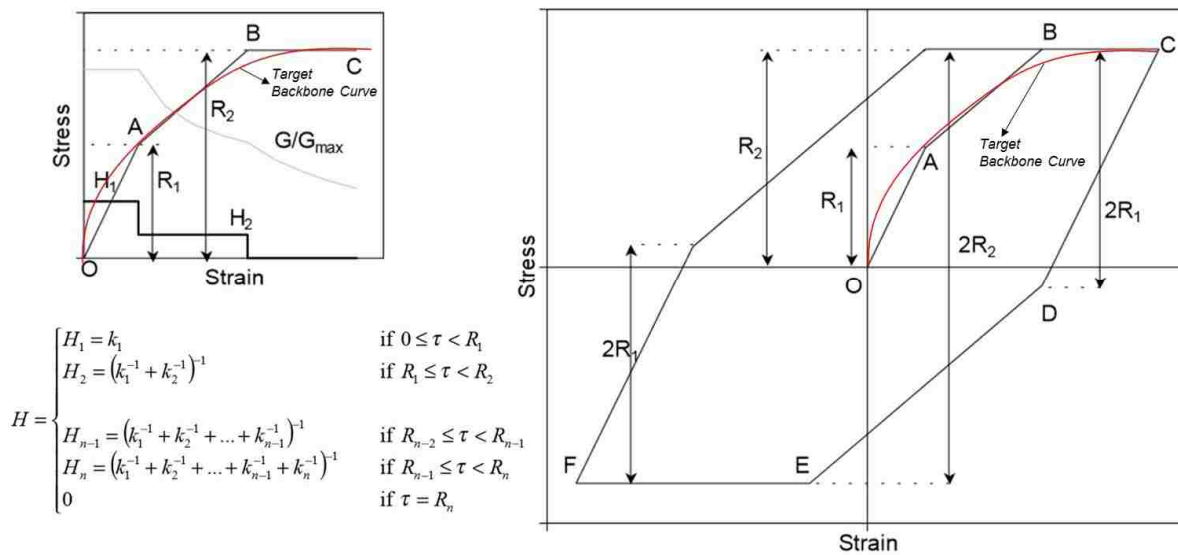
Figure 3.12. The IM model for using two spring and frictional element to match a target backbone curve in red line. (Modified from Bardet & Tobita, 2001)

Damping Model

During the computation, NERA does not require any viscous damping matrix to solve the governing equation, which means that no small strain damping is employed. IM model cause zero damping at very small strain since the stress-strain curve is only represented by a straight line (zero nonlinearity) for small elements number. Figure 3.14 show an example that NERA calculates the

zero material damping ratio in the small strain range. For some cases, it might raise an issue such as higher prediction of intensity, however recent study by Kaklamanos et al (2015) presents that the exclusion of viscous damping can mitigate the issue of overdamping at large strains. For hysteretic damping, the right curve in Figure 3.12 show an example how IM model generate the unloading and reloading curve based on Masing (1926) rules that is incorporated in NERA.
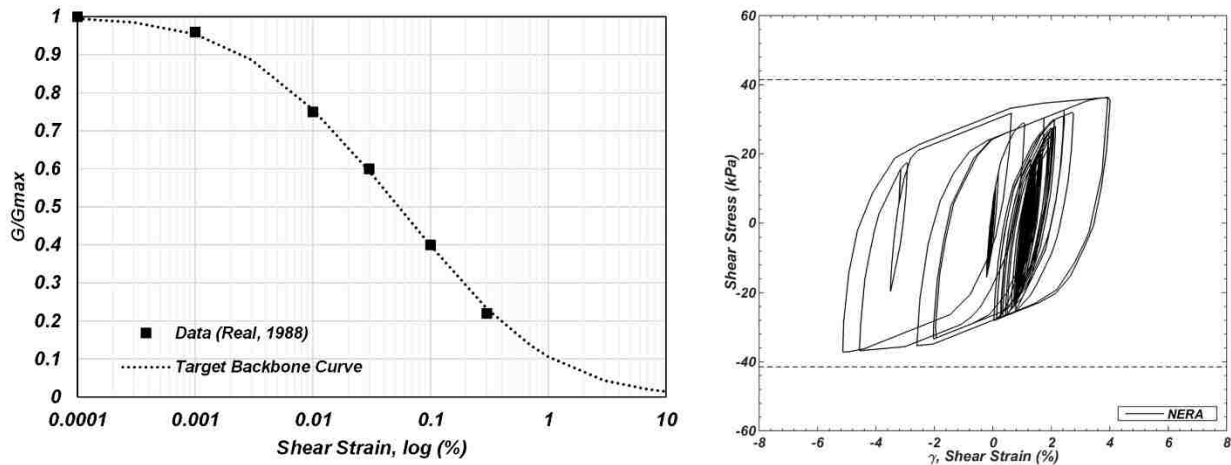
Figure 3.13. The IM model for using two spring and frictional element to match a target backbone curve in red line. (Modified from Bardet & Tobita, 2001)
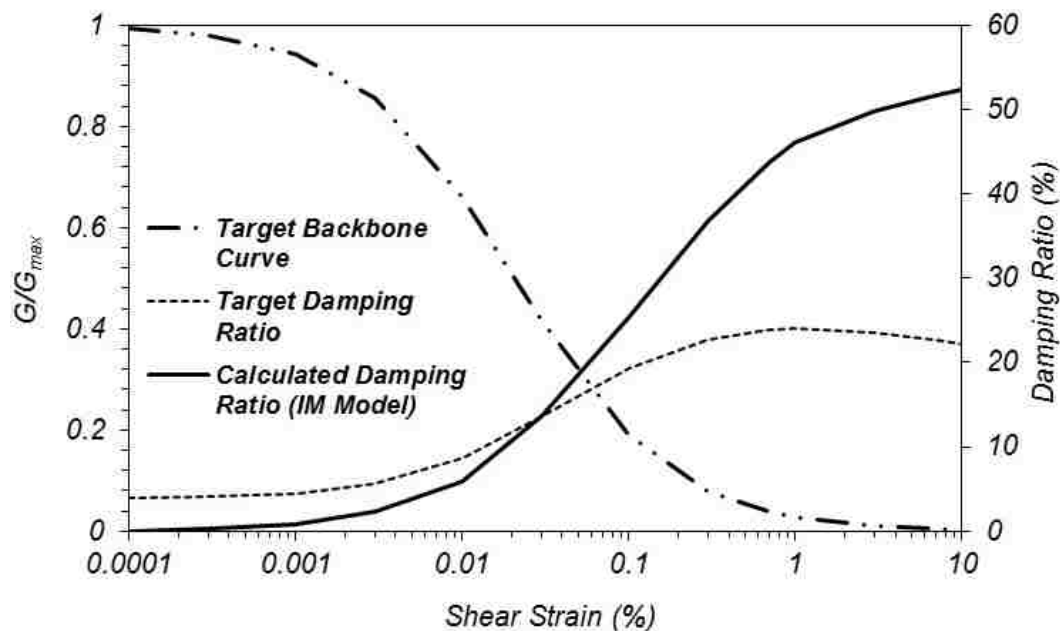
Figure 3.14. The damping ratio computed by IM model following a published curve / laboratory data of target backbone curve indicating zero damping ratio at very small strain.

3.2.4   *FLAC*

FLAC (Fast Langrangian Analysis of Continua) is a two-dimensional explicit finite difference (FD) program that is commonly used to perform static and dynamic analyses of geomechanics problems. In this research, a 1D soil column will be modeled in two-dimensional plane-strain represented by a stack of rectangular soil element in vertical direction that has one unit length in horizontal direction. FLAC is developed to solve the full equations of motion using lumped grid point masses derived from the real density of surrounding zones (Itasca, 2011). The computational sequence using FD approach is similar to the time integration method. At first, using explicit FD approach, the velocity and displacement at all element nodes are computed by solving the equation of motion and computing the strain from the nodes displacement. Then, using the constitutive relation, the corresponding stiffness is updated for the next time step and the whole process is repeated over the earthquake duration. The critical timestep using in FLAC depends on the area of the rectangular zone, length of its diagonal and speed of longitudinal wave (Itasca, 2011). The full explanation about FLAC is beyond of the scope of this thesis, but the general overview regarding the procedure to model 1D NL site response analysis in FLAC (i.e., boundary condition, height of element, specification of input motion, nonlinear soil and damping model) used in this research will be briefly discussed. The FLAC version used in this research is FLAC 2D 7.0 (Itasca, 2011).

Boundary Condition & Input Motion

The modeling of the side and bottom boundary condition play an important role within 1D seismic site response analysis framework using FLAC 2D. The boundary condition for right and left side of the column is straightforward as it will be set to move freely in x-direction (horizontal) by applying the fixity condition only upon the y-direction (vertical). In FLAC analyses, seismic input must be applied at the base of the soil column. The bottom boundary condition depends on the type of the base modeled in the analysis includes "rigid base" or "elastic base".

When analyzing 1D soil column with significant difference of impedance contrast (e.g., very soft profile underlain by very rigid bedrock), the downward propagating motion will be reflected back upward to the soil deposit. A "rigid base" is an appropriate type and an acceleration-time histories input motion should be specified at the base of FLAC mesh (Mejia & Dawson, 2006). From the type of input motion standpoint, when "within motion" through deconvolution procedure

(Figure 3.15) or a control motion recorded at depth within the vertical array site is used, the input motion should be used without any modification in conjunction with a "rigid base" (Kwok et al, 2007) as explained in the section 2.3.

For cases where some portion of downward propagating motion is absorbed by underlying bedrock with finite rigidity, an "elastic base" is an appropriate type to be used. Lysmer & Kuhlemeyer (1963) dashpot is a common way to model this boundary problem and it is employed in FLAC analyses. The product of velocity time history and the dashpot coefficient will be a shear stress time history as the seismic input motion (Itasca, 2011). It specifies the upward propagating motion into the soil column, but the actual response at the base will be the superposition of the reflected and transmitted motion (Mejia & Dawson, 2006). Figure 3.15 shows an illustration of how to model boundary condition at the bottom of soil column through a deconvolution procedure as usually performed using SHAKE in the practice of 1D seismic site response analysis. The selection of type of base in FLAC is an important issue that could lead to erros in the predicted surface motion (Mejia & Dawson, 2006).
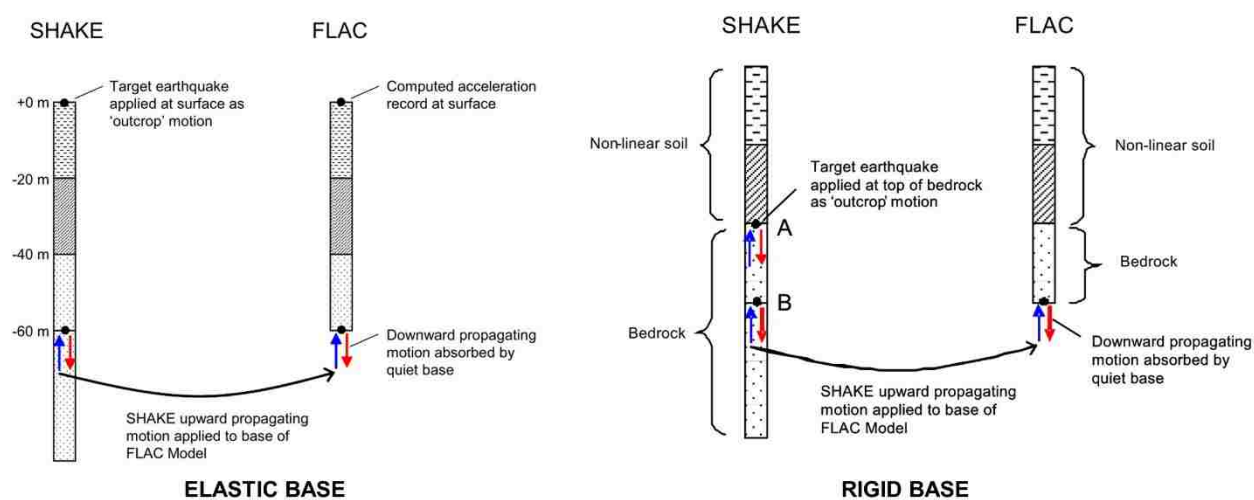
Figure 3.15. Deconvolution procedure for compliant and rigid halfspace base for FLAC analysis (after Mejia and Dawson, 2006)

Height of Element

In order to prevent numerical distortion in performing the wave propagation analysis, the height of elements in the 1D soil column should be adjusted. Kuhlemeyer and Lysmer (1973) reveal that it should be smaller than approximately one-tenth to one-eight of the wavelength

associated with the highest frequency component of interest. For example, if the frequency of a seismic wave is 4 Hz and it propagates through a soil column with shear wave velocity of 100 m/s, the wavelength will be 25 m. Hence, the height of the element should be smaller than 2.5 m.

Nonlinear Soil Model

Similar to nonlinear soil models used in D-MOD2000 and DEEPSOIL, FLAC utilizes an equation to match a target G/G_{max} curve for 1D NL site response analysis framework. The soil element is modeled as an elastic material to provide the small strain shear modulus (G_{max}). Then, as the strain increase, the stress-strain curve then will follow the hysteretic damping equation to model the nonlinearity of the soil. The hysteretic damping equation used in this research is the *sigmoidal* (sig3) model as given by Equation 3.8.

$$M_S = \frac{a}{1+exp\left(-\frac{L-x_0}{b}\right)} \; ; \quad L = \log_{10}(\gamma) \tag{3.9}$$

where M_S is the normalized secant modulus (G/G_{max}) and *a, b, x_0* are the curve fitting parameters to fit the target G/G_{max} curve. Figure 3.17 shows how the sig3 model fits the Vucetic & Dobry (1991) target curve using FLAC simulation to model cyclic Direct Simple Shear test on a single element.

Damping Model

For numerical analysis using FLAC, very small strain damping should be utilized to prevent natural oscillation modes of the system. FLAC has capability to utilize small strain damping using Rayleigh damping formulation that is available in many structural or geotechnical literature (e.g., Chopra, 2012; Wood, 2004). The implementation of Rayleigh damping in FLAC analysis is using simplified Rayleigh damping as shown in the red dot (ω_{min}, ξ_{min}) in Figure 3.16. Those values are computed by the equation shown in Figure 3.16 and the recommendation to select the ω_1 and ω_2 will be dependent on the natural frequency of 1D soil column as proposed by Stewart et al (2008). The unloading and reloading rules used to construct the hysteretic material damping behavior in FLAC follow the Masing (1926) rules. The implementation of sig3 model and Masing rule is presented in Figure 3.18.
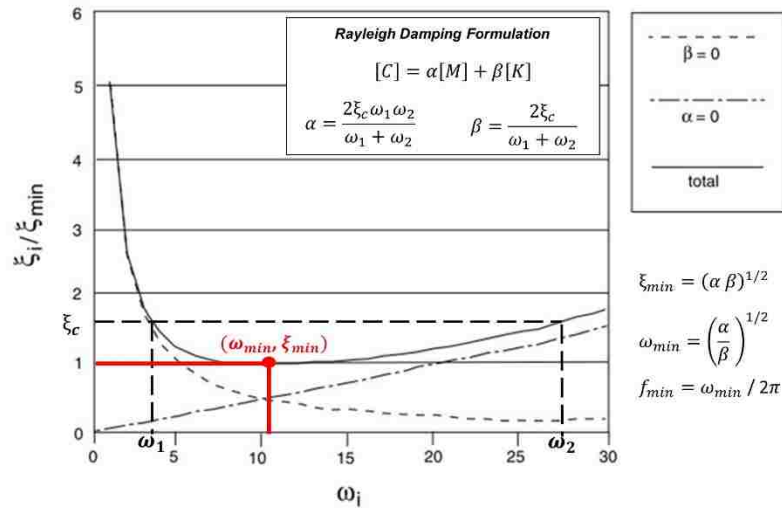
Figure 3.16. Illustration of Rayleigh Damping implementation in FLAC analysis
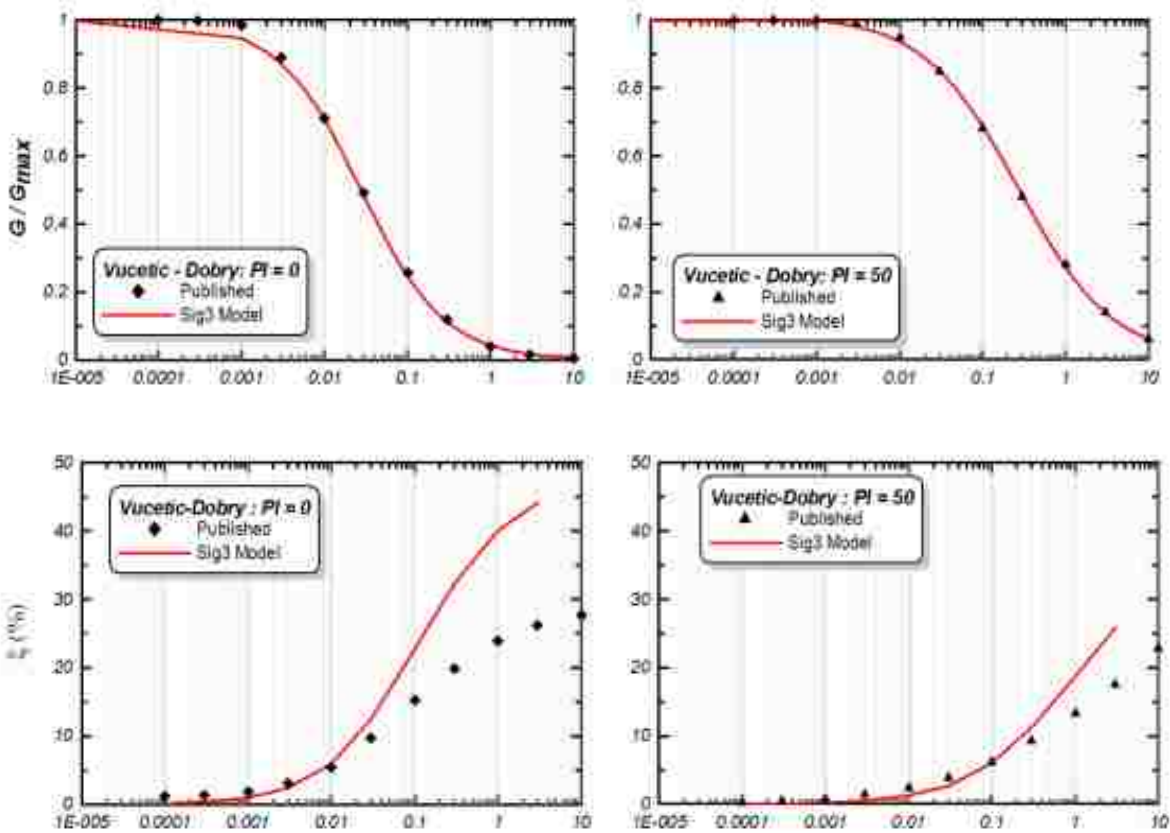
Figure 3.17. Example of Sig-3 model in FLAC fitting the target curves and results of single element undergoing cyclic Direct Simple Shear simulations to compute the damping ratio of the model (Ziotopoulou, 2010)
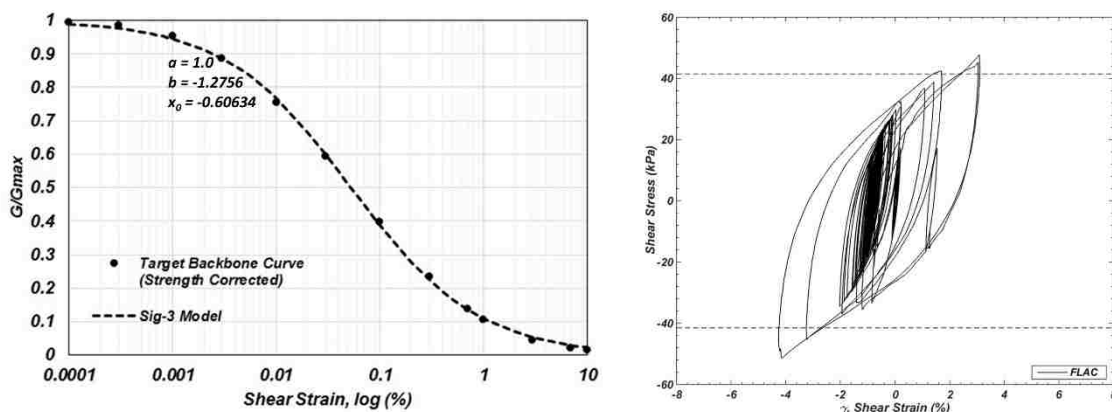
Figure 3.18. Implementation of Sig3 model and Masing (1926) rule to capture cyclic stress-strain behavior at high strain level.

The curve fitting procedure of matching a target backbone curve causes similar problems as presented in Figure 3.9. The Sig-3 model is not capable of reaching an asymptotic value of shear stress at high strain level due to the limitation of its equation as experienced in MKZ soil model. It also overpredicts damping at high strain levels. Therefore, careful consideration is required if FLAC 2D is used to analyze 1D NL seismic site response analysis subjected to high intensity motion inducing high strain level.

3.2.5 *OPENSEES*

OPENSEES (Open System for Earthquake Engineering Simulation) is a finite element (FEM) analysis program. The geometry of the model analysis in OPENSEES is similar to what is adopted in FLAC. However, in the FEM, several important aspects have to be considered carefully including: the element connectivity, type of element used in the analysis (Lee & Bathe, 1993), number of Gauss integration point, quality of element mesh geometry and constitutive model used in the analysis. A detailed explanation of the FEM is beyond the scope of this thesis but major aspect for its implementation in 1D site response analysis with total stress approach will be briefly discussed. The boundary condition model, the procedure to apply the input motion and implementation of Rayleigh damping are similar to what is done in FLAC analysis. Figure 3.19 illustrates the 1D soil column model used in FEM analysis showing the element connectivity, implementation of Lysmer & Kuhlemeyer's dashpot and procedure proposed by Joyner & Chen (1985).
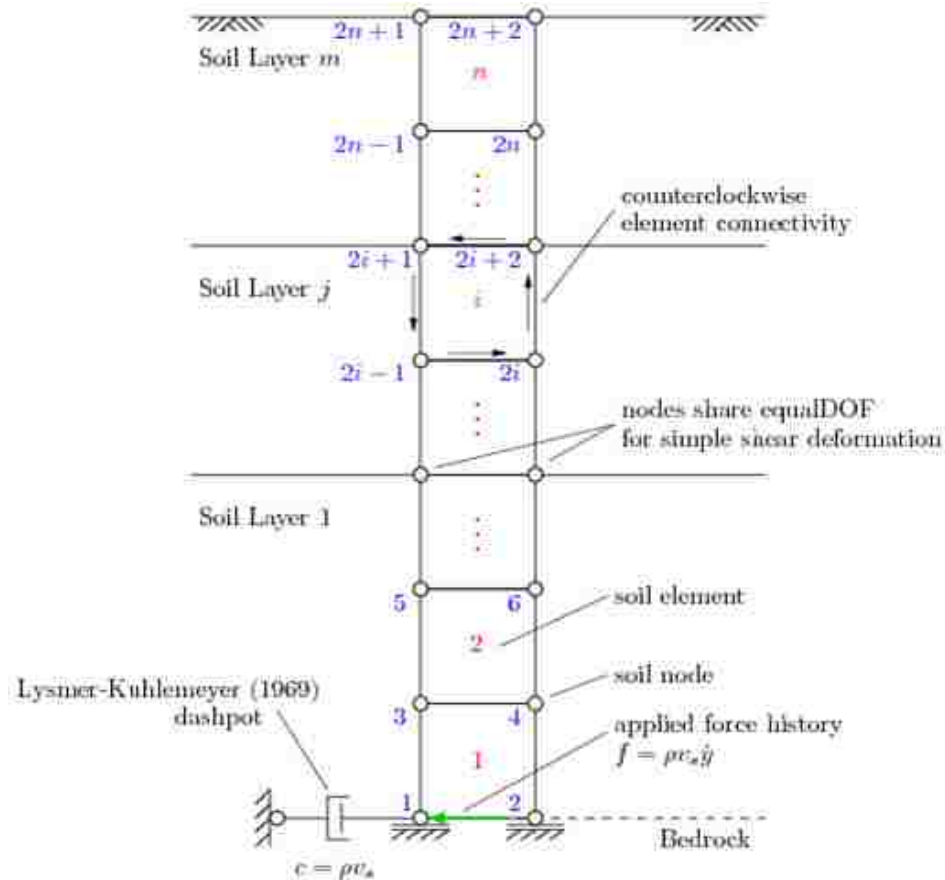
Figure 3.19. Schematic representation of the finite element mesh used in the 1D NL site response analysis used in this research (from McGann & Arduino, 2010) based on the procedure proposed by Joyner & Chen (1975).

Mesh Geometry

The problem of 1D seismic site response analysis is relatively straightforward since it deals only with one degree of freedom (horizontal movement). The implementation of 4 node quadrilateral elements for this analysis is sufficient to give an accurate result as long as the element mesh could maintain a low aspect ratio/element distortion. However, the analysis should ensure that sufficient number of elements are able to capture the propagation of the shear waves at a particular frequency that is represented by wavelength, ($\lambda = V_s / f$). In this research the total number of elements will depend on the maximum cutoff frequency that is required to be propagated.

Soil Constitutive Model

The objective of the soil constitutive model is to provide the path of stress-strain relationship and simulate complex soil behavior under loading, unloading and reloading condition accurately.

The ground site response analysis module in OPENSEES employs soil constitutive model based on Yang & Elgamal (2000) referred as Pressure Independent Multi Yield (PIMY) model developed at the University of California at San Diego. This model is independent from confining pressure and based on the framework of multi-surface plasticity (Iwan 1967; Mroz 1967 and Prevost 1985). Parameters such as friction angle and cohesion are required construct the yield function following the Von Mises yield criteria. PIMY is developed particularly for material where the analysis of generation of pore water pressure is not necessary. The most appropriate implementation of this model is to simulate monotonic or cyclic response of material where the failure behavior is independent to the the confining stress. Such material include cohesive soil deposit or organic soil subjected to fast undrained loading. The reader should refer to the original manuscripts (e.g., Yang, 2000 ; Yang & Elgamal, 2000; and Yang, Lu and Elgamal, 2008) for more detail explanations. The PIMY soil model follows the kinematic loading model proposed by Mroz (1967) to predict the unloading and reloading behavior. Figure 3.20 illustrate the cyclic behavior of soil predicted by PIMY soil model at high strain level and the capability of the constitutive relation to predict the stress-strain curve based on input soil properties. As expected, for models following the Masing rules, the large strain damping ratio is very high.
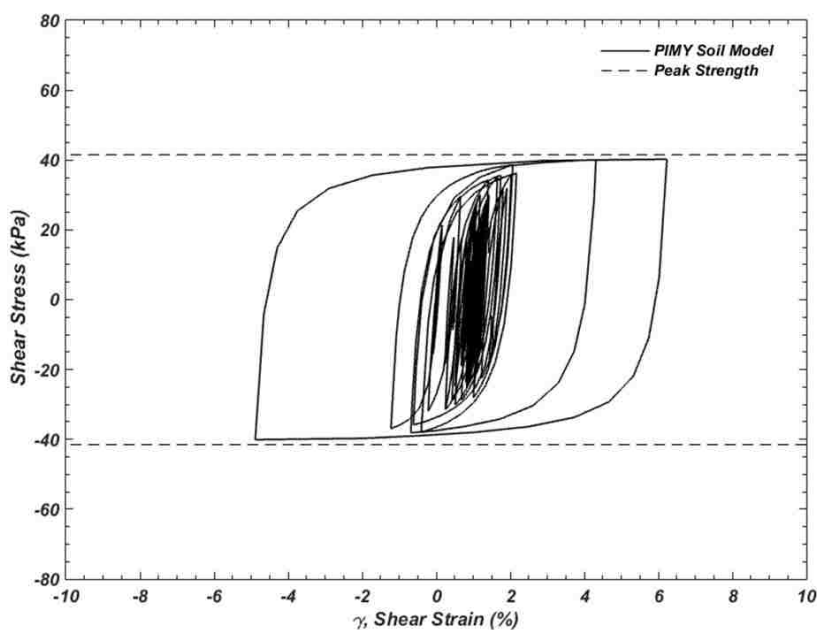
Figure 3.20. Example of cyclic behavior of soil predicted by PIMY soil model. The data is the result of totals stress analysis from Turkey Flat vertical array for shallow alluvium data shaken by 2004 Parkfield Earthquake input motion that is scaled to 1.0g.

3.2.6   *FLIP*

FLIP (Finite element analysis program for Liquefaction Process) was originally developed at Port and Harbor Research Institute (PARI), Ministry of Transport of Japan and in cooperation with Kyoto University. It utilizes the FEM approach to perform multidimensional effective stress analyses, and has been widely used for seismic analysis of quay walls and embankments. For 1D site response analyses standpoint, FLIP uses a simplified set of input commands. In general, modeling of the geometry, boundary condition and the specification of the input motion is similar to what is done in FLAC or OPENSEES since it utilize similar computation methods to solve the dynamic equation.

Soil Constitutive Model

The soil constitutive model used in FLIP is originally based on the multi-spring model element proposed by Towhata & Ishihara (1985). It is also capable to perform effective stress analysis using the excess pore water pressure generation model by Iai (1990). For unloading and reloading behavior, the multi-spring model follows the modified Masing rules proposed by Ishihara et al (1985). As described earlier, Masing's rules does not realistically represent the hysteresis loop when the level shear strain amplitude is high or at stress level approaching the peak strength of the soil. Figure 3.21 show an example of stress-strain curve constructed by multi-spring model and the generalized Masing's rule proposed by Ishihara et al (1985) using total stress approach.
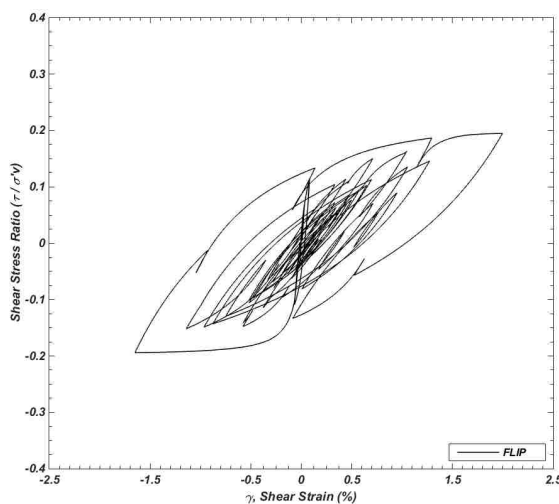
Figure 3.21. Example of cyclic behavior of soil predicted by multi-spring soil constitutive model.

In their study, attempts are made to address the drawback of Masing's rule by introducing scaling parameters that allows the model to better fit to the laboratory data of hysteretic damping. The soil constitutive relation requires important parameters to be defined and it is clearly described in the manual (FLIP Consortium, 2011).

3.3   SUMMARY

This chapter outlines the basic theory, soil model and computational procedure implemented in 1D site response analysis. Moreover, it also summarizes the common nonlinear soil model and advanced constitutive model and discusses the limitation for each model. The detail of each models are listed in Table 3.3 giving clear summary of soil models that are being analyzed in this thesis. The last part of this chapter discusses the aspects that must be taken into account to perform 1D non-linear site response analysis as follow:

- The minimum thickness of the layer during the analysis is designed to propagate maximum frequency of at least 25 Hz.
- The specification of input motion and type of underlying halfspace follow the recommendation based on Stewart et al (2008) :
    - Outcropping motion is used without modification with an elastic base.
    - If the response simulation of a vertical array data is required, recorded within motion is used without modification in conjunction with a rigid base.
- Calibration of Rayleigh damping is required and it is performed using procedure based on Kwok et al (2007). The natural and 5 times of site frequency will be used as the target frequencies following full Rayleigh damping formulation.
- The peak shear strength correction is required and this study will follow the procedure proposed by Groholski et al (2016).

Table 3-2. Summary of the 1D nonlinear codes and soil model used in this research

Codes	ID	Computational Method	Viscous Damping Matric, [C]	Nonlinear Soil Model		Reference for Soil Model	Reference for Computer Code
				Backbone Curve	Hysteretic Damping		
D-MOD2000	DMOD2000	1D time integration (Newmark β) solving dynamic equation (Lumped Mass system)	Full Rayleigh Damping[1]	Modified Kondner & Zelasko (MKZ)	Extended Masing Rules (Vucetic, 1990)	Kondner & Zelasko (1963); Matasovic & Vucetic (1993)	Matasovic & Ordonez (2011)
DEEPSOIL	DS-MKZ		Frequency Independent (Hashash, 2009)	Extended MKZ	Non Masing Rules (MRDF) – Phillips & Hashash (2009)	Park & Hashash (2001)	Hashash et al (2015)
	DS-GQ/H			GQ/H		Groholski et al (2016)	
NERA	NERA	1D forward Finite Difference (FD) solving stress wave propagation using Central Difference algorithm.	N/A	IM Soil Model	Follow the behavior of unloading-reloading behavior similar to Masing (1926) rules.	Iwan (1967) ; Mroz (1967)	Bardet & Tobita (2001)
FLAC	FLAC	2D forward FD solving full dynamic equation. (Distributed Mass)	Full Rayleigh Damping	Sigmoidal (Sig3)		Itasca, 2011	Itasca, 2011
OPENSEES	OPENSEES	2D Finite Element Method (FEM) solving full dynamic equation. (Distributed Mass)		Pressure Independent Multi Yield surface (PIMY)		Yang (2000); Yang & Elgamal (2000)	McKenna & Fenves (2006)
FLIP	FLIP	2D Finite Element Method (FEM) solving full dynamic equation. (Distributed Mass)		Multi-Spring Model	Generalized Masing Rules (Ishihara et al, 1985)	Towhata & Ishihara (1985), Iai et al (1990), Iai et al (2011)	FLIP Consortium (2011)

---

[1] All codes using full Rayleigh damping formulation is based on the recommendation of Kwok et al (2007)

Chapter 4. EVALUATION AGAINST SIMPLE SITE PROFILES

This chapter will present the evaluation of each 1D site response analysis computer code based on the protocols described in Chapter Three. The analysis involves a set of sites underlain by relatively simple shear wave velocity profiles subjected to input motions of different intensity. The sites are underlain by 30 meters depth of cohesive soil deposit with different shear wave velocity profile classified as soft soil, S_E ($V_{s30} < 180$ m/s), stiff soil, S_D (180 m/s $< V_{s30} < 360$ m/s) and very stiff soil, S_C (360 m/s $< V_{s30} < 760$ m/s) based on NEHRP site classification. The 1D EQL and NL site response analyses are then performed utilizing input motions scaled to a wide range of peak ground acceleration (PGA) values. Moreover, the last part of this chapter discusses the variability of the 1D NL site response analysis results in order to give better understanding in the implementation of site response analysis framework.

4.1 SITE CHARACTERISTICS

The characteristics of the site considered herein are designed to represent a range of site conditions. Three shear wave velocity profiles were used for each V_{S30} value. These profiles had constant, layered, and parabolically increasing shear wave velocity. The ground water level was assumed to be at the ground surface. However, since total stress analyses were performed, the ground water depth will not influence the results.

The shear modulus reduction and damping ratio curve for this study were based on the published curves proposed by Darendeli (2001). In order to fulfil the shear strength criteria of the soil, the original Darendeli curve was adjusted using procedure proposed by Groholski et al (2016). Figure 4.1 presents the adjusted target G/G$_{max}$ curves, damping curves and adjusted backbone curves for the constant profile used in this study. The G/G$_{max}$ curve for other soil profile was determined using same procedure. The writer understands that the nonlinearity of the soil depends on the confining pressure as shown in Figure 2.4. However, to simplify the analysis, the Darendeli's curve will be set to yield the curve at confining pressure of 1 atm, 10 number of cycles

and loading frequency of 10 Hz. As long as the analysis use an identical target curve, it should give consistent results since it is not attempting to match any vertical array data.
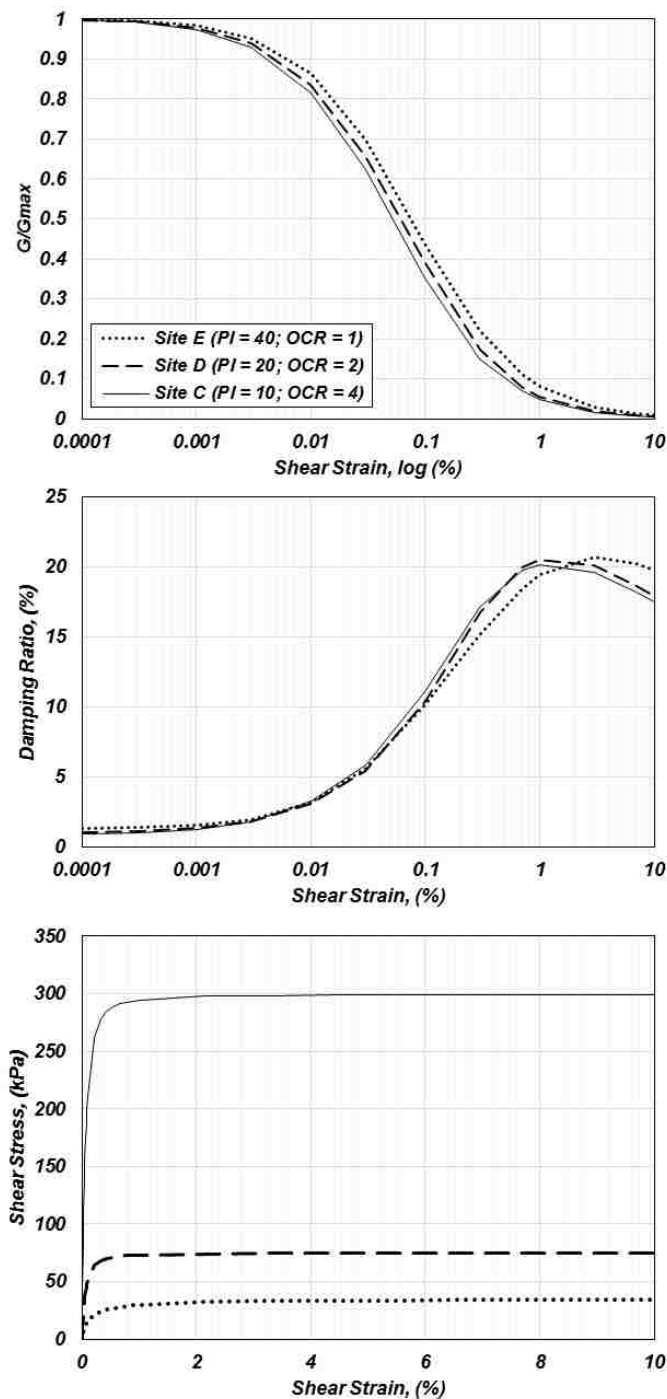
Figure 4.1. Shear modulus reduction curve, damping ratio curve and adjusted stress-strain curve used for the Constant soil profile extracted from Darendeli (2001) curve ($f = 1.0$ Hz, 10 number of cycles) using procedure proposed by Groholski et al (2016).

The average shear wave velocity of the top 30 m of the profile was adjusted to represent three site classes based on NEHRP site classification system (i.e., Site S_E, Site S_D and Site S_C). Those sites will had V_{S30} values of 150 m/s, 270 m/s and 560 m/s, respectively, and other geotechnical parameters were adjusted to provide reasonable and consistent geotechnical characteristics. Figures 4.2 – 4.4 summarize the geotechnical properties including shear wave velocity, peak (implied) shear strength, unit weight, plasticity index and overconsolidation ratio for each of the profiles used in this study. These parameters were selected to produce reasonable shear modulus reduction and damping curves required for the profiles used in the analysis. For the shear strength of the soil, since the earthquake loading will yield undrained condition, the correlation proposed by Dickenson (1994) to estimate the undrained shear strength of the soil based on shear wave velocity, V_S (m/s) $= 23\ S_u^{0.475}$ was used.

In addition, response spectra are among the most important results of site response analyses. The most common way to estimate the response spectra at the ground surface is using the amplification factor suggested by standard (e.g., ASCE 7-10) which is based on the assumption of constant V_{S30} profile. The three types of shear wave velocity profiles used herein are expected to give insight that different shear wave velocity profiles will yield different amplification ratios at the surface even though they have identical V_{S30} values.

4.2   INPUT MOTION CHARACTERISTIC

An objective of this research is to evaluate the ability of each computer programs and soil model to predict the site response at cyclic shear stress level approaching the shear strength of the soil. Such conditions can be achieved by providing a strong enough seismic loading that will be applied to the soil column. The input motion used in this study will be extracted from the 1989 Loma Prieta earthquake that is recorded at Gilroy station. This motion will be scaled to the PGA levels of 0.05g, 0.20g, 0.50g and 1.00g in order to produce a wide range of shear strain levels. Figures 4.5 – 4.7 present the acceleration, velocity and displacement time histories respectively used in this study where Figure 4.8 show the characteristic of the input motion in terms of the duration and the frequency content. The detail of analysis model for each computer program and the analysis results is presented in the following sections.
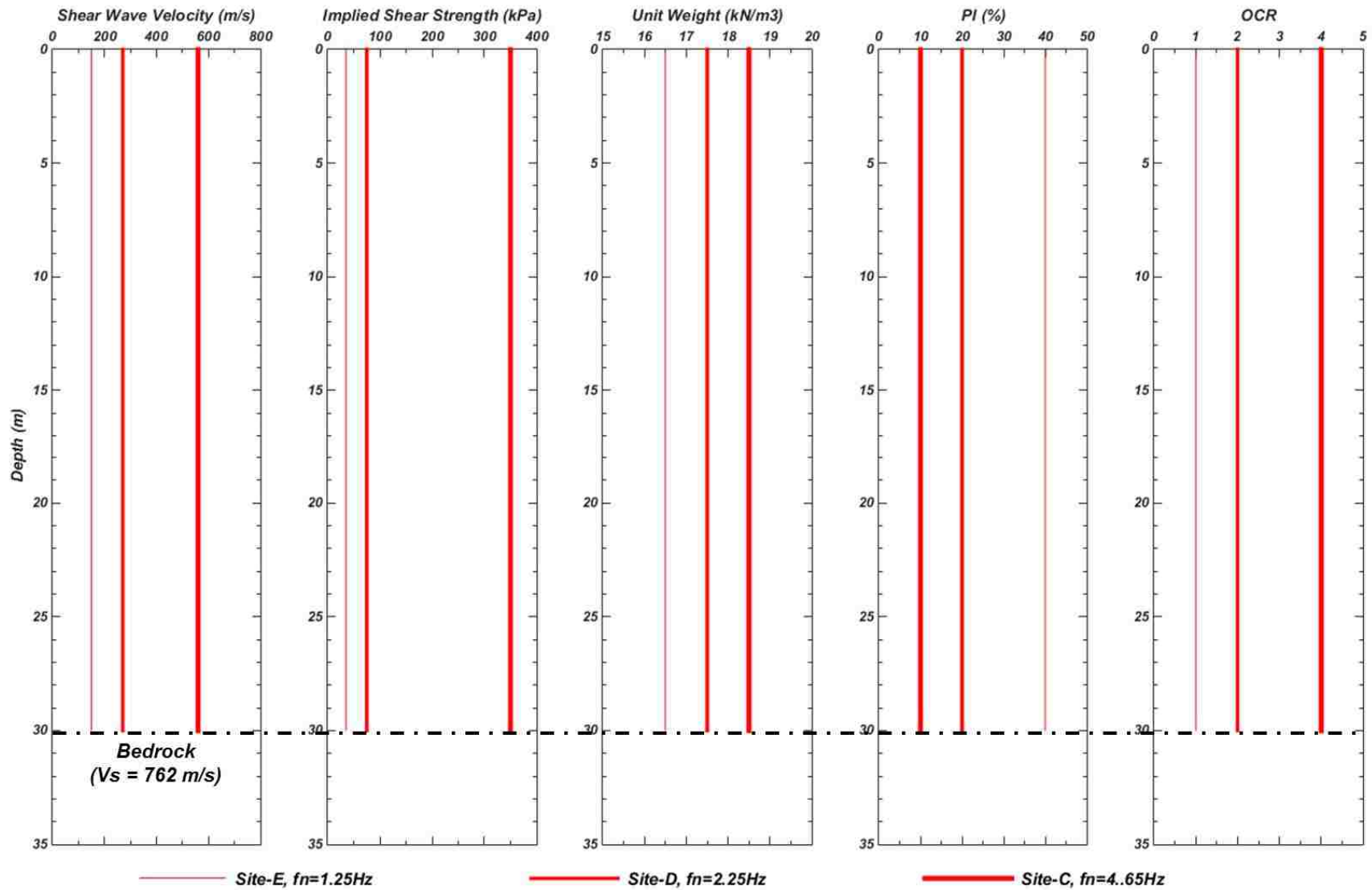
Figure 4.2. Geotechnical properties for a site with constant velocity profile with 30 m depth used in this study. The thicker line represent the stiffer site characteristic
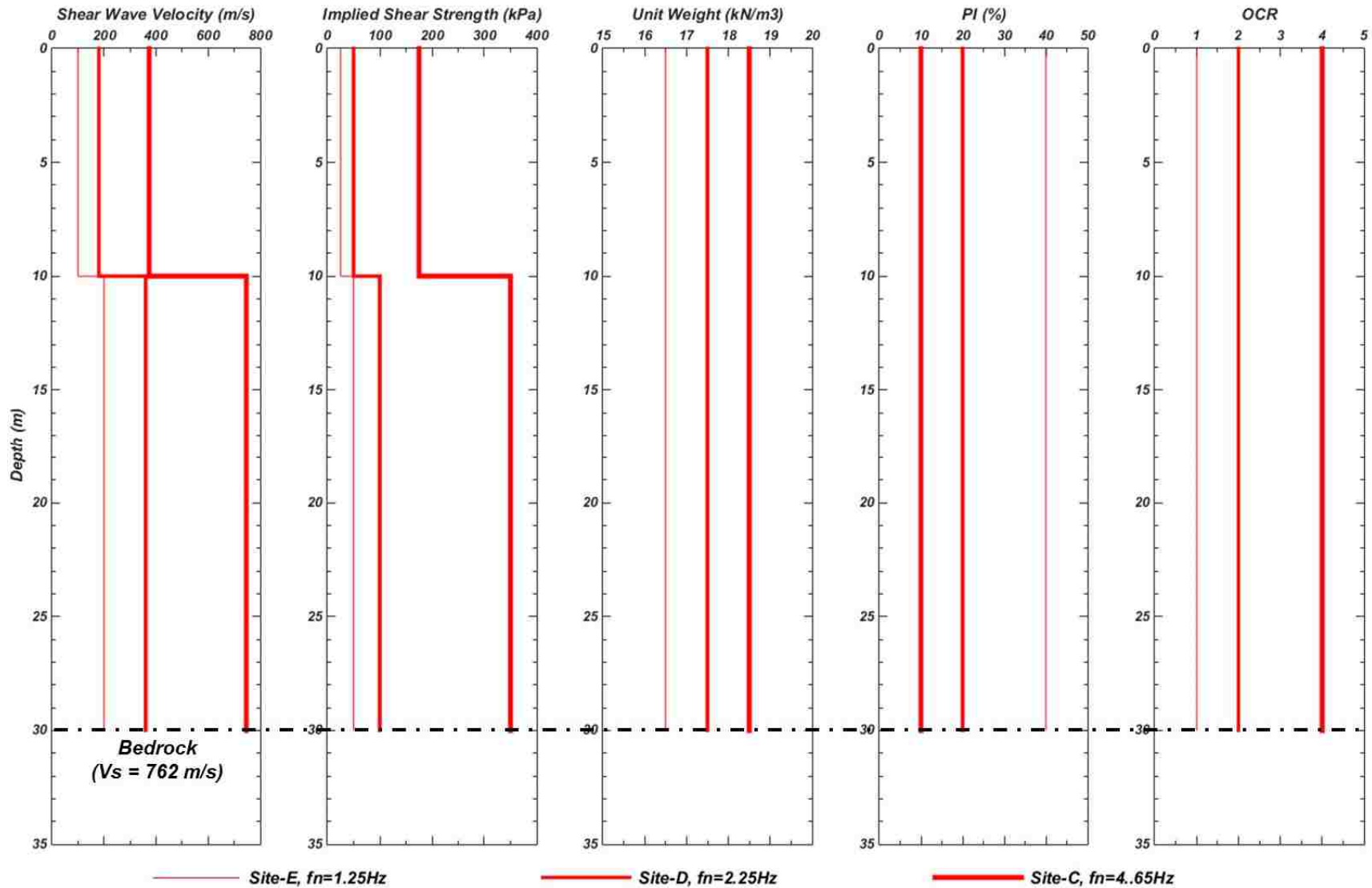
Figure 4.3. Geotechnical properties for a site with 2 layered shear wave velocity profile with 30 m depth used in this study. The thicker line represents stiffer site characteristic
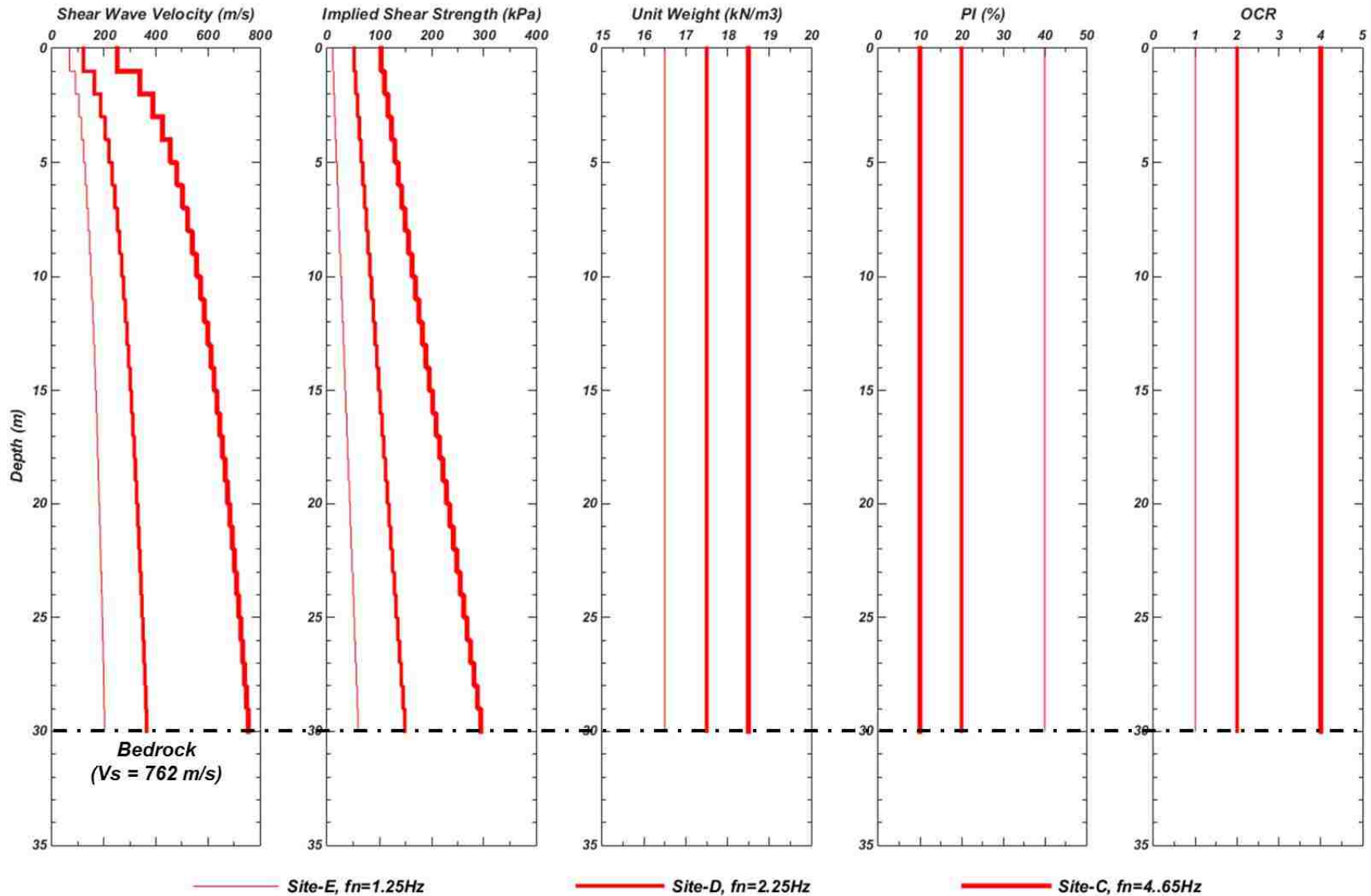
Figure 4.4. Geotechnical properties for a site with parabolically increasing shear wave velocity profile with 30 m depth used in this study. The thicker line represents stiffer site characteristic
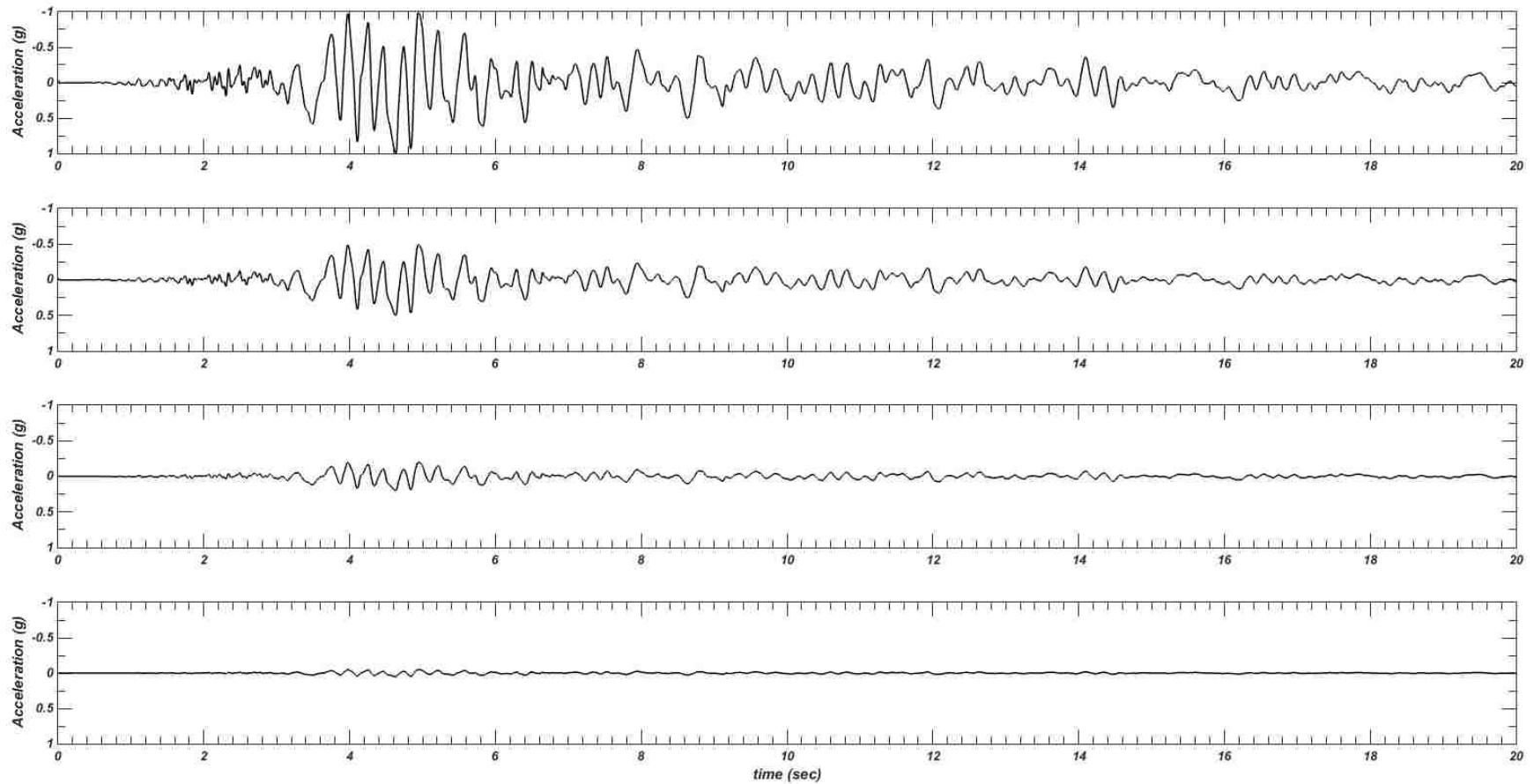
Figure 4.5. The acceleration time histories of input motion used in the analysis taken from 1989 Loma Prieta Earthquake recorded at Gilroy station that is scaled to different PGA level (i.e., from the top to bottom scaled to 1.0g, 0.5g, 0.2g, 0.05g). The original recording is up to 40.0 sec measurement.
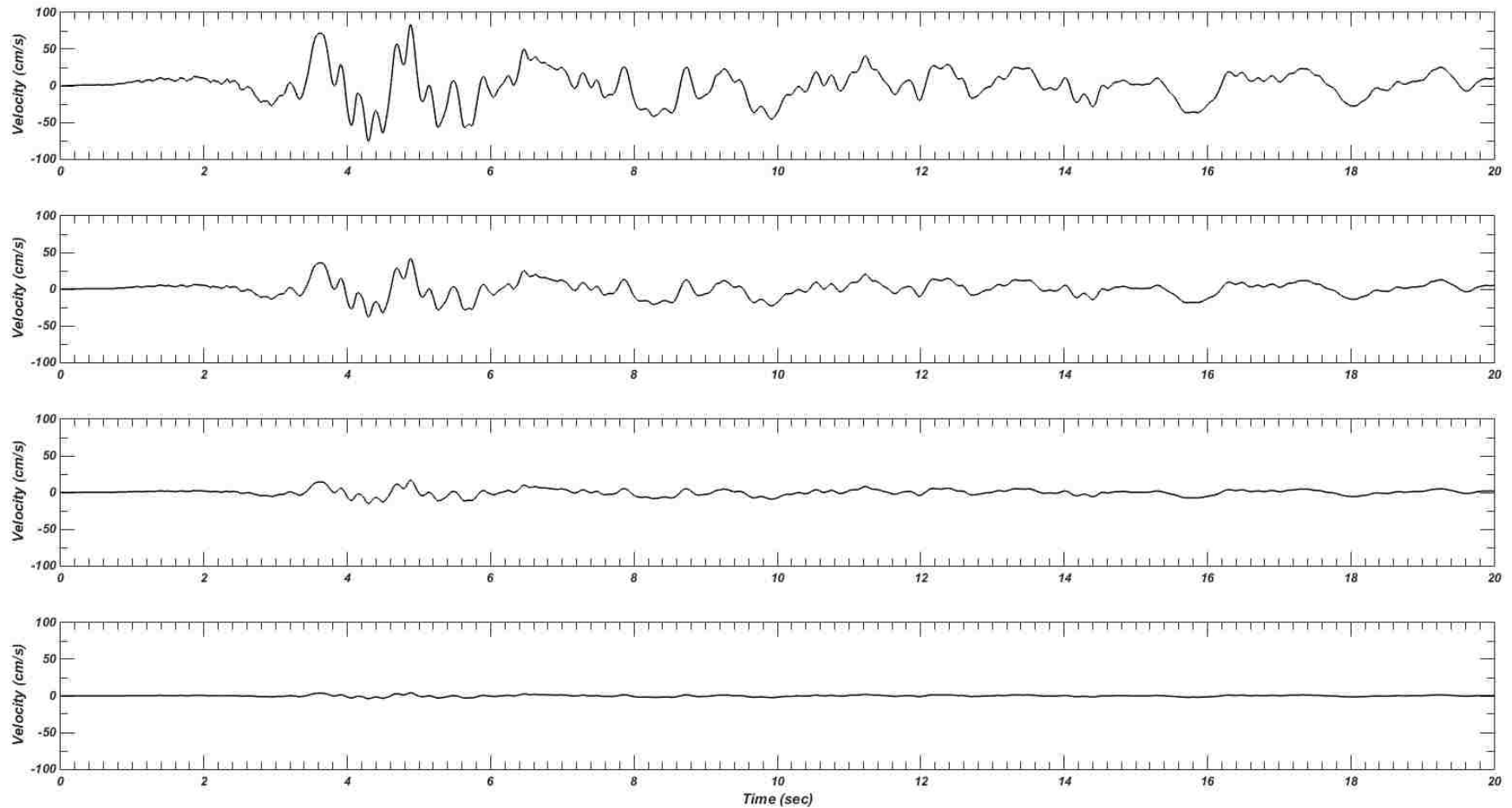
Figure 4.6. The velocity time histories of input motion used in the analysis taken from 1989 Loma Prieta Earthquake recorded at Gilroy station that is scaled to different PGA level (i.e., from the top to bottom scaled to 1.0g, 0.5g, 0.2g, 0.05g). The original recording is up to 40.0 sec measurement.
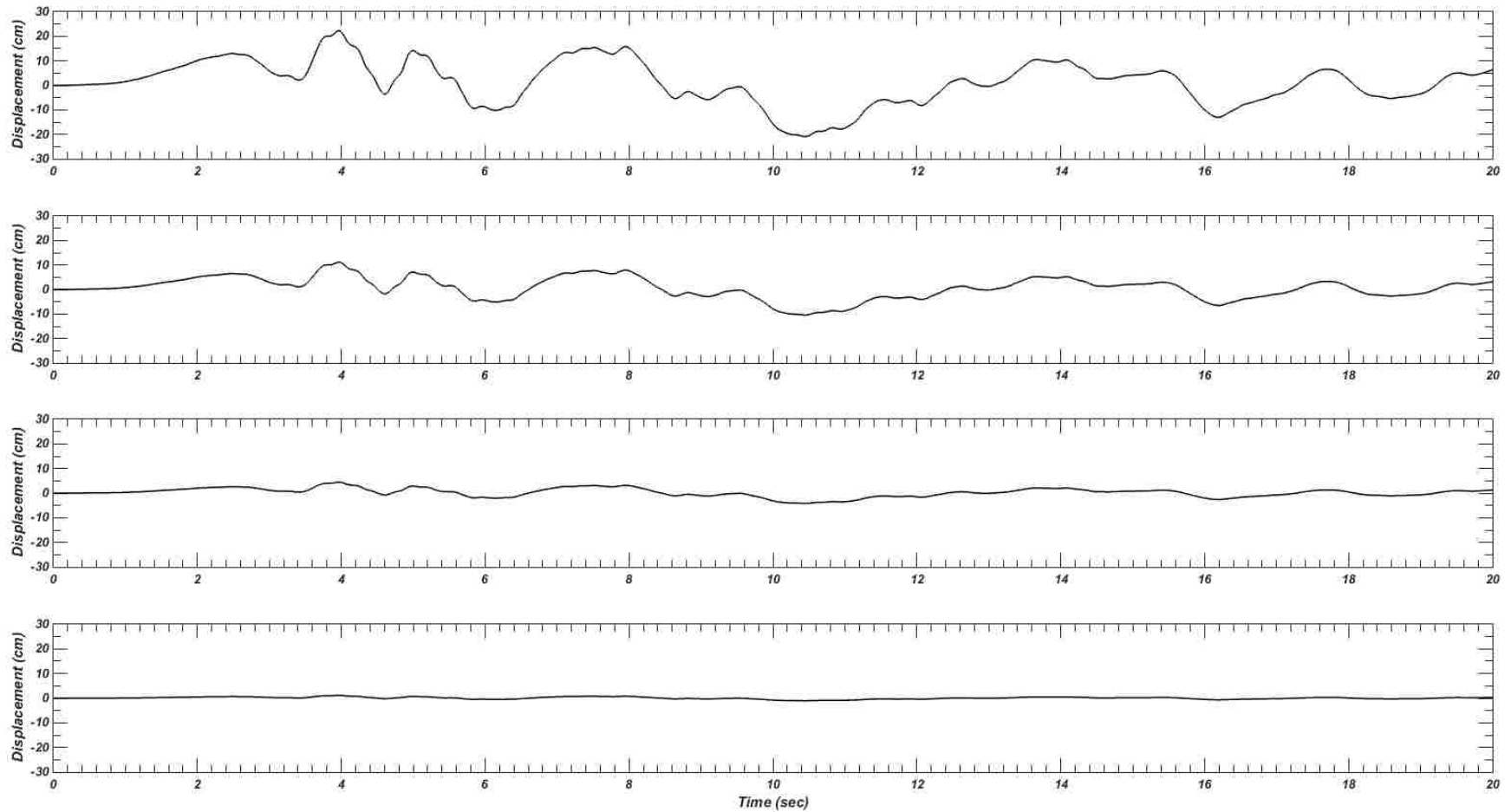
Figure 4.7. The displacement time histories of input motion used in the analysis taken from 1989 Loma Prieta Earthquake recorded at Gilroy station that is scaled to different PGA level (i.e., from the top to bottom scaled to 1.0g, 0.5g, 0.2g, 0.05g). The original recording is up to 40.0 sec measurement.
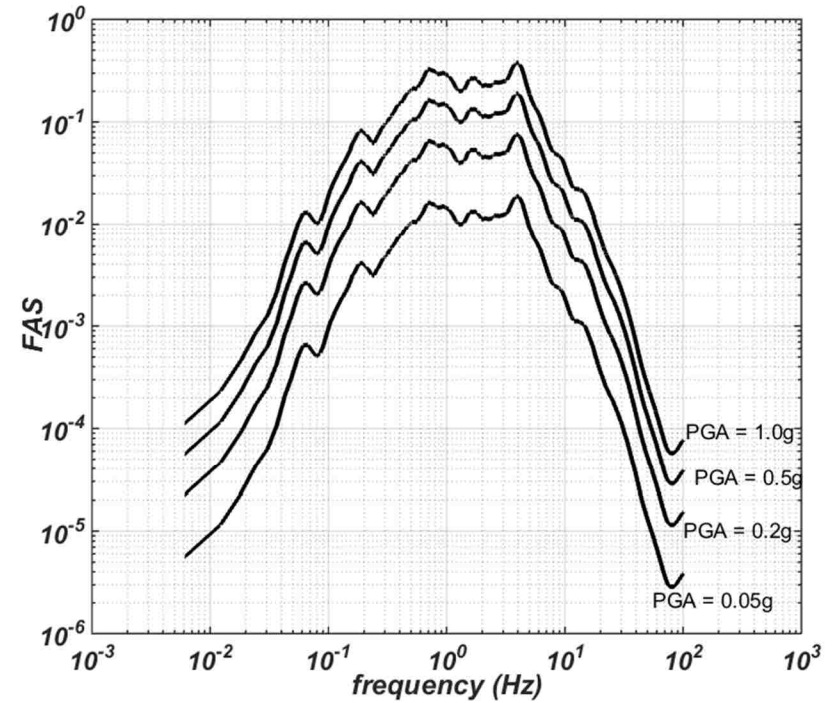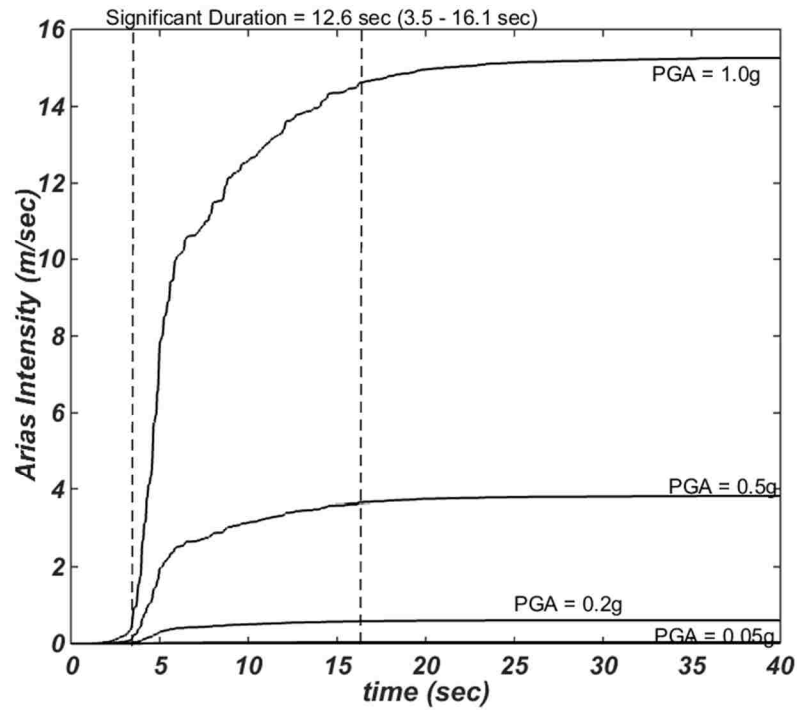
Figure 4.8. The input motion characteristic considered in this study. The left chart show the plot of Arias Intensity and the significant duration of the input motion is from 3.5 sec to 16.1 sec and it last for 12.6 sec. The right chart show the plot of Fourier Amplitude Spectrum over frequency to show the dominant frequency of the input motion ranging from 0.7 – 4 Hz or dominant period ranging from 0.25 – 1.5 sec.

4.3 MODEL ANALYSIS

The implementation of the 1D site response analysis models and procedures described in Chapter Three are presented in this section. All parameters and model prior to perform the analysis will be clearly explained.

Layer Thickness

The layer thicknesses were set to 1 m for each layer with total 30 layers. Time steps were then selected to allow a maximum frequency of at least 30 Hz to be propagated through each profile.

Specification of Half-Space and Input Motion

The implementation of outcropping motion along with elastic base was utilized for the site response analysis in this chapter. It employs the Lysmer & Kuhlemeyer (1969) dashpot and the concept of application of shear stress time history as the product of velocity time histories and the dashpot coefficient (Joyner & Chen, 1975) for the input motion. The density of elastic halfspace was 2243 kg/m^3 with finite rigidity corresponding to a shear wave velocity of 762 m/s. The example of application of shear stress time histories at the base of the column is shown in Figure 4.9 as modeled using FLAC.

Rayleigh Damping Calibration

Table 3-3 indicates that several NL codes require implementation of small strain Rayleigh damping to prevent oscillation of the system. However, it should not overdamp the system particularly at large strain levels that might cause underprediction of the intensity of ground motion at the surface. NERA does not require the implementation of Rayleigh damping since it employs the IM soil model and includes only hysteretic damping. DEEPSOIL utilizes a new formulation of the viscous damping matrix that is independent of frequency. Therefore, only FLAC, OPENSEES, D-MOD2000 and FLIP require the calibration of Rayleigh damping. The calibration follows the procedure explained in Section 2.3.3 to fit the EQL result at shear strain level less than 0.05% for each profile (Figure 3.25). The first guess of the Rayleigh damping coefficient used a target damping ratio equal to the small strain damping obtained from the target damping curve (1.5 -2.0 %) with the two target frequencies set to be the 1st mode natural site frequency (f_n) and 5 f_n.
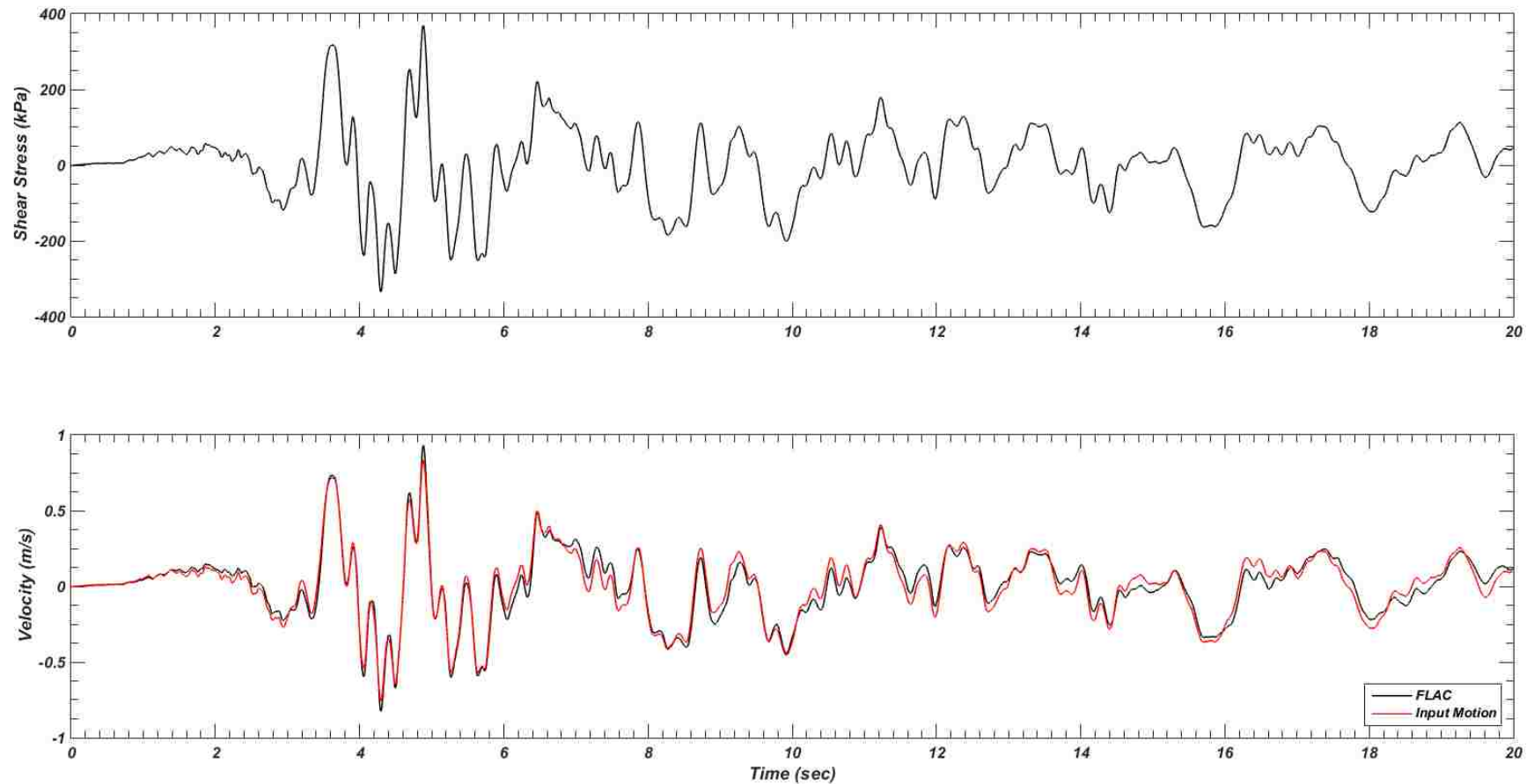
Figure 4.9. Example of input motion (PGA = 1.0g) applied as shear stress history at the base of 1D soil column (Top plot) modeled in FLAC. The bottom plot show the comparison of the particle velocity at the base of the column resulted from FLAC analysis compared to the original input motion (red line). Shear stress time history specifies the upward propagating motion into the soil column, but the actual response (particle velocity) at the base will be the superposition of the reflected and transmitted motion.

4.3.1   *Equivalent Linear Approach*

The EQL analysis in this chapter were performed using the STRATA program (Kottke & Rathje, 2008). The analysis used target G/G_{max} and damping curves as presented in Figure 4.1 for the constant velocity site profile and also identical to what is used in other codes for other site profile. The error tolerance for the iterative procedure is 2% with 10 numbers of iteration.

4.3.2   *Non-linear Approach*

The NL codes considered in this chapter are D-MOD2000, DEEPSOIL, NERA, FLAC, OPENSEES and FLIP. In general these codes are divided into one-dimensional and two-dimensional site response analysis codes.

One-Dimensional Codes

D-MOD2000, DEEPSOIL, and NERA are the one-dimensional site response analysis codes employed in this research. The model and procedure implemented for the analysis follow the protocols explained previously in Chapter 2. The analysis will discretize the soil profile into 30 layers (1m thickness) and will be fitted to corresponding target G/G_{max} and damping ratio curve. As described earlier, D-MOD2000 and DEEPSOIL utilize an equation featured by curve fitting parameters to match the target curve. The curve fitting procedure is performed automatically via built in user interface for each program. The value of curve fitting procedure will not be listed for the analysis in this chapter but it will be clearly listed for the analysis in Chapter Four.

NERA use the IM soil model in which the performance of the model depends on the number of spring and friction elements used within the analysis. The program will determine automatically the minimum required number of those elements to reach the convergence criteria based on the number of points inputted as the target modulus reduction curve. The higher the number of elements, the more accuracy to be achieved. Joyner & Chen (1975) utilized 50 elements that provided a good result and 100 element with reasonable computation time at that time.

Two-Dimensional Codes

OPENSEES, FLAC and FLIP are multidimensional numerical analysis programs that were used as one-dimensional analyses in this research. The most important aspects to perform the

analysis using these programs are the model geometry, boundary conditions and specification of input motions. The schematic illustration in Figure 4.10 presents all those aspects implemented in these multidimensional program. The location of computed response in these analysis will be identical to which computed by 1D programs having height of 1 m (30 layers). The prediction results computed by all these codes are presented in the next section.
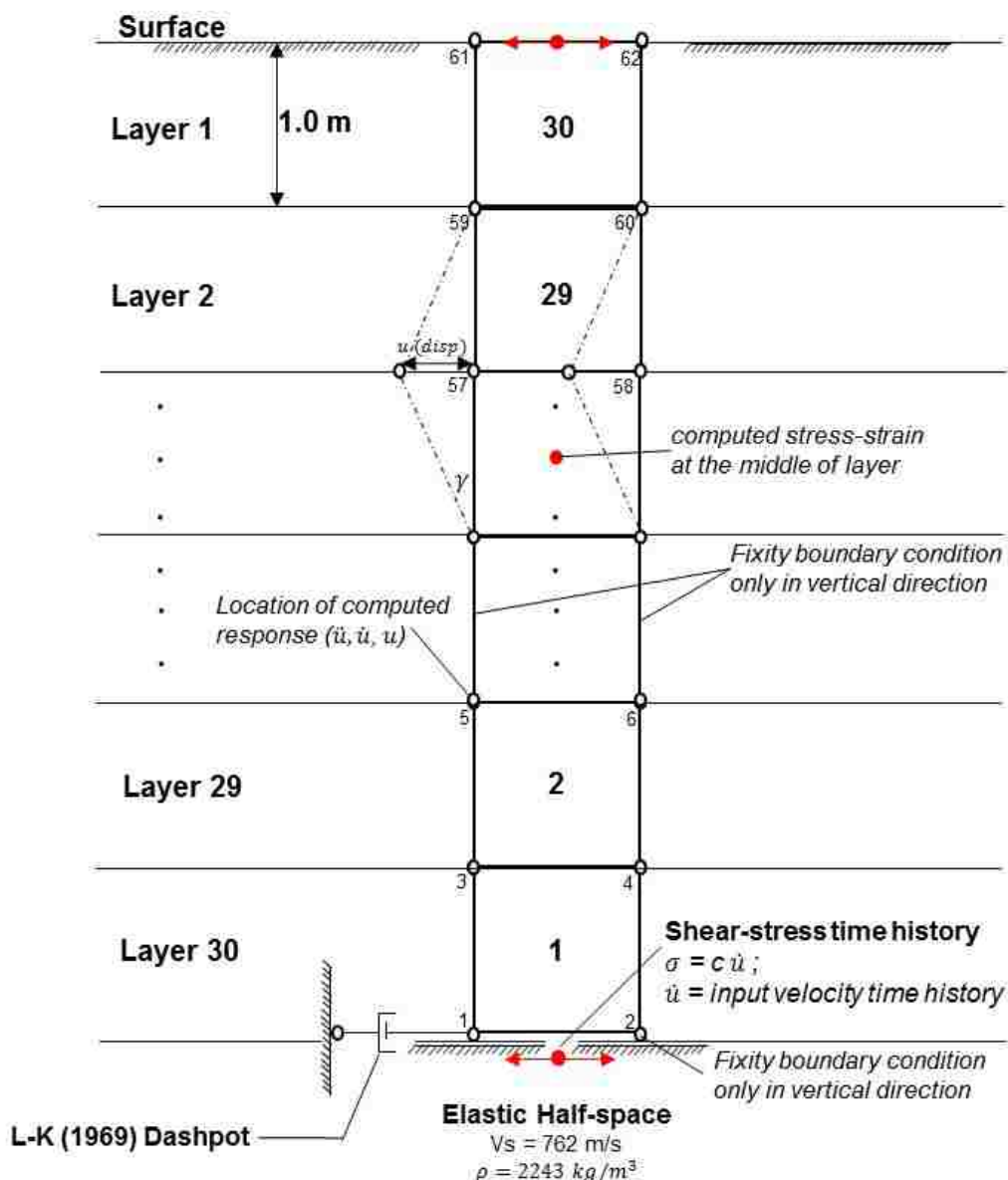
Figure 4.10. The model geometry implemented in multidimensional analysis to perform the dynamic analysis of a one dimensional soil column in Chapter Three. It model to be a stack of 30 quadrilateral elements with 62 nodes with stress history applied at the base of the column as proposed by Joyner & Chen, 1975. (Modified from McGann & Arduino, 2010)

From the standpoint of soil constitutive modeling, OPENSEES allows the computation to determine the number of yield surfaces either automatically or by user-defined. For the automatic option, it will construct the PIMY constitutive relation based on the modified rules by Yang (2000). In this research, the number of yield surfaces employed in the computation will corresponds to the user defined *G/Gmax* curve requiring the number of yield surfaces should be less than 40. This approach constructs the stress-strain relationship based on Mroz (1967) constitutive model and it will be implemented only for the small to moderate strain level to compare the response prediction of each codes using identical target G/G$_{max}$ curve. For large strain level, the computation will set the number of yield surfaces to be determined by PIMY rules to allow the model to predict the cyclic behavior accurately.

FLIP employs an advanced soil constitutive model based on the multi-spring model (Towhata & Ishihara, 1985). There is no option to adapt a target G/G$_{max}$ curve in FLIP that might provide unidentical stress-strain relationship with other codes. Based on this assumption, the prediction resulted by FLIP might deviate from others particularly at high strain level because FLIP will generate the stress-strain relationship that completely follows the rules governed by the model. Lastly, the nonlinear soil model in FLAC utilizes the Sigmoidal-Sig3 model (Itasca, 2011) to compute the seismic response at each nodes. This model is incapable of capturing the peak strength of the soil at large strain levels, thus it will predict unrealistic shear stress at large strain level.

4.4   SITE RESPONSE RESULTS

The 1D seismic site response analysis in this chapter involved three types of sites with different shear velocity profile (constant, layered and parabolic) and ranging from soft to very stiff site (Vs-30 of 150 m/s, 270 m/s and 560 m/s) subjected to four different scaled intensity motions. The combinations of all those analyses will provide 36 results over a wide range of shear strain levels. The characteristics of the results are typical to each other at similar shear strain level, thus, in order to simplify the variability analysis, the detail of the results presented herein only consider one single case for each strain range or nonlinearity level. The range of soil nonlinearity considered in this research is divided into four groups based on G/G$_{max}$ ranges as illustrated in Figure 4.11.

4.4.1   *Results Summary*

Table 4-1 lists all the 1D site response results computed from the combination of different shear wave velocity profiles, site classifications and various intensity motions. These results are beneficial to evaluate the variability of each code in predicting the site response over a wide range of soil nonlinearity and shear strain level, from very small strain ($\gamma < 0.003\%$) to very large strain ($\gamma > 6\%$) data.

The predictions in each group typically give similar variance behavior, hence, the variability analysis will be presented by only a single case for each group (highlighted in Table 4-1). The cases presented herein include median shear strain levels of 0.005%, 0.05%, 0.57%, 2.32% and 6% as indicated in Figure 4.11. Those strain levels corresponds to G/G_{max} value of 0.92, 0.54, 0.16, 0.02 and 0.01 respectively. In general, all codes predicted similar results at low shear strain level since they were still in the linear zone of soil behavior. On the contrary, the variability tends to increase at the higher soil nonlinearity levels induced by stronger intensity motions. The detailed analysis regarding the variance of each prediction is presented in the following section.
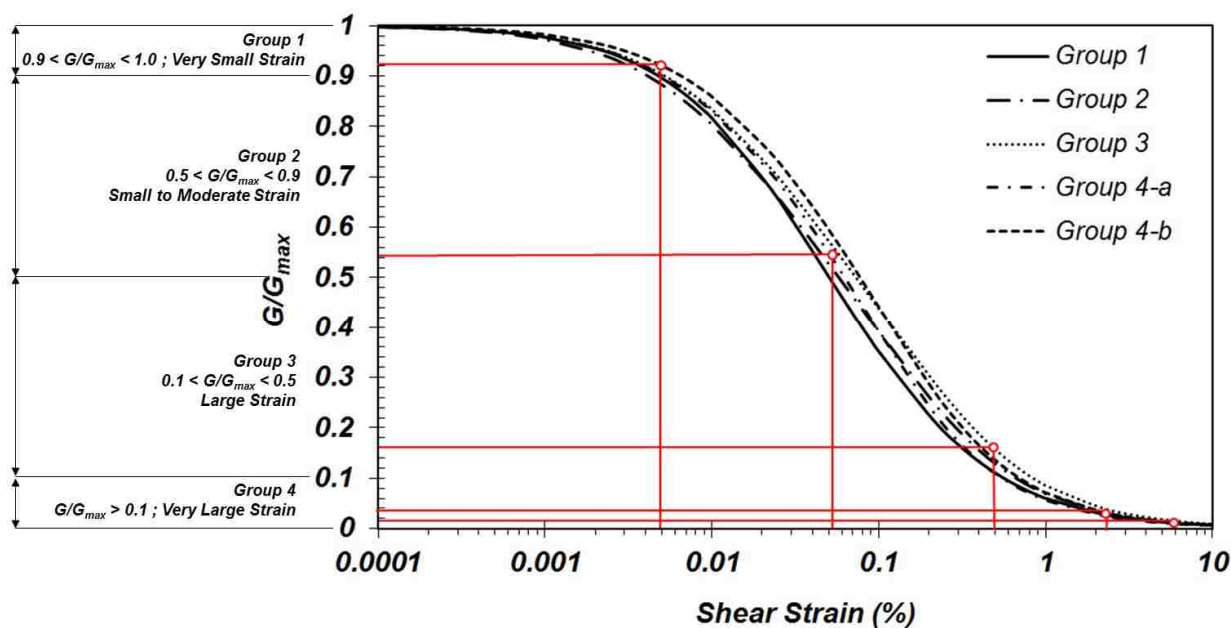
Figure 4.11. The range of soil nonlinearity level employed in this research that is divided into 4 groups based on the G/G$_{max}$ value. The red line indicates the 5 cases presented in this chapter to study the variability of each codes at each range of nonlinearity and these 5 cases is highlighted in Table 3-1. The selected G/Gmax curve corresponds to the chosen profile and particular depth.

Table 4-1. Summary of the 1D nonlinear analysis results resulted from 36 cases

Shear Velocity Profile	Site	PGA (g) Input Motion	Median Strain[†] (%)	Group	Shear Velocity Profile	Site	PGA (g) Input Motion	Median Strain (%)	Group	Shear Velocity Profile	Site	PGA (g) Input Motion	Median Strain (%)	Group
Parabolic	S_E	*0.05*	*0.05*	*2[‡]*	Constant	S_E	0.05	0.08	3	2-Layer	S_E	0.05	0.112	2
Parabolic	S_E	0.2	0.4	3	*Constant*	S_E	*0.2*	*0.57*	*3*	2-Layer	S_E	0.2	1.5	4
Parabolic	S_E	0.5	0.9	4	Constant	S_E	0.5	1	4	2-Layer	S_E	0.5	4	4
Parabolic	S_E	1	2.7	4	Constant	S_E	1	7	4	*2-Layer*	S_E	*1*	*6*	*4*
Parabolic	S_D	0.05	0.01	2	Constant	S_D	0.05	0.02	2	2-Layer	S_D	0.05	0.03	2
Parabolic	S_D	0.2	0.11	3	Constant	S_D	0.2	0.17	2	2-Layer	S_D	0.2	0.36	3
Parabolic	S_D	0.5	0.61	3	*Constant*	S_D	*0.5*	*2.32*	*4*	2-Layer	S_D	0.5	2.6	4
Parabolic	S_D	1	1.7	4	Constant	S_D	1	4	4	2-Layer	S_D	1	5.5	4
Parabolic	S_C	0.05	0.003	1	Constant	S_C	0.05	0.005	1	*2-Layer*	S_C	*0.05*	*0.0051*	*1*
Parabolic	S_C	0.2	0.01	2	Constant	S_C	0.2	0.03	2	2-Layer	S_C	0.2	0.04	2
Parabolic	S_C	0.5	0.1	3	Constant	S_C	0.5	0.15	3	2-Layer	S_C	0.5	0.15	3
Parabolic	S_C	1	0.3	4	Constant	S_C	1	0.5	4	2-Layer	S_C	1	1.5	4

[†] The median value of shear strain (computed by all codes) at depth where maximum shear strain along the soil profile is resulted.
[‡] The highlighted row indicates the data representing each range of nonlinearity level presented in this chapter.

4.4.2   *Profiles*

This section presents the variability of computed profiles of PGA, peak shear strain and peak shear stress versus depth as indicated from Figures 4-12 to 4-16. These three parameters were selected since they represent the amplitude of the node displacement at each depth. It should be noted that the variability analysis considered only the results computed by nonlinear (NL) codes to examine at which strain level the EQL code deviate from NL codes. The discussion will be organized to correspond with the nonlinearity groups described earlier.

Group 1 (1.0 < G/G$_{max}$ < 0.9 – Very small strain)

The case with the two layer shear wave velocity profile as depicted in Figure 4.12 having V$_{S30}$ of 560 m/s (S_C) subjected to input motion scaled to 0.05g is selected to represent the variance behavior of Group-1. The combination of very stiff soil column shaken by weak motion yields very small strain amplitudes with median value 0.0051% at 9.5 m depth (Figure 4.12). This strain level corresponds to an 8% of reduction of shear modulus (*G/G$_{max}$* = 0.92) indicating very low nonlinearity level. The results are relatively similar for all parameters as indicated in Table 4-2 or Figure 4.12, except for FLIP, which predicts softer behavior (greater strain with weaker cyclic stress). It may be because FLIP draw the stress-strain relationship based on the constitutive model that might have very narrow linear zone. Furthermore, the coefficient of variation (CoV) of NL codes prediction computed by dividing the standard deviation and the mean value is relatively low for all parameters. In conclusion, either both EQL or NL codes based on any soil model and hysteretic behavior predict relatively consistent seismic site response which is make sense since it is still in the linear part.

Table 4-2 Results of computed profiles of PGA, peak shear strain and peak shear stress for the two-layer profile shaken by 0.05g input motion (Group-1) at depth of 9.5 m

Parameters	EQL	OPEN SEES	DS-GQ	DS-MKZ	FLIP	FLAC	NERA	DMOD	median (NL only)	σ std.dev (NL only)	CoV (NL only)
PGA (g)	0.075	0.072	0.076	0.077	0.078	0.075	0.078	0.075	0.076	0.002	3%
Peak Shear Strain (%)	0.0048	0.0048	0.0051	0.005	0.0053	0.0046	0.0051	0.0052	0.0051	0.0002	5%
Peak Shear Stress (kPa)	11.56	11.48	12.06	12.04	*9.95*	11.68	11.97	11.99	11.97	0.75	7%
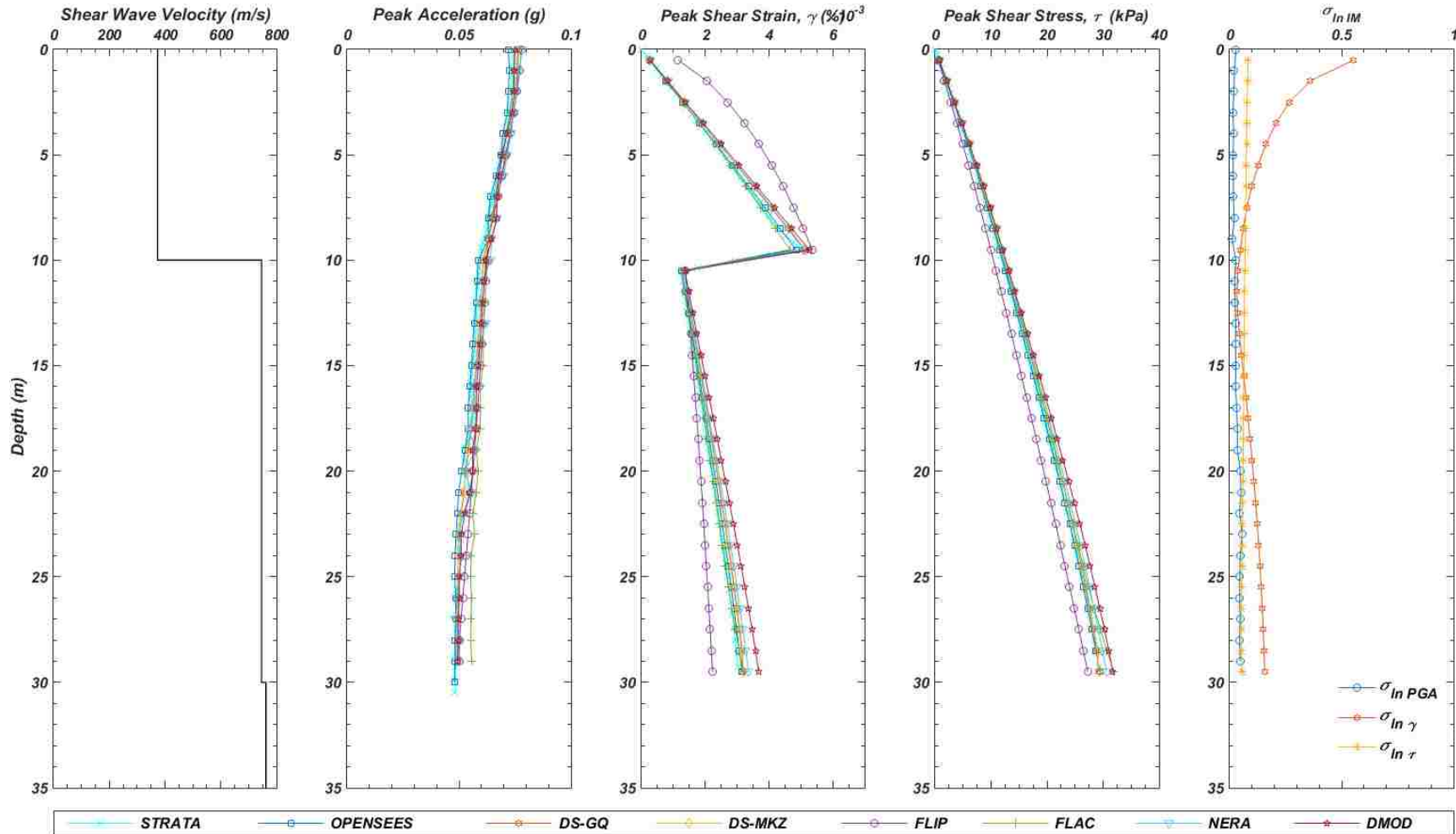
Figure 4.12. Plot of profiles of computed response versus depth representing the variance behavior of very low nonlinearity or very small strain level group (Group-1). The case includes very stiff soil (V_{S30} = 560 m/s) subjected to low intensity motion (PGA = 0.05g) inducing peak shear strain level less than 0.006% at depth of 9.5 m. The plot of standard deviation of natural logarithm indicates that peak shear strain parameter have similarer variability to peak shear stress and PGA at low strain level.

Group 2 (0.9 < G/G_{max} < 0.5 – Small to moderate strain)

The case with parabolic shear wave velocity profile as depicted in Figure 4.13 having V_{S30} of 150 m/s (S_E) subjected to input motion scaled to 0.05g is selected to represent the variance behavior of Group-2. The combination of a soft soil column and weak motion yielded small to moderate shear strain levels with median value 0.051% at the depth of 7.5m. This strain level corresponds to a 46% reduction of shear modulus (G/G_{max} = 0.54) indicating moderate nonlinearity levels. Table 4-3 indicates the increasing of variability as the computation predict larger shear strain level and higher soil nonlinearity behavior compared to what is observed in Group-1. The increasing CoV value indicates that the results have greater deviation. The range of computed PGA (highest to lowest) at ground surface is 0.03g with median value of 0.09g. The highest prediction is given by EQL and NERA, while FLIP and DMOD predict lower PGA value.

Even though it predicts greater deviation, the prediction using EQL and NL codes still give reasonable accuracy at least for PGA value. The discussion of the variability for another S_a at different periods will be presented in the following section. For cyclic strain and stress parameters, Figure 4.13 indicates that FLIP predicts significantly greater shear strain profile that is confirmed later by hysteresis loop plot where it predicts greater cyclic strain with higher damping ratio. In conclusion, at this strain level the prediction of all codes still provide reasonable similarity particularly for PGA parameter, but the role of NL soil model in the site response prediction starts to be an important issue as it is already interact with moderate nonlinearity level.

Table 4-3 Results of computed profiles of PGA, peak shear strain and peak shear stress for the parabolic profiles shaken by 0.05g input motion (Group-2) at depth of 7.5 m

Parameters	EQL	OPEN SEES	DS-GQ	DS-MKZ	FLIP	FLAC	NERA	DMOD	median (NL only)	σ std.dev (NL only)	CoV (NL only)
PGA (g)	0.11	0.10	0.10	0.09	0.08	0.09	0.11	0.08	0.09	0.01	11%
Peak Shear Strain (%)	0.041	0.048	0.052	0.047	0.064	0.045	0.052	0.051	0.051	0.006	12%
Peak Shear Stress (kPa)	9.4	8.5	8.7	8.7	*7.3*	8.1	8.8	7.8	8.5	0.57	7%
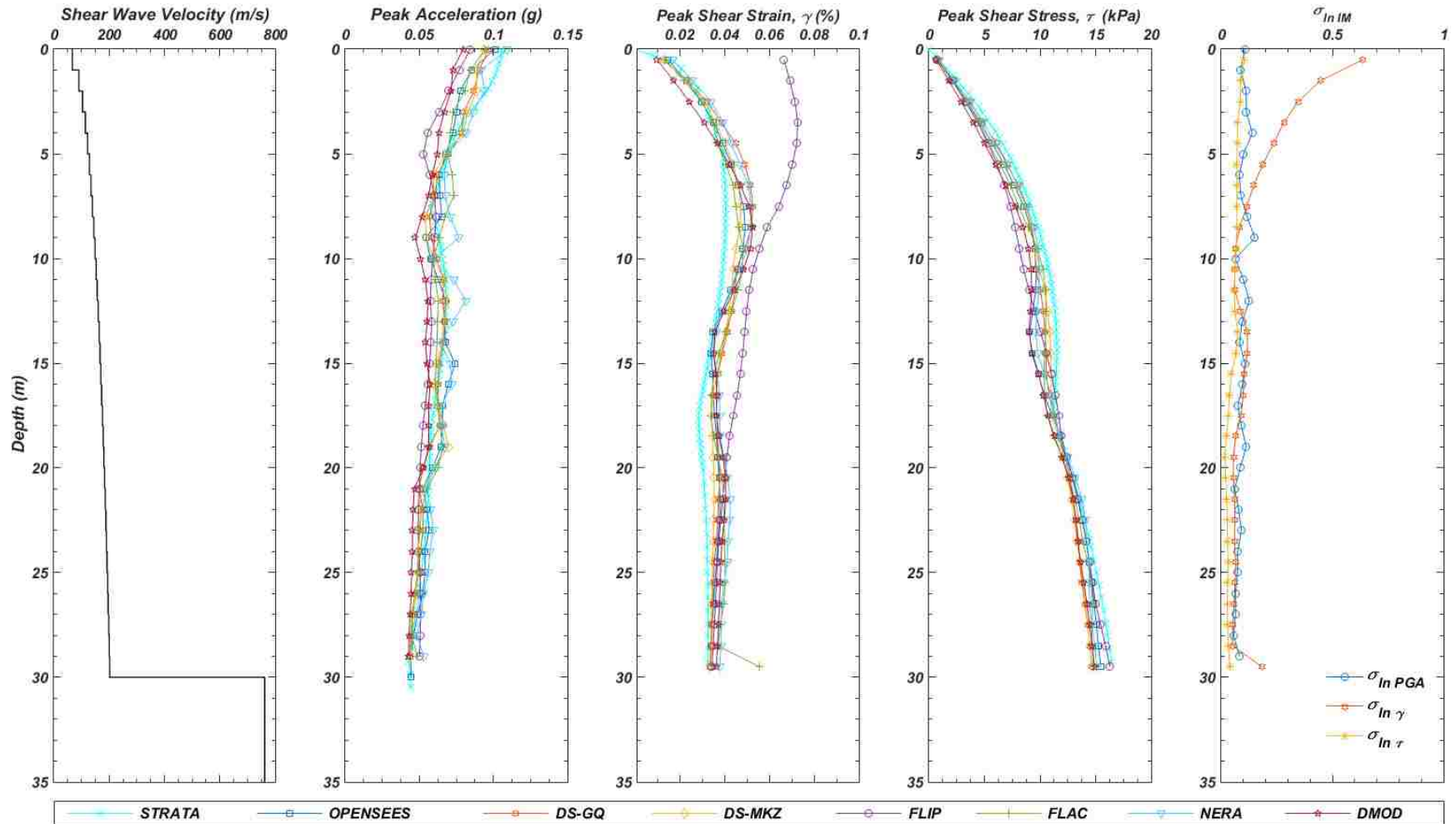
Figure 4.13 Plot of profiles of computed response versus depth representing the variance behavior of low to moderate nonlinearity or small to moderate strain level group (Group-2). The case includes very soft soil (V_{S-30} = 150 m/s) subjected to low intensity motion (PGA = 0.05g) inducing peak shear strain level less than 0.08%. The plot of standard deviation of natural logarithm indicates peak shear strain parameter have similar variability to peak shear stress and PGA at low strain level.

Group 3 (0.5 < G/G_{max} < 0.1 – Large strain)

The case with constant shear wave velocity profile as depicted in Figure 4.14 having V_{S30} of 150 m/s (S_E) subjected to input motion scaled to 0.20g is selected to represent the variance behavior of Group-3. The combination of a soft soil column and moderate intensity motion yielded large shear strain level with median value 0.57% at the depth of 29.5 m. This strain level corresponds to an 84% reduction of shear modulus (*G/G_{max}* = 0.16) indicating high nonlinearity level. Table 4-4 indicates higher variability than what is observed in Group-1 and Group-2. The CoV for PGA and shear strain parameters is up to five times than what was computed in Group-1. The range of computed PGA (highest to lowest) at ground surface is 0.09g with median value of 0.13g. The highest prediction is given by EQL and NERA, while FLIP, FLAC and DMOD predict lowest PGA value.

At this stage, DEEPSOIL and OPENSEES predicted the PGA value within the median range. NERA predicted a higher PGA value indicating the more seismic energy radiated to the ground surface. It is reasonable since NERA does not employ small strain damping (zero at small strain) that allows more energy to be propagated. Moreover, FLIP tends to predict lower intensity motion as shown in the plot of PGA provile versus depth in the Figure 4.14. The variability of the shear strain is even higher than other parameters. At this strain level, the soil has interacted with high soil nonlinearity level and almost reached the peak shear strength of the soil. The NL soil model will sensitively influence the computed response and the EQL codes are no longer accurate in modeling this phenomenon.

Table 4-4 Results of computed profiles of PGA peak shear strain and peak shear stress for the constant velocity profile shaken by 0.2g input motion (Group-3) at depth of 29.5m

Parameters	EQL	OPEN SEES	DS-GQ	DS-MKZ	FLIP	FLAC	NERA	DMOD	median (NL only)	σ std.dev (NL only)	CoV (NL only)
PGA (g)	0.21	0.13	0.15	0.14	0.12	0.12	0.18	0.12	0.13	0.02	16%
Peak Shear Strain (%)	0.3	0.49	0.75	0.66	0.57	0.9	0.52	0.55	0.57	0.147	23%
Peak Shear Stress (kPa)	39	29	31	30	29	32	30	31	30	1.11	4%
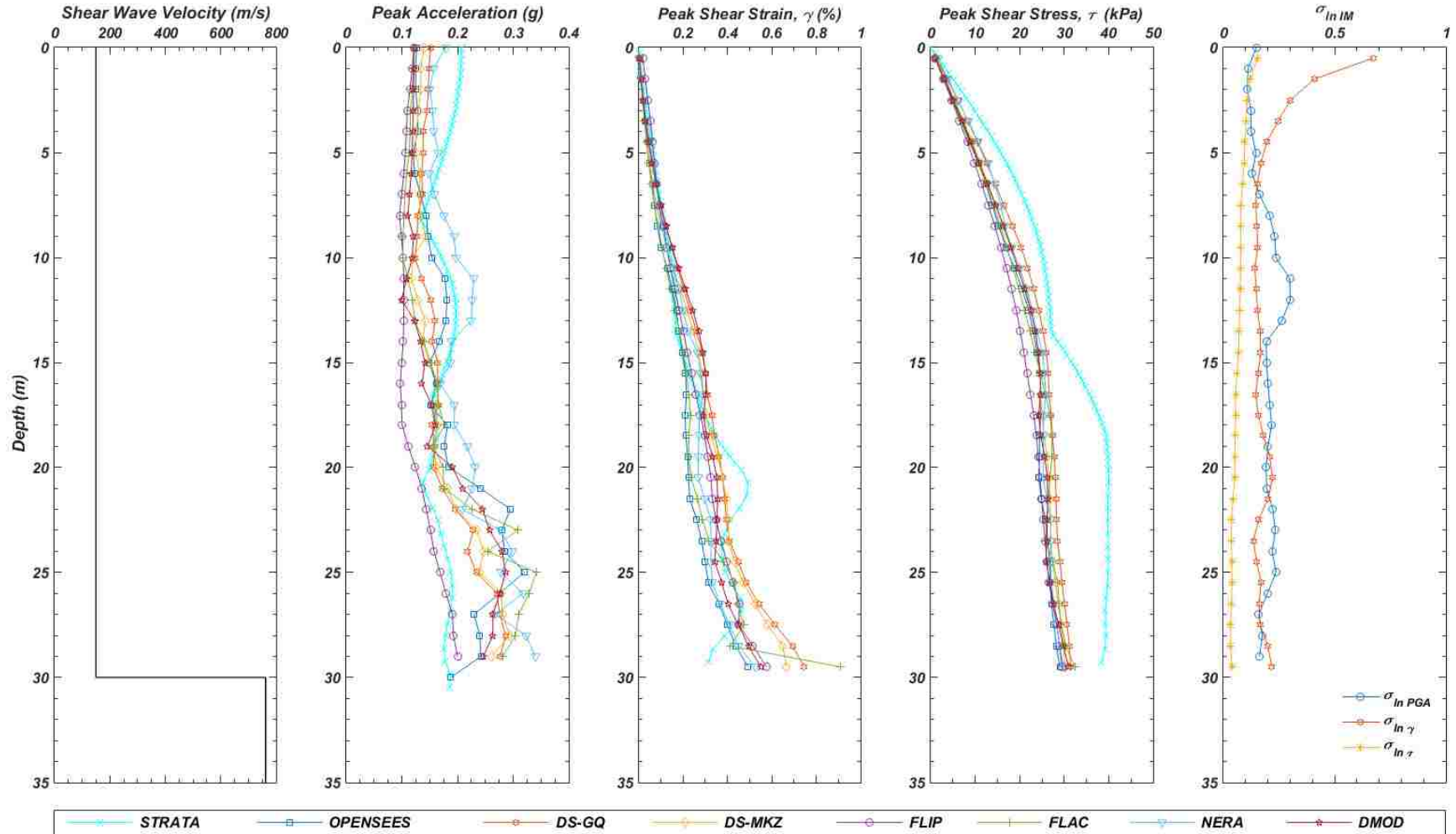
Figure 4.14 Plot of profiles of computed response versus depth representing the variance behavior of high nonlinearity or large strain level group (Group-3). The case includes very soft soil (V_{S30} = 150 m/s) subjected to medium intensity motion (PGA = 0.2 g) inducing peak shear strain level less than 1 %.

It can be seen that EQL codes predict stiffer behavior with higher prediction of shear stress and lower prediction of shear strain (Table 3-4). In conclusion, the prediction of all codes will be sensitively depends on the role of NL soil model at this stage since it has already interacted with high soil nonlinearity level.

Group 4-a and 4-b (0.1 < G/G$_{max}$ – Very large strain)

The case with constant shear wave velocity profile (Figure 4.15) having V$_{S30}$ of 270 m/s (S_D) subjected to input motion scaled to 0.50g is selected to represent the variance behavior of Group-4. The combination of a soft soil column shaken by high intensity motion yields very large shear strain levels with a median value of 2.32% at the depth of 30.0 m. This strain level corresponds to a 98% reduction of shear modulus (G/G_{max} = 0.02) indicating a very high nonlinearity level.

Table 4-5 indicates that the CoV for PGA and shear strain parameters are up to seven times larger than those computed for Group-1. The range of computed PGA (highest to lowest) at ground surface was 0.16g with a median value of 0.13g. The highest prediction was given by EQL and NERA, while FLIP predicted the lowest PGA value. At this stage, DEEPSOIL was relatively consistent in predicting PGA values within the median range. NERA tended to predict higher PGA value as described earlier due to the exclusion of small strain damping. Moreover, FLIP tended to predict lower intensity motion as shown in the plot of PGA profile versus depth in the Figure 4.15.

The variability of the shear strain was even higher and the shear stress due to seismic loading at this level reached the shear strength of the soil. The codes based on the nonlinear function to construct the NL soil model (i.e., DS-MKZ, D-MOD2000, FLAC) does not have ability to capture the peak strength aspect as explained in Chapter Three. If the model predicts shear stress higher than the shear strength it would underestimate the developed shear strain or below the median value (refer to Table 3-5). This aspect is well captured by NL codes that takes into account the peak strength of the soil (i.e., DS-GQ, OPENSEES, NERA and FLIP). In conclusion, at this strain level, the soil has reached the peak shear strength of the soil and the NL soil model that is incapable to predict this aspect is no longer accurate to compute the site respons.

The CoV for shear stress for Group-4 considered only results of OPENSEES, DS-GQ/H and FLIP since only these three codes that capable of predicting the peak strength. As the shear stress approaching the peak strength of the soil, the CoV is small.
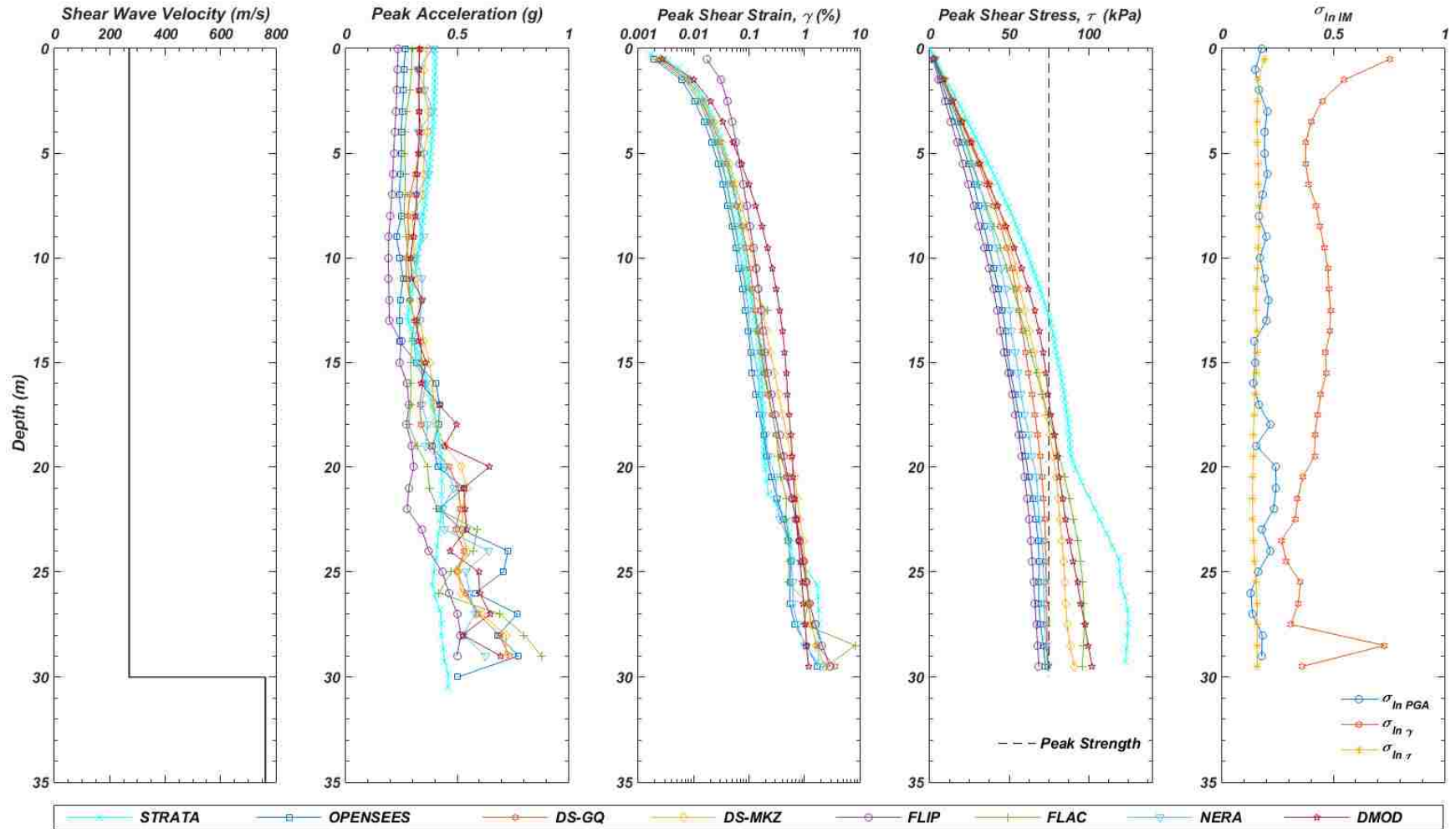
Figure 4.15 Plot of profiles of computed response versus depth representing the variance behavior of very high nonlinearity or very large strain level group (Group-4a). The case includes stiff soil (V_{S30} = 270 m/s) subjected to high intensity motion (PGA = 0.5g) inducing peak shear strain level up to 10% and shear stress approaching the peak strength of the soil. Note the logarithmic scale for shear strain. The plot of standard deviation of natural logarithm indicates that peak shear strain parameter have higher variability than peak shear stress and PGA.

Table 4-5 Results of computed profiles of PGA peak shear strain and peak shear stress for the constant velocity profile shaken by 0.50g input motion (Group-4a) at depth of 29.5m

Parameters	EQL	OPEN SEES	DS-GQ	DS-MKZ	FLIP	FLAC	NERA	DMOD	median (NL only)	σ std.dev (NL only)	CoV (NL only)
PGA (g)	0.40	0.27	0.33	0.37	0.24	0.30	0.39	0.33	0.32	0.05	17%
Peak Shear Strain (%)	1.8	1.73	3.56	2.32	2.91	2.49	2.03	1.18	2.32	0.779	34%
Peak Shear Stress (kPa)	125	73	74.54	91.07	*68.69*	95.97	74	102.3	74.54	13.3	2%

For the higher strain levels in Group-4, the two-layer shear wave velocity profile (Figure 4.16) having V_{S30} of 150 m/s (S_E) subjected to input motion scaled to 1.0g is selected to add another analysis for Group-4. The combination of a soft soil column with a strong impedance contrast shaken by very high intensity motion yielded very large peak shear strain level with a median value of 5.56% at a depth of 29.5 m. This strain level corresponds to a 99% of reduction of shear modulus ($G/G_{max} = 0.01$) indicating extremely nonlinearity level.

Table 4-6 indicates that the CoV for PGA and shear strain parameters is up to 10 times larger than what was computed for Group-1. The range of computed PGA (highest to lowest) at ground surface is 0.16g with a median value of 0.173g with CoV of 21%. The highest prediction was given by EQL and NERA, while FLIP predicted the lowest PGA value. At this stage, DEEPSOIL predicted the PGA values within the median range. NERA tended to predict higher PGA value as described earlier due to the exclusion of small strain damping. Moreover, FLIP tended to predict lower intensity motion as shown in the plot of PGA profile versus depth in the Figure 4.16.

Table 4-6 Results of computed profiles of PGA peak shear strain and peak shear stress for the soft two-layer profile shaken by 1.0g input motion (Group-4b) at depth of 29.5m

| Parameters	EQL	OPEN SEES	DS-GQ	DS-MKZ	FLIP	FLAC	NERA	DMOD	median (NL only)	σ std.dev (NL only)	CoV (NL only)
PGA (g)	0.339	0.223	0.236	0.238	0.196	0.251	0.366	0.260	0.253	0.053	21%
Peak Shear Strain (%)	1.59	9.35	10.85	5.593	3.038	4.414	10.4	2.463	5.593	3.55	54%
Peak Shear Stress (kPa)	75	48.71	49.83	61.99	*46.8*	72.25	49.81	76.27	49.83	12.23	1%
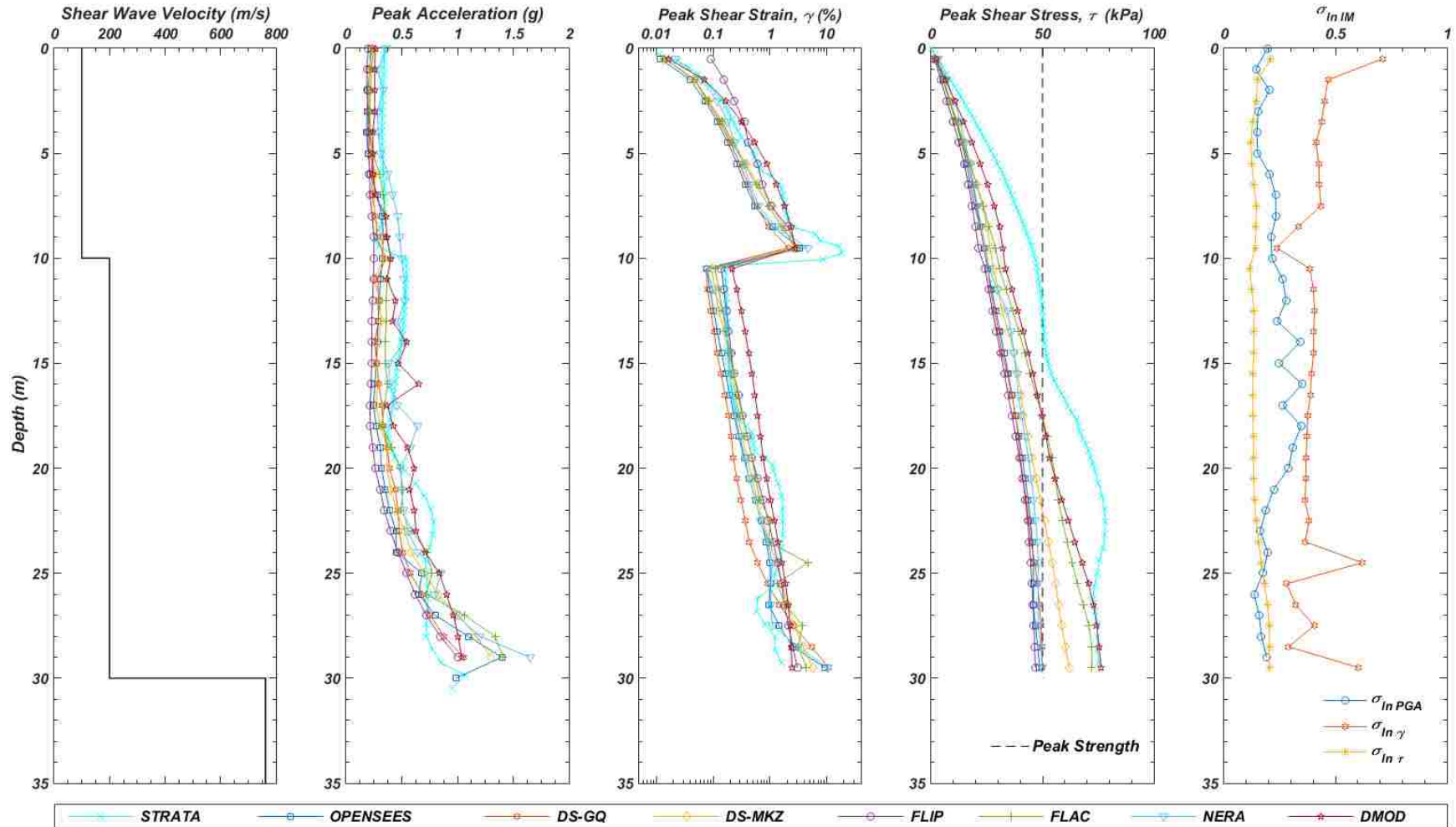
Figure 4.16 Plot of profiles of computed response versus depth representing the variance behavior of very high nonlinearity or very large strain level group (Group-4b). The case includes soft soil (V_{S30} = 150 m/s) subjected to very high intensity motion (PGA = 1.0g) inducing peak shear strain level more than 10% and shear stress approaching the peak strength of the soil. Note the logarithmic scale for shear strain. The plot of standard deviation of natural logarithm indicates that peak shear strain parameter have higher variability than peak shear stress and PGA.

4.4.3   *Response Spectrum*

Spectral acceleration is an important parameter for design in engineering practice. The previous section discussed the variability of this parameter only at a single period (zero seconds, i.e., PGA). This section presents the variability of computed spectral acceleration for a wide range of periods utilizing the response spectrum concept as shown in Figures 4.17 - 4.21. Additionally, the amplification factor correspond to the ratio of the spectral acceleration at ground surface and bedrock is also discussed.

Group 1 (1.0 < G/G_{max} < 0.9 – Very small strain)

The variability of spectral acceleration at higher periods was relatively similar indicating that the prediction of acceleration time-histories from all codes were nearly identical. Figure 4.17 indicates that the highest variability was at periods close to natural site periods where for Group-1 is 0.21 sec. In conclusion, at this strain level, all codes predicted similar results even through small variability was observed at periods close to the site period. It could predict similar shape of response spectra indicating similar prediction of acceleration time-histories. Regarding the amplification factor, the EQL and NL codes representing by each median tended to predict identical amplification ratios.

Group 2 (0.9 < G/G_{max} < 0.5 – Small to moderate strain)

The spectral acceleration tended to deviate to each other at periods of 0.06 to 0.8 seconds where the natural site period for this case was 0.21 sec as presented in Figure 4.18. The median value of amplification factor predicted by NL codes was still relatively similar to what is predicted by EQL.

Group 3 (0.5 < G/G_{max} < 0.1 – Large strain)

Figure 4.19 shows that NERA predicted higher spectral accelerations at low period but slightly lower values at periods higher than the natural period of the site. EQL predicts the highest prediction at the natural site period. There is a significant variability at this strain level that causes the median amplification factor predicted by NL codes to deviate from those predicted by EQL.

Group 4 (0.1 < G/G_{max} – Very large strain)

At this strain level, EQL predicted higher spectral acceleration of most periods. The variability in Group-4 was huge with prediction of the spectral ranging from 0.4 to 0.8 g even at higher periods (for example at T = 1 sec). The median value of amplification factor predicted by NL codes was lower than predicted by EQL in most of the period indicating the nonlinearity effect.
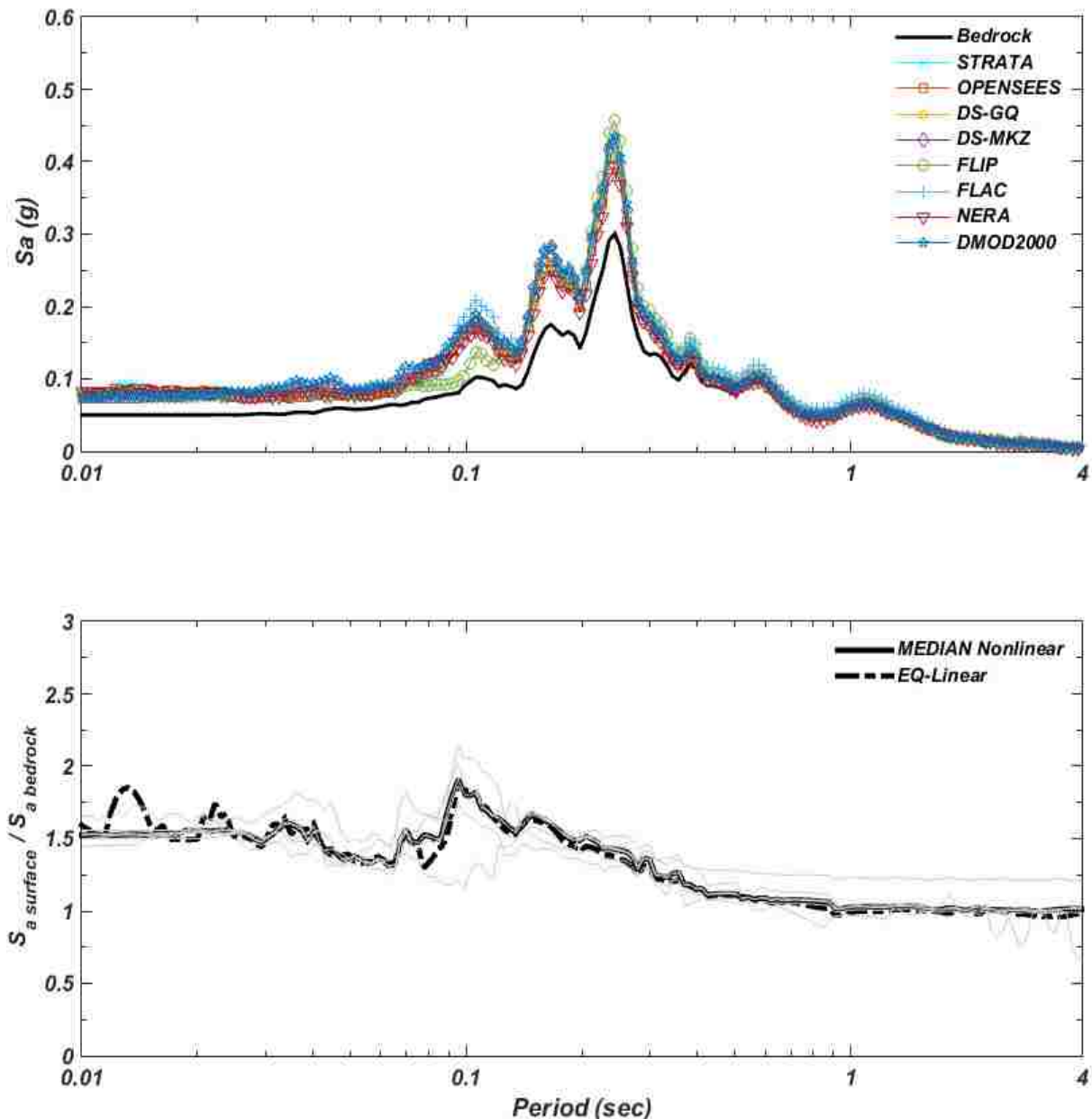
Figure 4.17. Plot of response spectrum at ground surface and amplification ratio (surface / bedrock) predicted by all codes for Group-1 case. The computed value is similar to each other at very small strain level. The natural site period for this case is 0.21 sec.
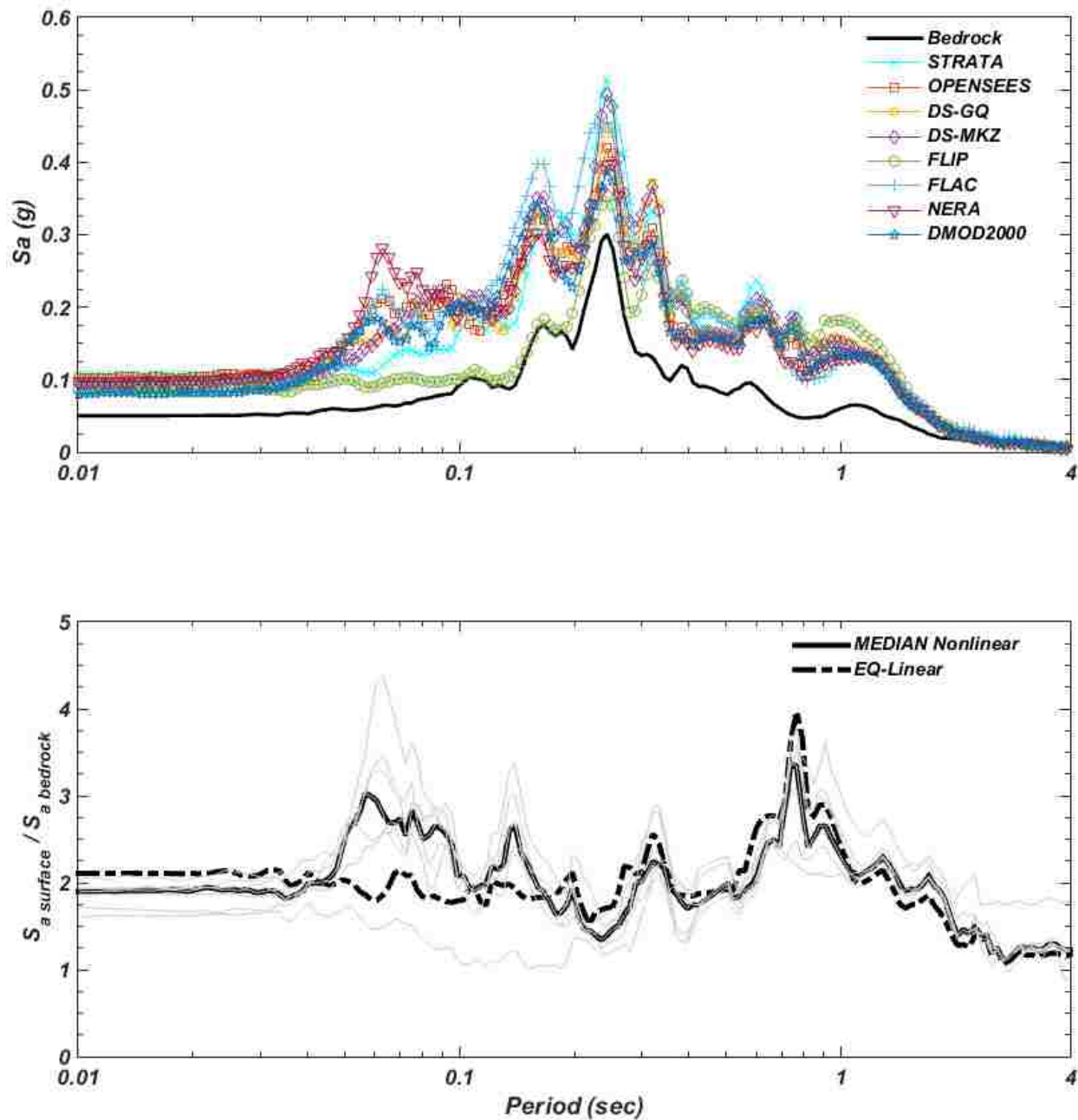
Figure 4.18. Plot of response spectrum at ground surface and amplification ratio (surface / bedrock) predicted by all codes for Group-2 case. The deviation of computed value started to increase at small to moderate shear strain level. The natural site period for this case is 0.21 sec.
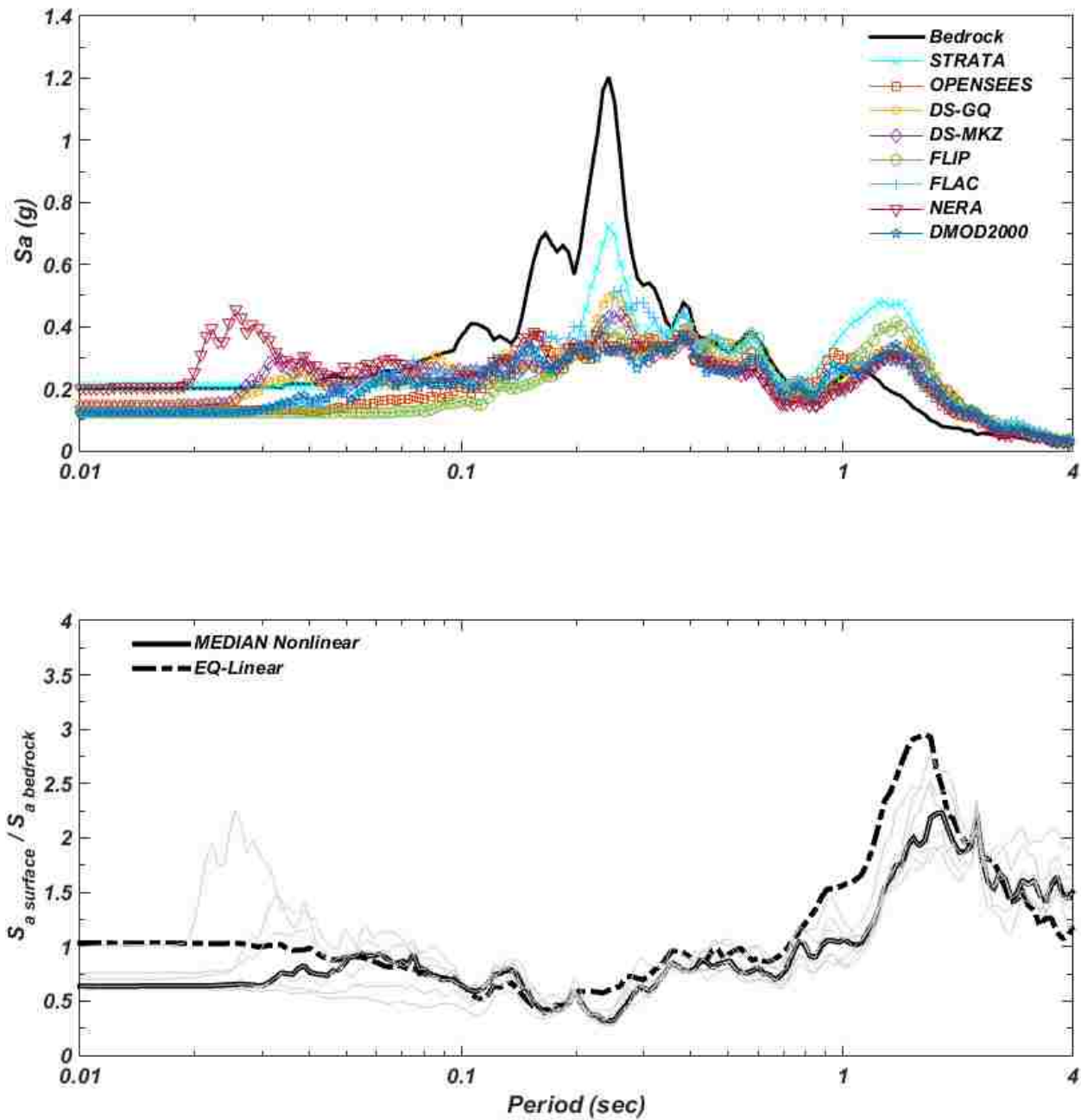
Figure 4.19 Plot of response spectrum at ground surface and amplification ratio (surface / bedrock) predicted by all codes for Group-3 case. The natural site period for this case is 0.44 sec.
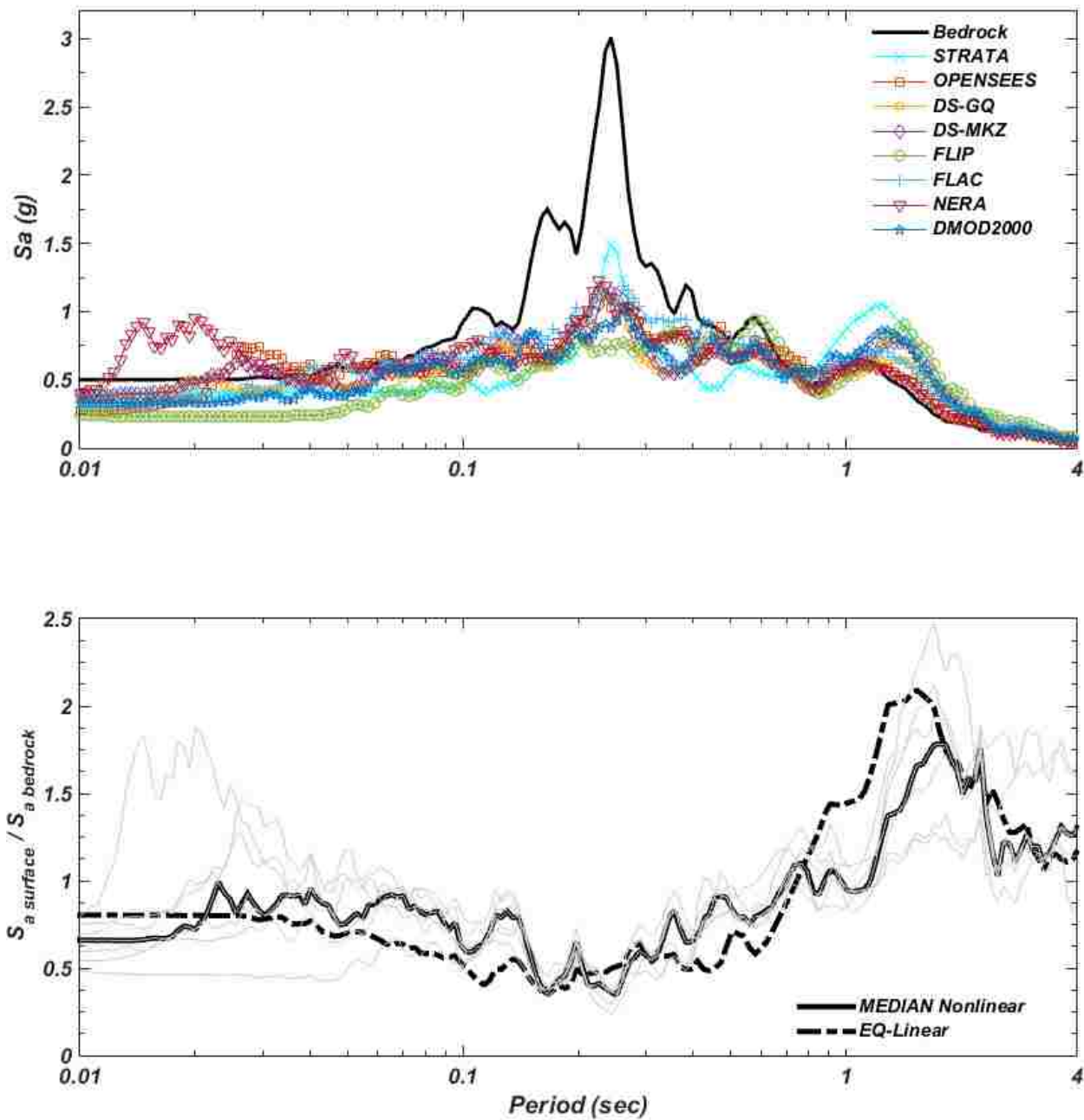
Figure 4.20 Plot of response spectrum at ground surface and amplification ratio (surface / bedrock) predicted by all codes for Group-4a case. The natural site period for this case is 0.8 sec
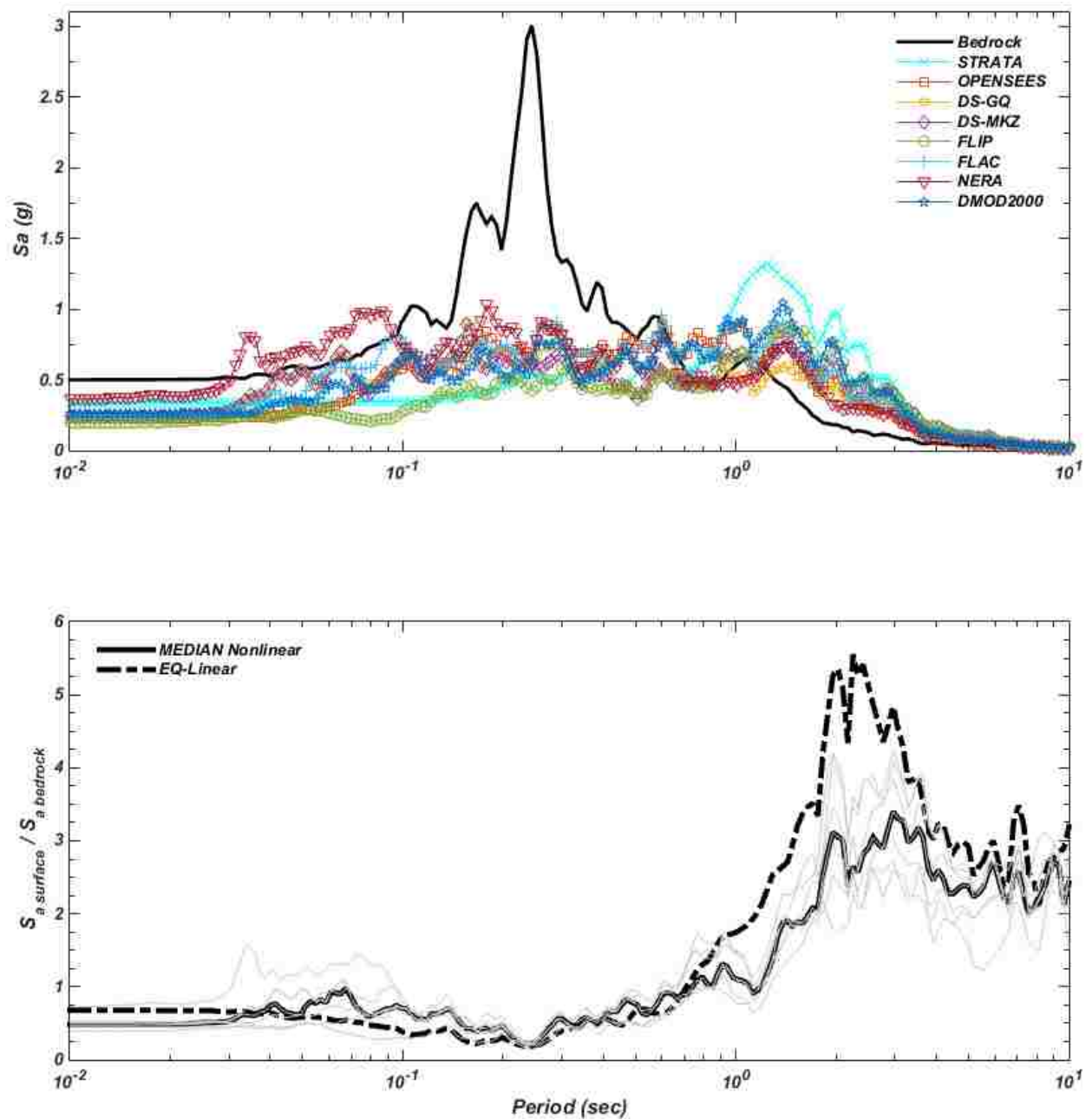
Figure 4.21 Plot of response spectrum at ground surface and amplification ratio (surface / bedrock) predicted by all codes for Group-4b case. The natural site period for this case is 0.8 sec

4.4.4   *Hysteresis Loops*

This section reviews the performance of each soil model in predicting the stress-strain curve for each strain level group. Figures 4.22 to 4.26 present plots of the results while the important aspect of a soil model such as peak strength correction and hysteretic damping will be discussed. Based on the results presented in section 4.4.2, each plot of stress-strain curve presented in this section was taken from the depth at which the maximum peak shear strain was developed.

Group 1 (1.0 < G/G$_{max}$ < 0.9 – Very small strain)

According to results in section 4.4.2, the stress-strain curves representing the maximum peak shear strain value for Group 1 (Figure 4.12) were recorded at depth of 9.5 m (Layer-10). At this depth, the soil had peak shear strength of 208 kPa at an effective stress of 82.5 kPa. The hysteresis loop are nearly straight lines indicating linear behavior at small strain levels with near zero damping ratio as shown in Figure 4.22. As described earlier, the prediction given by EQL and NL codes were similar at very small strain levels (Group-1). All NL codes except FLIP, predicted similar stiffness with small variations in the peak cyclic strain and cyclic stress ratio.

Group 2 (0.9 < G/G$_{max}$ < 0.5 – Small to moderate strain)

According to results in section 4.4.2, the stress-strain curves representing the maximum peak shear strain value for Group 2 (Figure 4.13) were recorded at depth of 7.5 m (Layer-8). At this depth, the soil had peak shear strength of 23 kPa at an effective stress of 50.2 kPa. The predictied slope of the stress-strain curve was similar between EQL and NL codes except that FLIP predicted slightly lower stiffness as indicated in Figure 4.23. FLIP does not employ the target G/G$_{max}$ curve as implemented in the other codes, instead it follows an advanced constitutive model to construct the stress-strain curve. This model tends to exhibit a very small linear portion and becomes nonlinear at lower strains than the other codes.

The stress-strain curve for Group 2 exhibits hysteretic damping starting to develop as the shear strain increases. DEEPSOIL utilizes the MRDF concept to construct the hysteretic damping and it represents relatively smaller damping ratio (hysteresis loop area) compare to what is predicted by

Figure 4.22. Plot of stress-strain curve predicted by all codes at very small strain and very low nonlinearity level (Group-1). The plot was taken at depth of 9.5 m of two-layered profile (S$_C$) shaken by PGA = 0.05g.All codes predict similar cyclic stress and cyclic strain indicating similar stiffness at linear zone.
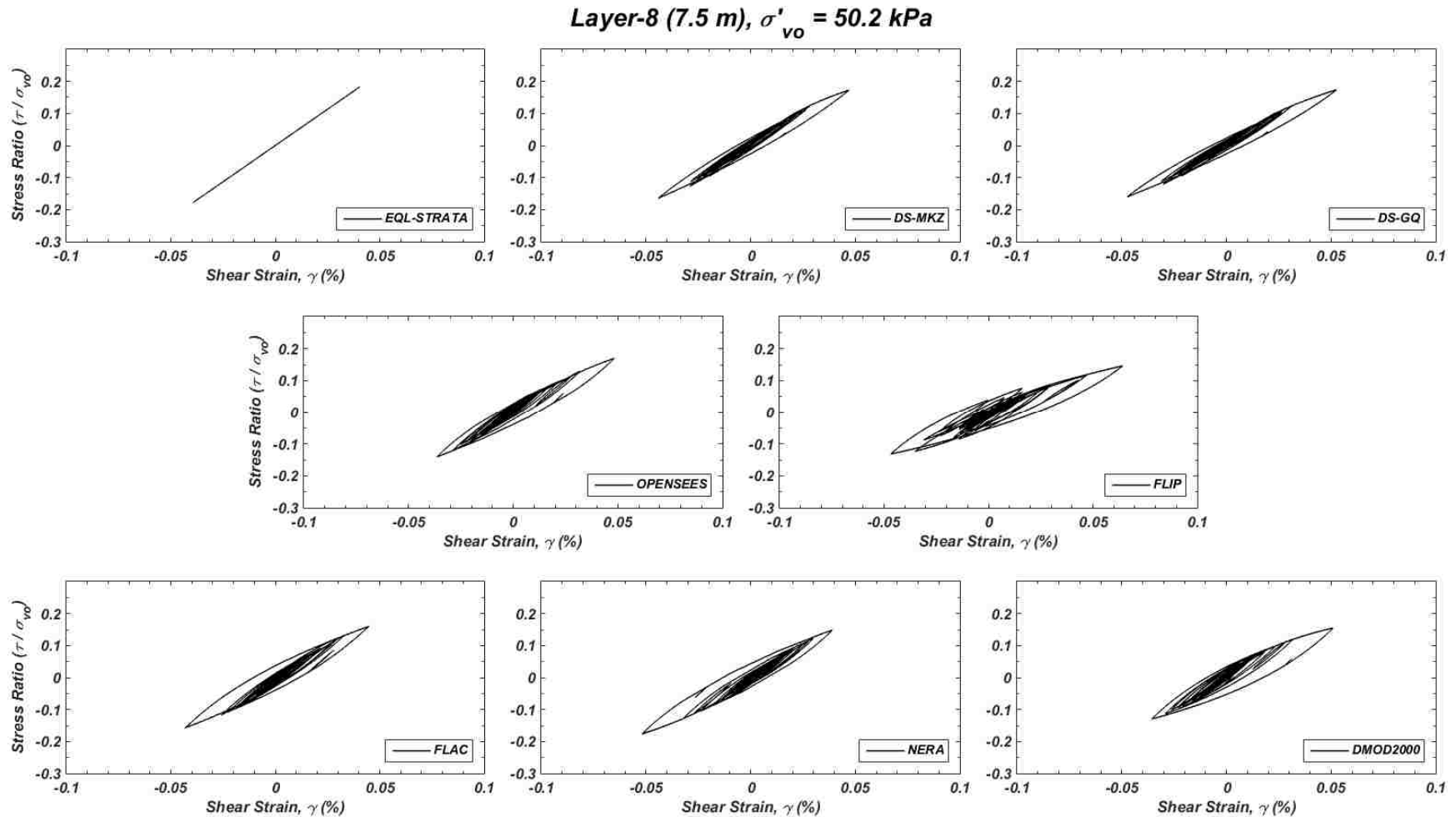
Figure 4.23. Plot of stress-strain curve predicted by all codes at small to moderate strain and low to moderate nonlinearity level (Group-2). The plot was taken at depth of 7.5 m of parabolically increasing velocity profile (S_E) shaken by PGA = 0.05g. All predictions tend to give similar stiffness compared to EQL result although the NL code started to predict damping effect.

other codes in Figure 4.23. Furthermore, the NL codes based on Masing rules (i.e., OPENSEES, FLAC, NERA and D-MOD2000) predicted similar damping behavior.

Group 3 (0.5 < G/G$_{max}$ < 0.1 – Large strain)

According to results in section 4.4.2, the stress-strain curves representing the maximum peak shear strain value for Group 3 (Figure 4.14) were recorded at depth of 29.5 m (Layer-30). At this depth, the soil had peak shear strength of 35 kPa at an effective stress of 198 kPa. At this strain level, the general slope of stress-strain curve predicted by EQL is relatively stiffer than NL codes as indicated in Figure 4.24. The backbone curve and hysteretic damping rules play the most important role for the site response prediction for Group-3. As describer earlier, DEEPSOIL predicts relatively smaller damping ratio (hysteresis loop area) compare to what is predicted by other codes in Figure 4.24. Moreover, the NL codes based on Masing rules (i.e., OPENSEES, FLAC, NERA and D-MOD2000) predicts similar damping behavior. At this strain level, most of NL codes gives reasonable prediction of the cyclic behavior of the soil although the codes based on Masing's rules may predict slightly greater damping than what is actually exists.

Group 4 (0.1 < G/G$_{max}$ – Very large strain)

According to results in section 4.4.2, the stress-strain curves representing the maximum peak shear strain value for Group 4 (Figure 4.15) were recorded at depth of 29.5 m. At this depth, the soil had peak shear strength of 75 kPa at an effective stress of 227 kPa. At this strain level, the soil has reached the shear strength of the soil indicating high soil nonlinearity level. The EQL code is no longer able to predict the cyclic soil behavior accurately at this stage of loading. Figure 4.25 shows that the EQL code predict shear stress exceeding the peak strength of the soil which is impossible. DS-MKZ utilize an equation to construct the backbone curve and MRDF procedure to construct the unloading-reloading behavior. The result shows that this model is incapable of reaching the peak shear strength of the soil. Furthermore, DS-GQ is the new model that can capture this important aspect. However, even though the damping formulation is better than Masing rules, the model does not approach the peak shear strength smoothly, which is different than actual soil behavior.
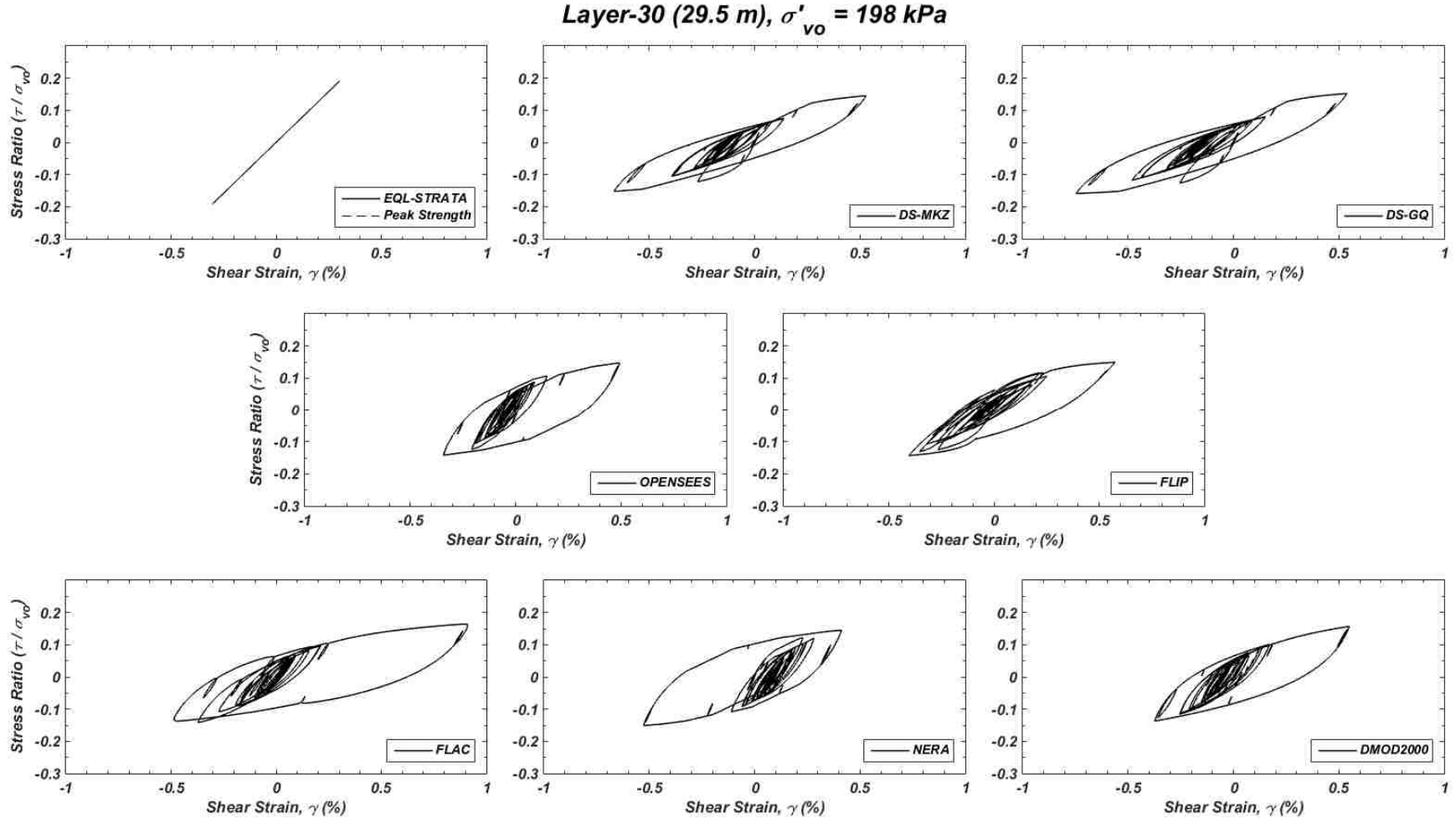
Figure 4.24. Plot of stress-strain curve predicted by all codes at large strain and high nonlinearity level (Group-3). The plot was taken at depth of 29.5 m of constant velocity profile (S$_E$) shaken by PGA = 0.2g. EQL starts to predict stiffer behavior than the prediction of NL codes. Codes those are based on non-Masing rule (DS-MKZ, DS-GQ and FLIP) construct smaller hysteresis loop area than what predicted by Masing's rule codes.
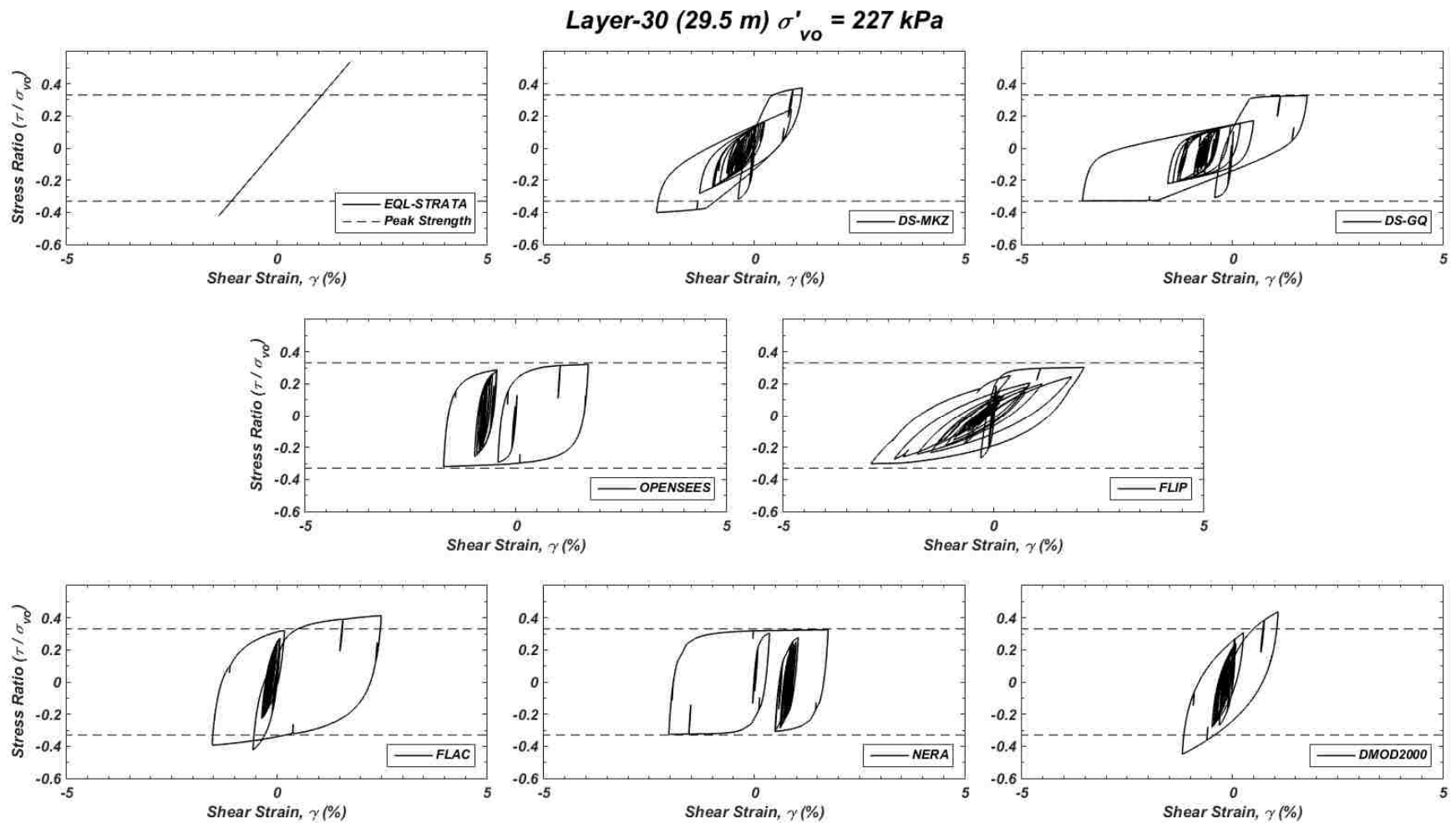
Figure 4.25. Plot of stress-strain curve predicted by all codes at very large strain and very high nonlinearity level (Group-4a). The plot was taken at depth of 29.5 m of constant velocity profile (S$_D$) shaken by PGA = 0.5g. EQL predicts stiffer and unreasonable behavior compared to the prediction of NL codes. NL codes those are used an advanced soil constitutive model has the ability to predict the peak shear strength of the soil.

OPENSEES and NERA utilize the constitutive model proposed by Iwan (1967) and Mroz (1967). This model is capable of tracking any type of stress-strain curve using multi-yield surfaces These two codes relatively give similar behavior where it can approach the peak strength smoothly and it utilize G_{max} value during unloading-reloading stage as shown in Figure 4.25 and Figure 3.26. However, the implementation of Masing rules cause these codes predict unrealistic damping ratio that overpredict what is exactly happening in reality at very large strain.

FLIP utilizes the constitutive model proposed by Towhata & Ishihara (1985) that utilize multi spring model that allow the curve to approach the peak strength smoothly. The stress-strain curve tends to predict reasonable damping behavior since it use the generalized Masing rules (Ishihara et al, 1985). However, it follows a different backbone curve in the early and later stages of loading. The other 2D site response analysis code considered here is FLAC. The sigmoidal-3 model is not capable of approaching the shear strength of the soil and the implementation of Masing rules caused similar problem to what is observed by OPENSEES and NERA. For D-MOD2000, the model does not predict that it will reach a peak value to represent failure. Additional data for Group- 4 is indicated in Figure 4.26. The stress-strain curves representing the maximum peak shear strain value for Group 4b (Figure 4.16) were recorded at depth of 29.5 m. At this depth, the soil had peak shear strength of 50 kPa at an effective stress of 198 kPa. This data also exhibit similar characteristics to what was described before.

In conclusion, codes such as DS-GQ, OPENSEES, FLIP and NERA are capable of predicting the peak shear strength of the soil during cyclic loading. Furthermore, DS-GQ and FLIP utilize non-Masing rules to construct the unloading-reloading behavior that may represent reasonable damping ratio. Lastly, the codes that are incapable of approaching the shear strength of the soil (i.e., DS-MKZ, DMOD2000, FLAC) generally predict lower shear strain level at high shear strain level. This makes sense, since in order to absorb similar seismic energy similar hysteresis loop area is required. When the stress-strain curve cannot increase in shear stress axis, the shear strain will consequently increase to accommodate similar hysteresis loop area.
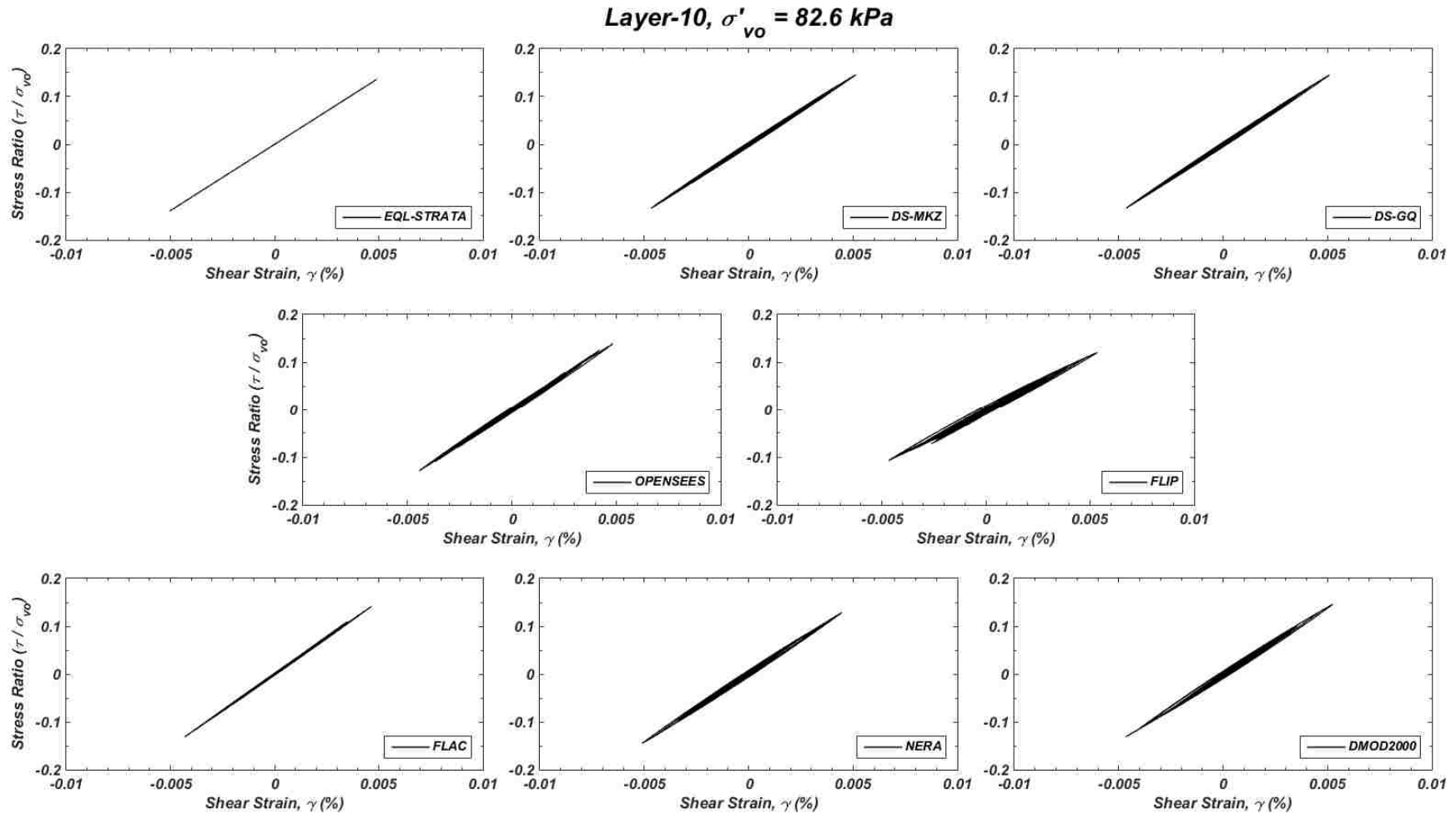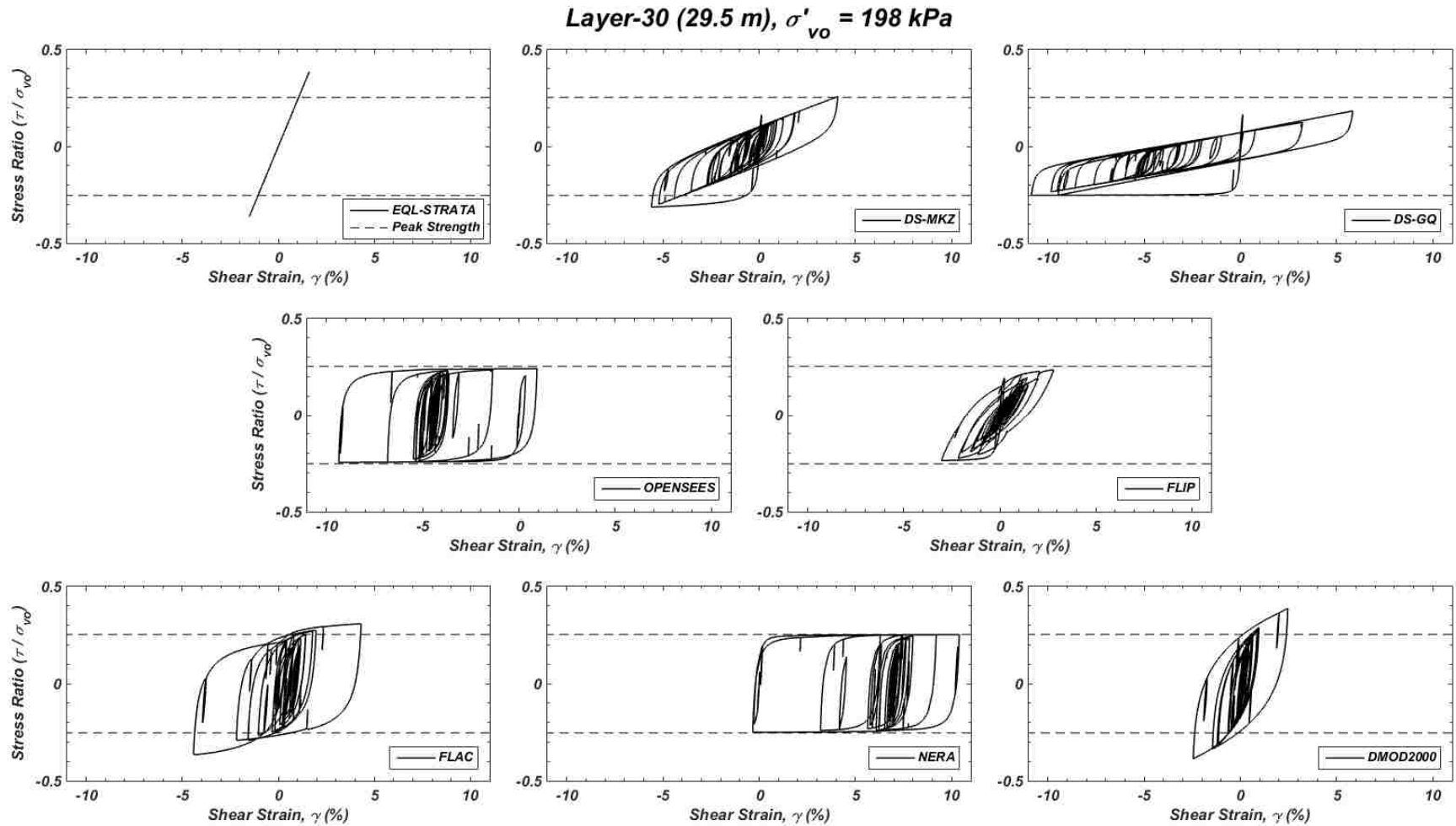
Figure 4.26. Plot of stress-strain curve predicted by all codes at very large strain and very high nonlinearity level (Group-4b). The plot was taken at depth of 29.5 m of two-layered profile (S_E) shaken by PGA = 1.0g. EQL predicts stiffer and unreasonable behavior compared to the prediction of NL codes. NL codes those are used an advanced soil constitutive model has the ability to predict the peak shear strength of the soil.

4.4.5   *Significant Duration and Intensity*

The durations of ground motion time histories are related to the duration for releasing the accumulated strain energy due to earthquake loading (Kramer, 1996). One of the useful parameter to evaluate duration is Arias Intensity (Arias, 1970). This parameter is obtained by integration of acceleration time histories over the entire earthquake duration. The plot of normalized Arias Intensity is referred to Husid plot that provide information the required time (significant duration) to release 5% to 95% energy as presented in Figure 4.27 to 4.31. As the intensity of input motion increases, the time required to release the energy will increase. This section present discussion regarding the duration and intensity variability predicted by each codes.

Group 1 (1.0 < G/G$_{max}$ < 0.9 – Very small strain)

At very small strain level, all codes predict similar response (e.g., acceleration time histories, PGA, shear strain, shear stress) since it is still in the linear portion of the stress-strain curve. The Arias Intensity (AI) predicted by all codes are similar as well with CoV of about 6%. The range of computed AI is 0.014 m/s with median of 0.0693. The Husid plot for Group-1 can be seen in Figure 4.27 that indicates relatively identical shape of normalized AI. The significant duration measured the duration from 5% energy released to 95% level is about 11 seconds and all codes predict identical results.

Table 4-7 Results of computed ground motion intensity and duration for Group-1

Parameters	EQL	OPEN SEES	DS-GQ	DS-MKZ	FLIP	FLAC	NERA	DMOD	median (NL only)	σ std.dev (NL only)	CoV (NL only)
Arias Intensity (m/s)	0.066	0.063	0.069	0.069	0.074	0.077	0.067	0.071	0.0693	0.0044	6%
Sig. Duration (D$_5$-D$_{95}$)	11.06	11.04	10.99	10.99	10.81	11.92	11.00	10.98	10.99	0.369	3%

Figure 4.27. The plot of normalized Arias intensity to predict required duration in dissipating 95% earthquake intensity for for Group-1. All codes predicts similar significant duration (D_5-D_{95}).

Group 2 (0.9 < G/G_{max} < 0.5 – Small to moderate strain)

As observed in section 3.4.2, the variability starts to increase in Group-2 as the CoV is increased to about double than what was computed in Group-1 (indicated in Table 4-8). The range

of AI for this group is 0.03 m/s with median of 0.167 m/s. FLIP tended to predict lower AI and longer significant duration but the accuracy compared to each other was reasonable. FLAC tended to predict shorter duration indicating that the damping mechanism implemented in the analysis absorbed greater seismic energy (Figure 4.28), as observed in Figure 4.23 where FLAC developed larger hysteresis loop areas than other codes. At this strain level, the performance of EQL and NL codes was relatively similar. The other NL codes excluding FLIP and FLAC predicted relatively similar intensity and significant duration.

Table 4-8 Results of computed ground motion intensity and duration for Group-2

Parameters	EQL	OPEN SEES	DS-GQ	DS-MKZ	FLIP	FLAC	NERA	DMOD	median (NL only)	σ std.dev (NL only)	CoV (NL only)
Arias Intensity (m/s)	0.17	0.16	0.18	0.19	0.14	0.17	0.19	0.16	0.1677	0.017	11%
Sig. Duration (D_5-D_{95})	15.59	15.82	16.25	16.20	17.59	12.72	16.00	16.25	16.195	1.486	9%

Group 3 (0.5 < G/G_{max} < 0.1 – Large strain)

The nonlinearity level of Group 3 correspond to reduction of shear modulus level of 0.16 indicating high nonlinear behavior. At this nonlinearity level, EQL code predicts shorter duration compared to NL codes as shown in Figure 4.29 due to stiffer prediction of the site response. This behavior might underestimate the intensity motion at the ground motion. Table 4-9 listed that FLAC tends to predict shorter duration than other NL codes due to higher damping ratio developed as shown in Figure 4.24. In conclusion, at this strain level the prediction of EQL and NL codes is no longer give similar prediction.

Group 4 (0.1 < G/G_{max} – Very large strain)

Table 4-10 and Table 4-11 listed the prediction results of AI and significant duration for all codes for very large strain level. The D_5-D_{95} is getting higher as the intensity motion increased with median value of 18.29 seconds and 26.5 seconds respectively. The EQL codes still predict shorter duration than what is predicted by NL codes. Figure 4.30 and Figure 4.31 present the Husid

plot predicted by all codes. General prediction of the surface motion intensity and duration present consistent variance behavior from small to large strain level as indicated by increasing CoV value and increasing D_5-D_{95}. It supports what is observed in section 3.4.2 that a single analysis using soil model might be is not sufficient to give an accurate prediction due to a lot of uncertainties.

Table 4-9 Results of computed ground motion intensity and duration for Group-3

Parameters	EQL	OPEN SEES	DS-GQ	DS-MKZ	FLIP	FLAC	NERA	DMOD	median (NL only)	σ std.dev (NL only)	CoV (NL only)
Arias Intensity (m/s)	0.58	0.49	0.51	0.47	0.53	0.57	0.65	0.49	0.508	0.062	12%
Sig. Duration (D_5-D_{95})	15.90	19.85	19.96	20.1	20.03	17.49	19.84	20.00	19.95	0.939	5%

Table 4-10 Results of computed ground motion intensity and duration for Group-4a

Parameters	EQL	OPEN SEES	DS-GQ	DS-MKZ	FLIP	FLAC	NERA	DMOD	median (NL only)	σ std.dev (NL only)	CoV (NL only)
Arias Intensity (m/s)	2.16	2.94	2.24	2.49	2.78	3.14	3.60	2.81	2.81	0.439	15%
Sig. Duration (D_5-D_{95})	15.16	18.04	20.33	19.86	22.37	16.70	17.58	18.29	18.29	1.939	10%

Table 4-11 Results of computed ground motion intensity and duration for Group-4b

Parameters	EQL	OPEN SEES	DS-GQ	DS-MKZ	FLIP	FLAC	NERA	DMOD	median (NL only)	σ std.dev (NL only)	CoV (NL only)
Arias Intensity (m/s)	4.68	4.26	2.50	3.15	3.07	4.44	5.80	4.70	4.26	0.004	29%
Sig. Duration (D_5-D_{95})	25.12	26.3	28.995	28.26	28.73	23.86	26.02	26.505	26.505	0.369	7%
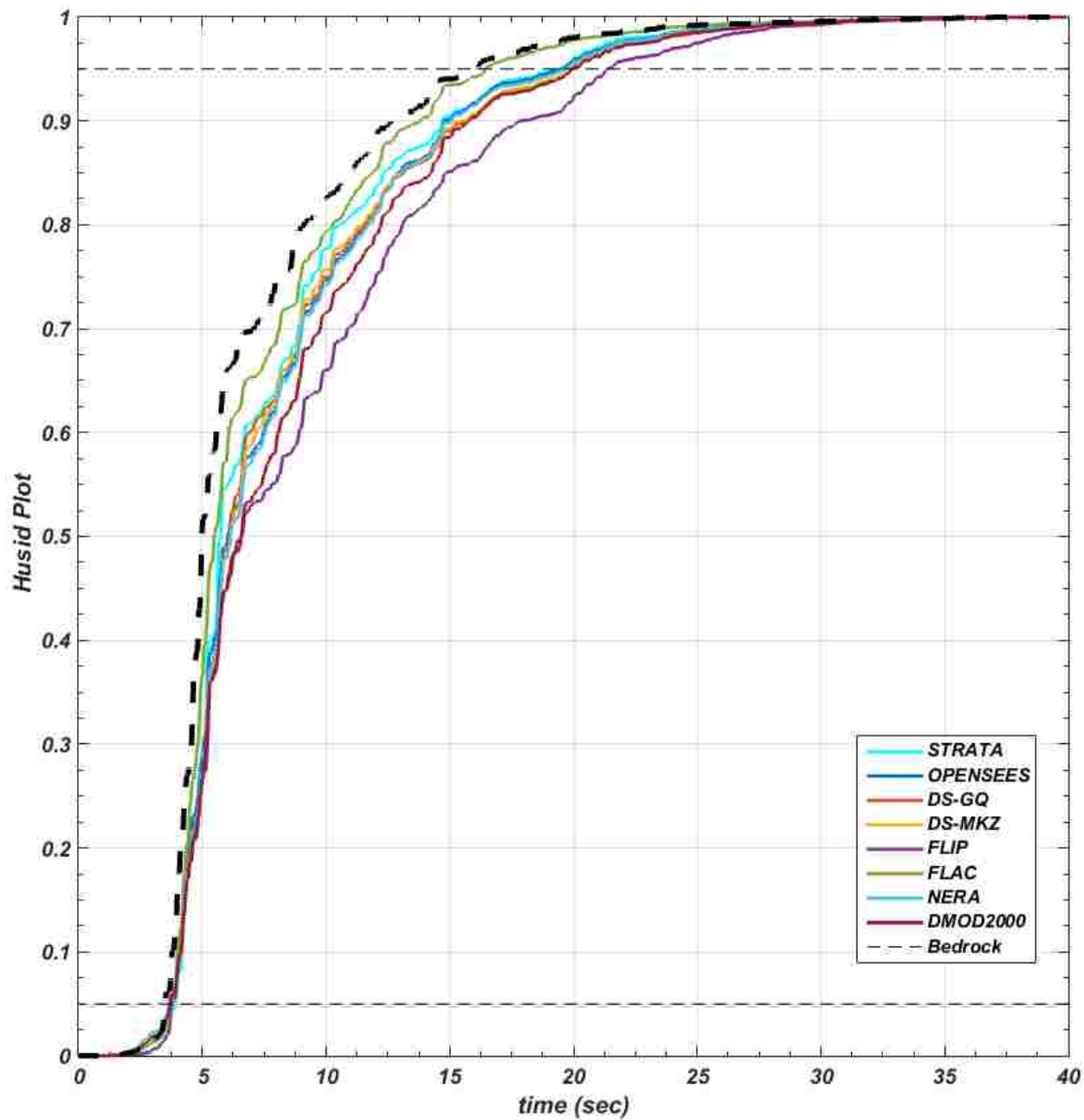
Figure 4.28. The plot of normalized Arias intensity to predict the required duration in dissipating 95% earthquake intensity for Group-2. The variability of significant duration prediction start to increase at small to moderate nonlinearity level.
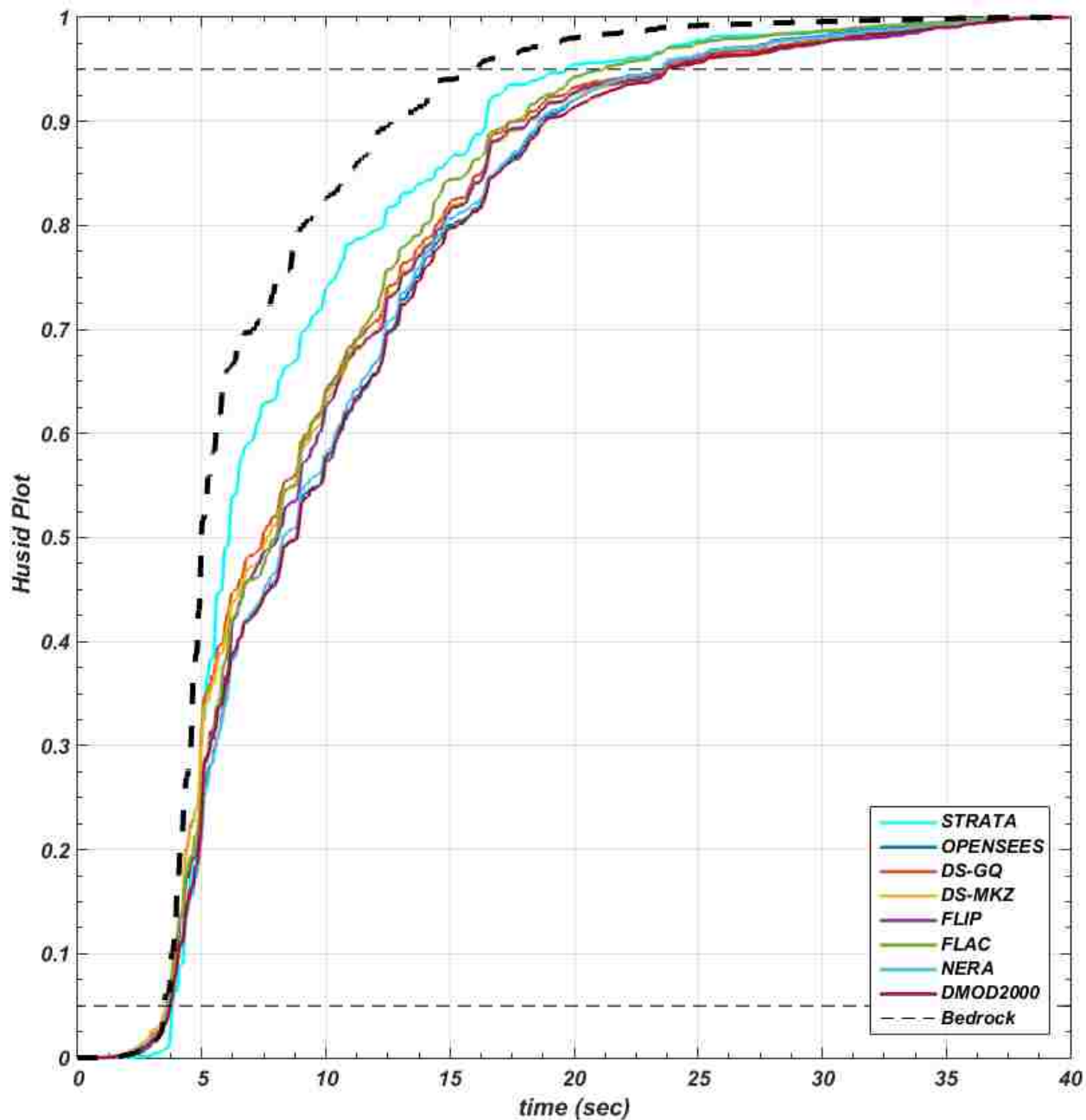
Figure 4.29. The plot of normalized Arias intensity to predict the required duration in dissipating 95% earthquake intensity for Group-3. The variability of significant duration prediction start to increase and longer duration is computed due to stronger intensity motion. At this strain level, EQL is no longer give accurate prediction and it gives shorter duration indicating stiffer behavior of the soil column
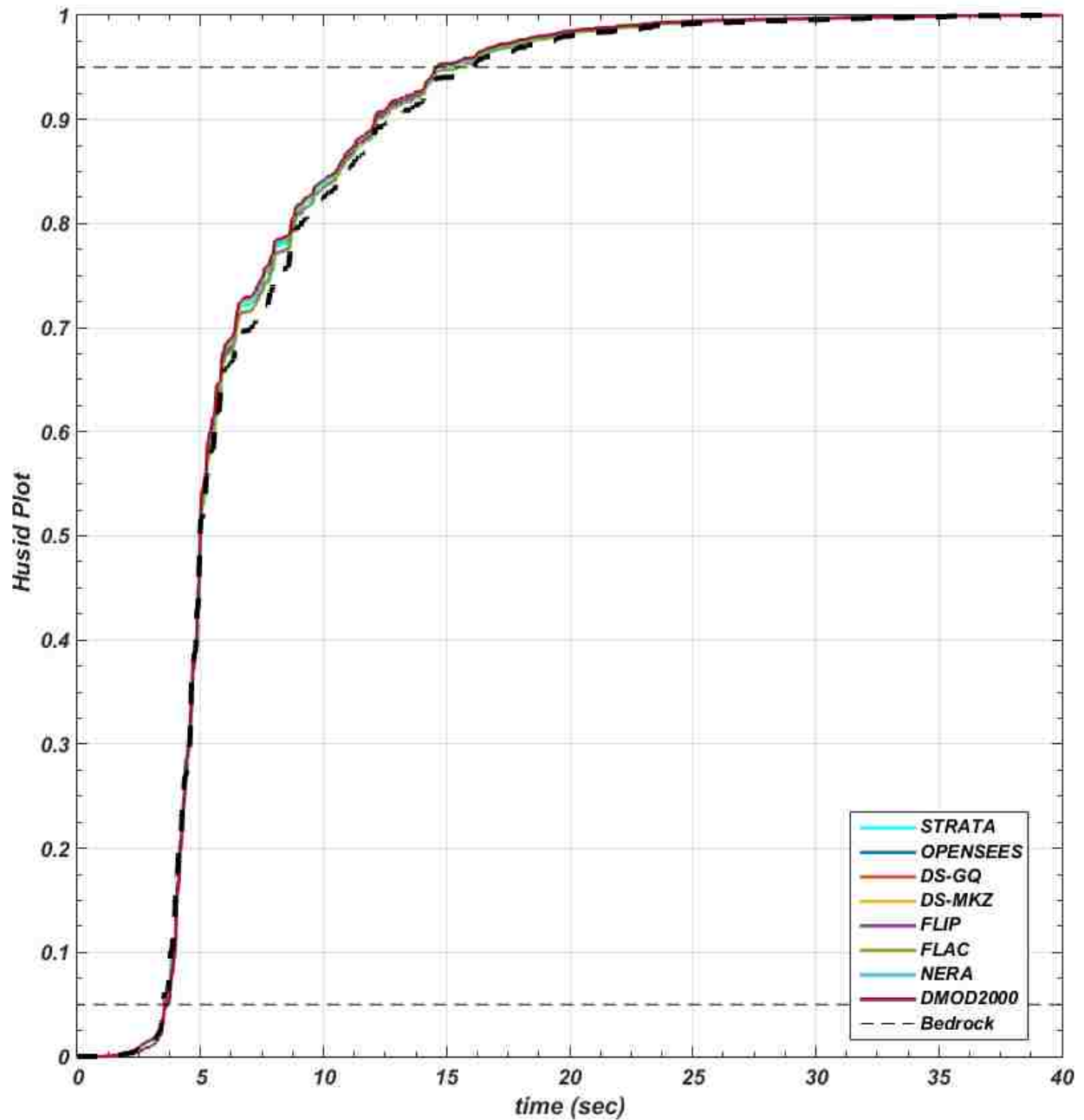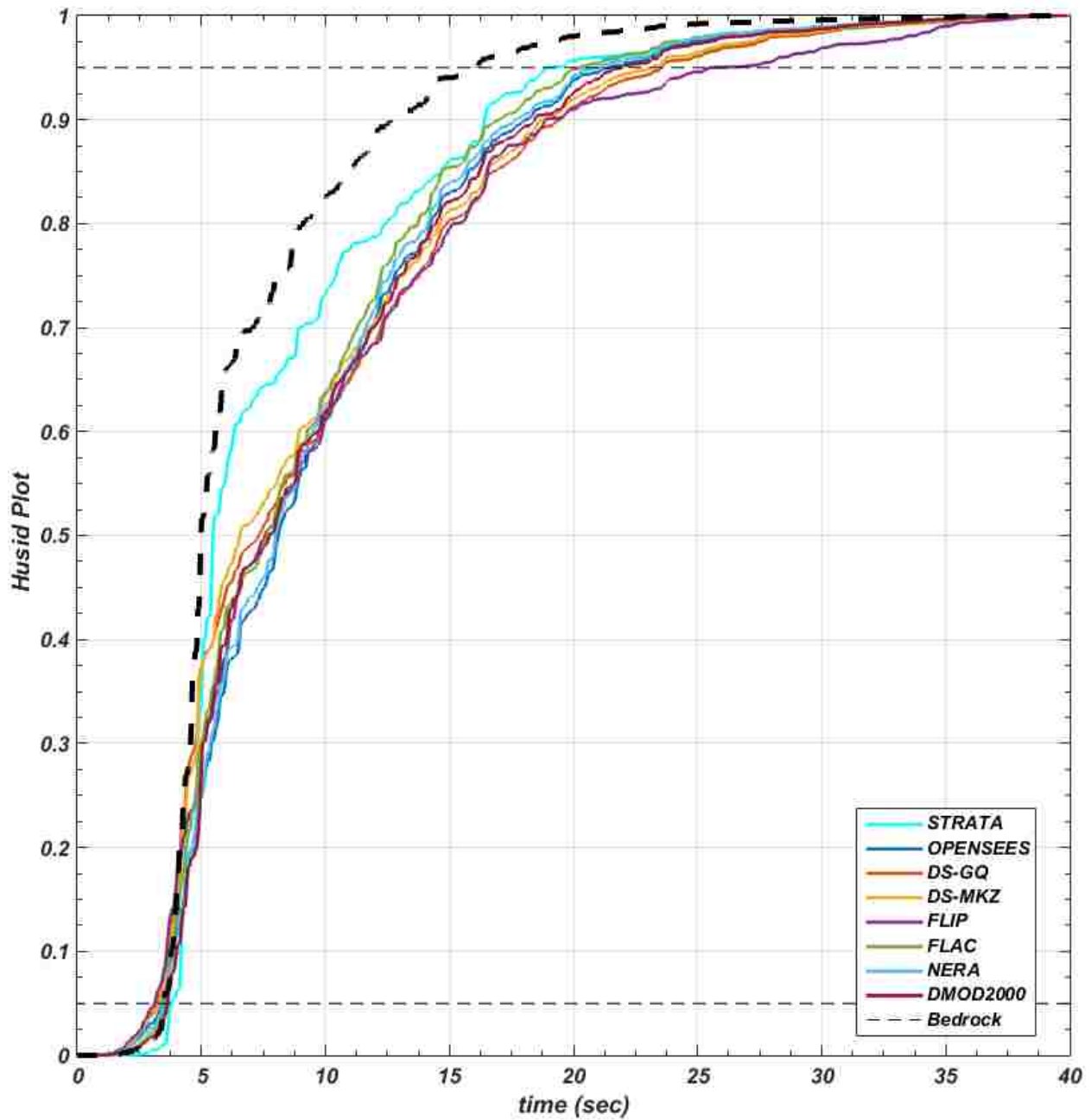
Figure 4.30 The plot of normalized Arias intensity to predict the required duration in dissipating 95% earthquake intensity for Group-4a. The EQL result predicts shorter duration of significant duration (D_5-D_{95}).
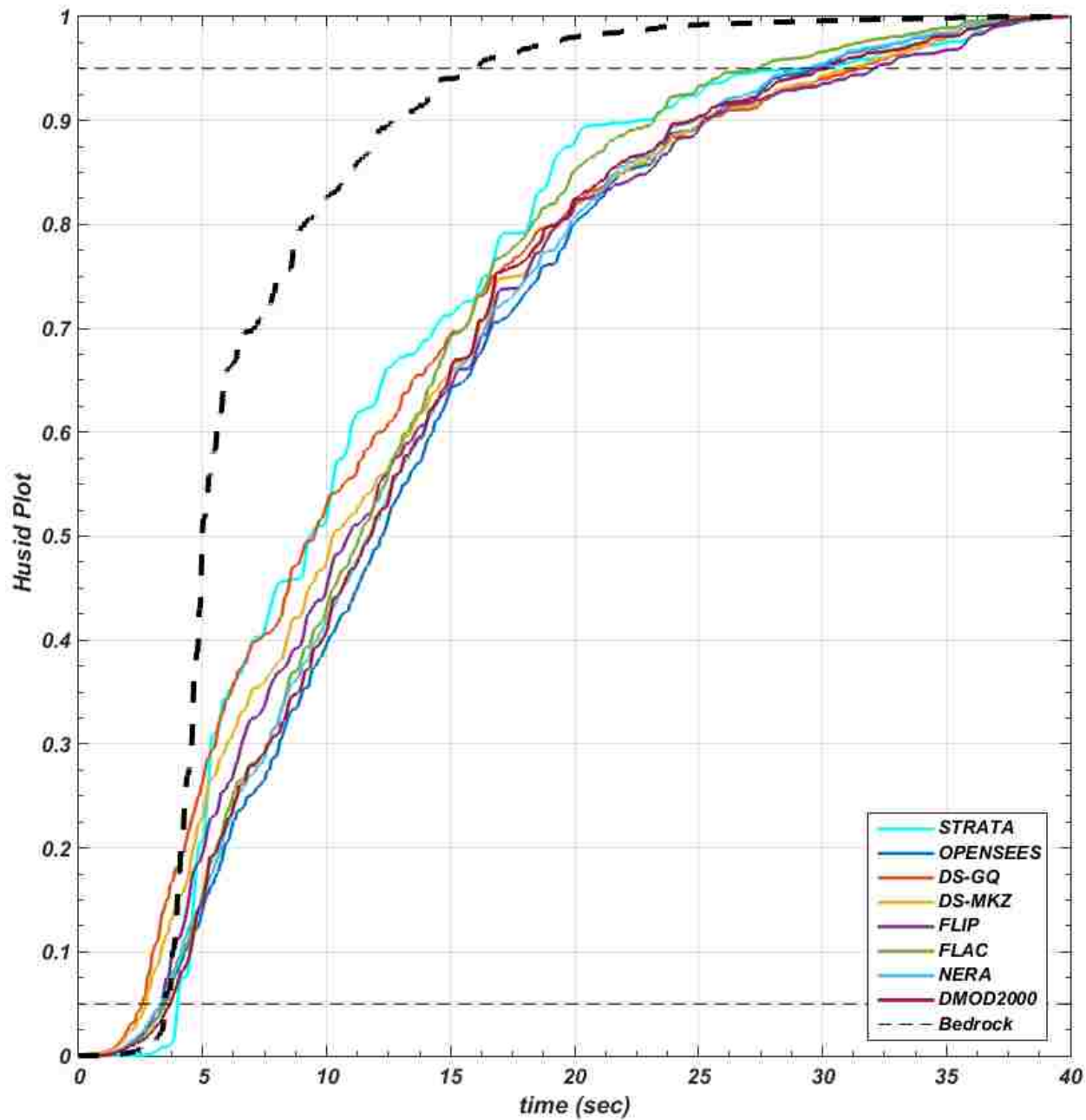
Figure 4.31. The plot of normalized Arias intensity to predict the required duration in dissipating 95% earthquake intensity for Group-4b. The EQL result predicts shorter duration of significant duration (D_5-D_{95}).

4.5 SUMMARY

This chapter presents a comparison of the results of 1D site response analysis using available codes for various types of site profile and site classes subjected to a wide range of intensity motions. The analyses evaluate the results over a wide range of soil nonlinearity and shear strain levels and tries to characterize the variability in the computed response. Moreover, the capability of the soil models to predict site response at a wide range shear strain level is assessed. This chapter has observed several important things:

- The prediction of seismic site response performed using all codes are relatively similar with reasonable accuracy at very small strain to moderate strain level (Group 1 and Group 2)

- Starting from high shear strain level (Group 3) the EQL codes tend to predict stiffer behavior that is no longer accurate to be used in 1D site response analysis.

- In general, NERA tends to predict higher intensity motion than other codes since NERA excludes the small strain damping to be implemented in the IM model.

- FLIP does not utilize an identical backbone curve to those as implemented in other codes. Instead, it follows an advanced constitutive model that might cause the result to deviate from others.

- The stress-strain curves constructed by several NL soil models (e.g., DS-MKZ, FLAC, and D-MOD2000) are unable to approach the peak shear strength of the soil, and therefore produce unrealistic cyclic behavior at very high shear strain levels.

- Several codes (e.g., OPENSEES, NERA, DS-GQ, and FLIP) are capable of approaching the shear strength of soil with reasonable behavior. However, some limitations are exist due to unrealistic hysteresis damping ratio and incapability to approach the shear strength smoothly.

- The variability of the ground motion parameters predicted by all NL codes tend to increase as the shear strain level increase as shown in Figure 4.32 to Figure 4.36. The coefficient of variation resulted at high strain level for parameters such as PGA, PGV, CAV, AI and significant duration are 30%, 20%, 15%, 30% and 15% respectively as indicated in Figure 4.32 to Figure 4.36
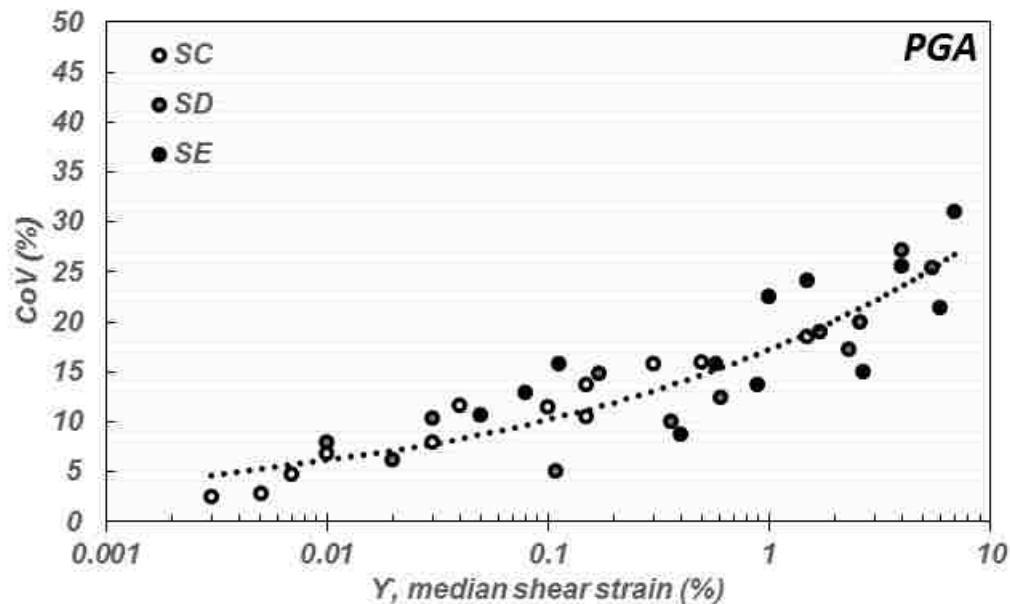
Figure 4.32. Plot of coefficient of variation of PGA at ground surface versus median shear strain computed from all 36 cases considered in this chapter. The variability resulted by all NL codes in PGA parameters increased as the shear strain increase
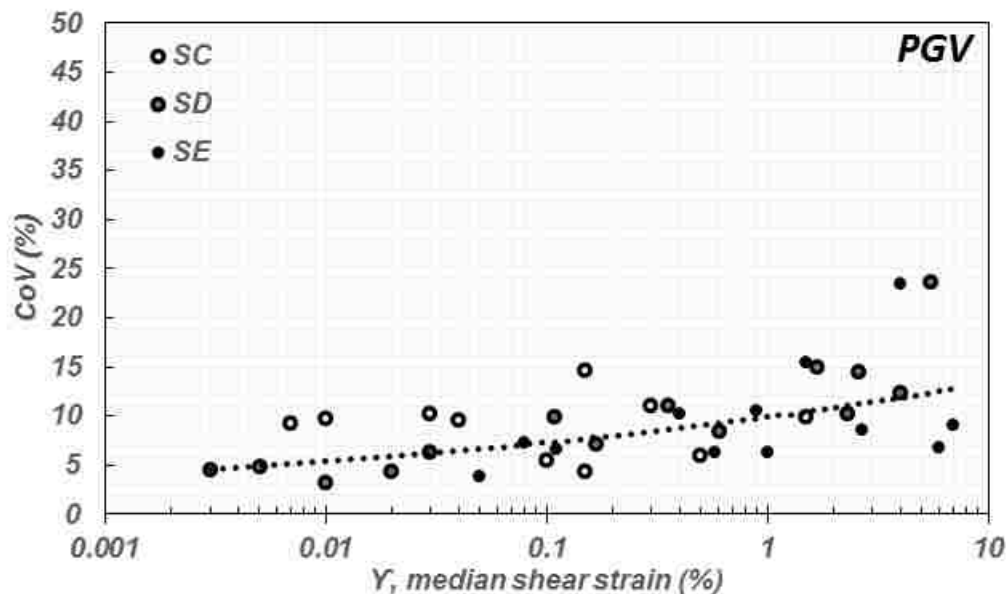
Figure 4.33. Plot of coefficient of variation of PGV at ground surface versus median shear strain computed from all 36 cases considered in this chapter. The variability resulted by all NL codes in PGV parameters increased as the shear strain increase but slightly lower than PGA parameter.
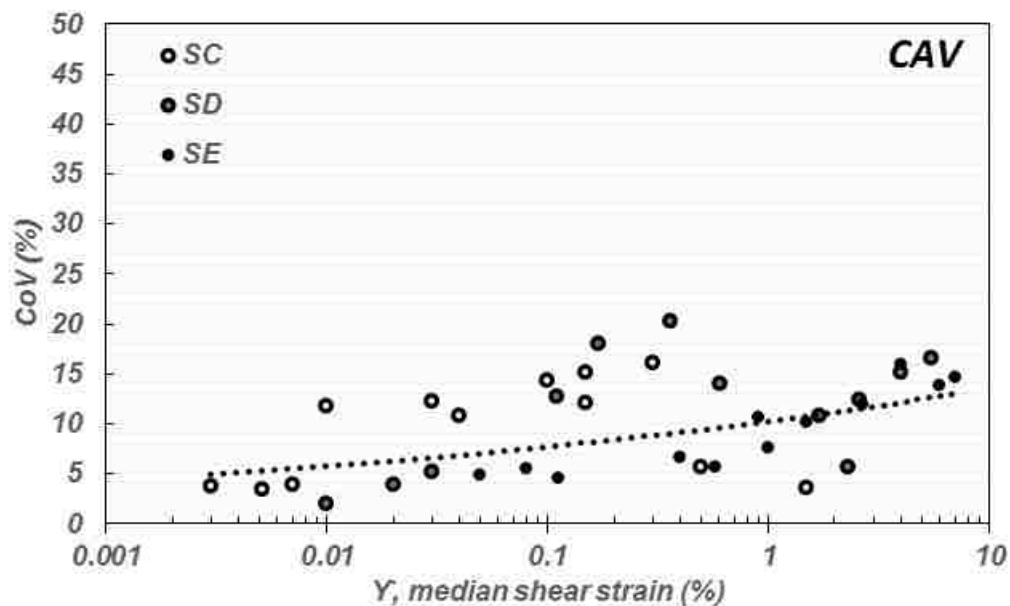
Figure 4.34. Plot of coefficient of variation of Cumulative Absolute Velocity (CAV) at ground surface versus median shear strain computed from all 36 cases considered in this chapter. The variability resulted by all NL codes in PGA parameters increased as the shear strain increase
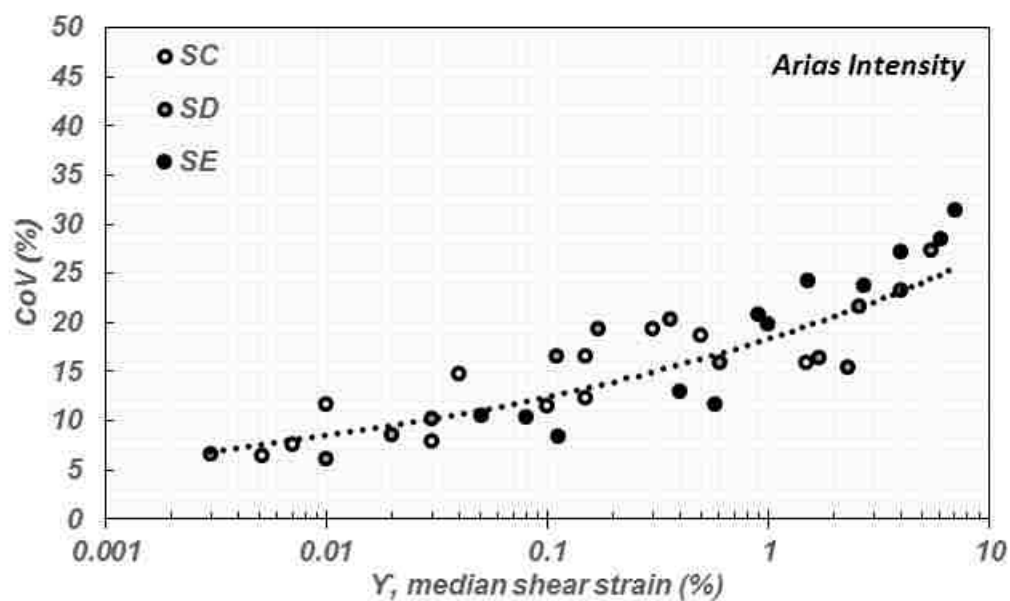
Figure 4.35. Plot of coefficient of variation of Arias Intensity (AI) at ground surface versus median shear strain computed from all 36 cases considered in this chapter. The variability resulted by all NL codes in PGA parameters increased as the shear strain increase
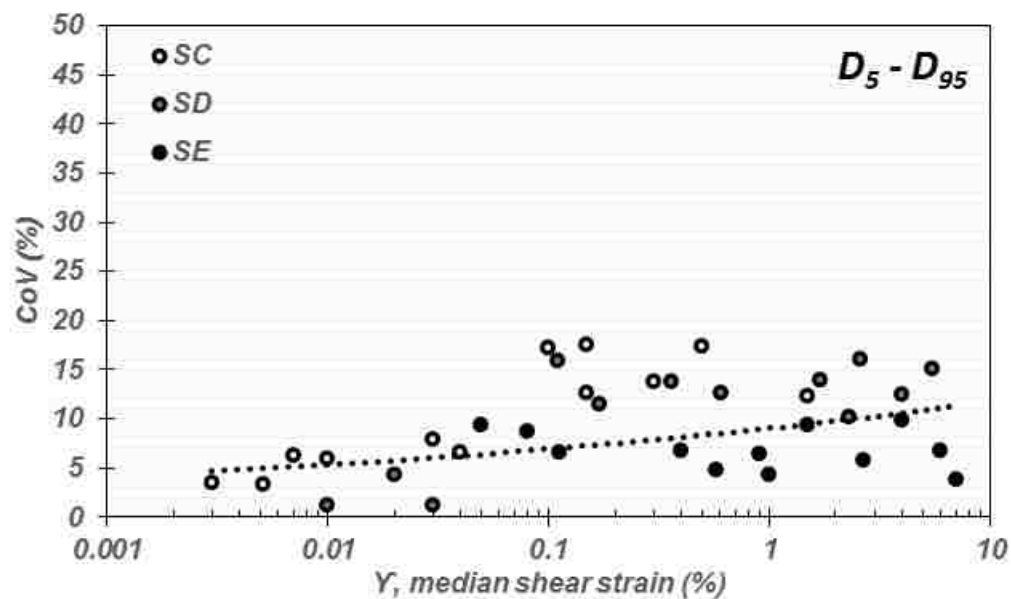
Figure 4.36. Plot of coefficient of variation of significant duration (D_5-D_{95}) at ground surface versus median shear strain computed from all 36 cases considered in this chapter. The variability resulted by all NL codes in PGA parameters increased as the shear strain increase.

Chapter 5. EVALUATION AGAINST VERTICAL ARRAY

The objective of this chapter is to validate the site response analysis protocols and codes described earlier to the motions from a well-recorded vertical array data. Prior to the analysis, the characteristics of the vertical array site and previous studies are presented. The validation will be conducted against the data of September 28, 2004 M_w 6.0 Parkfield earthquake that provide the recorded motion at bedrock and ground surface level. Analyses similar to those described in Chapter Three will be performed in order to document the variability analysis resulting from 1D nonlinear analysis against an actual, relatively well characterized site.

5.1 TURKEY FLAT SITE

The California Geological Survey (CGS) initiated installation of a seismic site instrumentation area at a site called Turkey Flat in 1988. The objective of this project was to investigate the reliability of current seismic site response analysis for estimating the effects of nearly surface geological condition on surface motion characteristic (Tucker and Real 1986). The Turkey Flat site is located 8 km southeast of the town of Parkfield about 5 km east of San Andreas Fault in central California as shown in Figure 5.1a. In 2004, an M_w 6.0 earthquake event occurred on the Parkfield segment of the San Andreas Fault and generated the strongest motion ever recorded at the Turkey Flat array.
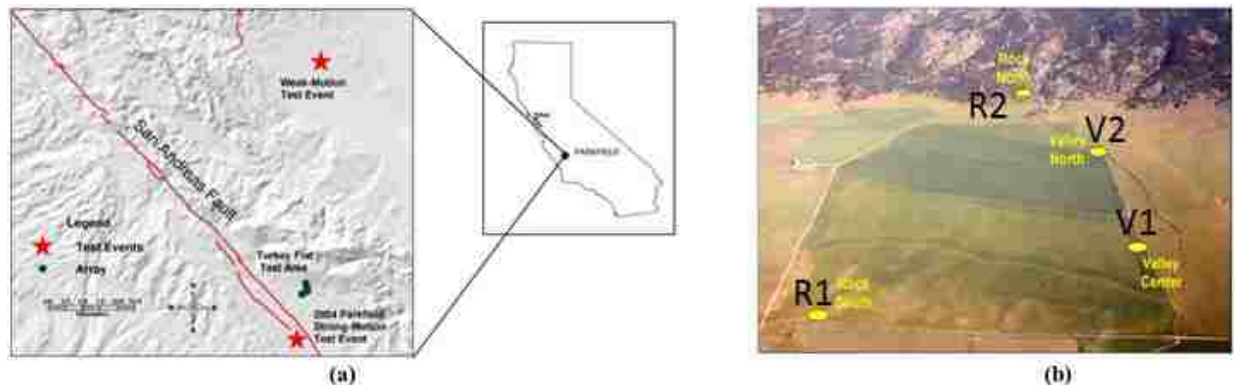
Figure 5.1. (a) Turkey Flat Site Effects Test Area, (b) Aerial view of Turkey Flat strong motion vertical array station. (Real et al, 2008).

5.1.1   *Strong Motion Instrumentation*

CGS's Strong-Motion Instrumentation Program (CSMIP) established the seismic instrumentation at Turkey Flat site in 1987. The set of instrumentation was established on a flat valley with unsaturated sediments near the San Andreas Fault in central California. It is composed of four recording sites including two on rock outcrops (Rock North and Rock South) and two on the sediments (Valley North and Valley Center) as shown in the photo in Figure 5.1b. The recording equipment was placed at different depth as illustrated in the cross section profile in Figure 5.2. The surface Rock South is composed of two recording equipment (R1 and D1) and the Valley Center is composed of three recording (D3, D2 and V1) all at different depth. This research only considered motions recorded at the Valley Center location including switch D3, D2 and V1 having position at depths of 0 m, 10 m and 24 m, respectively (Real et al, 2005). The rock level motion is represented by D3 and motion recorded at soil is presented by D2 and V1 (surface) instrumentation.
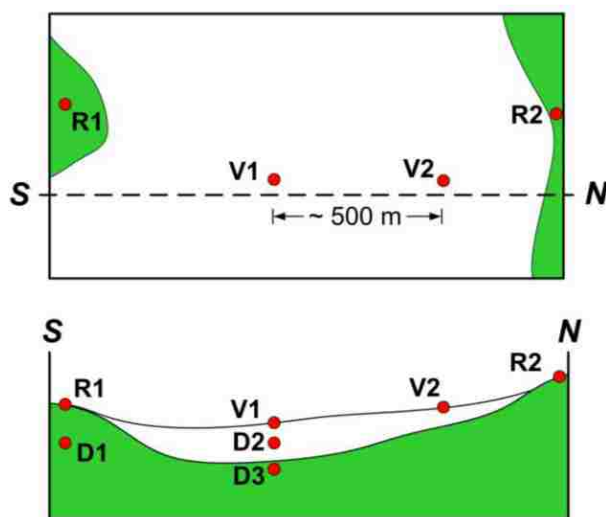
Figure 5.2. Schematic illustration of Turkey Flat instrumentation layout. Top figure illustrate the layout of instrumentation as indicated in Figure 5.1b. Bottom figure illustrate the cross-section profile of S-N line. Green color indicates rock (after Tucker and Real, 1986)

2004 M6.0 Parkfield Earthquake

Historical earthquakes in the Parkfield section of the San Andreas faults indicates consistent recurrence intervals over the past years (Kramer, 2010). At 10:15 am on September 28, 2004 an

earthquake with M_w 6.0 occurred on the Parkfield segment and was recorded by multiple stations resulted a wide range of peak acceleration values as shown in Figure 5.3.

The best set of motions recorded by the Turkey Flat array to validate the protocols of 1D site response analysis are those recorded at Valley Center (V1). The instrumentation in V1 includes the motion at bedrock, mid depth and surface level having recordings in the horizontal east west (E-W) and north-south (N-S) direction. Figures 4.4 to 4.6 show the recorded motion at each depth. The peak accelerations at bedrock level are 0.069 g and 0.065 g for E-W and N-S component. The wave propagation phenomenon at Turkey Flat indicates that amplification of motion occurred as shown by a peak acceleration of 0.3 g at ground surface level, which was nearly five times greater than the bedrock motion. The Turkey Flat data from 2004 Parkfield Earthquake data provides a good opportunity to validate the 1D site response analysis. The site profile and geological condition that will be explained in next section are considered to fit the basic assumption of 1D approach.
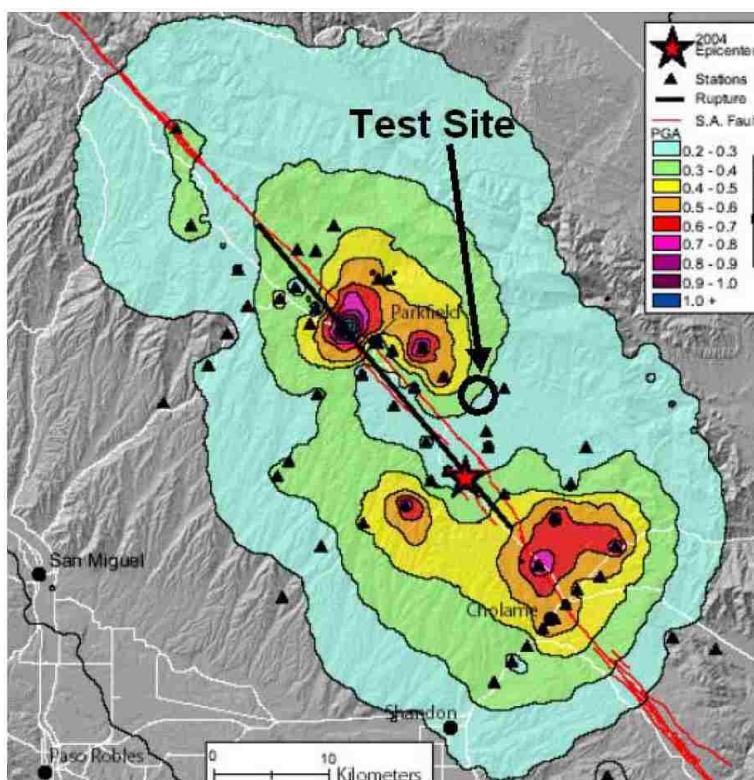
Figure 5.3. Contour of peak ground surface acceleration map of M 6.0 2004 Parkfield Earthquake (Shakal et al., 2005)
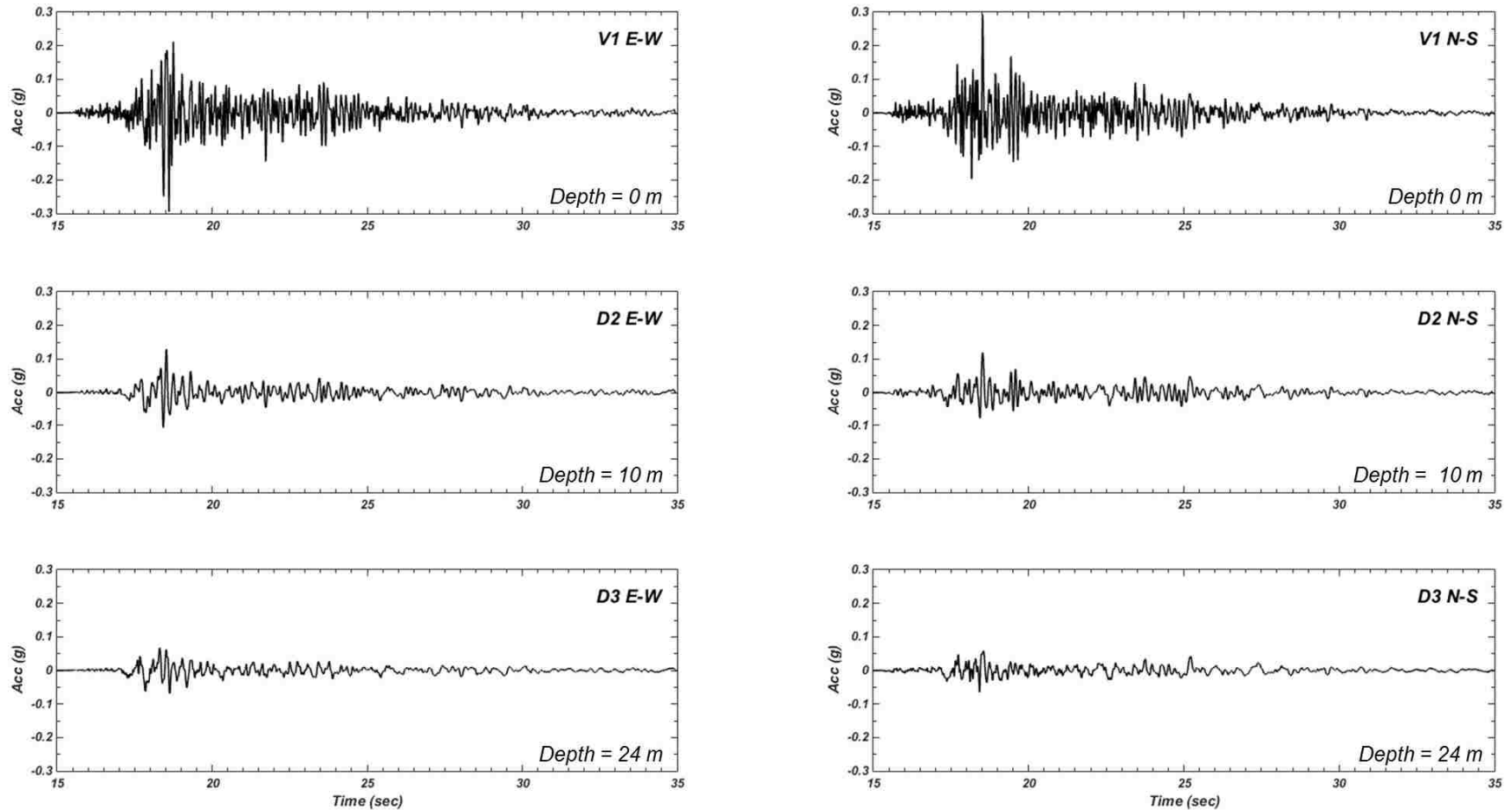
Figure 5.4. Acceleration time histories recorded at different depth by Turkey Flat array instrumentation at Valley Center (V1). The motion recorded at D3 instrumentation presents the bedrock level motion while others are recorded on soil deposit at mid depth and surface level. Original motion recorded the data from 0 to more than 80 seconds.
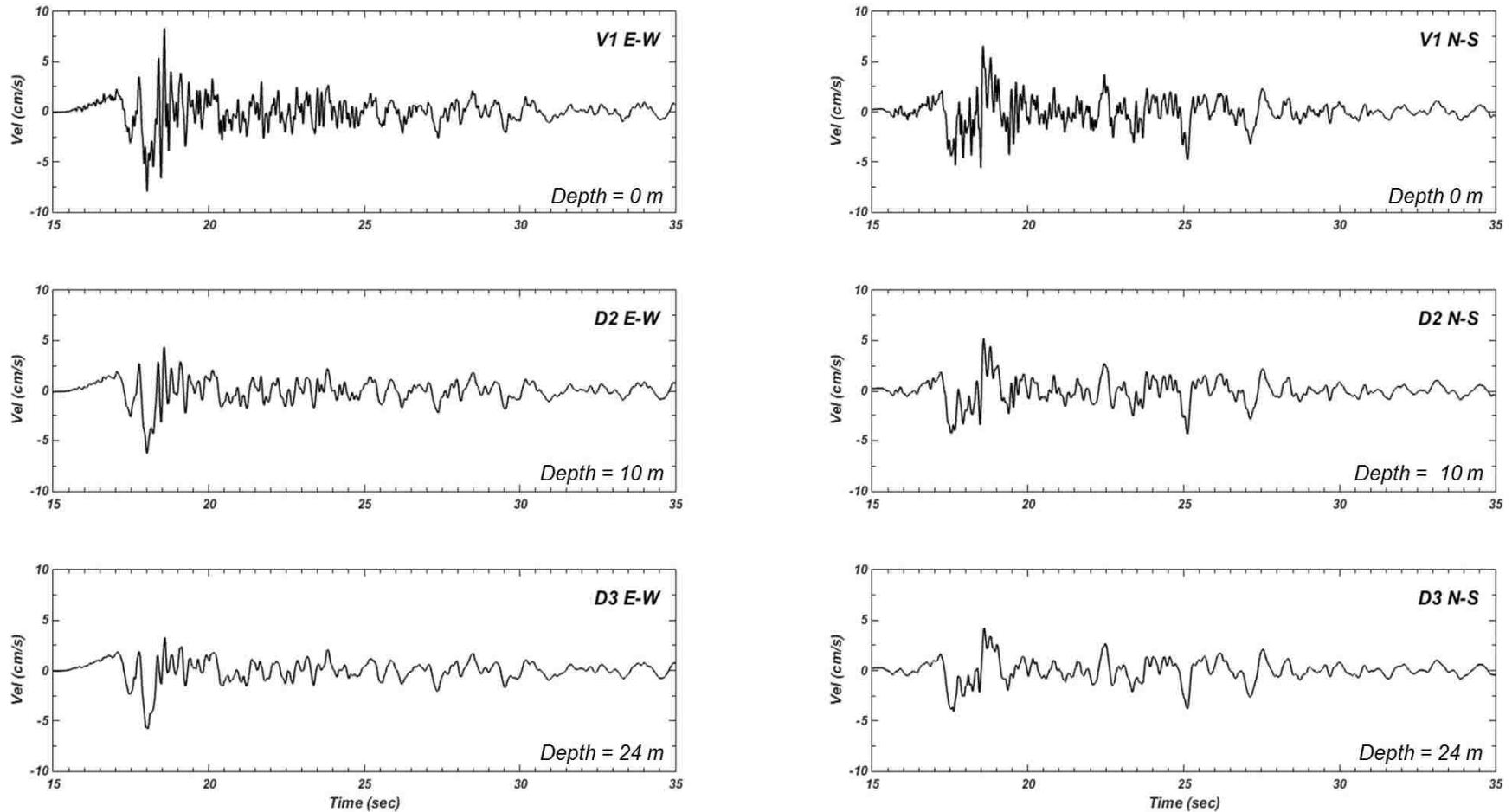
Figure 5.5. Velocity time histories recorded at different depth by Turkey Flat array instrumentation at Valley Center (V1). The motion recorded at D3 instrumentation presents the bedrock level motion while others are recorded on soil deposit at mid depth and surface level. Original motion recorded the data from 0 to more than 80 seconds.
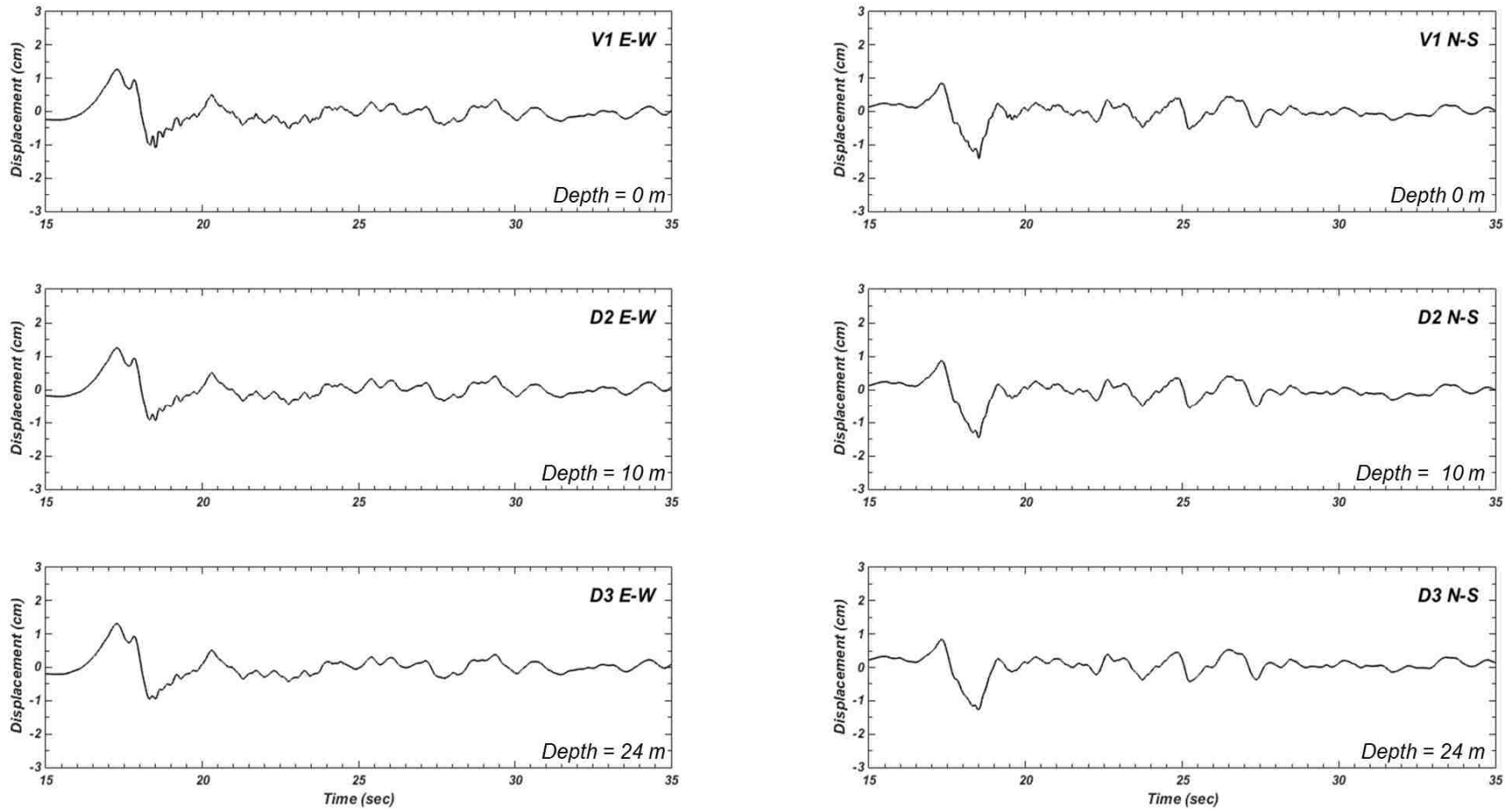
Figure 5.6. Displacement time histories recorded at different depth by Turkey Flat array instrumentation at Valley Center (V1). The motion recorded at D3 instrumentation presents the bedrock level motion while others are recorded on soil deposit at mid depth and surface level. Original motion recorded the data from 0 to more than 80 seconds.

5.1.2   *Turkey Flat Site Condition*

As depicted in Figure 5.1b, Turkey Flat is a shallow valley having a flat ground surface bounded to the northeast and the southwest by mountains. The valley is filled with unsaturated alluvial sediments and can be best described as a shallow stiff-soil site. It is composed mainly of sandy clays with intermittent layers of gravel and occasional strands of boulders (Real, 1988).

In order to obtain well characterized site data, CGS through CSMIP held an extensive site investigation which was conducted in 1988 by multiple experts and investigation teams from the U.S. and abroad (e.g., LeRoy Crandall and Associates, Hardin Lawson Associates, QEST Consultants, OYO Corporation, Kajima Corporation, the California Division of Mines and Geology, and Woodward-Clyde Consultants). The collective information obtained from all the investigators indicated the presence of three primary soil layers. The upper layer consisted of dark brown silty clay (at the Valley Center) to sandy clay (at Valley North). The middle and lower layer consisted predominantly of clayey sand that contained gravel and sandy clay where more gravel are found at lower layer.

In Turkey Flat, the shear wave velocity profiles were measured using several different techniques including seismic refraction, seismic reflection, downhole velocity, crosshole velocity, etc. Detailed descriptions of the field and laboratory testing program and all the results are given in Real (1988). Measurements performed by all investigators provided results with variability that can be affected by different interpretations of the velocity profile. In order to standardize the shear wave velocities at the Turkey Flat for future research and analysis, Real 1988 provided the standard profile listed in Table 5-1, which was employed for the analysis in this research.

Laboratory investigations (i.e., resonant column and cyclic triaxial test) using samples from the Turkey Flat seismic instrumentation site provided dynamic soil properties for seismic site response analyses as listed in Table 5-2. However, the normalized shear modulus reduction and damping curve data was limited to shear strain levels of 0.3%. Thus, this set of curves needed to be extended to perform the site response analysis shaken by stronger motion. The extension of G/G_{max} will be set to approach a peak strength of the soil in order to predict real cyclic behavior using protocols described earlier in Chapter Two. The shear strength of alluvium material is given in Table 4-1. The first layer is composed of dark-brown silty clay material having relatively low shear wave velocity, therefore correlation to estimate the shear strength from shear wave velocity

based on Dickenson (1994) is utilized. For the mid and lower alluvial deposits, the shear strength of the material is determined by personal judgement by using consideration of the shape of stress-strain curve and the measured G/G_{max} curve as indicated in Figure 5.7. The underlying material is a sandstone bedrock profile similar to the rock south area.

Table 5-1. Seismic Velocities at soil site Valley Center – Turkey Flat (After Real, 1988)

ID	Depth Range (m)	Shear Wave Velocity (m/s)	Compression Wave Velocity (m/s)	Density (gr/cm³)	Implied Shear Strength (kPa)
Alluvium 1	0.0 – 2.4	135	320	1.5	41.5 [4]
Alluvium 2	2.4 – 7.6	460	975	1.8	400 [5]
Alluvium 3	7.6 – 21.3	610	975	1.9	700 [5]
Sandstone	Below 21.3	1340	2715	2.2	--

Table 5-2. Dynamic Soil Properties at Valley Center (Real, 1988)

Strain, γ (%)	G/G_{max}	Damping Ratio (%)
0.0001	1.00	1.5
0.001	0.96	2.0
0.01	0.75	4.0
0.03	0.60	6.5
0.1	0.40	10.0
0.3	0.22	13.0

Figure 5.7 presents the target G/G_{max} curve after considering the shear strength correction as the crucial protocols described in previous chapter. The G/G_{max} curve is extended by using the procedure proposed by Groholski et al (2015) that can provide the flexibility to match the target data at low shear strain by reaching a peak strength at large strain.

---

[4] Based on Dickenson (1994) assuming that Alluvium-1 consists of cohesive deposit.
[5] Based on personal judgment estimated from data given by Real, 1988 (shear wave velocity and G/Gmax, square-marker in Figure 4.1b) and undrained shear strength range correspond to NEHRP site class.
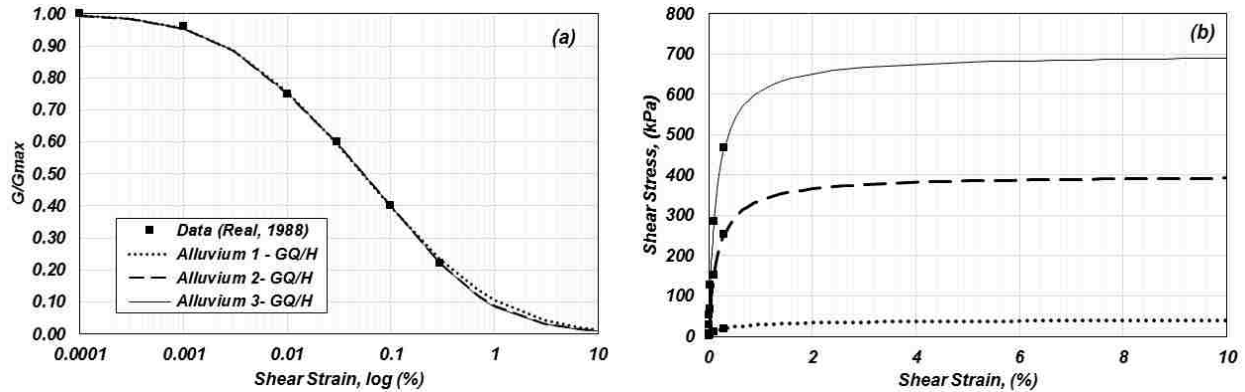
Figure 5.7. Dynamic behavior of alluvium material in Valley Center, Turkey Flat, CA used in this study approximated based on General Quadratic/Hyperbolic (GQ/H) model (Groholski et al, 2016). (a) Plot of measured laboratory data from Real (1988) and G/G_{max} curve used in this study. (b) Backbone curve extended from strain = 0.3% (original data) by using GQ/H equation that allows implementation of peak shear strength correction. All calculation and fitting procedure is conducted via DEEPSOIL (Hashash, 2015) user interface program.

5.2   MODEL ANALYSIS

This section presents the results of analyses intended to validate all site response analysis codes against the recorded motions at the Turkey Flat site. The validation implements similar protocols described in Chapter Three and only different important matters that will be presented in this section.

Layer Thickness

The thickness of the alluvial sediment of Valley Center (V1) at Turkey Flat vertical array site is 21.3 meters above the sandstone bedrock. The profile was discretized into 20 layers in order to accommodate the maximum frequency that had to be propagated through the profile as indicated in Figure 5.8. By utilizing the 1D soil column model in Figure 5.8, the analysis is capable to propagate maximum frequency greater than 40 Hz.

Specification of Half-Space and Input Motion

Kwok et al (2007) gives recommendation in modeling the underlying half-space and the input motion for validation against vertical array (Figure 3.23). Herein, the recorded "within" motions (D3) are implemented as the input motion without any modification and applied at the top of a

rigid base. For codes that do not provide the analysis for rigid half-space, another option to perform the calculation using this model is to use shear wave velocity of bedrock up to 30000 m/s (Stewart, 2008).

Type	Unit Weight (kN/m³)	Layer	Thickness (m)	Recording Depth	Shear Wave Velocity (m/s)	Max. Frequency (Hz)
					0 500 1000	0 50 100 150
Alluvium 1	14.72	1	0.8	V1		
		2	0.8			
		3	0.8			
Alluvium 2	17.66	4	1.3			
		5	1.3			
		6	1.3			
		7	1.3			
Alluvium 3	18.64	8	1.2			
		9	1.2	D2		
		10	1.0			
		11	1.0			
		12	1.0			
		13	1.0			
		14	1.0			
		15	1.0			
		16	1.0			
		17	1.0			
		18	1.0			
		19	1.0			
		20	1.3			
Sandstone (Rock)	21.58			D3	Vs = 1340 m/s	
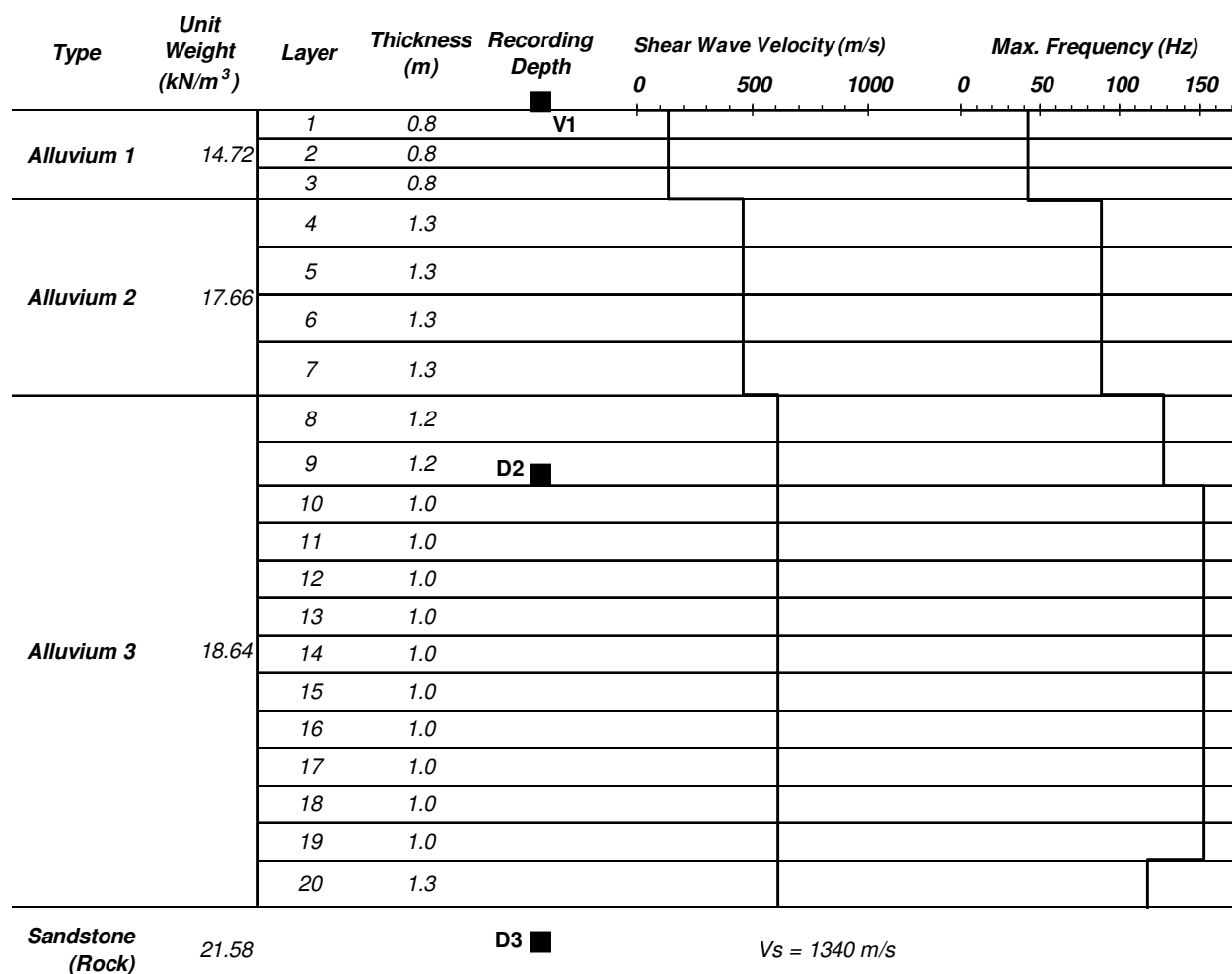
Figure 5.8. Layer discretization model of Valley Center at Turkey Flat vertical array site. The maximum frequency that can be propagated is more than 40 Hz in all layer. The model discretize the profile into 20 layers to provide more accuracy.

Implementation of Small Strain Damping

The NL site response codes that require the implementation of Rayleigh damping formulation are FLAC, OPENSEES, D-MOD2000 and FLIP. The analysis in this section follows the calibration procedure explained in section 2.3.3 to fit the EQL result at small shear strain levels. As recommended by Kwok et al (2007), the Rayleigh damping coefficients are computed using the

target small strain material damping ratio which is 1.5% as presented in Real (1988) and the two target frequencies are set to be fundamental site frequency, 4.85 Hz and five times that frequency, or 24.25 Hz. The calibration procedure indicated that, using this first guess, all codes matched the EQL results with reasonable accuracy, therefore, this set of coefficients was used for further analysis.

5.2.1   *Equivalent Linear (EQL) Approach*

The EQL analysis was performed against the soil profile indicated in Figure 5.8 using a similar protocol to that described in Chapter Three.

5.2.2   *Non-linear (NL) Approach*

The nonlinear site response analyses of the Turkey Flat array site were based on the 1D site profile presented in Figure 5.8. All the important aspects of the analysis were similar to those presented in Chapter Three except for the rigid half-space boundary condition. The details of the analyses, including codes and site response parameters, are attached in the appendices part.

One Dimensional Codes

D-MOD2000, DEEPSOIL and NERA are the 1D site response analysis codes employed in this research to validate the Turkey Flat vertical array data. The soil models for each code were set to fit the target G/G_{max} curve shown in Figure 5.7. Detailed parameters for the analysis are listed in the appendices. D-MOD2000 and DEEPSOIL provides the user with the "Rigid Bedrock" option, therefore this options will be activated. For NERA, the shear wave velocity for underlying bedrock was set to 30000 m/s to model the rigid bedrock. All the input motion (D3) were applied without any modification.

Multi-Dimensional Codes

OPENSEES, FLAC and FLIP are the multidimensional site response analysis codes employed in this research to validate the Turkey Flat vertical array data. The geometry models for these codes were similar to Chapter Three except the model of the underlying bedrock. In order to accommodate rigid bedrock, OPENSEES and FLIP set the underlying bedrock shear wave velocity to 30000 m/s. Furthermore, FLAC used the acceleration time histories directly as the input motion

applied at the base of the soil column. This accommodated the interface boundary to completely reflect the seismic wave to the soil deposit instead of transmitting to the underlying bedrock (Itasca, 2009). The G/G$_{max}$ curves shown in Figure 5.7 were used in the computations using OPENSEES and FLAC. The procedures to apply the soil model are exactly the same as explained previously. On the other hand, FLIP employs the multispring soil constitutive model instead of adapting a target G/G$_{max}$ curve. As described earlier, this might yield a prediction that can deviate from other analyses. For further reference, the detail command lines for each codes are listed in the appendices.

5.3   VALIDATION RESULTS

This section presents the results of the analyes using all codes compared to the measured vertical array data at middle depth (D2) and ground surface layer (V1). Each recording had two different component consisting of east-west and north-south component as depicted in Figure 5.4. Furthermore, site response analysis results utilizing stronger motions are also presented in order to evaluate the performance of each soil model at higher shear strain levels. The evaluation is performed by comparing results including profiles of node response versus depth, response spectra, hysteresis loops and shaking duration.

5.3.1   *Turkey Flat Vertical Array*

The validation of 1D site response analysis process against the Turkey Flat vertical array data follows similar procedure that what has been done in Chapter Three. The 2004 Parkfield Earthquake produce motion strong enough to induce significant shear strain in the Valley Center soil column. According to the nonlinearity group presented in Chapter Three, the Turkey Flat results indicates moderate soil nonlinearity level (Group 2 - $0.9 < $ G/G$_{max}$ $ < 0.5$). It means that the response of the analysis should be similar with what predicted in Chapter Three.

Profiles

Tables 5-3 and 5-4 list the prediction results computed by all codes at ground surface level. The V1 instrumentation recorded peak ground accelerations of 0.295g and 0.292g for east-west and north-south components, respectively. For more detailed presentation, Figure 5.9 and Figure 5.10 depict the profiles of all computed response versus depth predicted by all codes. Most of the codes predicted the peak ground acceleration with reasonable accuracy except FLIP, which predicted relatively lower PGA. The prediction results were mostly determined by the first soil layer at Turkey Flat profile due to relatively high impedance contrast.

Table 5-3 Results of computed PGA, peak cyclic strain and peak stress for E-W Component

Parameters	EQL	OPEN SEES	DS-GQ	DS-MKZ	FLIP	FLAC	NERA	DMOD	median (NL only)	σ std.dev (NL only)	CoV (NL only)
PGA (g)	0.277	0.273	0.288	0.289	0.234	0.287	0.299	0.25	0.282	0.057	13%
Shear Strain (%)	0.037	0.049	0.052	0.053	0.083	0.042	0.049	0.033	0.049	0.015	30%
Shear Stress (kPa)	6.75	6.67	7.24	7.24	8.99	7.14	6.974	5.51	7.14	1.028	14%

Table 5-4 Results of computed PGA, peak cyclic strain and peak stress for N-S Component

Parameters	EQL	OPEN SEES	DS-GQ	DS-MKZ	FLIP	FLAC	NERA	DMOD	median (NL only)	σ std.dev (NL only)	CoV (NL only)
PGA (g)	0.310	0.274	0.268	0.270	0.25	0.325	0.305	0.267	0.272	0.026	9%
Shear Strain (%)	0.044	0.051	0.052	0.054	0.092	0.05	0.058	0.044	0.052	0.0159	28%
Shear Stress (kPa)	7.76	7.2	7.29	7.40	9.57	7.98	7.77	6.65	7.4	0.9301	12%

The peak ground acceleration predicted by 1D site response codes ranged from 0.234 g to 0.299 g with a median value of 0.282 g for validation against east-west component. Similar to the variance behavior in Chapter Three, FLIP predicted the lowest peak acceleration and NERA predicted the highest acceleration value. Based on previous analysis, the soil model and the target G/G_{max} curve is the major aspects for the accuracy of the site response prediction. FLIP utilized advanced constitutive model instead of using the target G/G_{max} curve that might cause the deviation
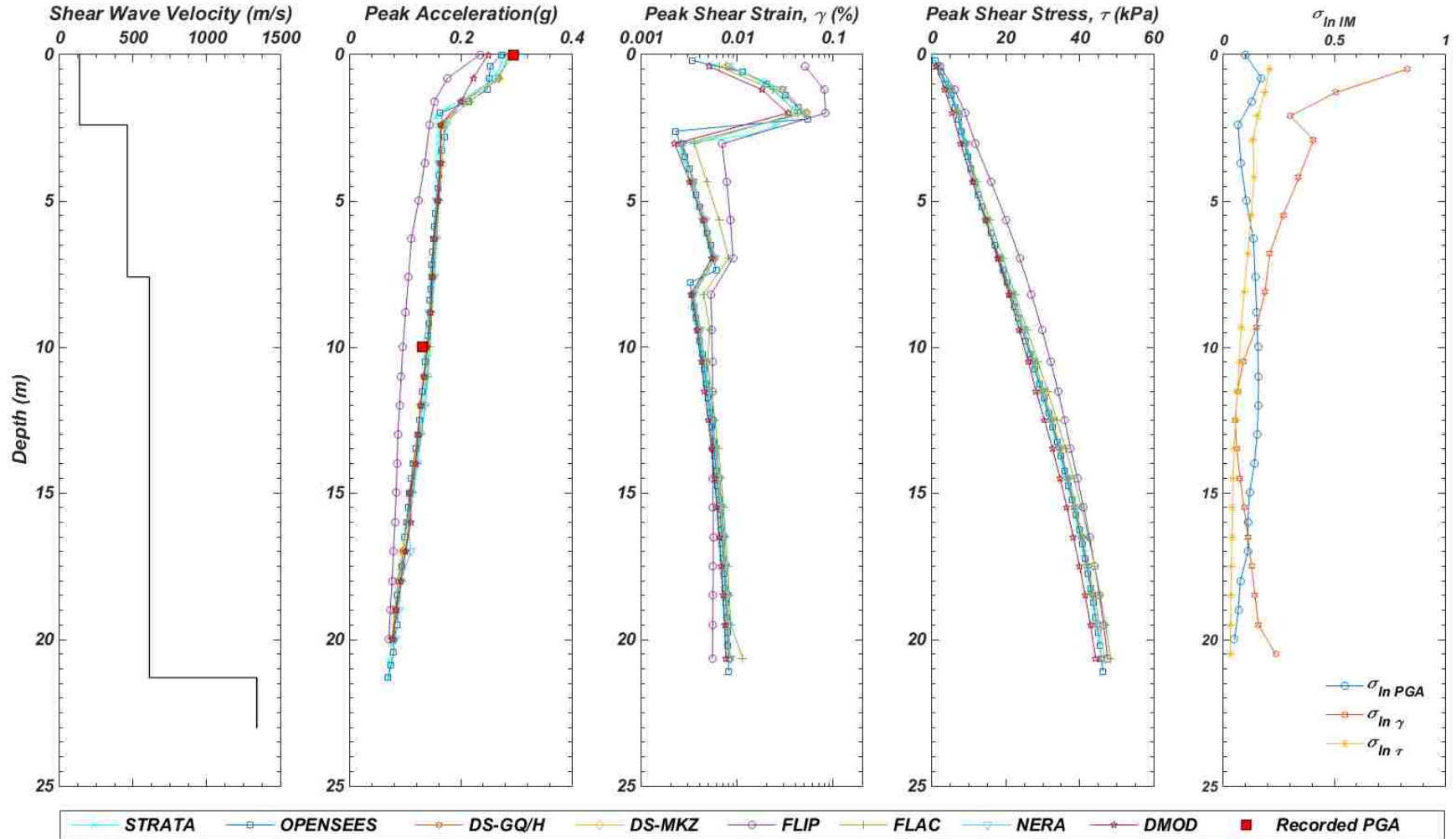
Figure 5.9. Results prediction of Turkey Flat vertical array site using East-West (E-W) component of input motion (D3-EW). From left to right are plot of shear wave velocity, peak acceleration, shear strain and shear stress versus depth predicted by all codes. Most of the codes predicts similar peak acceleration at ground surface level except for FLIP. The plot of standard deviation of natural logarithm indicates the PGA, peak shear strain and peak shear stress at each depth.
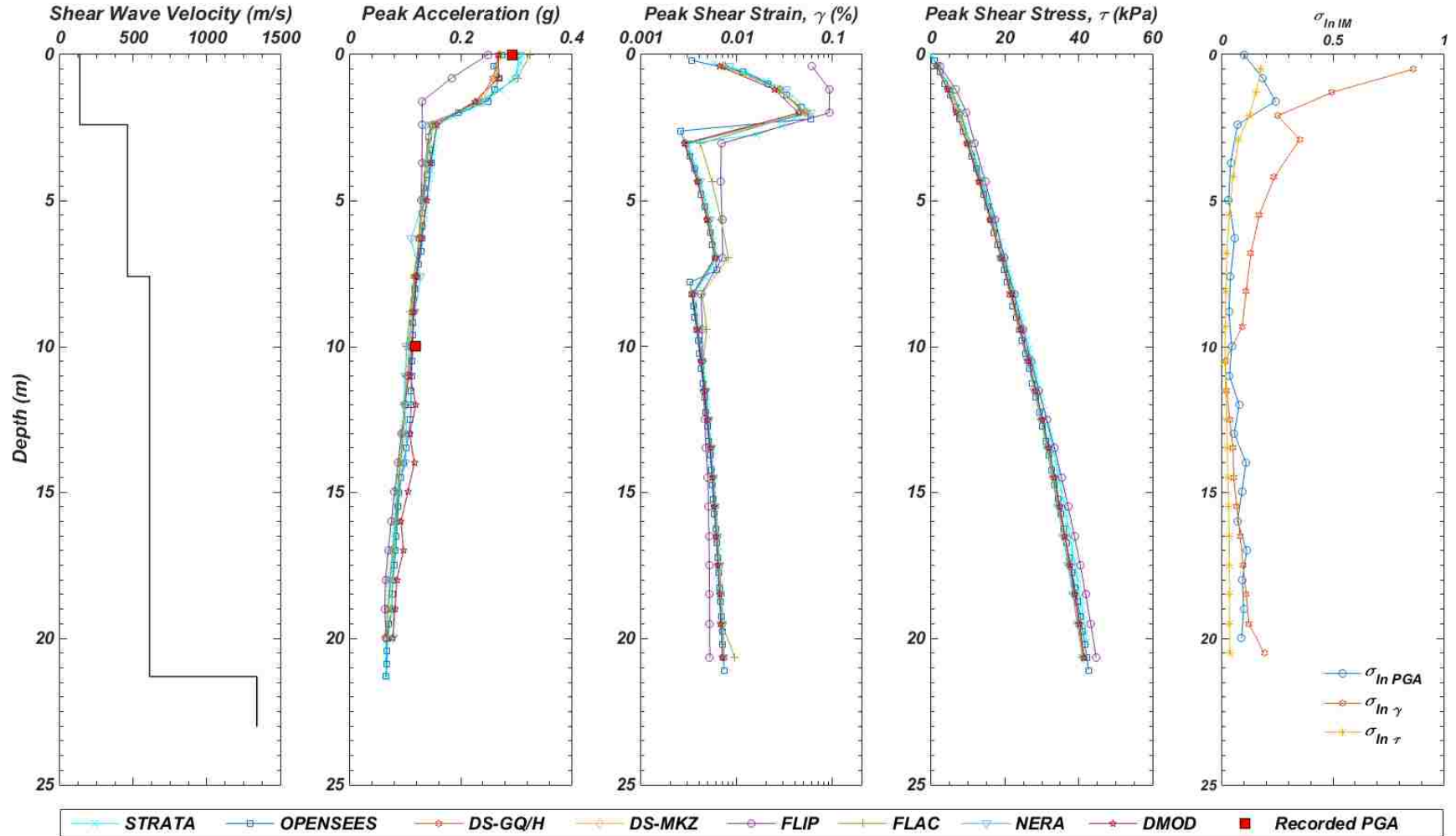
Figure 5.10. Results prediction of Turkey Flat vertical array site using North-South (N-S) component of input motion (D3-NS). From left to right are plot of shear wave velocity, peak acceleration, shear strain and shear stress versus depth predicted by all codes. Most of the codes predicts similar peak acceleration at various depth but less accuracy at ground surface level. The plot of standard deviation of natural logarithm indicates the PGA, peak shear strain and peak shear stress at each depth.

of the results. In terms of cyclic shear strain & shear stress, FLIP predicted different response although it has similar stiffness as shown later in the hysteresis loop part.

For validation against the north-south component, the peak ground acceleration predicted by 1D site response codes ranged from 0.25 g to 0.325 g with a median value of 0.272 g. FLIP predicted the lowest prediction and DEEPSOIL predicted an acceleration close to the median value. All the cases of analyses predicted higher variability of cyclic shear strain than cyclic stress and peak acceleration. Figures 5.9 and 5.10 depict more detailed descriptions of the variability predicted by all codes for validation data against Turkey Flat vertical array data. Most of the codes, except for FLIP, predicted peak acceleration relatively close to what was recorded at D2 and V1. FLIP utilizes an advanced constitutive hysteresis model (Towhata & Ishihara, 1985) to construct the cyclic stress versus cyclic strain curve instead of using the data reported by Real (1988) as implemented in other codes. This causeed FLIP results to deviate from then other codes.

Time Histories

Figure 5.11 presents the results of simulated time histories and how well one of site response codes (NERA) predicted the strong motion data at the ground surface level. It can be concluded that the amplitude of motion at D2 is relatively lower than V1 because D2 is located in stiffer material. All site response codes predicts relatively similar acceleration time history as depicted in Figure 5.11 and these are listed in the appendices.

Hysteresis Loops

This section reviews the performance of all soil models in predicting the cyclic stress and cyclic strain behavior of Valley Center site shaken by 2004 Parkfield earthquake. Figures 5.12 and 5.13 depict plots of stress-strain curves for the E-W and N-S component of input motion. The curves are recorded at depth of 2.0 m within the Alluvium-1 soil layer with the peak shear strength and effective shear stress are 41.5 kPa and 29.43 kPa respectively. Figures 5.9 and 5.10 indicate that along the soil profile, the maximum induced shear strain developed at 2.0 m depth so that depth was chosen to study the cyclic hysteresis loop of the model.

The dynamic engineering properties documented by Real (1988) were implemented for all analysis except for FLIP, which utilizes its own advanced constitutive soil model. All results predicts similar stiffness at moderate shear strain level but with slight variation in damping ratio,
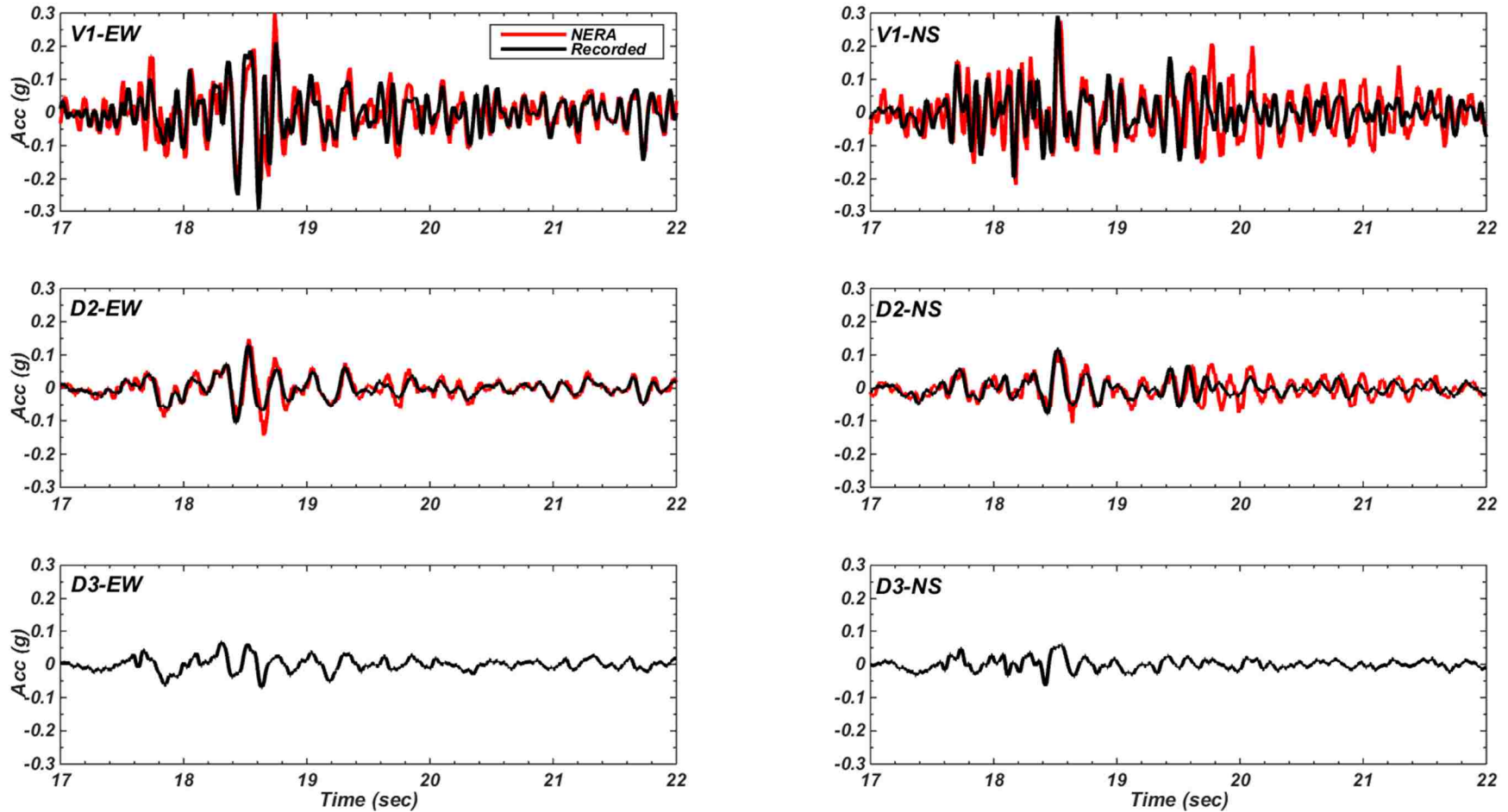
Figure 5.11. Example of acceleration time histories predicted by NERA compared to the D2 and V1 instrumentation data. Results shown for two horizontal directions and two elevations (V1, ground surface; D2, 10 m depth). The other prediction by all codes is listed in the appendices.
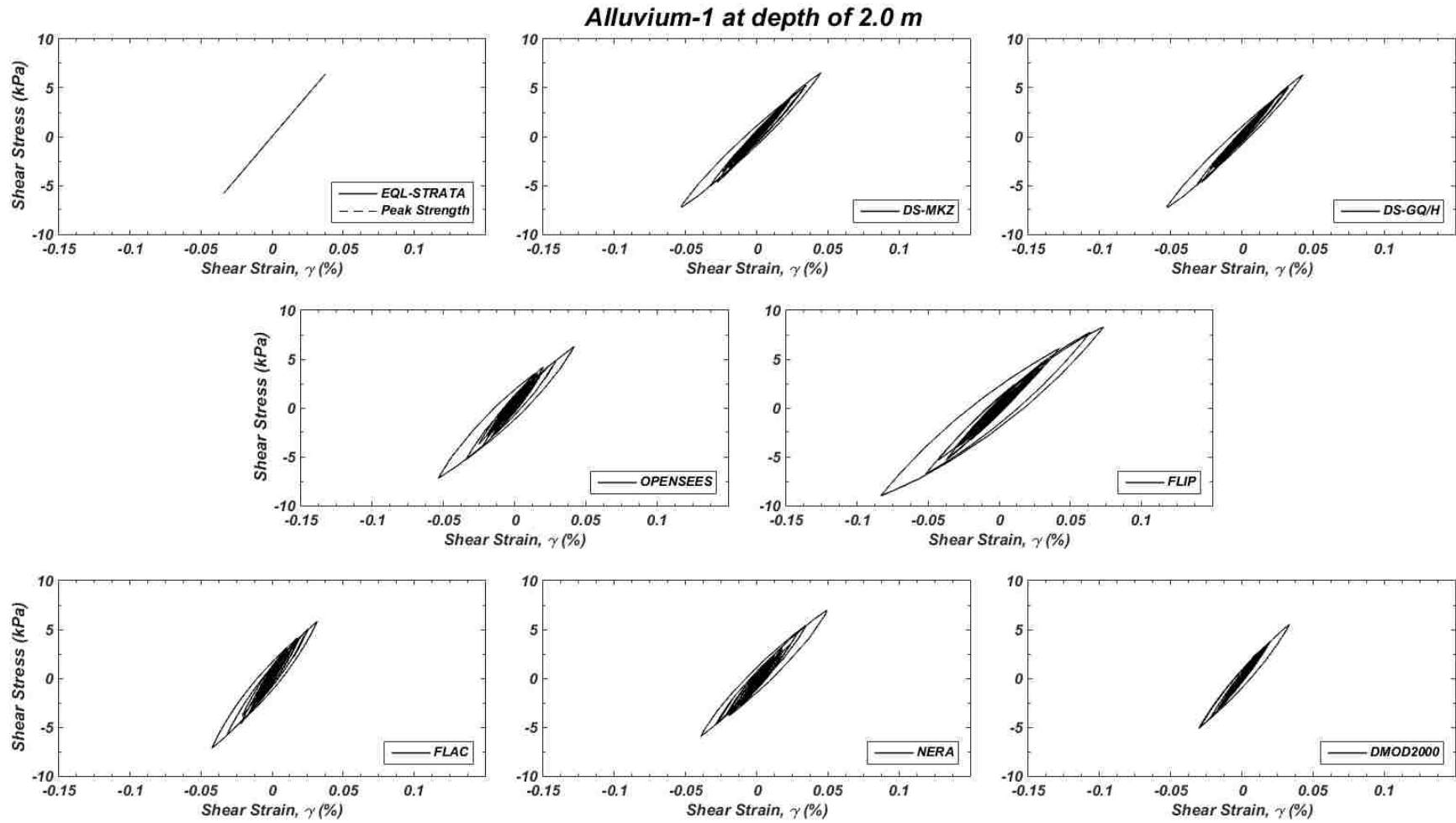
Figure 5.12. Plot of cyclic stress versus cyclic strain curve predicted by all codes during the validation against the V1 recording turkey flat data using the East-West (E-W) component of input motion. The response is chosen from Alluvium-1 layer at 2.0m depth.
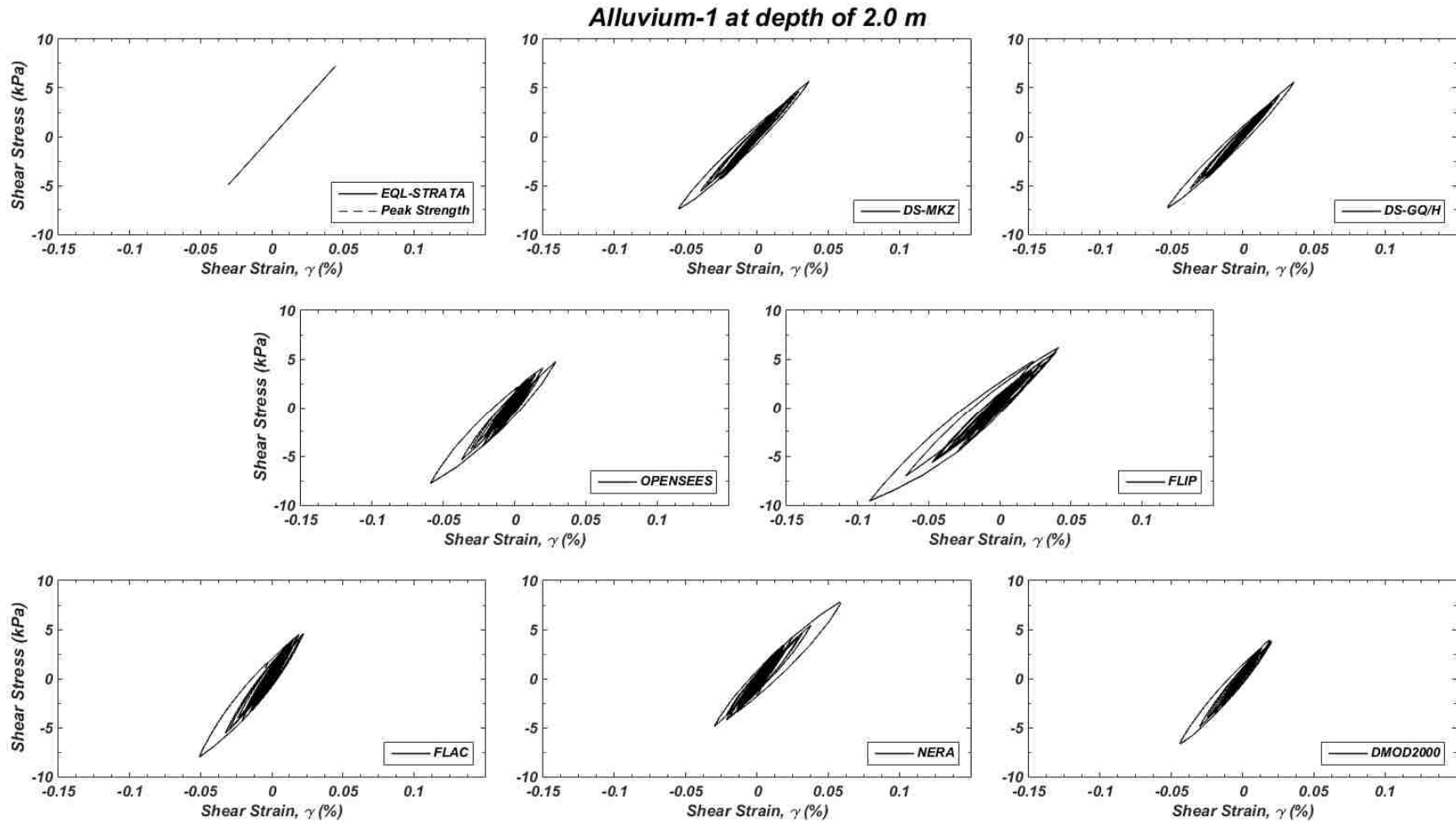
Figure 5.13. Results prediction of Turkey Flat vertical array North-South (N-S) component of input motion (D3-NS). From left to right are plot of shear wave velocity, peak acceleration, shear strain and shear stress versus depth predicted by all codes. Most of the codes predicts similar peak acceleration at ground surface level except for FLIP and D-MOD2000.

the amplitude of shear strain and shear stress. The backbone curve implemented in all codes were identical to each other so the variation is low at this strain level as indicated by low coefficient of variation of the peak shear strain.

The cyclic response of the soil predicted by all codes indicates that the current site response analysis codes are sufficient to predict the ground motion at the ground surface for low nonlinearity level. At this strain level, the prediction of nonlinear codes gives similar accuracy with equivalent linear code as indicated with the similar stiffness and small strain damping ratio.

Response Spectra

Response spectra can provide a clear way to evaluate the acceleration time histories predicted at ground surface level as depicted in Figures 5.14 and 5.15. The natural fundamental period of Turkey Flat site was 0.21 sec and beyond that period, the simulation results match the surface V1 recordings either for E-W and N-S horizontal component. All codes also gave very similar predictions at this period range which was expected. At shorter periods (T < 0.08 sec), the predictions generally underpredicted the recorded motions especially for the E-W component; all codes tended to predict results with higher variability. At medium periods, all predictions predicted generally lower values than the V1 recorded motion for E-W component but generally higher values for the N-S component. In conclusion, at this strain level, all codes is capable to predict with reasonable accuracy the phenomena of seismic wave propagation via 1D site response analysis.

Significant Duration & Intensity

Another important parameter that can be validated include the ground motion duration that can clearly presented by analyzing the plot of normalized Arias Intensity. Figures 5.16 and 5.17 show the plots of normalized Arias Intensity and the significant duration of the prediction of Turkey Flat vertical array site. Either for E-W and N-S component, all site response analysis codes tended to predict slightly longer duration than V1 recorded motion. The variance behavior of significant duration and intensity resulted in this case is similar to what is discussed in Chapter Three.
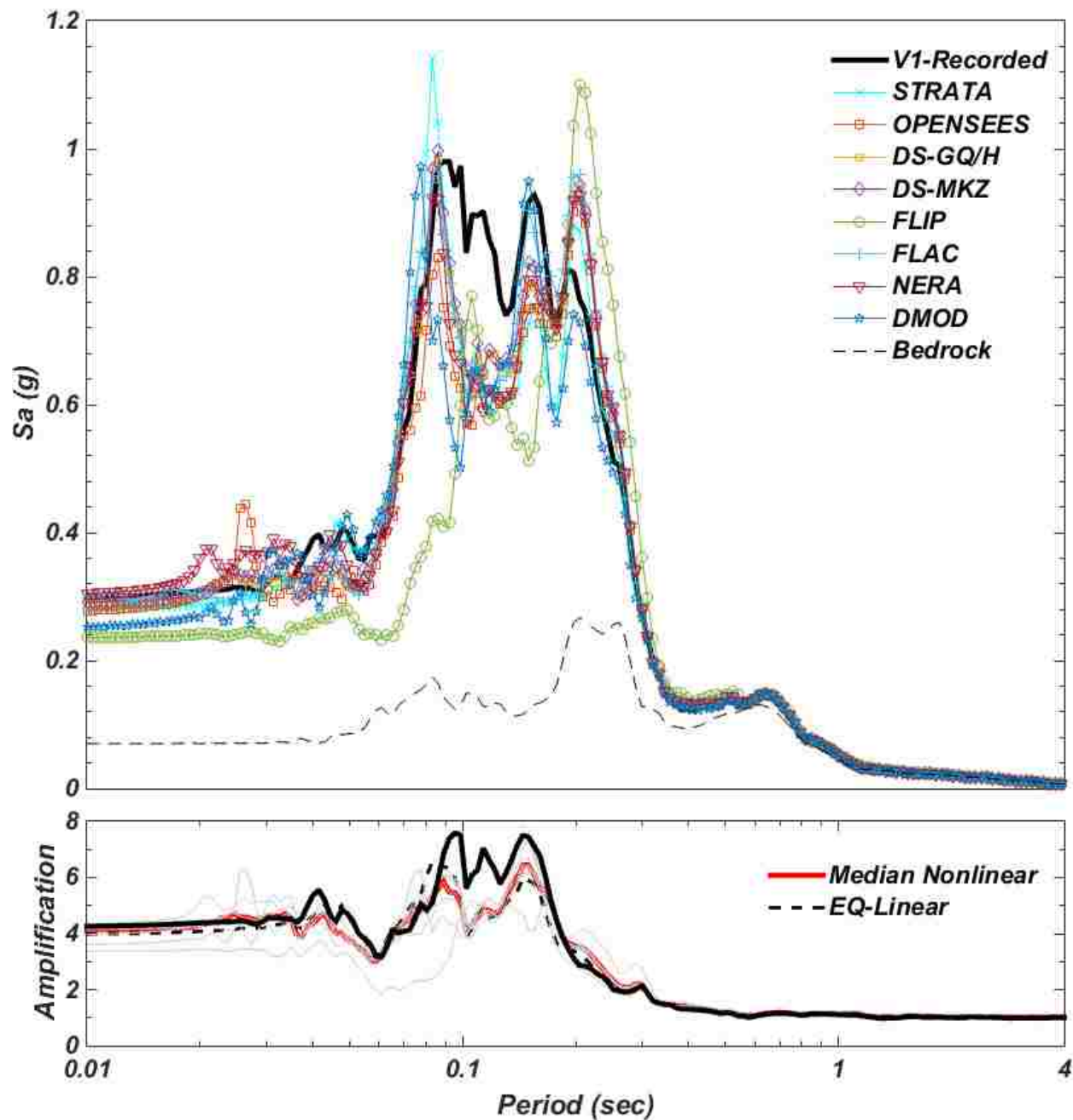
Figure 5.14. Prediction of response spectra of Turkey Flat vertical array site using East-West (E-W) component of input motion (D3-EW). Top figure depicts the spectral acceleration versus period and the bottom figure depicts the spectral amplification ratio predicted by nonlinear and equivalent linear analysis.
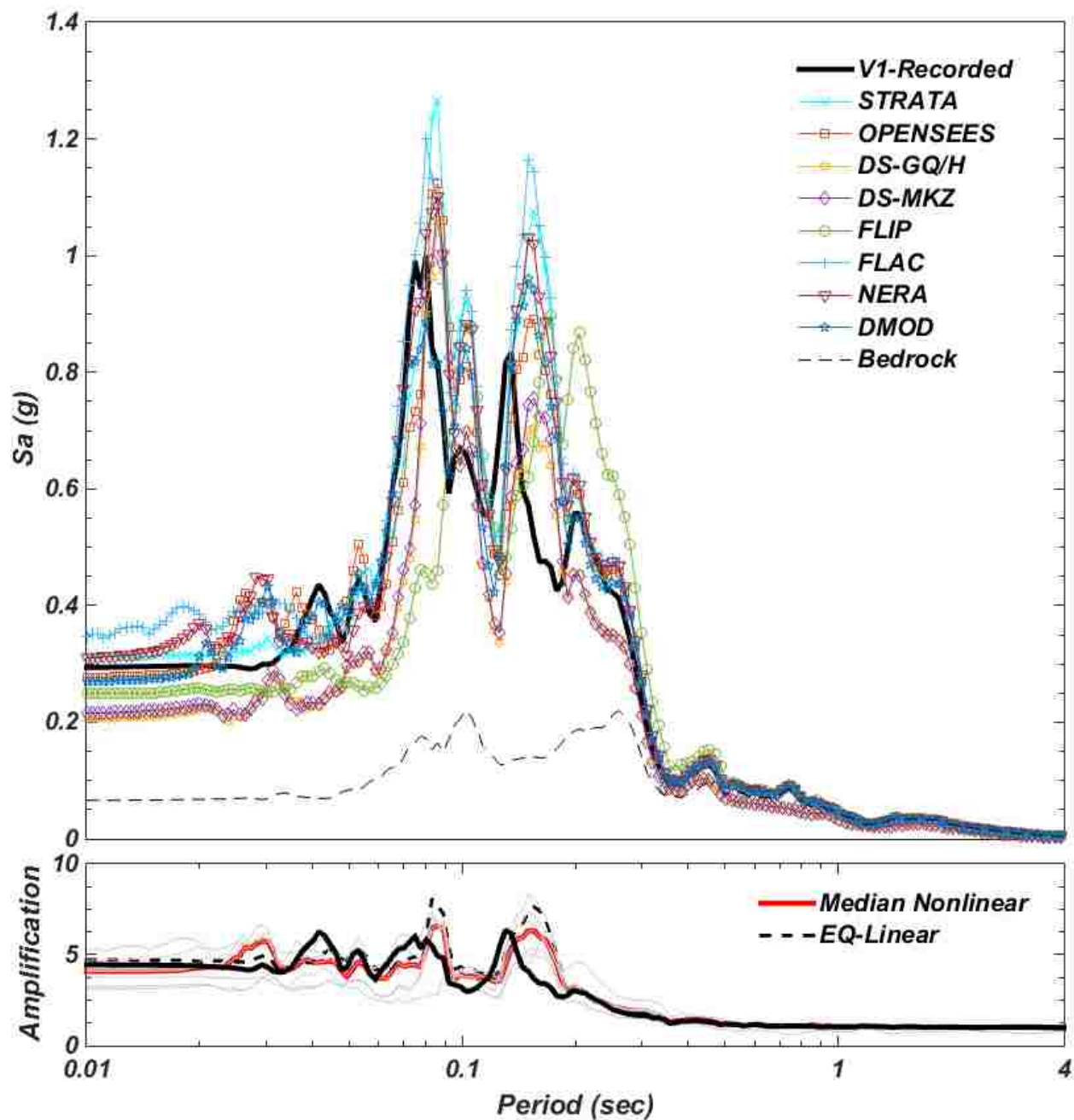
Figure 5.15. Prediction of response spectra of Turkey Flat vertical array site using North-South (N-S) component of input motion (D3-NS). Top figure depicts the spectral acceleration versus period and the bottom figure depicts the spectral amplification ratio predicted by nonlinear and equivalent linear analysis.
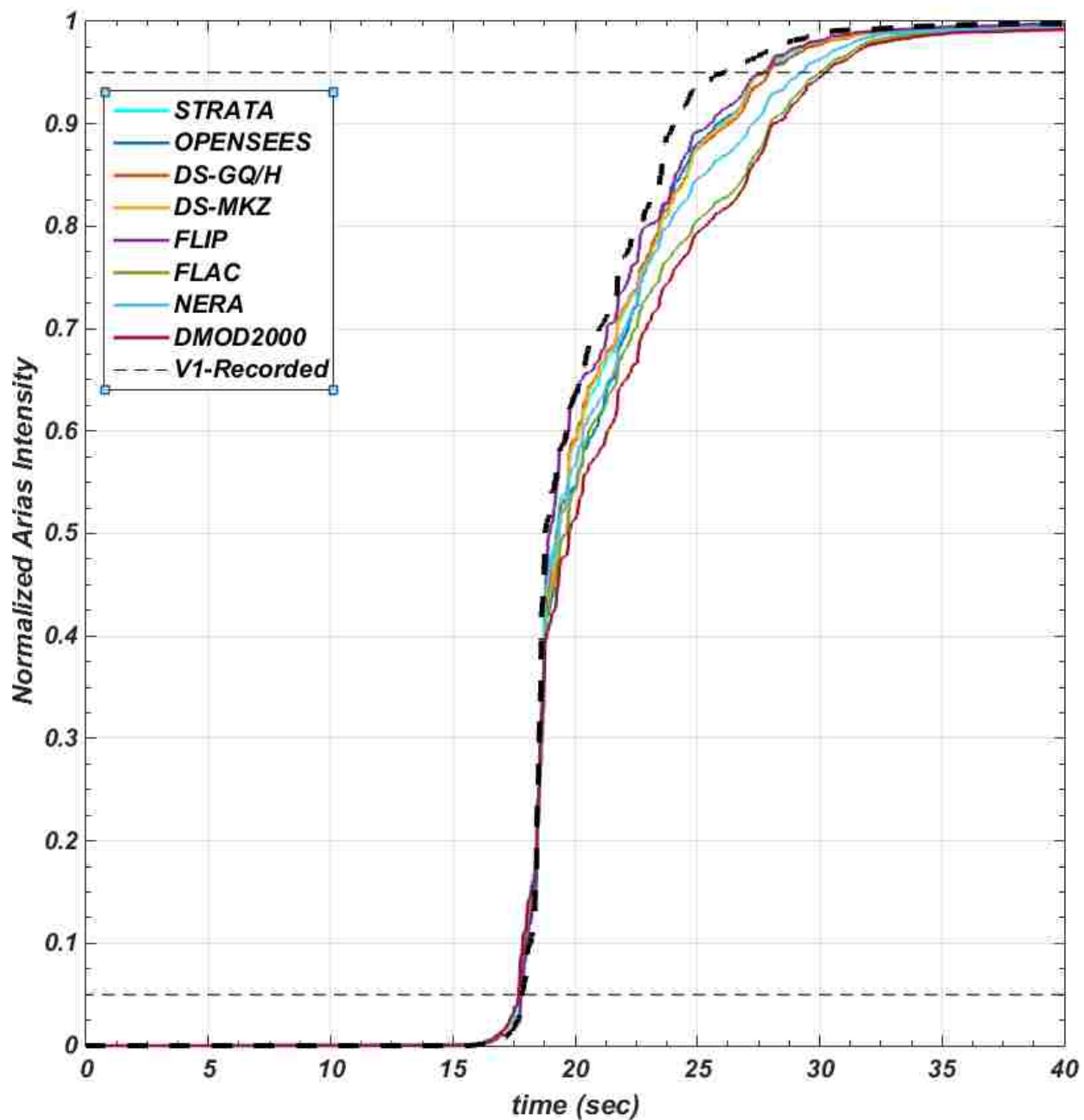
Figure 5.16. The plot of normalized Arias Intensity of Turkey Flat vertical array site shaken by East-West (E-W) component of input motion (D3-EW) of 2004 Parkfield Earthquake. All codes tend to predict longer duration than what is recorded.
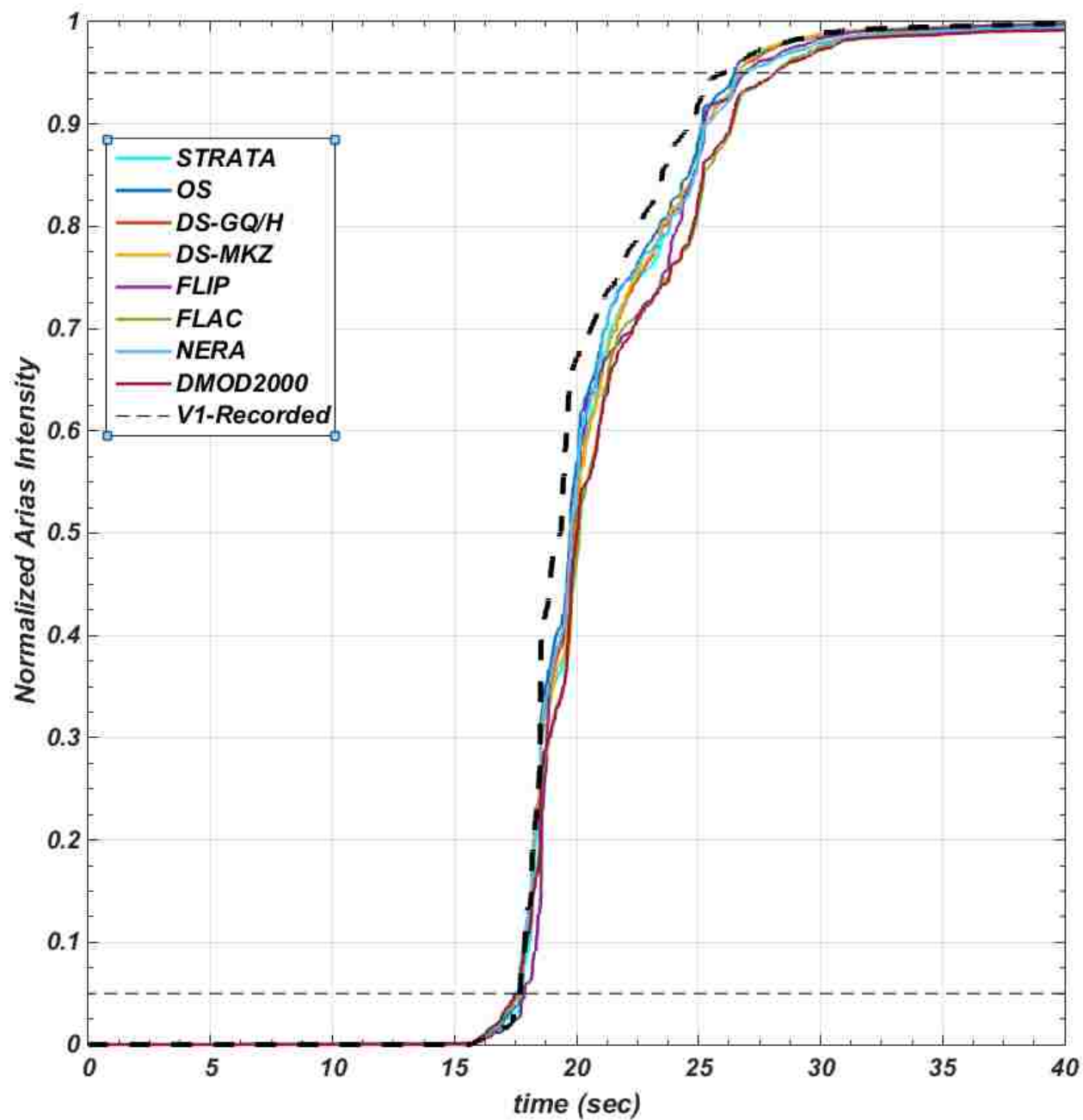
Figure 5.17. The plot of normalized Arias Intensity of Turkey Flat vertical array site shaken by East-West (N-S) component of input motion (D3-NS) of 2004 Parkfield Earthquake. All codes tend to predict slightly longer duration than what is recorded.

5.3.2   *Response at High Nonlinearity Level*

This section presents the results of 1D site response analysis using Valley Center soil profile shaken by 2004 Parkfield Earthquake motion (D3-East West component) scaled to 0.2, 0.5 and 1.0 g, respectively. These results correspond to high and very high nonlinearity levels which help illustrate the variability of each code in predicting the cyclic behavior at larger strain level taken from a well characterized site and vertical array data.

Profiles

When the D3 input motion was scaled to 0.2 g and is applied at the base of the Valley Center soil profile, it induced median shear strains of 0.4% indicating high soil nonlinearity level based on the G/G_{max} curve in Figure 5.7. This result is summarized in Table 5-5 and Figure 5.18. The PGA values produced by all codes are ranged from 0.629 to 0.834 g with a coefficient of variation of 12%. In general, the variability resulted from the analysis in this section exhibits similar behavior with what was observed in Chapter Three. The plot of profiles of site response in Figure 5.18 indicates that FLIP results deviated from other codes because it did not implement identical target G/G_{max} curves in the computation. However, it still gave reasonable accuracy and response compare to other codes. It also can be concluded that the variability of shear stress is lower than the variability of computed PGA and shear strain in site response prediction.

Table 5-5 Results of computed profiles of PGA, cyclic strain and stress at Valley Center shaken by D3-EW motion scaled to 0.2 g

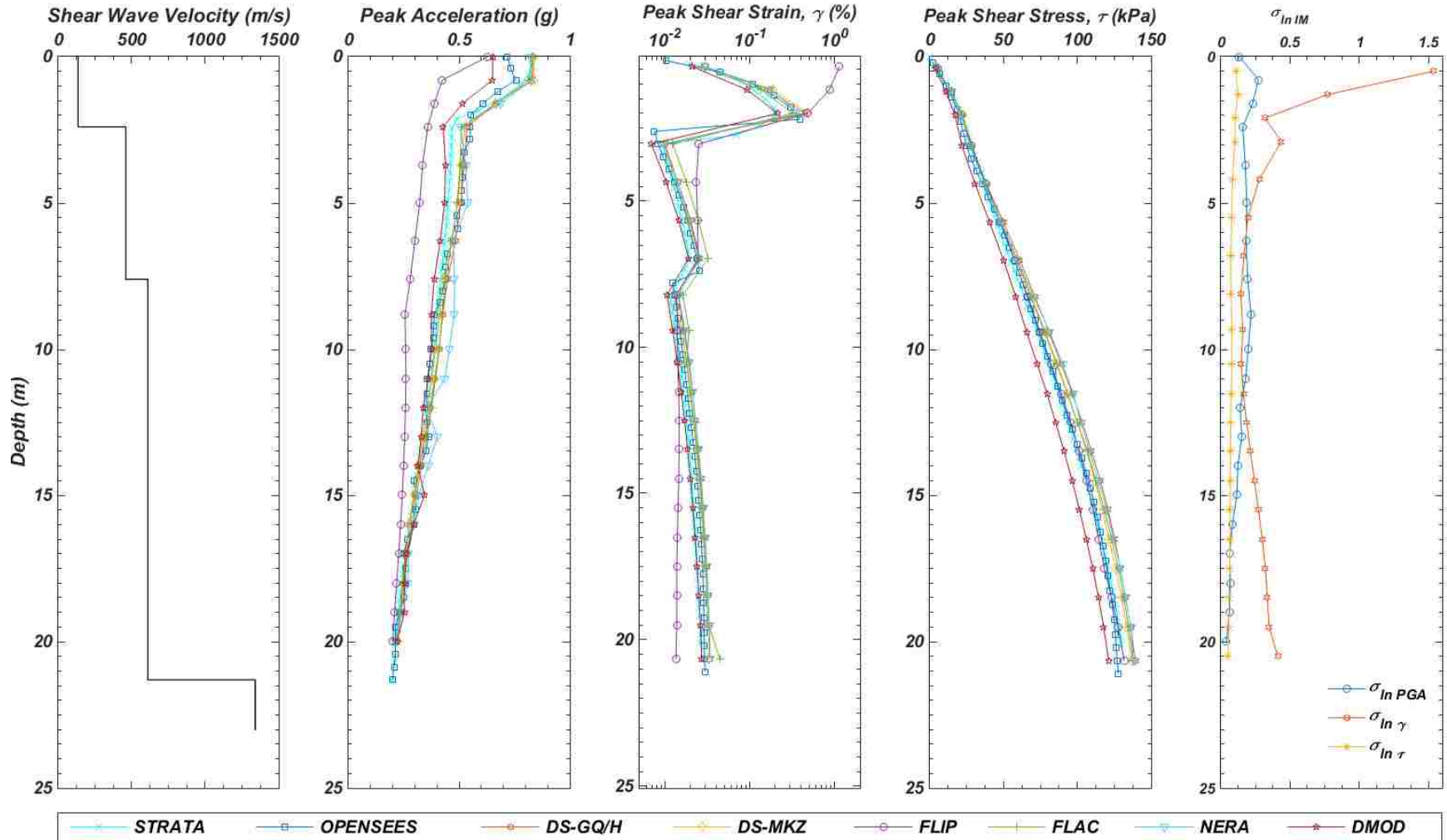| Parameters	EQL	OPEN SEES	DS-GQ	DS-MKZ	FLIP	FLAC	NERA	DMOD	median (NL only)	σ std.dev (NL only)	CoV (NL only)
PGA (g)	0.834	0.718	0.834	0.834	0.629	0.831	0.819	0.651	0.819	0.091	12%
Shear Strain (%)	0.196	0.341	0.445	0.496	0.485	0.323	0.391	0.214	0.391	0.1008	26%
Shear Stress (kPa)	21.4	19.5	22.53	22.54	*21.27*	21.58	21.21	17.13	21.27	1.922	9%

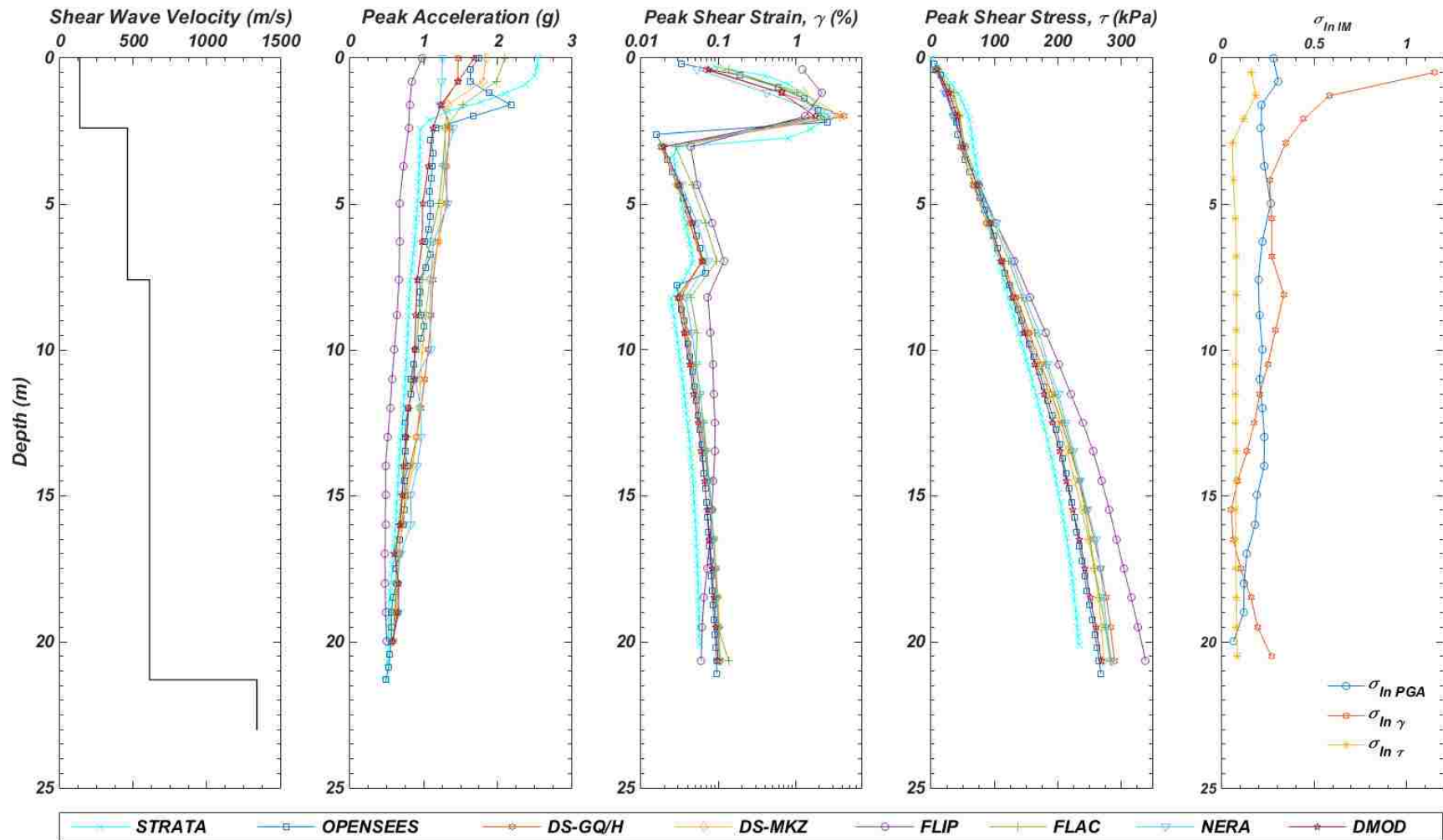Figure 5.18. Results prediction of Turkey Flat vertical array site using East-West (E-W) component of input motion (D3-EW) scaled to 0.2 g. From left to right are plot of shear wave velocity, peak acceleration, shear strain and shear stress versus depth predicted by all codes. The plot of standard deviation of natural logarithm indicates the PGA, peak shear strain and peak shear stress at each depth.

For stronger motions scaled to 0.5 and 1.0 g, the median peak shear strain were 2.1% and 5.2%, respectively, indicating very high nonlinearity levels. These results are depicted in Tables 5-6 and Table 5-7, Figures 5.19 and 5.20. The variability of the shear strain in these two results are relatively high indicating higher discrepancy of the node's movement prediction during earthquake event. The NL soil model will dramatically influence the computed response because all the NL codes construct different stress-strain curve at higher shear strain level. Figure 5.19 and Figure 5.20 also indicates that FLIP gave results that deviated from the others and it confirms the sensitivity of selected backbone curve to the accuracy of the site response prediction.

Table 5-6 Results of computed profiles of PGA, cyclic strain and stress at Valley Center shaken by D3-EW motion scaled to 0.5 g

Parameters	EQL	OPEN SEES	DS-GQ	DS-MKZ	FLIP	FLAC	NERA	DMOD	median (NL only)	σ std.dev (NL only)	CoV (NL only)
PGA (g)	2.54	1.75	1.46	1.84	0.97	2.09	1.25	1.68	1.68	0.379	24%
Shear Strain (%)	2.21	2.12	4.2	3.72	1.33	2.09	2.82	1.77	2.12	1.05	41%
Shear Stress (kPa)	58	39.1	37.05	45.4	*35.82*	45.5	35.14	41.7	39.1	4.33	11%

Table 5-7 Results of computed profiles of PGA, cyclic strain and stress at Valley Center shaken by D3-EW motion scaled to 1.0 g

Parameters	EQL	OPEN SEES	DS-GQ	DS-MKZ	FLIP	FLAC	NERA	DMOD	median (NL only)	σ std.dev (NL only)	CoV (NL only)
PGA (g)	2.626	1.823	1.575	2.156	0.837	2.246	1.354	2.795	1.8237	0.644	35%
Shear Strain (%)	5.21	3.45	6.821	6.063	5.64	4.261	5.303	4.585	5.303	1.146	22%
Shear Stress (kPa)	63	37.2	38.58	52.98	*42.84*	51.27	37.83	58	42.84	8.447	19%

Figure 5.19. Results prediction of Turkey Flat vertical array site using East-West (E-W) component of input motion (D3-EW) scaled to 0.5 g. From left to right are plot of shear wave velocity, peak acceleration, shear strain and shear stress versus depth predicted by all codes. The plot of standard deviation of natural logarithm indicates the PGA, peak shear strain and peak shear stress at each depth.
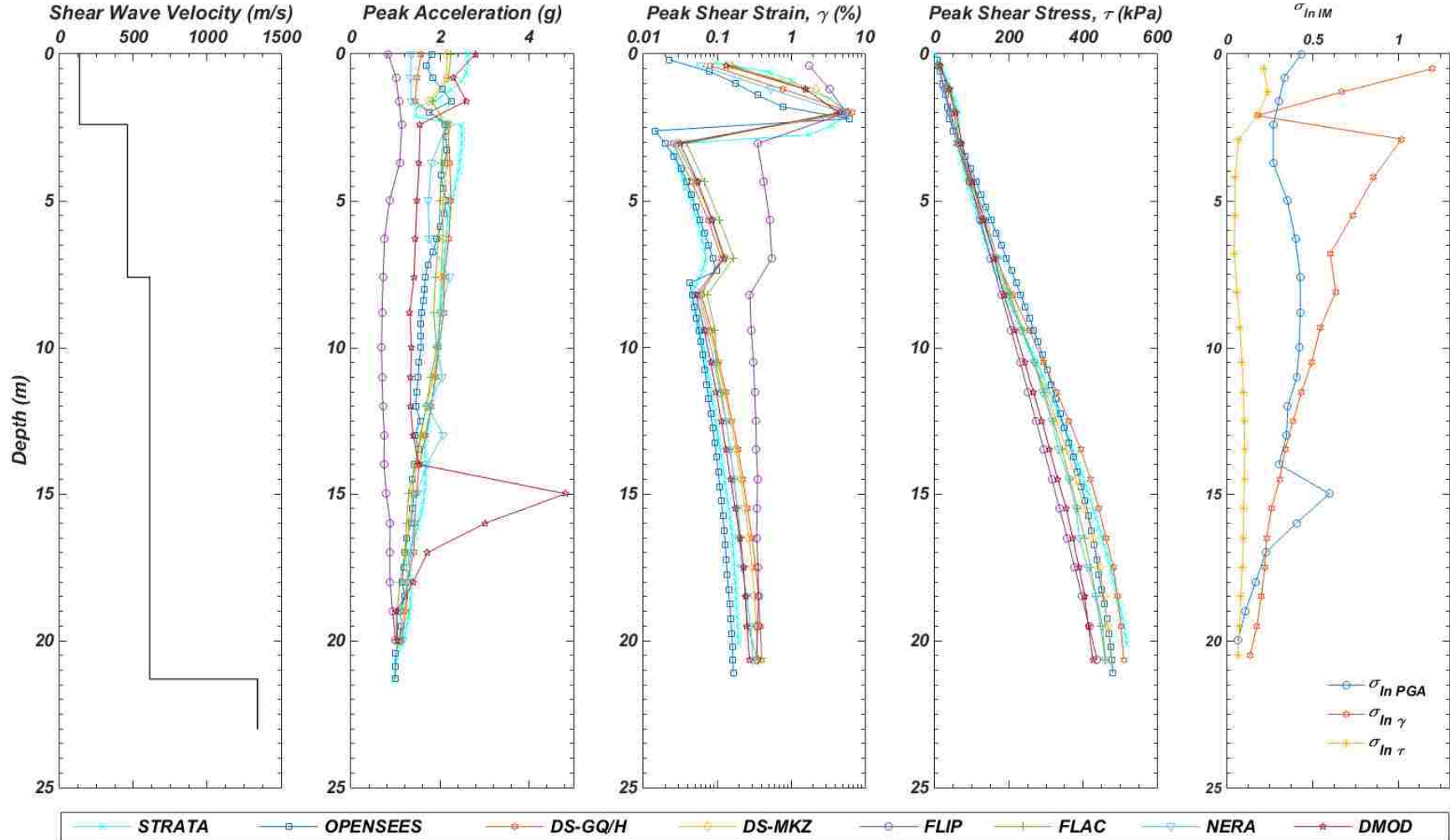
Figure 5.20. Results prediction of Turkey Flat vertical array site using East-West (E-W) component of input motion (D3-EW) scaled to 0.5 g. From left to right are plot of shear wave velocity, peak acceleration, shear strain and shear stress versus depth predicted by all codes. The plot of standard deviation of natural logarithm indicates the PGA, peak shear strain and peak shear stress at each depth.

Hysteresis Loops

The stress-strain curves are crucial to evaluate the performance of site response codes in predicting cyclic behavior at higher nonlinearity levels. Figure 5.21 shows the cyclic stress-strain behavior at moderate shear strain level at Turkey Flat site. All codes predicted similar stiffness and behavior in terms of the area of hysteresis loop. These results were similar to what was observed for Group-3 in Chapter Three. Furthermore, for the higher soil nonlinearity level (Group-4), all codes started to give different cyclic behavior. From the results shown in Figures 5.22 and 5.23, several nonlinear codes (i.e., DS-MKZ, D-MOD2000 and FLAC) were not capable of capturing the peak shear strength behavior that is crucial in site response prediction. On the other hand, OPENSEES and NERA were able to capture this important aspect although those codes exhibited greater damping ratios than actually occur in real conditions. Codes such as DS-GQ/H and FLIP employ non-Masing rules that allow the hysteresis loop construct smaller area indicating lower damping ratio. At this nonlinearity level, the EQL is no longer accurate to predict site response since it tends to predict stiffer behavior as depicted in Figures 5.21 to 5.23

Response Spectra

The response spectra predicted by all codes are presented in Figures 5.24 to 5.26. The results for Group-3 indicated similar shapes of response spectra and a little variability. The median amplification predicted by NL codes were similar to EQL prediction. Moreover, the results for Group-4 indicated very high variability especially for periods around the natural site period. These results are aligned with what was observed in the previous chapter.

Arias Intensity

Ground motion duration is another important parameter evaluated in this section, and the results are depicted in Figures 5.27 to 5.29. At large strain levels, the code-to-code variability is relatively low as indicated in Figure 5.27. All codes predicted similar durations and intensity levels. Moreover, the code to code variability tended to increase and become high at very high shear strain level as depicted in Figures 5.28 and 5.29. The EQL codes tended to predict shorter durations since they predict stiffer behavior than what is predicted by NL codes. FLIP predicts longer duration because of different target G/G_{max} curve implemented in the computation.
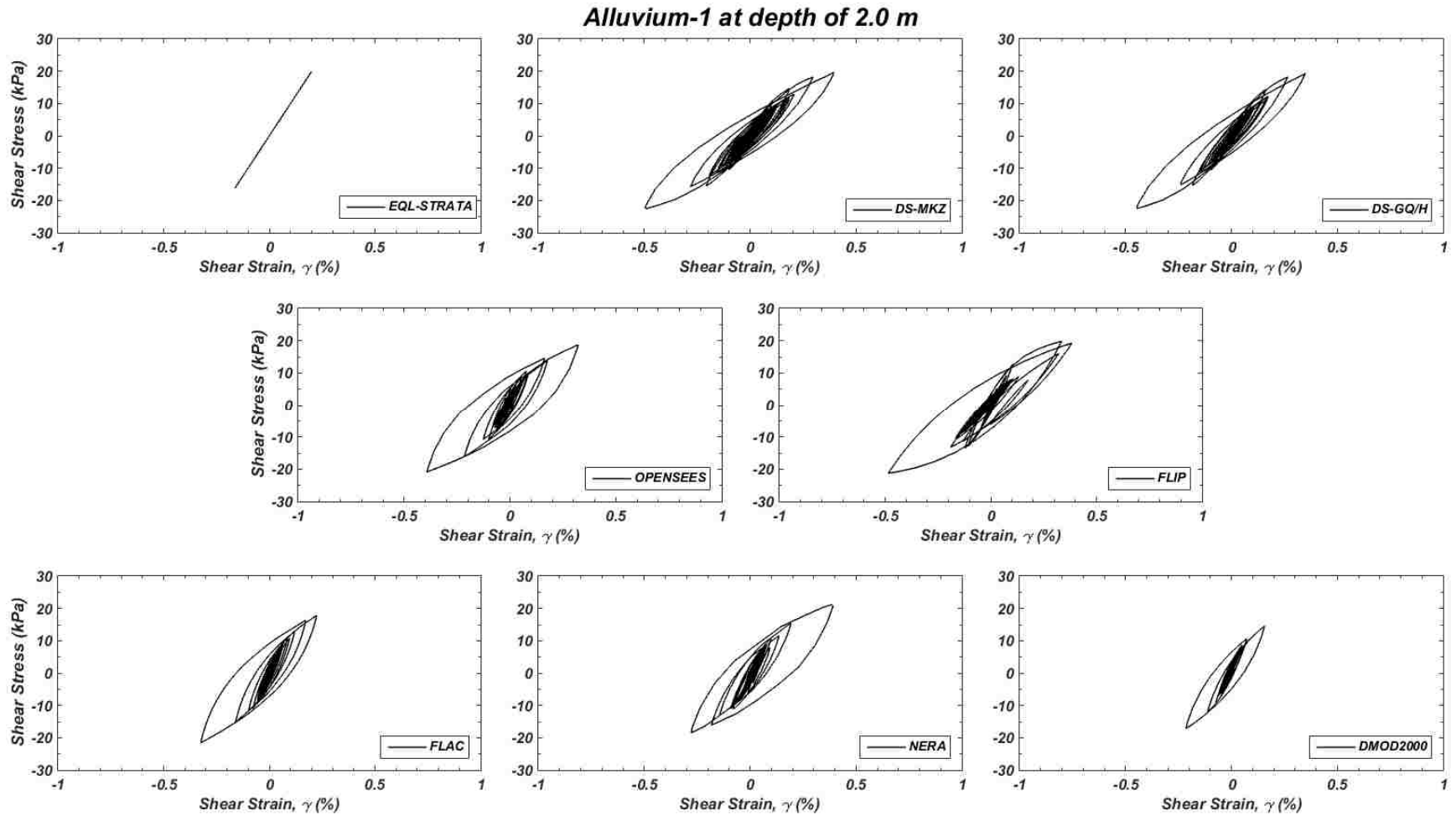
Figure 5.21. Plot of stress-strain curve predicted by all codes at moderate shear strain level (Group-3) at Turkey Flat site. At this strain level, all codes predicts relatively similar behavior.
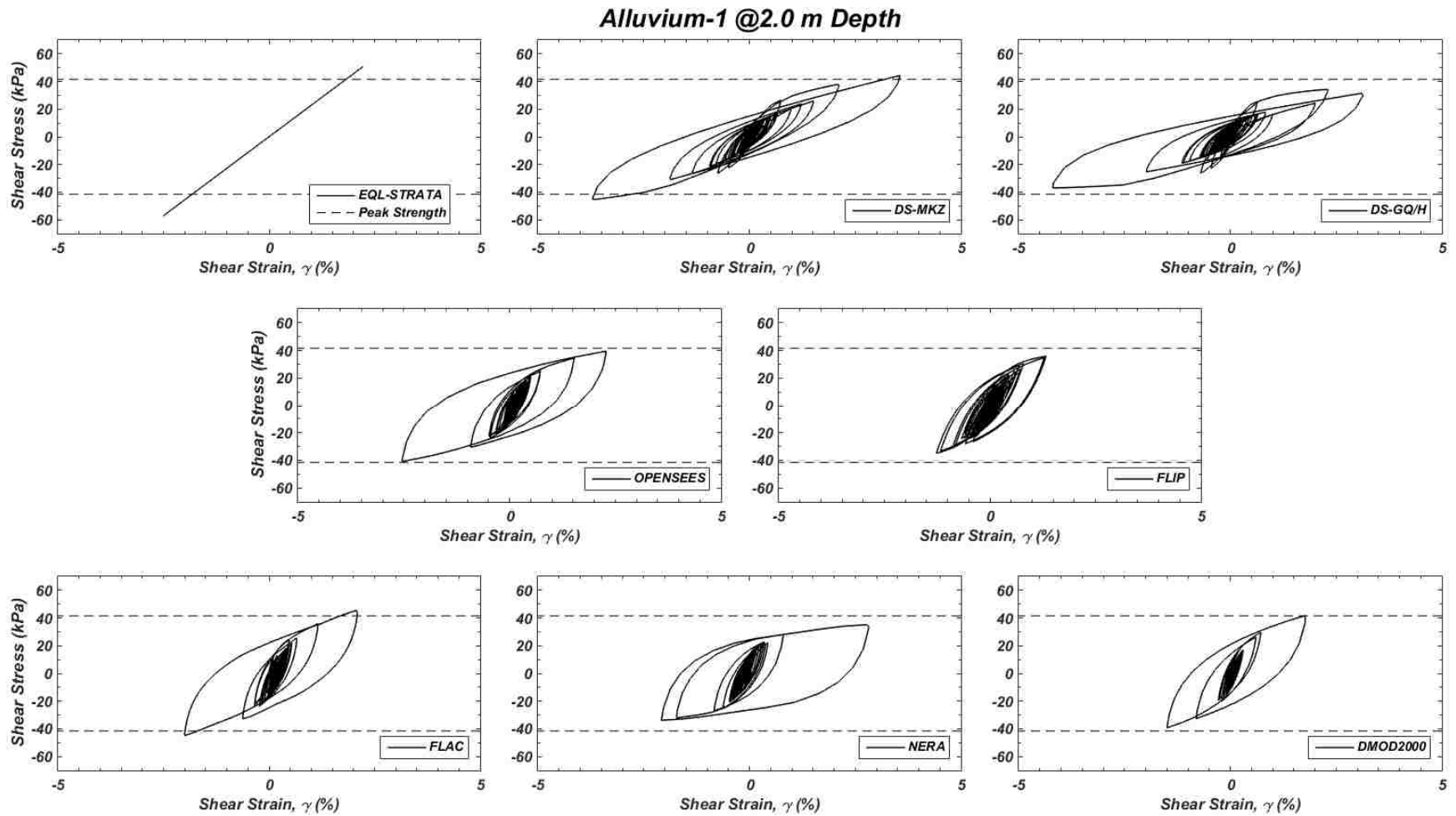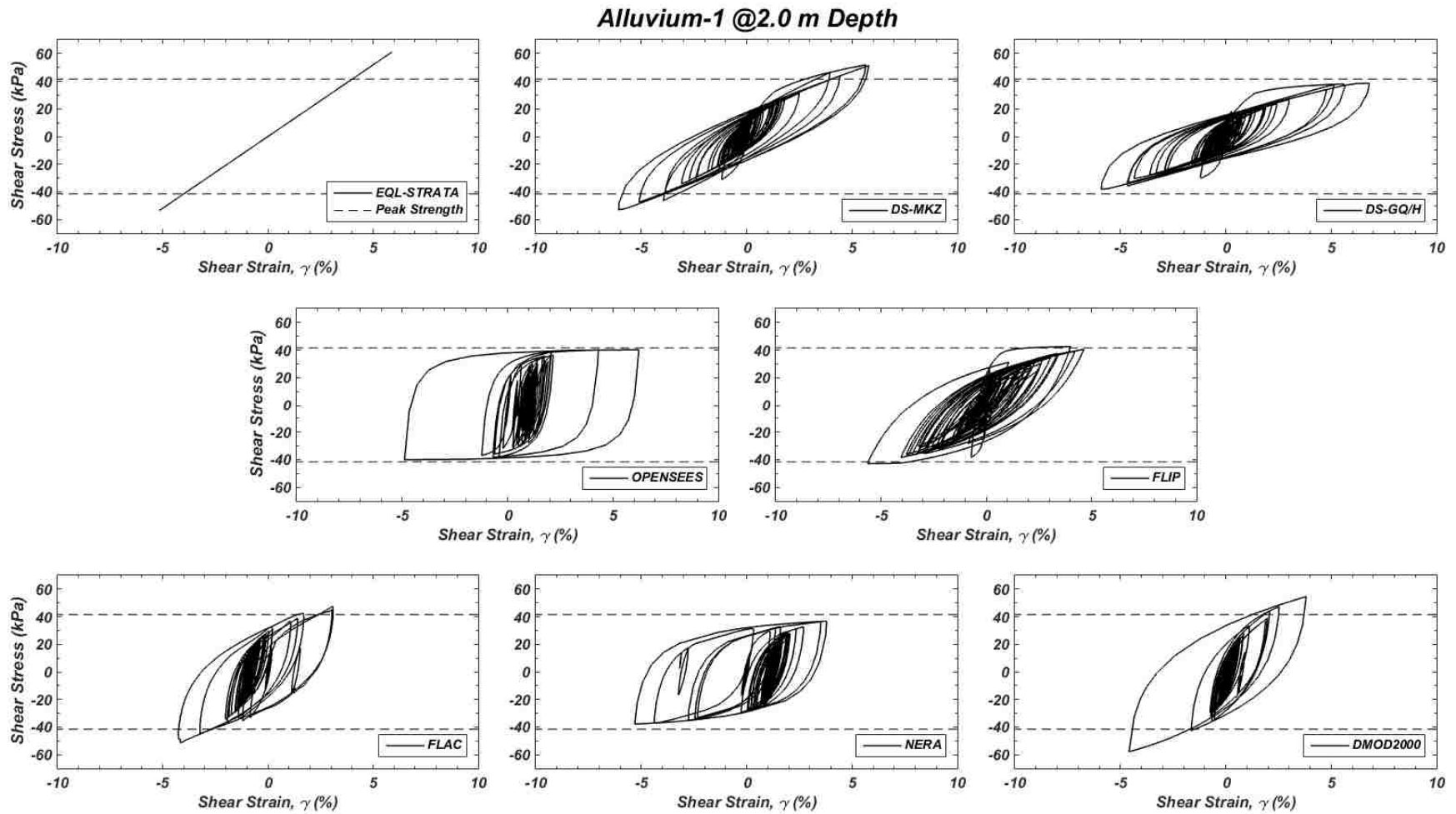
Figure 5.22. Plot of stress-strain curve predicted by all codes at moderate shear strain level (Group-4) at Turkey Flat site. At this strain level, all codes predicts relatively similar behavior.

Figure 5.23. Plot of stress-strain curve predicted by all codes at moderate shear strain level (Group-4) at Turkey Flat site. At this strain level, all codes predicts relatively similar behavior.
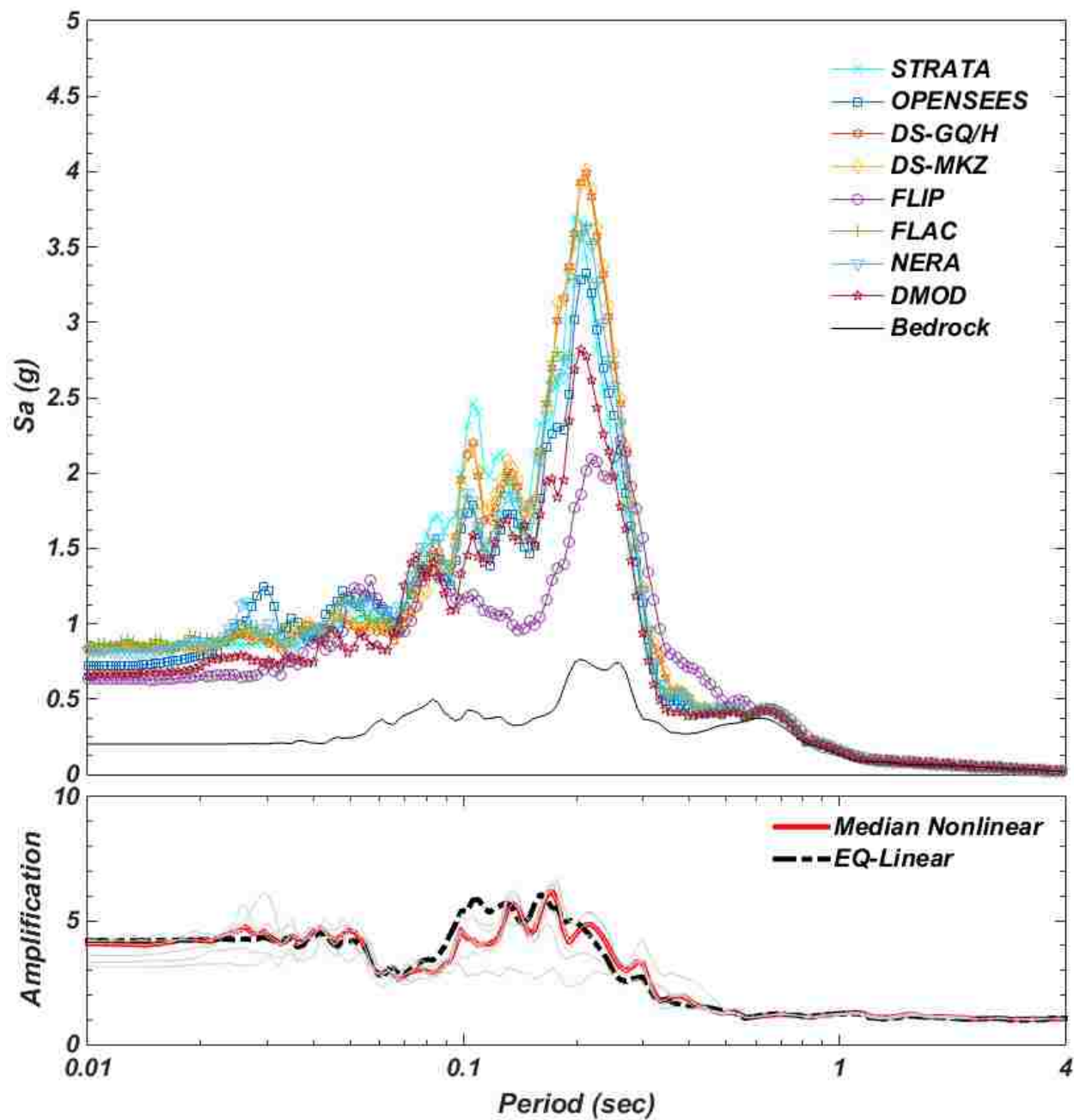
Figure 5.24. Plot of response spectrum at ground surface and amplification ratio (surface/bedrock) predicted by all codes at Turkey Flat site shaken by D3-EW motion scaled to 0.2g. The variability of the spectral acceleration increase around the natural site period of the Valley Center soil profile.
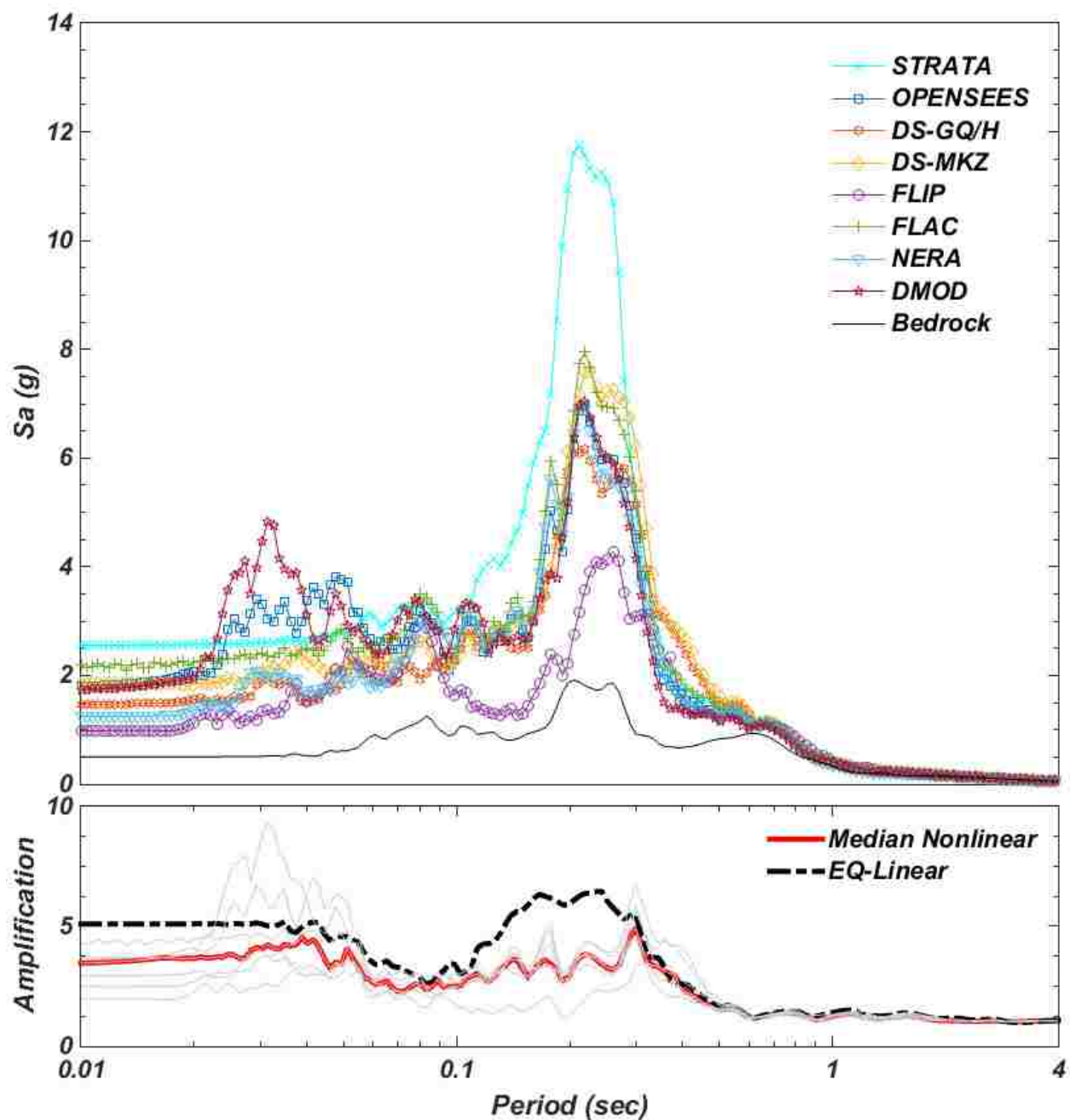
Figure 5.25. Plot of response spectrum at ground surface and amplification ratio (surface/bedrock) predicted by all codes at Turkey Flat site shaken by D3-EW motion scaled to 0.5g. The variability of the spectral acceleration increase around the natural site period of the Valley Center soil profile.
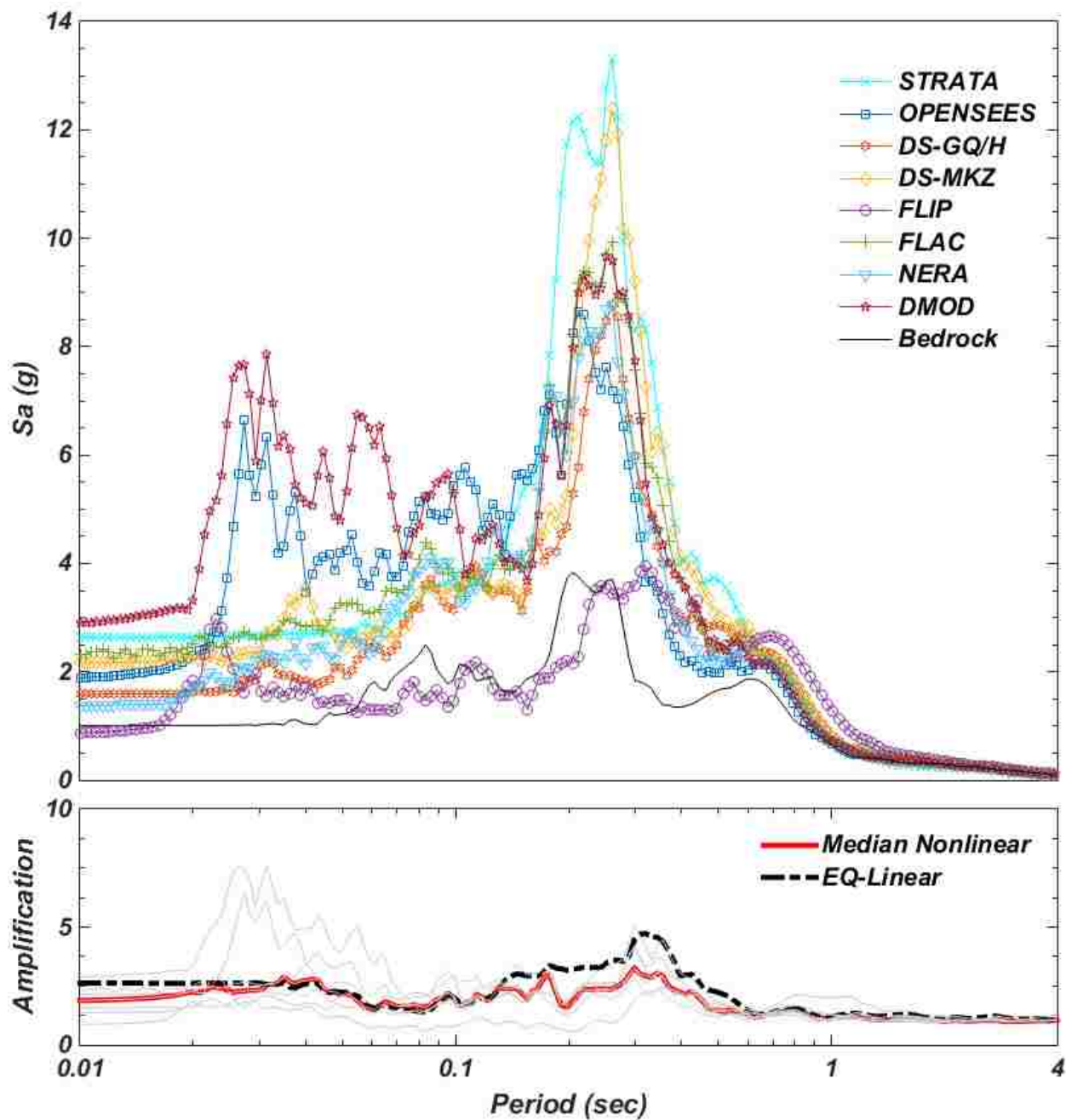
Figure 5.26. Plot of response spectrum at ground surface and amplification ratio (surface/bedrock) predicted by all codes at Turkey Flat site shaken by D3-EW motion scaled to 1.0g. The variability of the spectral acceleration is high at all periods until 0.5 second. At this strain level, the prediction is full with uncertainty.
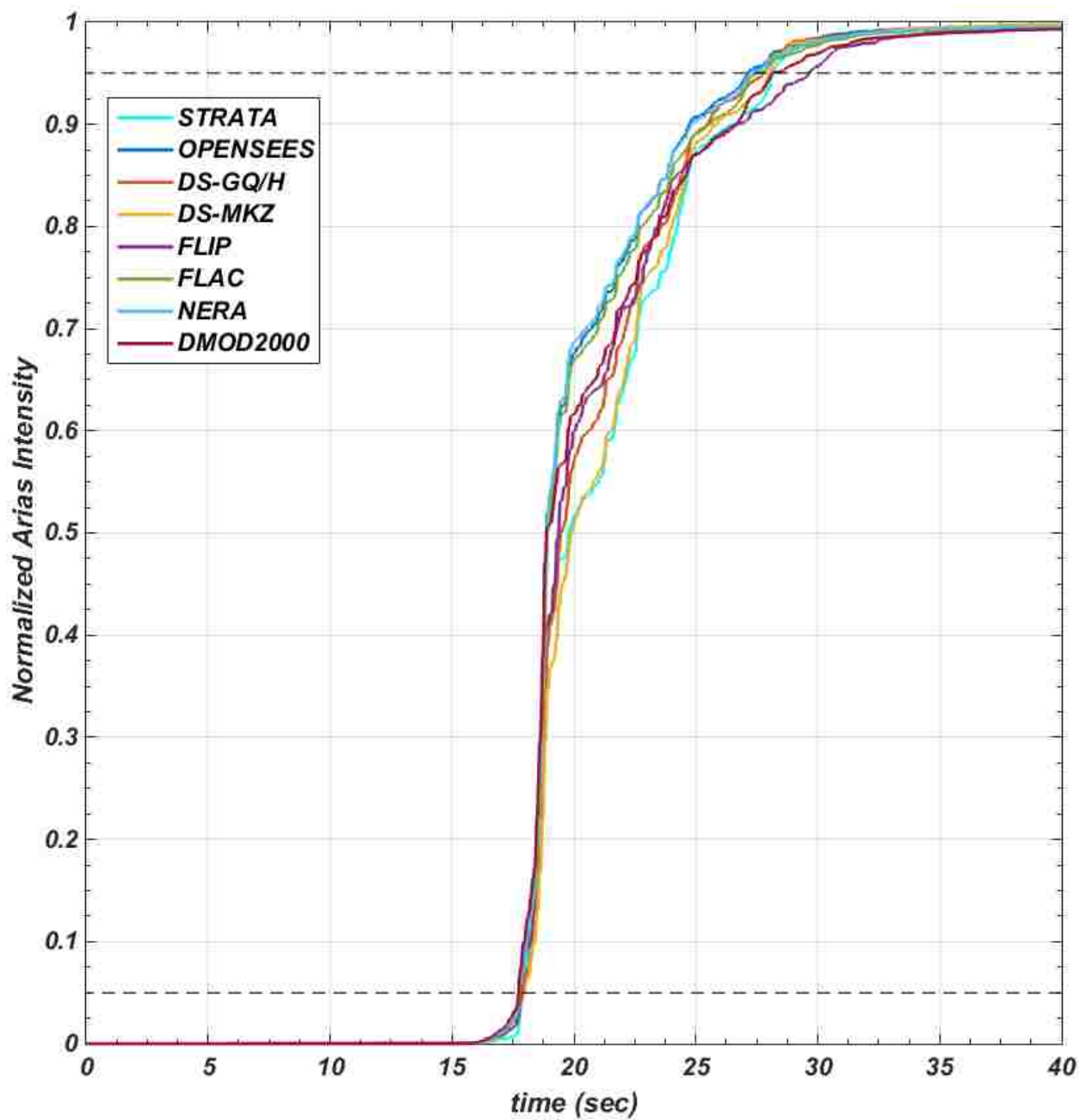
Figure 5.27. Plot of normalized Arias Intensity predicted by all codes at Turkey Flat site shaken by D3-EW motion scaled to 0.2g. Code to code variability at this strain level is relatively low.
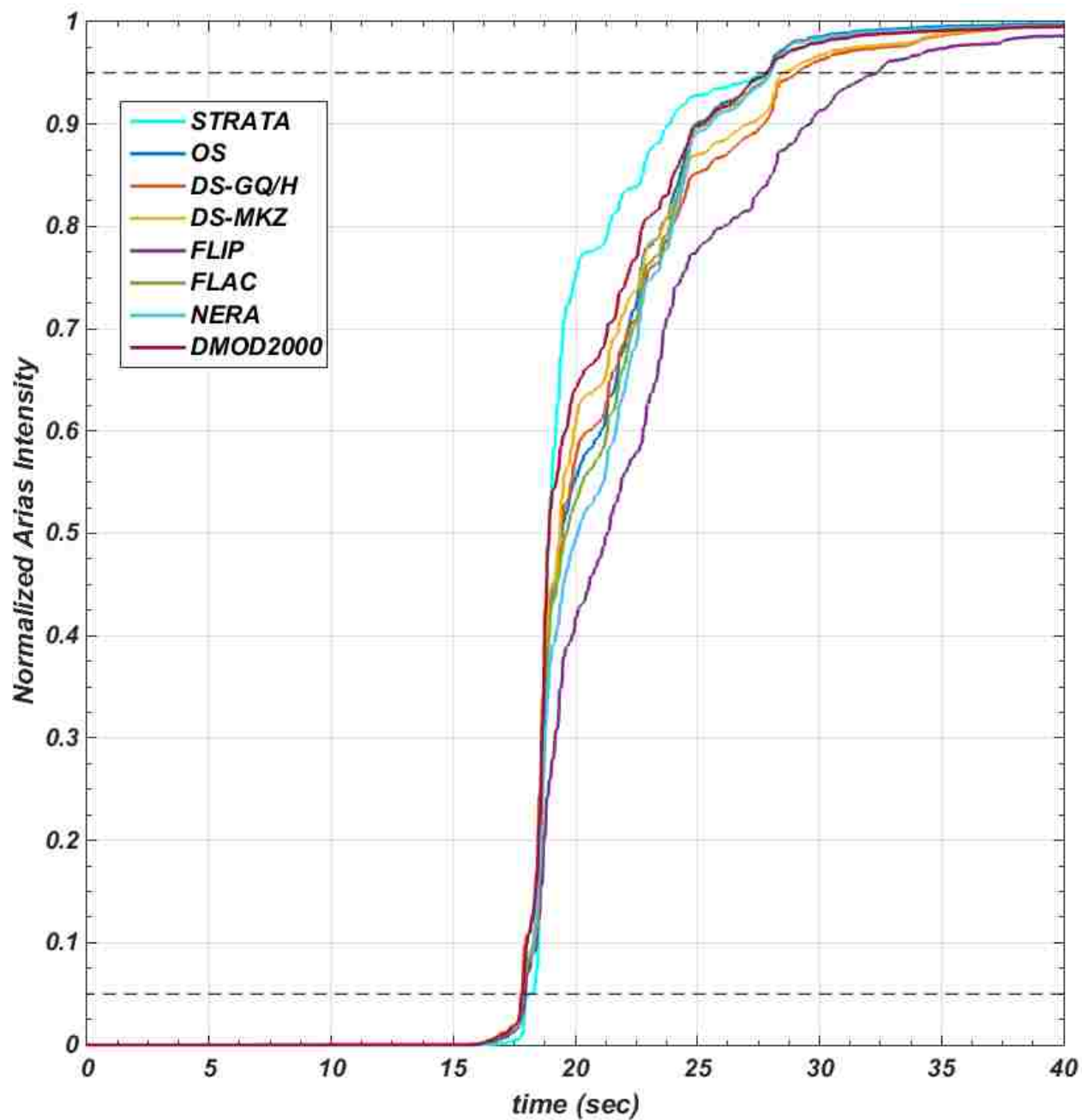
Figure 5.28. Plot of normalized Arias Intensity predicted by all codes at Turkey Flat site shaken by D3-EW motion scaled to 0.5g. Code to code variability at this strain level start to increase while the EQL codes predict shorter duration due to stiffer behavior.
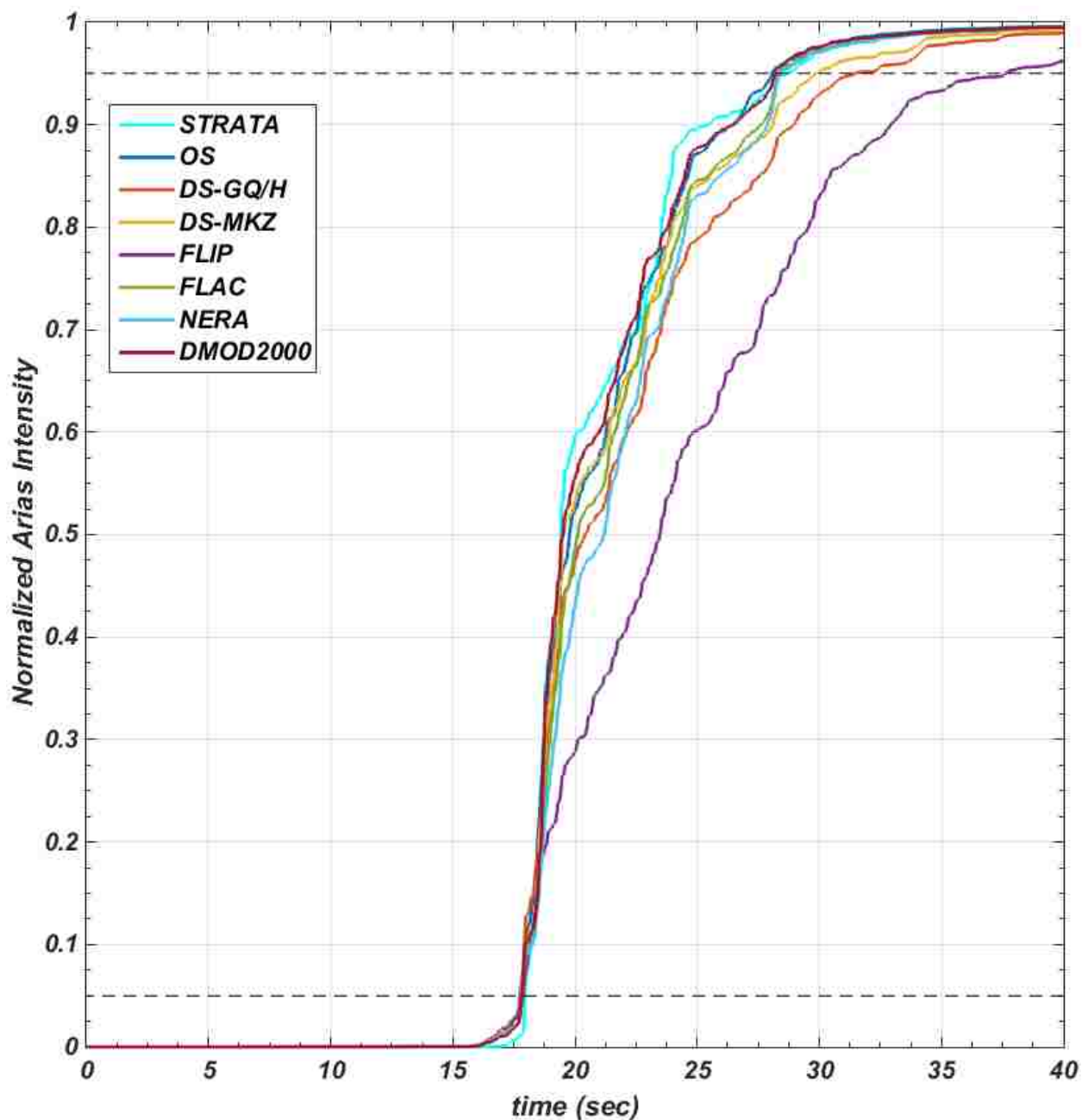
Figure 5.29. Plot of normalized Arias Intensity predicted by all codes at Turkey Flat site shaken by D3-EW motion scaled to 1.0. Code to code variability at this strain level start to increase while the EQL codes predict shorter duration due to stiffer behavior and FLIP predicts longer duration than other codes.

The site prediction resulted in this chapter are align with what were observed in previous chapter in terms of the variance behavior. The plot of coefficient of variation versus shear strain for 5 additional cases at Turkey Flat site is depicted in Figure 5.30 to Figure 5.34.
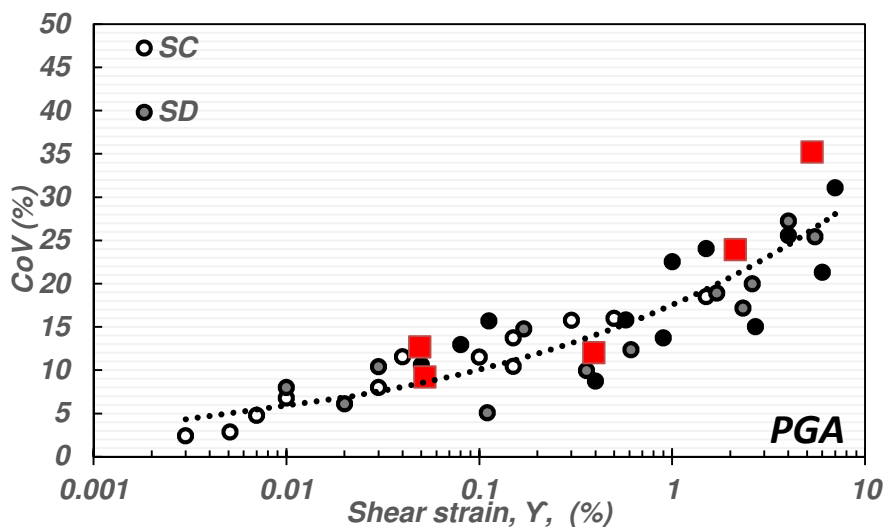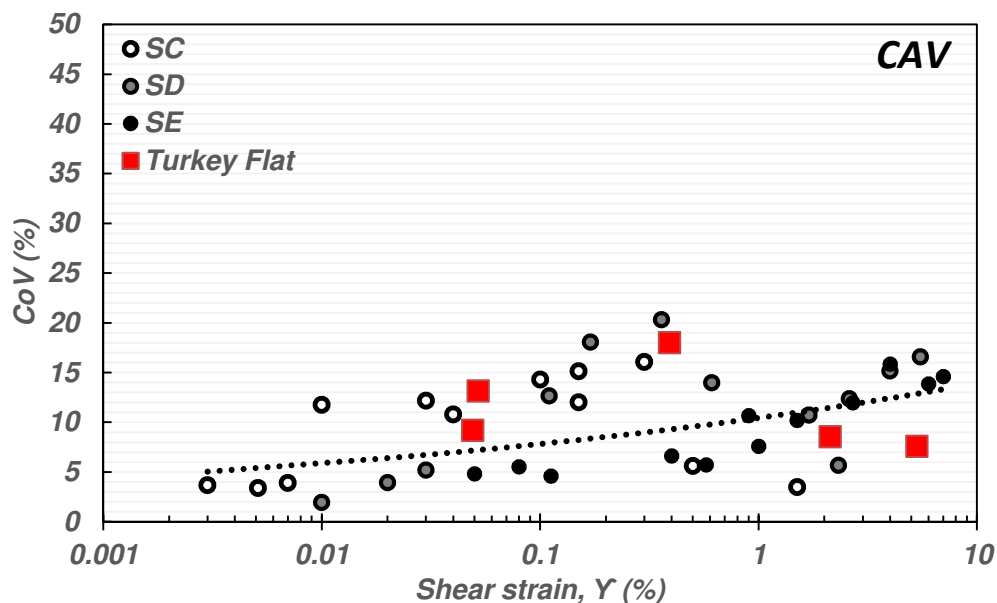

Figure 5.30. Plot of coefficient of variation of PGA at ground surface versus shear strain computed from all site response analysis performed in this research. The Turkey Flat data indicates similar variance behavior compared to what is observed in other results.
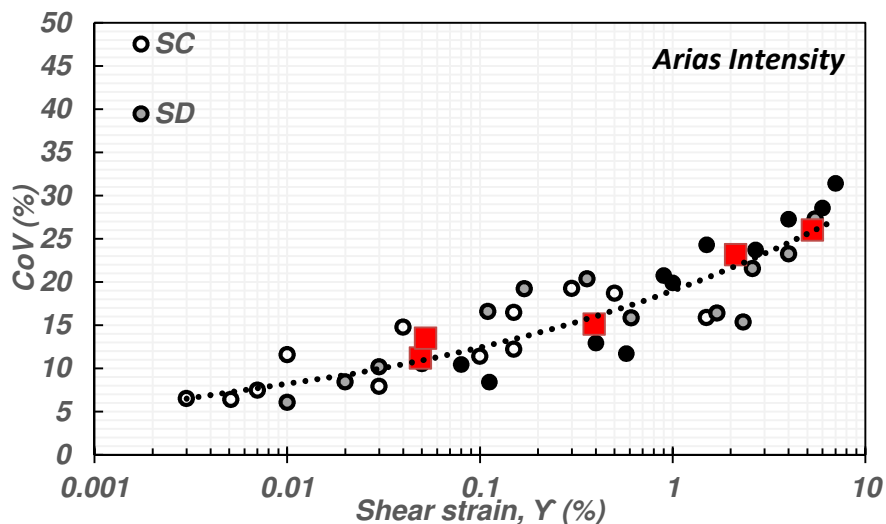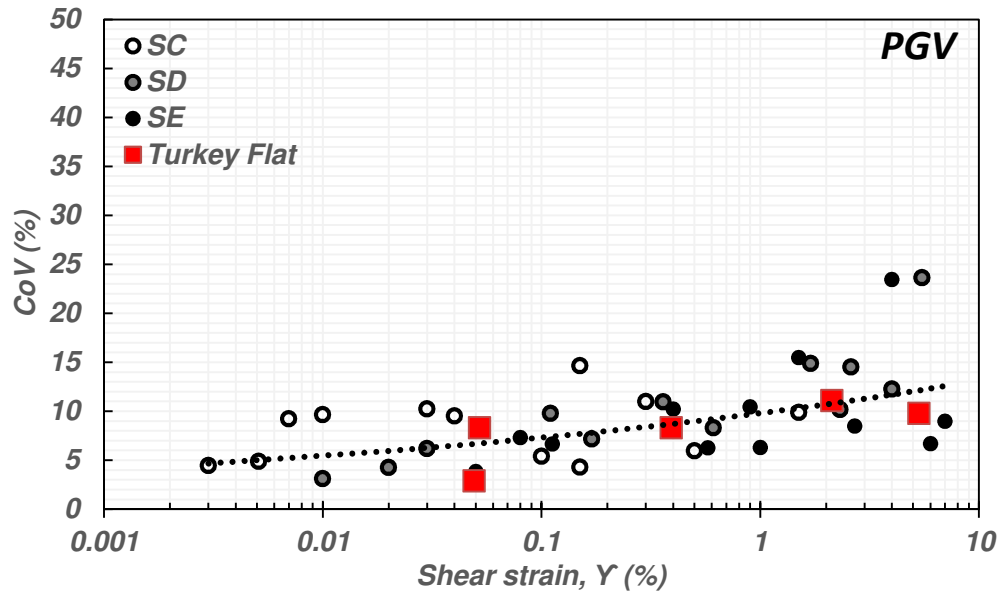

Figure 5.31. Plot of coefficient of variation of Arias Intensity for the acceleration time histories resulted at ground surface versus shear strain computed from all site response analysis performed in this research. The Turkey Flat data indicates similar variance behavior compared to what is observed in other results.
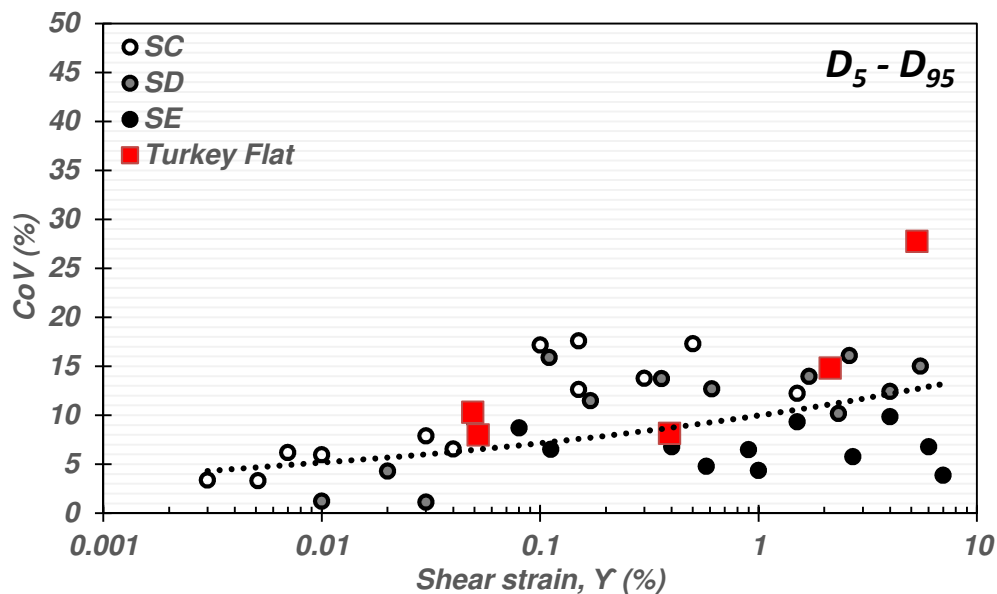
Figure 5.32. Plot of coefficient of variation of significant duration for the acceleration time histories resulted at ground surface versus shear strain computed from all site response analysis performed in this research. The Turkey Flat data indicates similar variance behavior compared to what is observed in other results.

Figure 5.33. Plot of coefficient of variation of Cumulative Absolute Velocity at ground surface versus shear strain computed from all site response analysis performed in this research. The Turkey Flat data indicates similar variance behavior compared to what is observed in other results.

Figure 5.34. Plot of coefficient of variation of PGV at ground surface versus shear strain computed from all site response analysis performed in this research. The Turkey Flat data indicates similar variance behavior compared to what is observed in other results

5.4   SUMMARY

This chapter has presented the results of a comparison of the predictions of 1D site response analysis codes against a recorded data from vertical array at a site near the San Andreas Fault in California, USA. Turkey Flat site is located on top of an unsaturated deposit and that is a suitable site to validate the 1D assumption. The soil profile at Valley Center was analyzed using all considered site response codes and the results compared to recorded motions at Turkey Flat site. Several findings were observed in this chapter:

- The seismic site response predicted by all codes was similar compared to that recorded at the Turkey Flat site. The induced shear strain of the Turkey Flat site during 2004 Parkfield earthquake was at a moderate nonlinearity level (Group-2 – $G/G_{max} > 0.5$) that made the site response prediction yield result with good accuracy.

- All of the site response codes predicted relatively similar results for cases limited to moderate nonlinearity and shear strain levels. Beyond this limit, the code-to-code variability started to increase and became very high at very large shear strain levels.

- At very large strain levels, the EQL codes tended to predict stiffer behavior while the NL codes are capable to simulate better prediction. However, not all NL codes predicted correct behavior since codes such as DS-MKZ, FLAC and D-MOD2000 were not capable to accurately capture the peak shear strength.

- FLIP does not employ identical G/G*max* curve as implemented in other codes. This condition causes FLIP results to deviate from other results. FLIP employs its own constitutive model with non-Masing rules as implemented in DS-GQ/H in this research.

- Codes such as OPENSEES and NERA are capable of predicting the peak shear strength of the soil although they still predict unreasonable damping ratios at large strain level since they utilize the Masing rules.

- The variability in predicting the shear strain is higher than the prediction of PGA and peak shear stress due to the different soil model implemented in the analyses.

Chapter 6. SUMMARY AND CONCLUSIONS

6.1 SUMMARY & CONCLUSION

Scope of Work

The prediction of ground shaking under earthquake events is typically accomplished via one-dimensional (1D) site response analysis. These analyses are often performed using the equivalent linear approach (EQL) since it requires straightforward soil properties and computational procedures. Recently, 1D nonlinear (NL) site response analyses have gained more popularity due to the capability to better simulate the soil nonlinearity level at higher shear strain levels at which the EQL approach is no longer accurate. The nonlinear soil model implemented in every NL codes play an important role in producing reasonable and accurate results.

In this research, current EQL and NL site response codes are evaluated at small to large strain levels in order to further study their capabilities in predicting seismic response at shear stress levels approaching the shear strength of the soil. The variability of the predictions is documented and important aspects of the analyses are discussed. In this research, the 1D site response analyses employ current recommendations and soil models that are typically implemented in engineering practice. This research also reviews the nonlinear soil models employed in the analyses to predict the cyclic behavior of soil at various strain levels. The 1D total stress site response analyses are performed against a set of simple soil profiles and a vertical array recording at a well characterized site using available codes (i.e., STRATA, DEEPSOIL, OPENSEES, NERA, FLAC 2D, FLIP and D-MOD2000).

Research Findings & Conclusion

The evaluation against current 1D site response analysis procedure have been performed in this researches and resulting several findings and conclusions as follow:

- 1D site response prediction utilizing EQL or NL codes gives relatively similar results for cases with moderate nonlinearity ($G/G_{max} > 0.5$) level or referred as Group 2 in this research. This similarity includes the node response along the profile (i.e., time histories,

response spectra), cyclic stress-strain behavior and duration. The protocols (e.g., Rayleigh damping calibration, specification of input motion and underlying halfspace, backbone curve modification and minimum layer thickness) explained in Chapter Two are recommended for another 1D total stress site response analysis and was successfully validated using Turkey Flat vertical array data during 2004 Parkfield earthquake.

- The plot of the profile versus several parameters results indicate that peak shear strain parameter had the highest variability compared to the PGA and the peak shear stress.

- The computed value of CoV of several ground motion parameters indicate that PGA and Arias Intensities have higher variability compared to the prediction of earthquake duration and Cumulative Absolute Velocity.

- For higher soil nonlinearity levels ($G/G_{max} < 0.5$), EQL codes predict results with unreasonable cyclic behavior indicated by stiffer behavior plotted in the stress-strain curve even though the other response might be similar to what is predicted by NL codes.

- Nonlinear soil models that are capable of predicting the peak shear strength will predict greater shear strain level at higher strain level as the compensation to accommodate same energy shaking. This condition leads the prediction of greater intensity motion, longer duration and greater displacement at ground surface than codes that are not capable of simulating the peak shear strength.

- Codes which are based on Masing rules (D-MOD2000, FLAC and OPENSEES) tend to predict generally lower PGA values at the ground surface due to high damping ratio during cyclic loading. For codes that are unable to capture the peak shear strength at high strain levels, this condition will underpredict the intensity motion at ground surface level.

- The IM Model implemented in NERA excluded viscous damping in the analysis that might prevent overdamping at large strain although it utilized the Masing rules to govern the unloading and reloading behavior. The results indicates that NERA tended to predict stronger intensity motion indicated by results that tend to be greater than the median value.

- Almost in all cases, DEEPSOIL tended to predict result close to the median value predicted by all NL codes.

- Nonlinear codes such as DEEPSOIL with Extended MKZ model, FLAC 2D and D-MOD2000 require special treatment during the prediction for the case with high nonlinearity level because they cannot capture the peak shear strength of the soil.

- The variability of the ground motion parameters predicted by NL codes tended to increase as the shear strain level increased. Parameters such as PGA, Arias Intensity have more sensitivity to higher shear strain level compare to other parameter such as Cumulative Absolute Velocity (CAV) and significant duration.

6.2   RECOMMENDATION FOR FUTURE WORKS

The results in this thesis indicates that several potential research that can improve the accuracy of 1D site response analysis in the future, as follow:

1. Current nonlinear soil model is capable to capture several important aspect of cyclic behavior of soil including the initial backbone curve, peak shear strength of soil, unloading-reloading behavior. However, the model is only valid for shear strain or nonlinearity level up to moderate level. The soil model to predict cyclic behavior of soil at high shear strain level is crucial and the unloading and reloading rules has not been fully understood. It could be validated against laboratory test results that can accommodate shear strain more than 5% to see the cyclic behavior of broader type of soil. Once the laboratory data is collected, a formulation to establish unloading-reloading rules at higher shear strain level could be formed.

2. The validation of site response analysis in this research only limited to total stress approach, alluvial deposit with relatively low shear strain and nonlinearity level. More validation with broader type of soil (e.g., sandy soil, peaty soil, etc), analysis approach (effective stress analysis) and higher shear strain cases from recorded earthquake event are required to gain more confidence to perform 1D site response analysis.

REFERENCES

Arefi, M.J., Cubrinovski, M., Bradley, B.A., (2013). "Site response analysis of Christchurch soil sites using a non-linear model." 2013 New Zealand Society for Earthquake Engineering Conference, New Zealand.

Arias, A. (1970). "A Measure of Earthquake Intensity," R.J. Hansen, ed. Seismic Design for Nuclear Power Plants, MIT Press, Cambridge, Massachusetts, pp. 438-483.

Baise, L. G., Glaser, S. D., and Dreger, D. (2003). "Site response at Treasure and Yerba Buena Islands, California." J. Geotech. Geoenviron. Eng., 129(5), 415–426.

Bardet, J. P., Tobita, T., 2001, NERA: A Computer program for Nonlinear Earthquake site Response Analyses of Layred soil deposits, Department of Civil Engineering, University of Southern California.

Chopra, A. K. (2012). Dynamics of structures: Theory and Applications to Earthquake Engineering, 4th Ed., Prentice-Hall, Englewood Cliffs, N.J.

Darendeli, M. B. (2001). "Development of a new family of normalized modulus reduction and material damping curves." Ph.D. dissertation, Univ. of Texas at Austin, Austin, TX, 396.

Dickenson, SE (1994). Dynamic Response of Soft and Deep Cohesive Soils during the Loma Prieta Earthquake of October 17, 1989, PhD thesis, Dept. of Civil and Enviro. Eng., University of California, Berkeley, CA.

Dobry, R., W.G. Pierce, R. Dyvik, G.E. Thomas, and R.S. Ladd. (1985). "Pore pressure model for cyclic straining of sand," Research Report, Civil Eng. Dept., Rensselaer Polytechnic Institute, Troy, New York

FLIP Consortium, (2011). "Computer program for evaluating damage to structures induced by liquefaction FLIP (Ver.7.2.3) Manual."

Groholski, D., Hashash, Y., Kim, B., Musgrove, M., Harmon, J., and Stewart, J. (2016). "Simplified Model for Small-Strain Nonlinearity and Strength in 1D Seismic Site Response Analysis." J. Geotech. Geoenviron. Eng. , *10.1061/(ASCE)GT.1943-5606.0001496* , *04016042*.

Hardin, B.O., Drnevich, V.P., (1972). Shear modulus and damping in soils: Design equations and curves. J. Soil Mech. Found., ASCE 98 (SM7), 289-324

Hashash, Y.M.A. and Park D. (2001). "Non-linear one-dimensional wave propagation in the Mississippi Embayment", Engineering Geology, v. 62 (1-3), 185-206.

Hashash, Y.M.A., Phillips, C. and Groholski, D. (2010). "Recent advances in non-linear site response analysis", Fifth International Conference on Recent Advances in Geotechnical Earthquake Engineering and Soil Dynamics, Paper no. OSP 4.

Hashash, Y.M.A., Musgrove, M.I., Harmon, J.A., Groholski, D.R., Phillips, C.A., and Park, D. (2015) "DEEPSOIL 6.0, User Manual" 125 p.

Iai, S., Matsunaga,Y. and Kameoka,T.(1990): Strain space plasticity model for cyclic mobility, Report of Port and Harbour Research Institute, Vol.29, No.4, pp.27-56.

Iai,S., Matsunaga,Y. and Kameoka,T.(1990): Parameter Identification for a Cyclic Mobility Model, Rep. of the Port and Harbour Res. Inst. Vol.29, No.4.

Idriss, I.M. and J.I. Sun (1992). User's Manual for SHAKE91. Center for Geotechnical Modeling, University of California, Davis, CA.

Ishihara,K., Yoshida,N. and Tsujino,S.: Modelling of stress-strain relations of soils in cyclic loading, Proc. of 5th International Conf. on Num. Methods in Geomechanics, Nagoya, Vol.1, pp. 373-380, 1985.

Itasca. (2011). FLAC - Fast Lagrangian Analysis of Continua, Version 7.0. Minneapolis, Minne sota: Itasca Consulting Group, Inc.

Iwan W. D. 1967. On a class of models for the yielding behavior of continuous and composite systems. Journal of Applied Mechanics, 34 (3), 612-617.

Joyner, W. B., and Chen, A. T. F. (1975) . "Calculation of nonlinear ground response in earthquakes." Bull. Seismol. Soc. Am., 65 (5) ,1315–1336.

Kaklamanos, J., Bradley, B. A., Thompson, E. M., and Baise, L. G. (2013). " Critical para-meters affecting bias and variability in site-response analyses using Kik-net downhole array data." Bull. Seismol. Soc.Am., 103(3), 1733 – 1749.

Kaklamanos, J., Baise, L.G., Thompson, E.M., Dorfman, L. (2015). " Comparison of 1D linear, equivalent-linear, and nonlinear site response models at six KiK-net validation sites", Soil Dynamics and Earthquake Engineering, v. 69 (2015) 207–219.

Kottke A., Rathje E.M. (2008). Technical manual for STRATA, PEER Report No. 2008/10, Pacific Earthquake Engineering Research Center, University of California, Berkeley, CA.

Kondner, R. L., and J.S. Zelasko (1963). "A hyperbolic stress-strain formulation of sands," Proc. of 2nd Pan American Conference on Soil Mechanics and Foundation Engineering, Sao Paulo, Brasil, 289–324

Kramer, S.L. (1996). "Geotechnical Earthquake Engineering", Prentice Hall, Upper Saddle River, 653 pp.

Kramer, S. L., and Paulsen, S. B. (2004) . "Practical use of geotechnical site response models." Proc., Int. Workshop on Uncertainties in Non-linear Soil Properties and their Impact on Modeling Dynamic Soil Response, PEER Center Headquarters, Richmond, Calif.

Kuhlemeyer, R. L., and J. Lysmer. (1973) "Finite Element Method Accuracy for Wave Propagation Problems," J. Soil Mech. & Foundations, Div. ASCE, 99(SM5), 421-427.

Kwok, A.O., Stewart,J.P., Hashash, Y.M.A., Matasovic, N., Pyke, R., Wang, Z.,and Yang, Z. (2007)."Use of exact solutions of wave propagation problems to guide implementation of nonlinear seismic ground response analysis procedures." J. Geotech.&Geoenv. Eng., ASCE, 133 (11), 1385-1398.

Laird, J.P., Stokoe, K.H. (1993). Dynamic properties of remolded and undisturbed soil samples test at high confining pressure. Geotechnical Engineering Report GR93-6, Electrical Power Research Institute

Lee, N., Bathe, K.J. (1993)/ "Effects of Element Distortions on the Performance of Isoparatmetric Elements. International Journal for Numerical Methods in Engineering, Vol. 36, 3553-3576. John Wiley & Sons, LLtd

Lysmer, J. M., and Kuhlemeyer, R. L. (1969). "Finite-dynamic model for infinite media." J. Engrg. Mech. Div., 95(4), 859–877.

Masing, G. (1926) . "Eigenspannungen and verfertigung beim messing."Proc., 2nd Int. Congress on Applied Mech., Zurich, Switzerland.

Matasovic, N., and Vucetic, M. (1993). "Cyclic characterization of liquefiable sands." J. Geotech. Engrg., 119 (11) , 1805–1822.

Matasovic, N. and Ordóñez, G.A. (2011). "D-MOD2000 – A Computer Program for Seismic Site Response Analysis of Horizontally Layered Soil Deposits, Earthfill Dams, and Solid Waste Landfills." GeoMotions, LLC; Lacey, Washington, USA.

McGann, C., and Arduino, P. (2010). "Site Response Analysis of a Layered Soil Column (Total Stress Analysis" Opensees Example Wiki. University of Washington

McKenna, F. and G.L. Fenves (2006). "The OpenSees command language manual, version 1.2." Pacific Earthquake Engrg. Research Center, Univ. of Calif., Berkeley. http://opensees.berkeley.edu/OpenSees/manuals/usermanual/OpenSeesCommandLanguage ManualJune2006.pdf

Mejia, L. H., and E. M. Dawson. (2006). "Earthquake Deconvolution for FLAC" in FLAC and Numerical Modeling in Geomechanics (Proceedings of the 4th International FLAC Symposium, Madrid, Spain, May 2006), pp. 211-219. P. Varona & R. Hart, eds. Minneapolis, Minnesota: Itasca Consulting Group Inc.

Mroz, Z. (1967). ''On the description of anisotropic work hardening.'' J. Mech. Phys. Solids, 15, 163–175.

Newmark, N. M. (1959). "A Method of Computation for Structural Dynamics," Journal of the Engineering Mechanics Division, ASCE, 85, pp. 67–94.

Nikolau, S. & Go, J. (2009). "Site-Specific Seismic Studies for Optimal Structural Design: Part II-Applications," Structure Magazine. Link: http://www.structuremag.org/wp-content/uploads/2014/08/C-StructuralDesign-Nikolaou-Dec091.pdf

Park, D. and Hashash, Y.M.A. (2003). "Soil damping formulation in nonlinear time domain site response analysis". Journal of Earthquake Engineering", v. 8, (2), 249-274.

Phillips, C. and Hashash, Y.M.A. (2009). "Damping formulation for nonlinear 1D site response analyses", Soil Dynamics and Earthquake Engineering, v. 29 (2009) 1143–1158.

Schnabel, P. B., Lysmer, J., and Seed, H. B. (1972). "SHAKE: A computer program for earthquake response analysis of horizontally layered sites." Report No. UCB/EERC-72/12, Earthquake Engineering Research Center, University of California., Berkeley, CA.

Rayleigh, J.W.S., Lindsay, R.B.,(1945) The theory of sound, Vol. 2(1). New York: Dover Publications.

Real, C.R. (1988). "Turkey Flat, USA site effects test area – Report 2: Site characterization," California Division of Mines and Geology TR 88-2.

Real, C.R. and A.F. Shakal (2005). "Turkey Flat, USA Site Effects Test Area – Report 7: Strong-Motion Test: Prediction Criteria and Input Rock Motions." California Geological Survey, OSMS 05-1, 33 p.

Real, C., Shakal, A., and Tucker, B. (2008) The Turkey Flat Blind Prediction Experiment for the September 28, 2004 Parkfield Earthquake: General Overview and Models Tested. Geotechnical Earthquake Engineering and Soil Dynamics IV: pp. 1-10.doi: 10.1061/40975(318)27

Schnabel, P. B., Lysmer, J., and Seed, H. B. (1972). SHAKE: A computer program for earthquake response analysis of horizontally-layered. University of California, Berkeley, CA: Earthquake Engineering Research Center.

Seed, H.B., Ugas, C., and Lysmer, J. (1976). ''Site-dependent spectra for earthquake resistant design.'' Bulletin of the Seismological Society of America, Vol. 66(1), 221–244.

Seed, H.B., Romo, M.P., Sun, J.I, Jaime, A., and Lysmer, J., (1988). "The Mexico earthquake of September 19, 1985 – Relationships between soil conditions and earthquake ground motions." Earthquake Spectra, Vol. 4(4), pp. 687-729.

Shakal, A., Graizer, V., Huang, M., Borcherdt, R., Haddadi, H., Lin, K., Stephens, C., and P. Roffers (2005). "Preliminary Analysis of Strong-motion Recordings form the 28 September 2004 Parkfield, California Earthquake." Seismological Research Letters 76 (1), 27-39.

Stewart, J.P., Kwok, A.O., Hashash, Y.M.A, Matasovic, N., Pyke, R., Wang, Z., Yang, Z. (2008). "Benchmarking of Nonlinear Geotechnical Ground Response Analysis Procedures." Pacific Earthquake Engineering Research Center Report 2008/04.

Stokoe, K.H., Darendeli, M.B., Menq, F.-Y. (1999). ROSRINE Project: Phases I and II summary of RC/TS laboratory test results. Symposium at MIT on Site Reponse Issues, March, 19, 1999.

Towhata,I. and Ishihara,K. (1985). Modelling soil behavior under principal stress axes rotation, Proc. 5th International conference on numerical method in geomechanics, Nagoya, pp.523-530.

Towhata, I. (2008). Geotechnical Earthquake Engineering. Springer Series in Geomechanics and Geoengineering

Tucker, B.E. and C.R. Real (1986). "Turkey Flat, USA site effects test area – report 1: needs, goals, and objectives," TR 86-1, Calif. Div. of Mines and Geology

Vucetic, M. and Dobry, R. (1991). "Effect of soil plasticity on cyclic response." Journal of Geotechnical Engineering. ASCE, 117(1), 89–107.

Vucetic, M. and R. Dobry (1986). "Pore pressure buildup and liquefaction at level sandy sites during earthquakes," Research report CE-86-3, Dept. Civil Eng., Rensselaer Polytechnic Institute, New York

Vucetic, M. (1990) . "Normalized behavior of clay under irregular cyclic loading." Can. Geotech. J., 27, 29–46.

Wood, D.M. (2004). "Geotechnical Modeling." Spoon Press: Taylor Francis Group. London.

Yang, Z. (2000). "Numerical modeling of earthquake site response including dilation and liquefaction." Ph.D. thesis, Dept. of Civil Engineering and Engineering Mechanics, Columbia Univ., New York.

Yang, Z and Elgamal, A. (2000). " Numerical modeling of earthquake site response including dilation and liquefaction.". Structural System Research Project. Report No. SSRP-2000/01. Department of Structural Engineering University of California, San Diego. La Jolla, CA.

Yee, E., Stewart, J., and Tokimatsu, K. (2013). "Elastic and Large-Strain Nonlinear Seismic Site Response from Analysis of Vertical Array Recordings." J. Geotech. Geoenviron. Eng., 139(10), 1789–1801.

Zalachoris, G., Rathje, E.M., 2015. Evaluation of one-dimensional site response techniques using borehole arrays. J. Geotech. Geoenviron. Eng. 141 (12), 04015053.

APPENDIX

TURKEY FLAT PREDICTION RESULTS
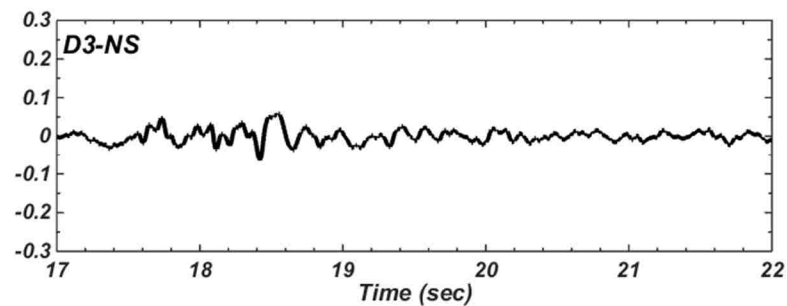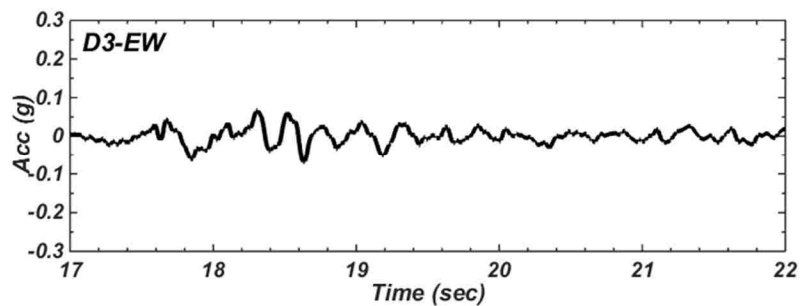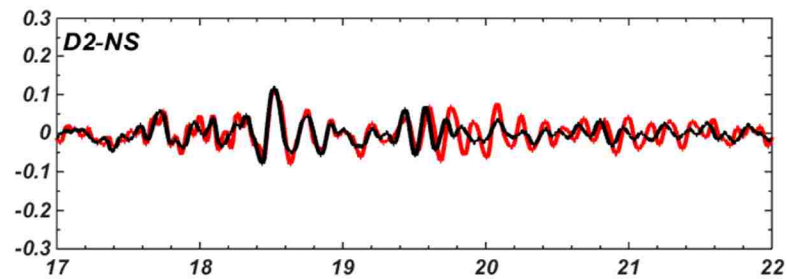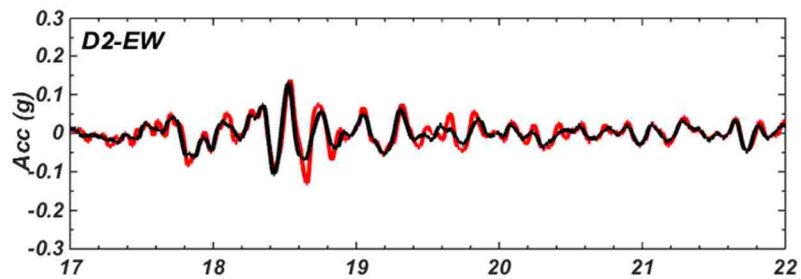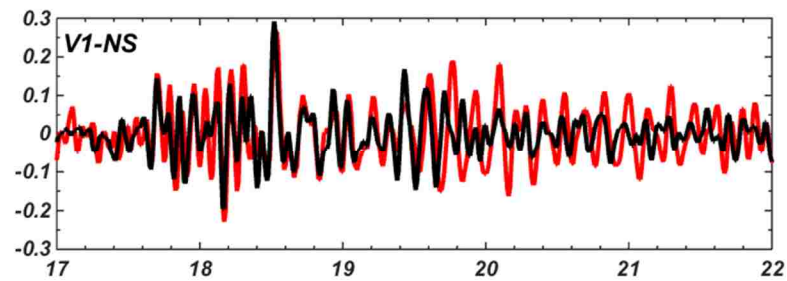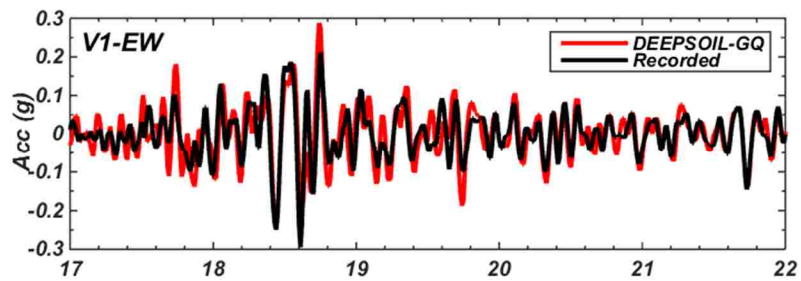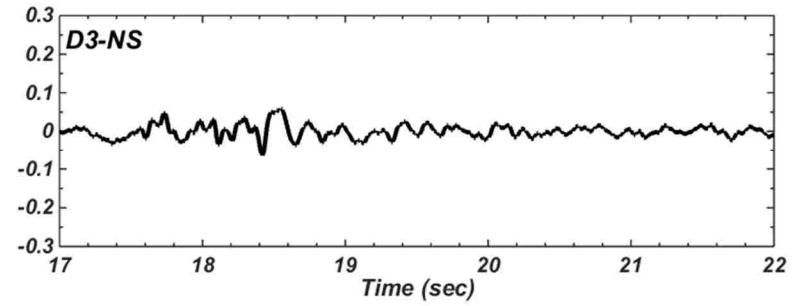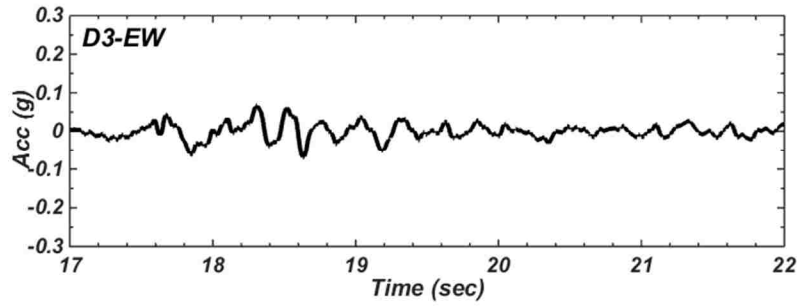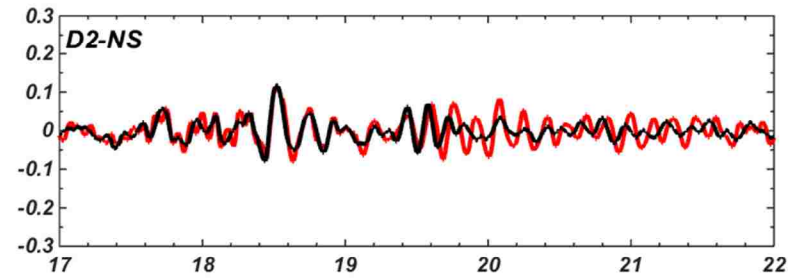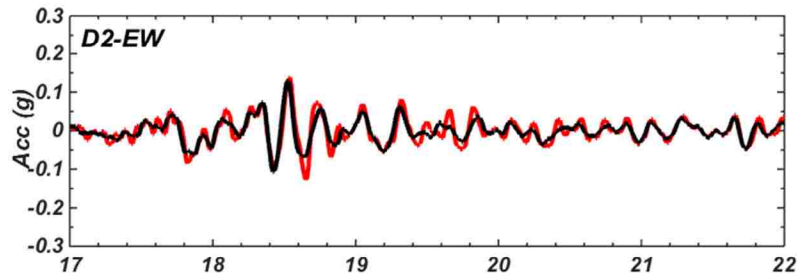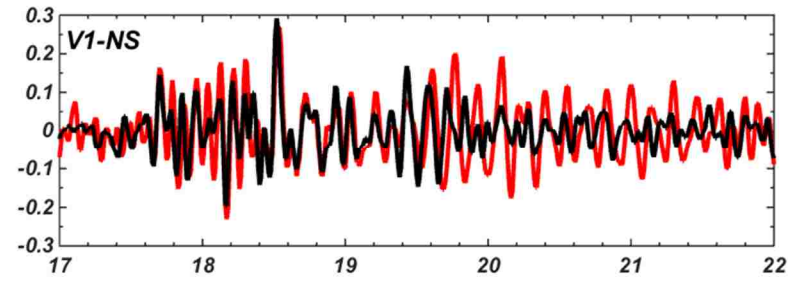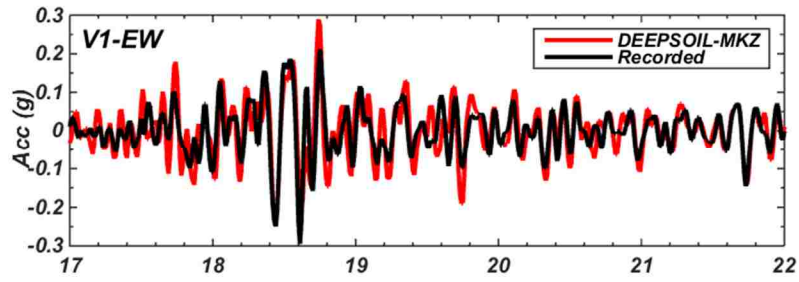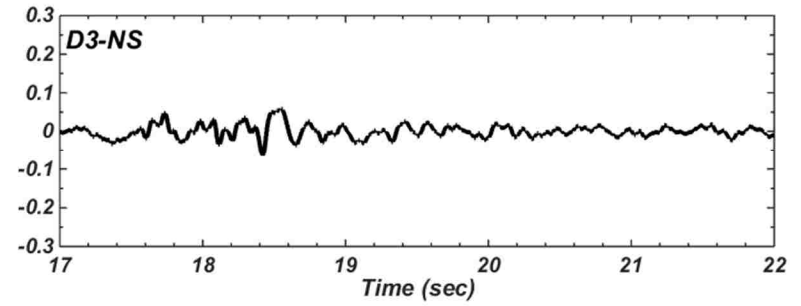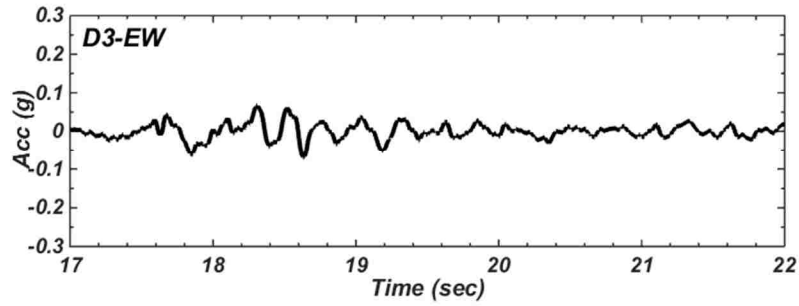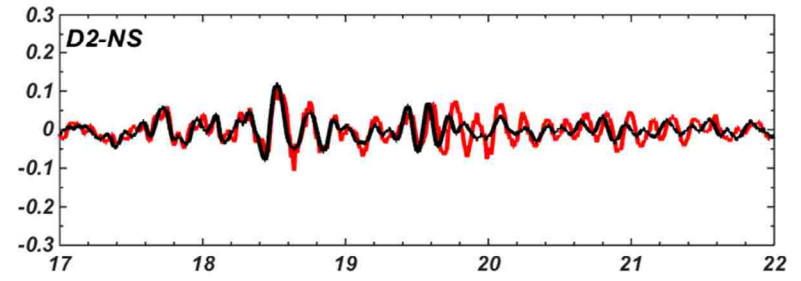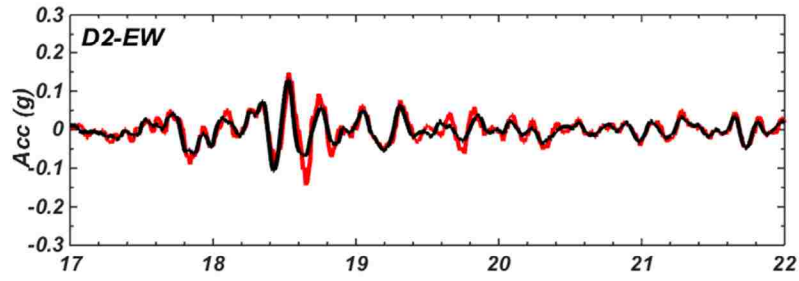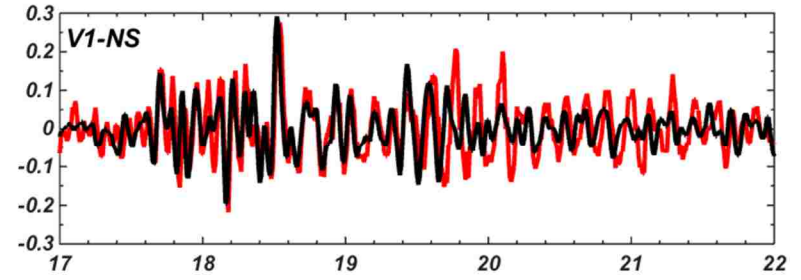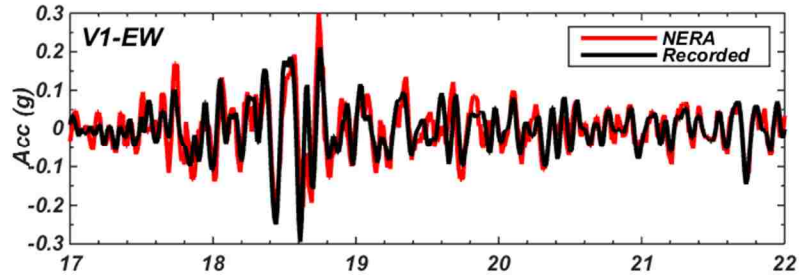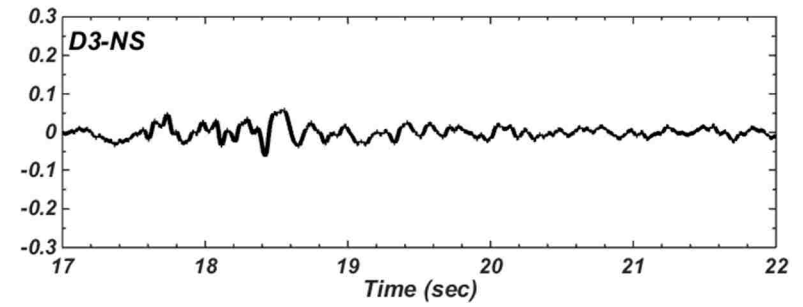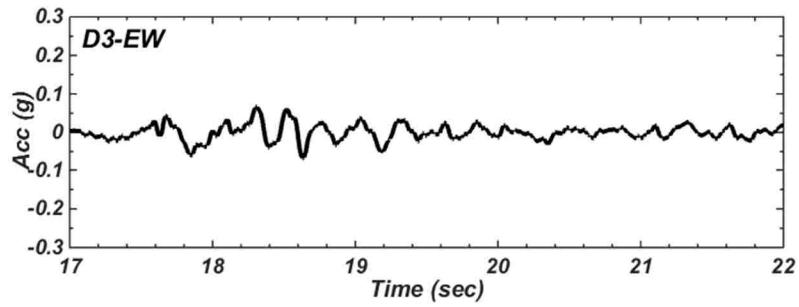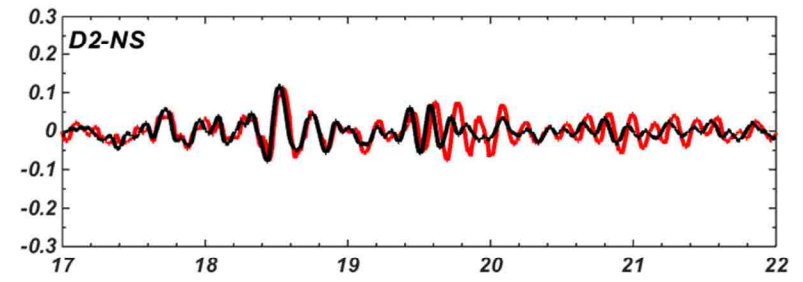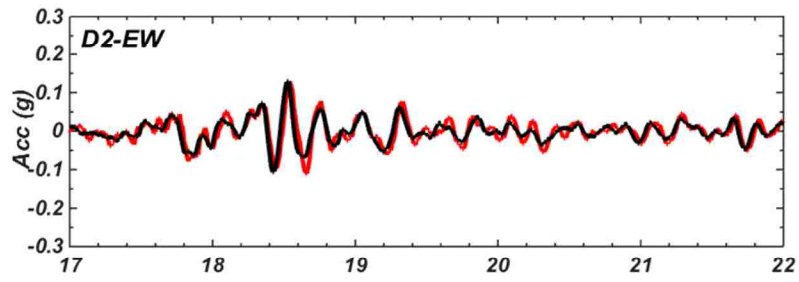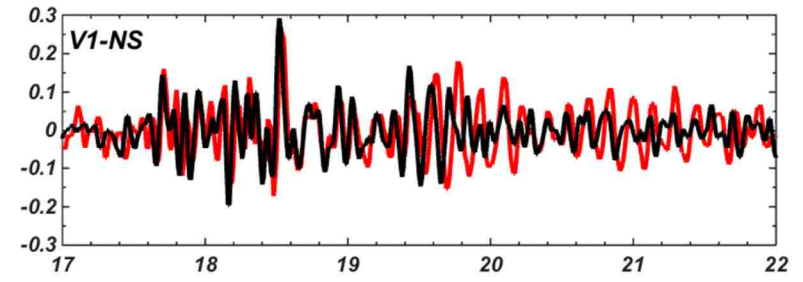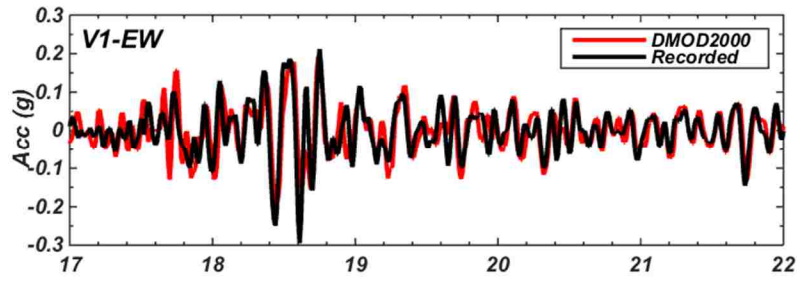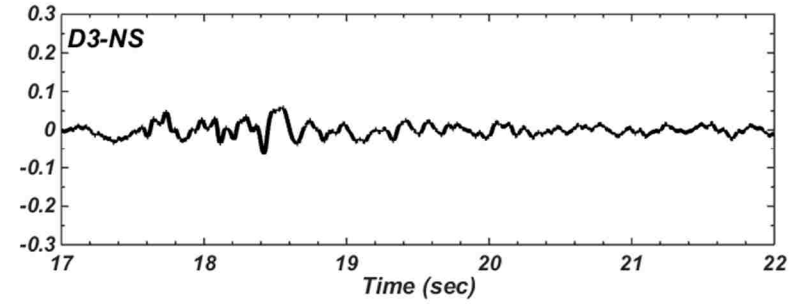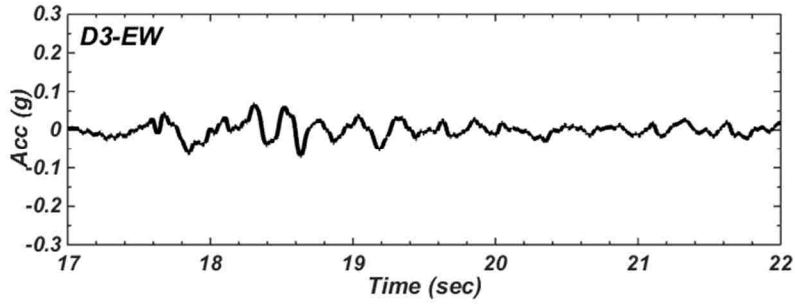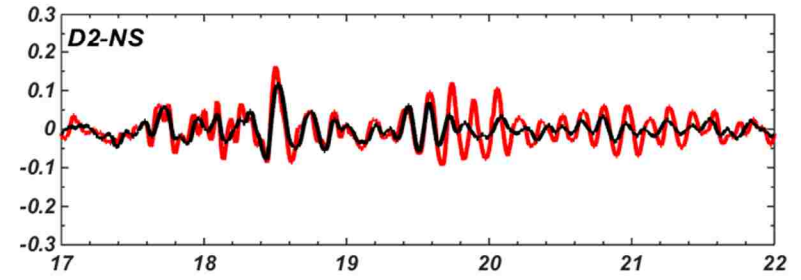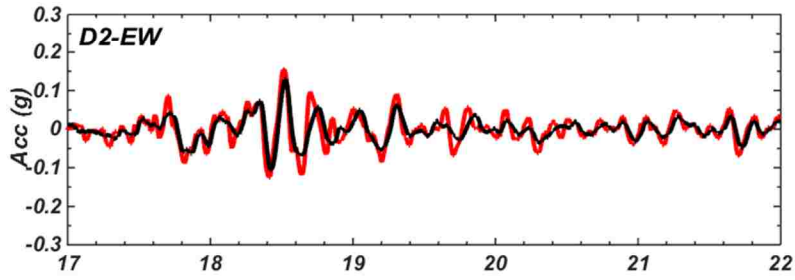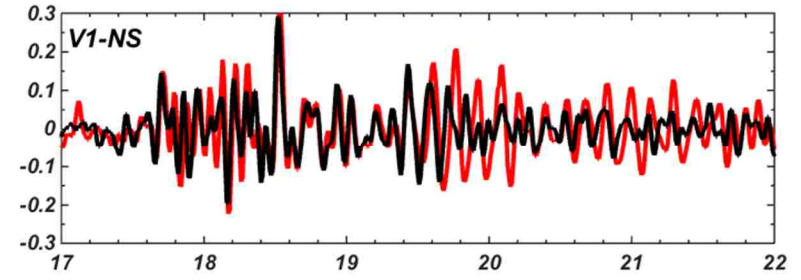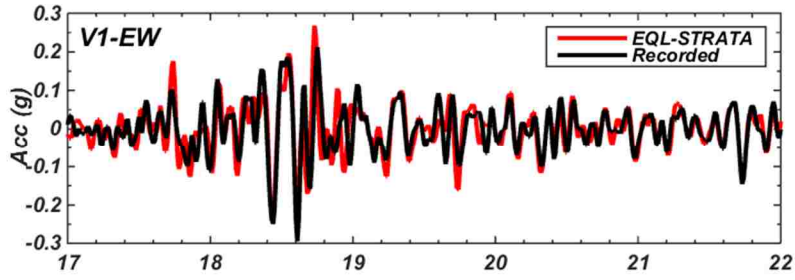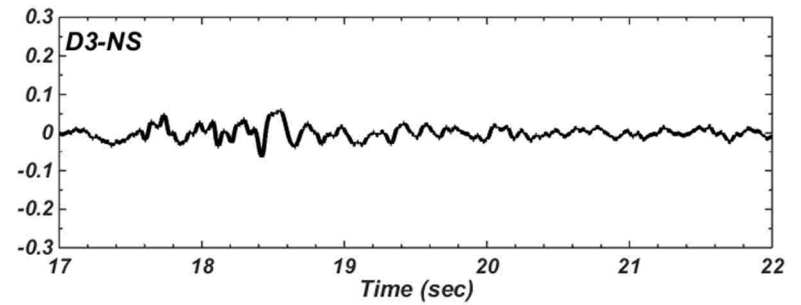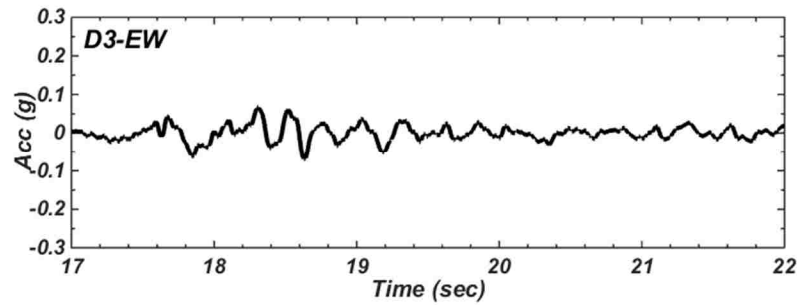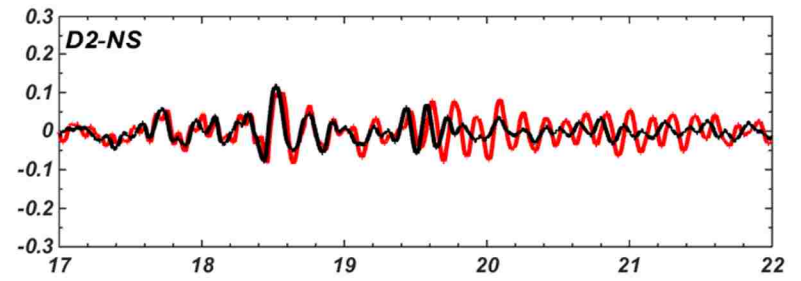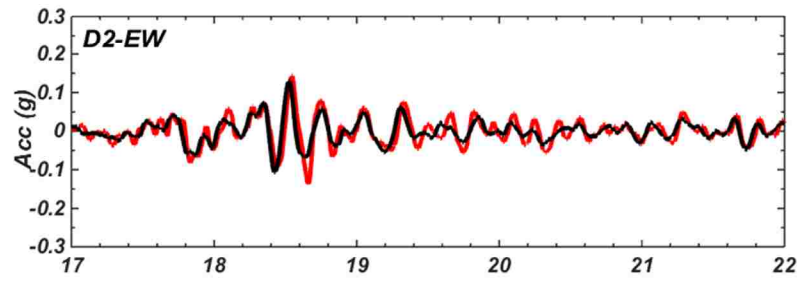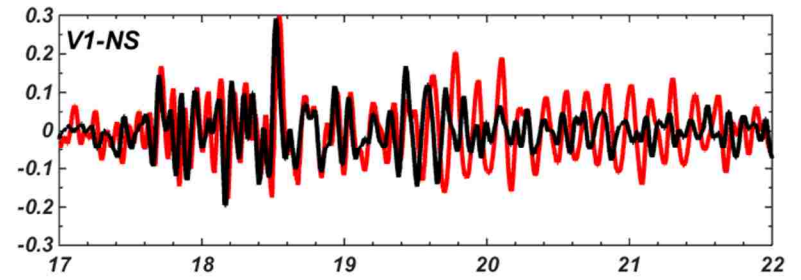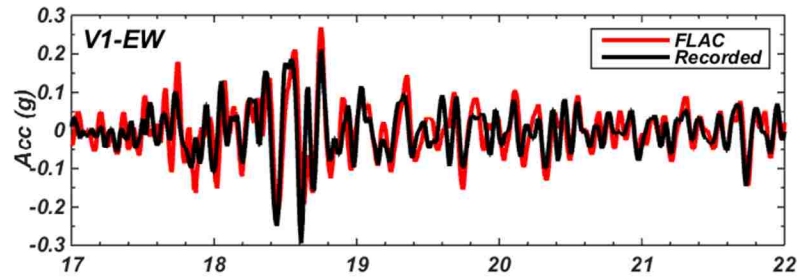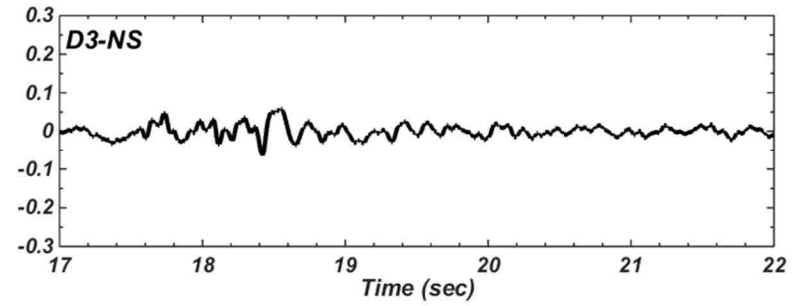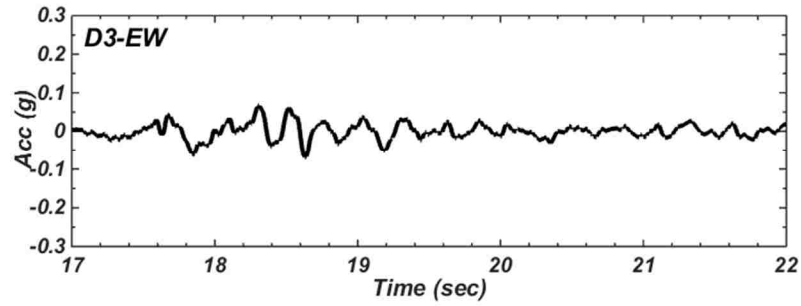
VITA

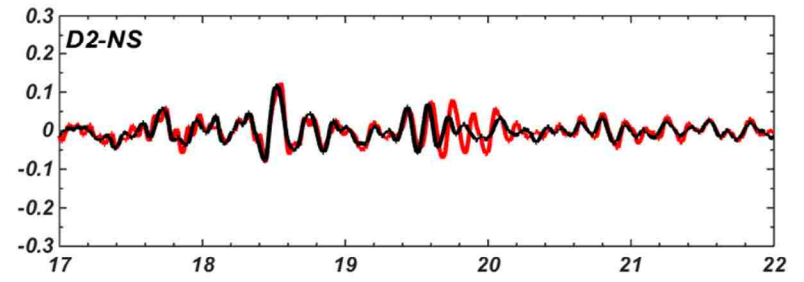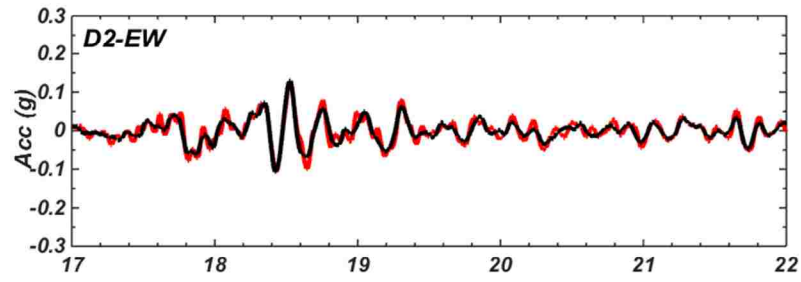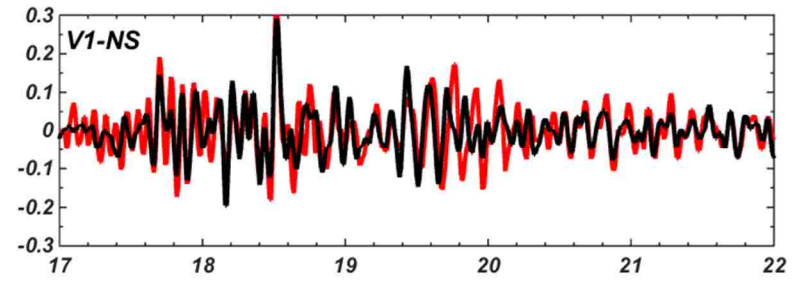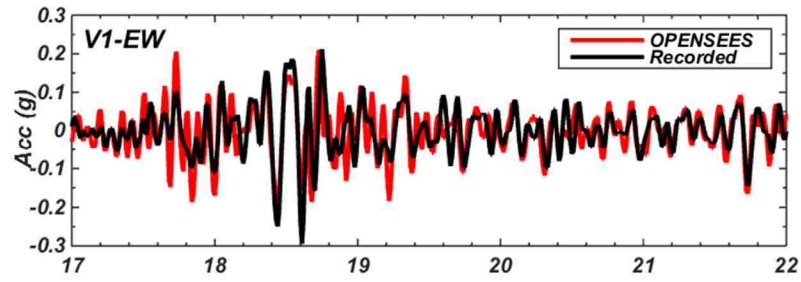Daniel Hutabarat was born in Palembang, Indonesia on September 29, 1988 to Ratmarani Bhadra br. Sihombing and Robert Hutabarat. He graduated from SMA Negeri 1 (High School) Bogor, Indonesia in 2006. In July 2010, he graduated with a Bachelor of Science degree in Civil Engineering from Institut Teknologi Bandung (ITB), Bandung, Indonesia. After graduation, he earned professional working experience as a geotechnical engineer for several years. He worked as a geotechnical engineer in geotechnical consultant company in Indonesia for 2 years and in ground improvement contractor company in Singapore for another year before continuing his M.S. study in the University of Washington in Autumn 2014.

Permanent email: hutabarat.dnl@gmail.com

This thesis was typed by Daniel Hutabarat